Late Holocene environmental and climate dynamics along the southern Cape coast of South Africa: High resolution multi-proxy records from the Wilderness Embayment

Nadia du Plessis

Thesis presented for the degree of

DOCTOR OF PHILOSOPHY

in the Department of Environmental and Geographical Science

University of Cape Town

October 2020

Declaration

I, Nadia du Plessis, declare that this work is my own and that all contributions from other people's work are properly referenced, cited and acknowledged.

I confirm that I have been granted permission by the University of Cape Town's Doctoral Degrees Board to include the following publication(s) in my PhD thesis, and where co-authorships are involved, my co-authors have agreed that I may include the publication(s):

du Plessis, N., Chase, B.M., Quick, L.J., Haberzettl, T., Kasper, T. & Meadows, M.E., 2020. Vegetation and climate change during the Medieval Climate Anomaly and the Little Ice Age on the southern Cape coast of South Africa: Pollen evidence from Bo Langvlei. *The Holocene*, 30(12), pp. 1716-1727.

du Plessis, N, Chase, BM, Quick, LQ & Meadows, ME. A late Holocene pollen and charcoal record from Eilandvlei, southern Cape coast, South Africa. Submitted, in review: *Palaeoecology of Africa*. Volume 35*:* Quaternary Vegetation Dynamics. Special Edition: Contributions to the African Pollen Database.

du Plessis, N, Chase, BM, Quick, LJ, Strobel, P, Haberzettl, T & Meadows, ME. A ~650 year pollen and microcharcoal record from Vankervelsvlei, South Africa. Submitted, in review: *Palaeoecology of Africa.* Volume 35*:* Quaternary Vegetation Dynamics. Special Edition: Contributions to the African Pollen Database.

SIGNATURE: Signed by candidate DATE: 19/10/2020

STUDENT NAME: Nadia du Plessis STUDENT NUMBER: DPLNAD003

Abstract

It is well documented that the South African palaeoenvironmental record is relatively limited in terms of both quantity and quality. This is mainly due to the region's highly seasonal rainfall regimes and generally arid to semi-arid environments which are not conducive to the preservation of sedimentary sequences and associated proxy records. The climate along the southern Cape coast is influenced by both tropical and temperate climate systems, and the region hosts highly diverse vegetation including fynbos and thicket elements and includes the Knysna Afrotemperate Region – the most extensive forest complex in southern Africa. The mechanisms controlling these tropical and temperate systems have responded to changing global boundary conditions and these changes have significantly impacted the regional vegetation mosaic. This ephemeral nature of the region's climate and vegetation suggests it is particularly sensitive to climate change, making it an ideal area to evaluate changes in these systems and how they interact over time.

For this study, four sets of records were produced from three wetlands along the southern Cape coast. The Eilandvlei palynological and microcharcoal records span the last ~3000 years with the pollen and microcharcoal records from adjacent Bo Langvlei covering the last ~1300 years. The most outstanding feature in these records are the time periods covering the Medieval Climate Anomaly (MCA; c. AD 950 – 1250) and the Little Ice Age (LIA; c. AD 1300 – 1850). The evidence indicates that conditions in the region during the MCA chronozone were relatively dry and perhaps slightly cooler than present. The most durable phase of forest expansion, and likely more humid conditions, occurred during the transition between the MCA and core cooling of the LIA with the LIA clearly identified as a period of cool, dry conditions between c. AD 1600 to c. AD 1850. In addition, the Eilandvlei pollen record demonstrates the effects of external physiographic dynamics on pollen accumulation and deposition within the lake basin. A complementary set of geochemical and sedimentological records have been generated for Bo Langvlei incorporating the last ~4200 years. These records suggest that the late Holocene evolutionary history of Bo Langvlei comprised of three phases: a marine/lagoonal phase extending until c. 1270 cal yr BP, a short transitional phase between c. 1270 and 1200 cal yr BP, and

the more recent lacustrine phase. A ~650 year pollen and microcharcoal record have been obtained from nearby Vankervelsvlei. Although discontinuous, this is the first palynological record from this unique waterbody covering this period.

In terms of climate, the mechanisms driving the observed changes in the records taken as a whole appear to relate to changes in temperature and dynamics in the influence of tropical systems, perhaps transmitted at least in part via the Agulhas Current and the development of localised precipitation systems. The findings further reinforce the proposed importance of summer rainfall in regulating moisture availability along the south coast of South Africa. The records also highlight the significant impacts of fluctuating sea levels and changes in dune morphology in shaping the embayment, and more recently, the effects of accelerated anthropogenic activities in the area.

Acknowledgements

Firstly, a big thank you to my main supervisor, Mike Meadows, who has been with me throughout my journey at UCT. Thank you for sticking with me, through the good and the bad.

To my co-supervisors, Torsten Haberzettl and Brian Chase, thank you for the trans-continental support and encouragement. This would definitely have not been possible without your help.

Lynne Quick, my dearest friend, teacher in the ways of pollen, co-supervisor and one of my biggest cheerleaders, I don't think the words "thank you" encapsulate the immense amount of gratitude I have for your role in getting me this far, both personally and academically.

Thank you to the University of Cape Town's Postgraduate Funding Office and the Bundesministerium für Bildung und Forschung (BMBF) (this work forms part of a bilateral - South African/German - project between the University of Cape Town and Friedrich Schiller University of Jena) for generously funding various parts of this research. The financial assistance of the National Research Foundation (NRF) towards some of this research is hereby acknowledged.

Finally, to my family – Mamma, Mia and John, and the little ones Grayson and Imogen – I can't thank you enough for all the love and support and encouragement! You've carried me through this crazy PhD ride, especially towards the end. I will forever be grateful for your support of my academic endeavours.

Vir Pappa

Table of Contents

List of Figures

List of Tables

Chapter 1
Introduction

The best way to predict the future is to study the past, or prognosticate

Robert Kiyosaki

How, then, can we use the past to predict the future? Of central importance in answering this question is the prerequisite of establishing an understanding of the natural climate and environmental variability of the more recent geological past. By studying these periods, we can gain important insights into modern day and predicted future climate states. Indeed, this has been highlighted before, i.e.

'The study of past climate provides an essential baseline from which to understand and contextualize changes in the contemporary climate' (Neukom et al. 2019, p 550).

'If we are to understand the background of natural variability underlying anthropogenic climate change, it is important to concentrate on climate of the more recent past' (Mayewski et al. 2004, p 243).

'Reconstructing past climate is essential for enhanced understanding of climate variability, and provides necessary background knowledge for improving predictions of future changes' (Moberg et al. 2005, p 614).

In this regard, the late Quaternary presents a key time frame against which contemporary, and future, environmental and climate change can be measured (Meadows 2001; 2012). **The Holocene (1.1)** epoch in particular is of major interest as it provides the best analogue for present-day boundary conditions (MacDonald et al. 2008; Norström et al. 2018).

Lakes and wetlands offer some of the few environments suitable for the preservation of Quaternary deposits in more arid southern Africa. **Lacustrine sediments (1.2)** provide a rich archive of palaeoenvironmental data and have been used extensively in the study and reconstruction of past vegetation histories and long term climate change. Situated within the year round rainfall zone, the lakes within **the Wilderness Embayment (1.3)** serve as a great example of such a setting.

Climatic conditions across southern Africa are affected by a complex interplay of atmospheric and oceanic circulation systems. A fundamental question relating to southern African palaeoclimatology is how the dynamics of these systems have influenced rainfall regimes across the subcontinent. Analysis of the available palaeoenvironmental records have concluded that regional climates have likely been highly dynamic over time (Chase and Meadows 2007), as the mechanisms controlling tropical and temperate systems have responded to changing global boundary conditions (Chase et al. 2017; Chase and Quick 2018). These changes have further significantly impacted the regional vegetation mosaic of the southern Cape (Martin 1968; Quick et al. 2016; Quick et al. 2018). As such, this area is ideally situated to explore the diverse climatic regimes of southern Africa and the influence of these on regional environments. In addition, sea level oscillations has left its distinctive mark on the coastal regions of the southern Cape, moulding and shaping the Wilderness Embayment and associated lakes into its contemporary form (Cawthra et al. 2014; Martin 1962; Martin 1968; Wündsch et al. 2016a; Wündsch et al. 2018). More recently however, anthropogenic activities have become the main drivers behind landscape and vegetation change in both the catchments and within the lakes themselves. Consequently, there is a great need to understand the environmental and landscape dynamics of the region, not just from a broader climatic perspective but also in a more local context. Recent research initiatives along the southern Cape coast (e.g. Haberzettl et al. 2019; Kirsten et al. 2018; Quick et al. 2016; Quick et al. 2018; Reinwarth et al. 2013; Strobel et al. 2019; Wündsch et al. 2016b; Wündsch et al. 2016a; Wündsch et al. 2018) have made great inroads towards understanding the complex nature of climatic interactions, and the related environmental responses, in the region during the Holocene - there is, however, a lack of focus on finer scale variability, especially during the late Holocene.

1.1. The Holocene

The onset of the Holocene, the most recent stratigraphic epoch, is widely regarded as 11 500 cal yr BP (Mayewski et al. 2004; Walker et al. 2008; Walker et al. 2012; 2019) or, as per the most recent International Chronostratigraphic Chart (Cohen et al. 2020), 11 700 cal yr BP. This designates the end of the Younger Dryas, an unusual cold event during the late Pleistocene (Walker et al. 2008). Conditions during the Holocene, while globally regarded as more stable than the preceding glacial and late glacial phase, are typically recognized as comprising three phases or sub-epochs. Formally, as proposed by Walker et al. (2012; 2019), these phases were defined as the early, mid- and late Holocene with the boundaries between them represented by key climatic events. The latest classifications however now refer to these phases as the Greenlandian, Northgrippian and Meghalayan stages (Cohen et al. 2020).

The early and mid-Holocene (Greenlandian and Northgrippian) is separated by the "8.2 ka BP event" – a brief near-global cooling episode around 8200 cal yr BP, before the onset of Altithermal conditions (Walker et al. 2012; 2019). The so called Holocene Altithermal (also Hypsithermal or so-called climatic optimum) was a global phenomenon between ~8000 and 6000 cal yr BP characterised by warmer environments, especially in the Northern mid- to high latitudes (Wanner et al. 2008). The boundary between the mid and late Holocene (Northgrippian and Meghalayan) is placed at ~4200 cal yr BP where the "4.2 ka event" is associated with extensive aridity and warming in the Southern Hemisphere (Mayewski et al. 2004; Walker et al. 2012; 2019).

In addition, two rapid climate change events, as termed by Mayewski et al. (2004), characterise global climate over the past ~1200 years. The Medieval Climate Anomaly, extending from ~1000 to 700 cal yr BP (AD 950 – 1250) (Jones et al. 2001; Matthews and Briffa 2005), have largely been interpreted as a generally warmer period, both globally and in South Africa (Tyson 1999; Tyson et al. 2000). Recent evidence however indicates that conditions were not homogeneously so, but rather were marked by considerable variability in terms of both temperature and hydroclimate (Nash et al. 2016; Nicholson et al. 2013; PAGES2k 2013). The more recent Little Ice Age, defined primarily in the

Northern Hemisphere, represents a cooler interval between ~650 and 100 cal yr BP (AD 1300 – 1850) (Jones et al. 2001; Matthews and Briffa 2005; Nicholson et al. 2013; PAGES2k 2013).

1.2. Lacustrine Sediments as Palaeo-archives

Lacustrine systems are sensitive to both environmental and climatic changes. Essentially acting as a sediment trap, lakes accumulate sediment and preserve proxy material over time, providing an invaluable archive of palaeoenvironmental information. These sediments can contain evidence of past environmental changes, both within the lake and the surrounding catchment (Foster and Walling 1994). Even though lacustrine systems are limited in semi-arid southern Africa where the climate is not always conducive to the preservation of such palaeo-archives, lacustrine sediment has been used with great success to expand the palaeoenvironmental knowledge of the region, e.g. Finch and Hill 2008; Meadows and Baxter 2001; Norström et al. 2009; Neumann et al. 2010; Quick et al. 2018.

Multi-proxy analysis of the stratigraphic sequence in lacustrine sediments are used extensively for the reconstruction of long term environmental and climate change in both terrestrial and aquatic ecosystems (Andrén et al. 2015; Lotter et al. 1995). Different environmental dynamics are reflected by different proxies at various spatial scales, each with their own strengths and weaknesses (Birks and Birks 2006). When used together, these can provide a more complete picture of changing dynamics within an ecosystem (Birks and Birks 2006). An overview of the proxies utilised in this study is set out below.

1.2.1. Pollen and microcharcoal

Pollen analysis is one of the most widely applied methods for the investigation and reconstruction of Quaternary environments. Through the analysis of fossil pollen and spores changes in vegetation and, thereafter, climate and ecosystem dynamics, can be explored. Pollen grains are well adapted for analysis over extended timescales mainly due to their structure allowing for the preservation of these grains over millennia under particular conditions. The exine, or outer layer, contains the highly resistant material

sporopollenin, protecting the pollen grain from microbial decay (Faegri and Iversen 1989; Traverse 2008). This outer layer is also responsible for the various shapes and apertures (i.e. colpi and pores) making taxonomic identification of pollen grains possible (Moore et al. 1991). A notable limitation of this method however is that the identification of fossil pollen, especially in species-rich environments, may be difficult beyond family level (Meadows and Sugden 1991). A further consideration involves pollen production levels and the dispersal modes of grains from individual taxa (Lowe and Walker 1997), i.e. taxa with high pollen productivity as well as those dependent on wind dispersal (e.g. *Podocarpus*) tend to be over represented in the pollen record (Coetzee 1967; Hamilton 1972; Jackson and Kearsley 1998; Jackson and Williams 2004), which needs to be taken into account when interpreting the data. Similarly, the intricate relationship between pollen present at the specific sampling site and the vegetation cover it would represent in the data is an important consideration, as illustrated by Duffin and Bunting (2008).

The study of fossil charcoal particles in lacustrine sediments can provide information on past fire events and fire regimes in the region (Conedera et al. 2009; Tinner and Hu 2003). In conjunction with pollen data, charcoal assemblages can offer insights into fire-vegetation dynamics of the surrounding environment. An important consideration in the interpretation of charcoal records is the provenance of these deposited particles. Charcoal calibration studies (e.g. MacDonald et al. 1991; Tinner et al. 1998) have shown that microcharcoal particles (10-200 μm) can originate from 20 to 100 km from the eventual deposition site thus presenting more of a regional fire signal. Larger particles (100-200 μm), on the other hand, are typically not dispersed further than a few hundred meters from the fire providing evidence of local fire events (Conedera et al. 2009; Tinner et al. 1998).

1.2.2. Inorganic geochemistry: Elemental analyses

Geochemical elements in lacustrine sediments are important indicators of palaeoenvironmental conditions at the time of deposition and thereafter (Ma et al. 2016). The proportion of each element transported to and deposited within the lake depends on the erosional, geomorphological, geological, climatic and topographical conditions of the surrounding catchment (Hoffman 1988). Further

distribution and accumulation of these are influenced by amongst others, mineral composition, sediment texture and reduction/oxidation states (Kylander et al. 2011; Ma et al. 2016). As such, variations in sediment geochemistry can reflect sediment sources, hydrological changes, catchment dynamics, biotic processes and particle sorting (Dellwig et al. 2000; Kylander et al. 2011). For example, the elements K, Ti, Si, Al, Zr are commonly inferred to reflect minerogenic sediment input from the lake catchment (Haberzettl et al. 2005; Kasper et al. 2012), while Ca and Sr has frequently been used as marine indicators in lacustrine environments (Haberzettl et al. 2019; Watling 1977; Wündsch et al. 2018).

1.2.3. Organic geochemistry

The organic component of lake sediments provide several proxies for reconstructing past environmental and climate change (Last 2001; Meyers 2003). This organic matter originates from planktonic, terrestrial and degraded terrestrial sources, each with different properties and characteristics (Hoffman 1988), retaining evidence on its provenance and how it was transported and deposited (Meyers 2003). The accumulated organic matter further offer information on both intra and extra basin productivity and can be of use for climatic reconstructions (Meyers 1994; Meyers and Lallier-Vergès 1999).

The concentration of total organic carbon (TOC) in sediment is affected by both primary biomass production and the degree of degradation post deposition (Meyers 2003). It is an essential indicator of the amount of organic matter in sediments, representing the portion of organic matter that did not undergo remineralisation during the sedimentation process (Meyers 2003). Nitrogen contents are a further important proxy, most commonly used in C/N (or TOC/TN) ratios to distinguish between aquatic and land-derived sources of organic matter (Meyers and Lallier-Vergès 1999; Meyers 2003). Aquatic organic matter, i.e. algae, typically have C/N ratios of between four and ten while organic matter of terrestrial origin usually have ratios of 20 and above (Meyers 1994; 2003).

1.2.4. Particle size analysis

Particle size analysis provides information on transport- and depositional mechanisms as well as the provenance of the sediment delivered to the lake (Schillereff et al. 2014). Particle, or grain size is one of the key indicators of energy driven processes in lacustrine sequences (Gayantha et al. 2017; Last 2001) and can be used to reconstruct the depositional environment and rate of transfer, i.e. finer grained particles are typically representative of calmer conditions within the lake and catchment, whereas the coarser fraction typically indicates a more turbulent depositional environment and high energy events such as floods and storm surges (Last 2001; Schillereff et al. 2014). Variations in grain size can further reflect the dominant mode of transport, i.e. fluvial transport is generally associated with coarser particles while finer grain sizes suggest aeolian transport (Wohlfarth et al. 2008).

1.3. The Wilderness Embayment

The Wilderness Embayment (Figure 1-1), located along the southern Cape coast, is well known for the series of lakes and dune cordons. The embayment is backed by the Outeniqua Mountains in the north and bound in the west by the Touw River estuary with the eastern boundary defined by Buffels Bay (Bateman et al. 2011; Butzer and Helgren 1972). This section starts with the broader climate dynamics along the southern Cape coast before moving in closer to introduce the lakes within the Wilderness Embayment. This is followed by an overview of the geology and geomorphology, and contemporary vegetation distribution of the larger Wilderness region, ending off with a brief history of the establishment of the forestry industry in the region.

1.3.1. Southern Cape coast climate

South Africa can broadly be divided into three rainfall zones. The winter rainfall zone (WRZ) is focussed on the west and south western coast while the summer rainfall zone (SRZ) incorporates the largest part of the interior and the east Coast. At the convergence of these, centred on the southern Cape

coast, is the smaller intermediate year round or aseasonal rainfall zone (YRZ/ARZ) (*sensu* Chase and Meadows 2007) (Figure 1-1).

In the YRZ, winter rainfall is brought about by temperate westerlies in the form of ridging anticyclones and cut-off lows (Engelbrecht et al. 2015). Rainfall during the summer months is associated with tropical-temperate trough cloud bands and enhanced tropical easterly flow due to warmer Indian Ocean sea surface temperatures (Engelbrecht et al. 2015; Tyson and Preston-Whyte 2000). The contemporary climate of the region can be described as temperate oceanic ("Cfb"; Peel et al. 2007) with rainfall at a mean annual average ranging from 800 to 1 000mm (Allanson and Whitfield 1983; Russel et al. 2012). There is no distinct dry season, or marked seasonal rainfall pattern but slight increases in rainfall are experienced from March to April and September to October (Allanson and Whitfield 1983; Russel et al. 2012).

In addition to its setting within the YRZ, several local factors further influence local climatic conditions along the southern Cape coast:

i) The Outeniqua Mountains cause orographic uplift and atmospheric flux resulting in light rain, foggy and cloudy conditions as well as high relative humidity along the coast (Hunter 1987; Martin 1968).
ii) The Agulhas current has a major influence as conditions along the coast are particularly susceptible to changes in the upwelling system along the eastern Agulhas Bank (Cohen and Tyson 1995; Tyson and Preston-Whyte 2000). Moreover, warm water from the Agulhas current provides a source of moisture, generating increased humidity along the coast (Jury et al. 1993).
iii) Bergwinds follow a predominantly north-westerly to north-easterly direction from the drier interior, over the mountains towards the coast (Geldenhuys 1994). Most common during winter, bergwinds are linked to the movement of low pressure cells along the coast from west to east (Geldenhuys 1994). These winds are hot and desiccating resulting in large scale variability in temperature and moisture availability in the region (von Maltitz et al. 2003).

Bergwinds further play a key role with regard to fire regimes, and consequently the distribution of forests, in the region (Geldenhuys 1994).

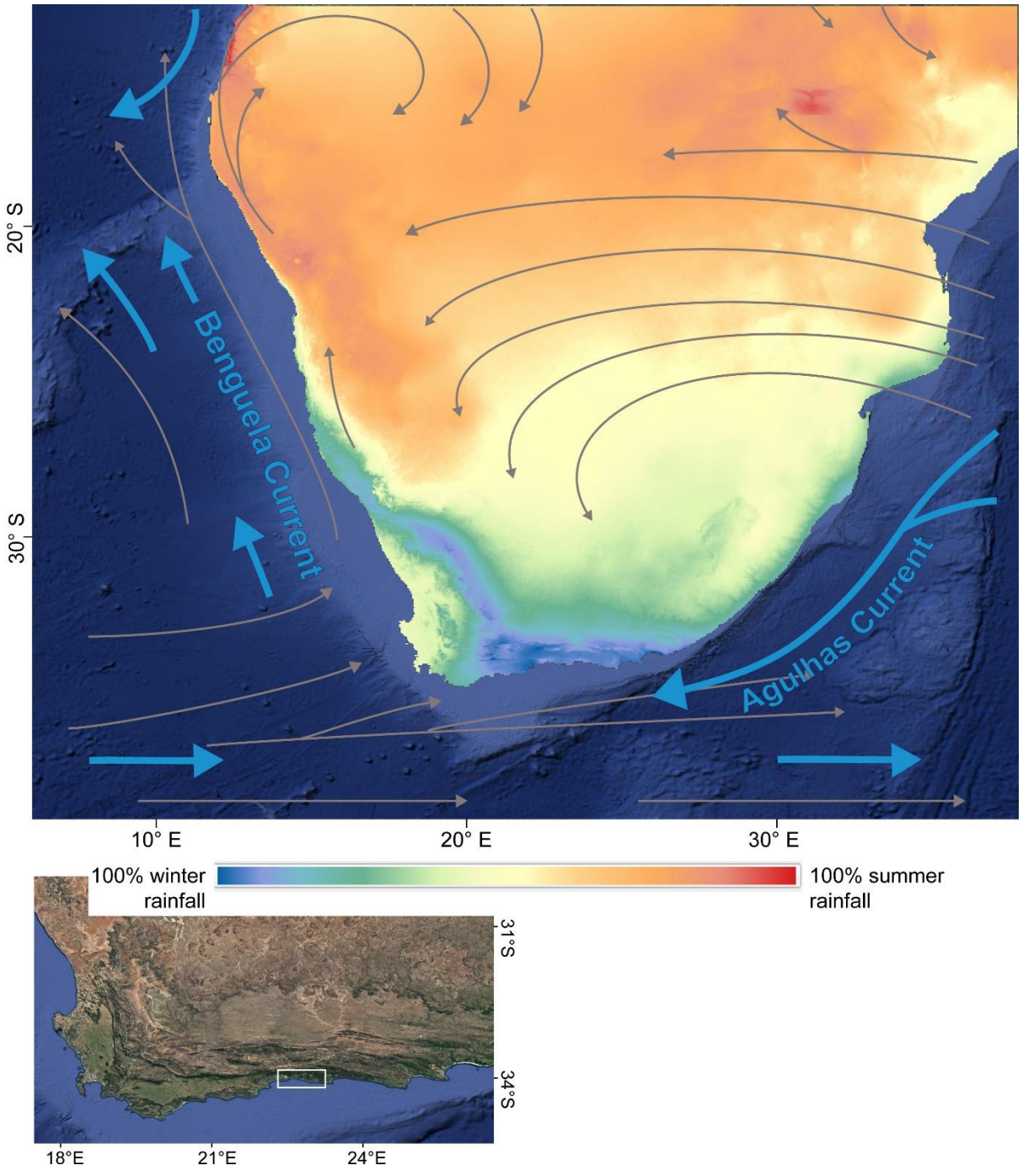

Figure 1-1: Map of southern Africa showing seasonality of rainfall and sharp climatic gradients dictated by the zones of summer/tropical (red) and winter/temperate (blue) rainfall dominance. Major atmospheric (grey arrows) and oceanic (blue arrows) circulation systems are indicated. The approximate location of the Wilderness Embayment is indicated by the white box in the inset.

1.3.2. Lakes of the Wilderness Embayment

The lakes within the Wilderness Embayment can essentially be divided into three units: the Wilderness Lakes system or complex, Swartvlei, and Groenvlei (Figure 1-2). Swartvlei is fed by the Karatara, Hoogekraal and Diep Rivers while the freshwater input to Groenvlei comes from seepage from the surrounding barrier dunes (Martin 1956; Russel et al. 2012). Three interconnected lakes define the Wilderness Lakes system - Eilandvlei, Bo Langvlei and Rondevlei. These are further connected to the Touw River and its estuary through the Serpentine channel (Russel et al. 2012).

Eilandvlei has a surface area of 1.48 km^2 (Watling 1977) and is largely fed by the Duiwe River (catchment size 42.1 km^2; Fijen and Kapp 1995) with its inflow along the north-eastern shore. Its name is derived from the island (island = eiland in Afrikaans) situated near the middle of the lake, presumed to be a remnant of the middle dune cordon (see section 1.3.3) separated through river and/or marine erosion (Martin 1962). Bo Langvlei (2.14 km^2; Watling 1977), the largest of the three lakes, mainly receives freshwater from Langvlei Spruit (catchment size 8.2 km^2; Fijen and Kapp, 1995), with occasional overflow from Rondevlei which is groundwater fed (Fijen and Kapp 1995). The narrow channel between Eilandvlei and Bo Langvlei is mostly obstructed by macrophytes but Bo Langvlei does periodically receive runoff from the Duiwe River via this connection.

The hydrodynamics of this lake system is complex, largely dependent on the state of the Touw River estuary mouth. The system typically drains in a westerly direction via the Serpentine Channel, the Touw River and ultimately the Touw River estuary, into the ocean (Watling 1977). The flow direction is however reversed at times, usually when the Touw River mouth is closed by a sandbar, resulting in the back ponding of discharge from the river back into the lakes (Martin 1962; Russel et al. 2010).

Vankervelsvlei lies further towards the east on the landward edge of the Wilderness Embayment (Illenberger 1996; Bateman et al. 2011), about 5 km inland of Groenvlei. It is situated on a fossilised aeolian dune at an elevation of ~150 mamsl (Illenberger 1996; Bateman et al. 2011). Today, Vankervelsvlei is a ~0.5 km^2 irregular shaped endorheic waterbody with no surface inflow or outlet

(Irving and Meadows 1997; Quick et al. 2016). It is covered with a floating vegetation mat primarily comprising of several Cyperaceae species, and some Bryophytes and Pteridophytes (Irving and Meadows 1997; Quick et al. 2016).

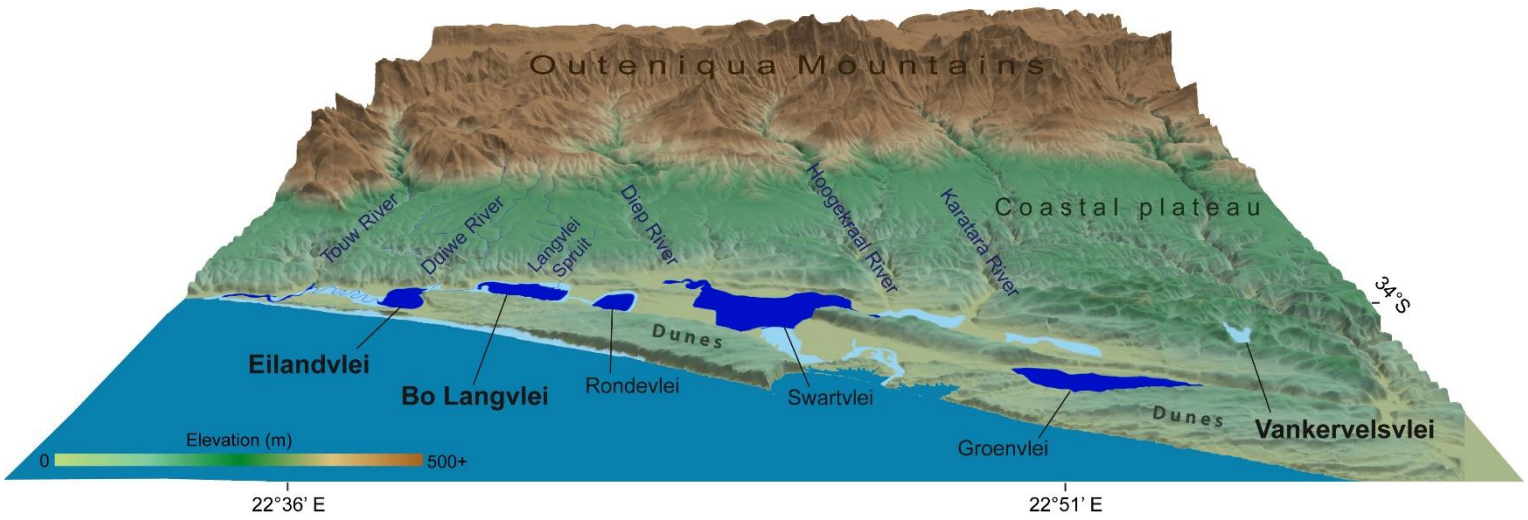

Figure 1-2: The Wilderness lakes region indicating the locations of Eilandvlei, Bo Langvlei and Vankervelsvlei, and the primary rivers feeding the Wilderness lakes.

1.3.3. Geology and geomorphology

The Wilderness region is characterised by three geomorphic units: the Outeniqua Mountains in the north, the coastal plateau and the coastal embayment (Figure 1-2). The Outeniqua Mountains are primarily composed of quartzites and sandstones of the Table Mountain Group with a maximum altitude of 1600 mamsl (Balfour and Bond 1993; Booth 2011). The coastal plateau represents the old sea floor of Tertiary origin, comprised of Table Mountain sandstones, pre-Cape granite and Kaaiman Group sediments (Bateman et al. 2011; Illenberger 1996; Marker and Holmes 2002; 2010; Martin 1962). The coastal embayment dates from the Pleistocene and predominantly consists of dune deposits forming the characteristic dune cordons (Bateman et al. 2011; Illenberger 1996; Martin 1962).

The dune ridges are characterised by three sets of sub-parallel cordons, identified as the landward, middle and seaward barriers (Bateman et al. 2004; 2011; Illenberger 1996). The landward barrier is the oldest, located towards the east extending up to 280 mamsl (Bateman et al. 2004; 2011;

Illenberger 1996). Vankervelsvlei lies within this dune field, estimated to be 205 – 250 ka old (Bateman 2011). The middle barrier ranges to a height of 210 mamsl, spanning the area between Bo Langvlei and the Goukamma River (Bateman et al. 2011; Illenberger 1996). The seaward cordon, the youngest of the barriers, borders the coast to the west in the region between Wilderness and Brenton-on-Sea (Bateman et al. 2011; Illenberger 1996). These dune cordons were formed during the Pleistocene interglacials with successive sea level highstands resulting in increased aeolian activity (Martin 1962; Illenberger 1996). Dune building phases are further attributed to prevailing westerly winds, the most recent of which occurred during the late Holocene between c. 3.7 and 2.4 ka and from c. 1.7 to 0.6 ka (Bateman et al. 2011).

1.3.4. Contemporary vegetation

Vegetation in the greater Wilderness region consists of a mosaic of fynbos and coastal thicket with pockets of Afrotemperate forest forming the most extensive forest complex in southern Africa (Cowling and Heijinis 2001; Geldenhuys 1993; Midgley et al. 2004) (Figure 1-3). Several factors control the distribution of these vegetation types, including climate, topography, edaphic conditions and fire (Cowling 1983; Geldenhuys 1991; Manders 1990; Mucina and Rutherford 2006; Quick et al. 2016). Fire, specifically, is a key component in maintaining fynbos-forest boundaries; in the absence of fire, fynbos becomes senescent and vulnerable to invasion especially by thicket and forest elements (Cowling 1992; Manders 1990; Manders and Richardson 1992; Midgley et al. 2004; Mucina and Rutherford 2006).

A variety of fynbos types occupy large parts of the region, varying from the coastline and surrounding dunes, across the coastal plains towards the mountains along the coastal plateau. The plateau is characterised by Garden Route Shale Fynbos comprising tall dense proteiod and ericaceous fynbos (Mucina and Rutherford 2006). Northward of the lakes, Knysna Sand Fynbos is present on the coastal plains, mainly represented by *Erica curvifolia*, *Metalasia densa* (Asteraceae) and *Passerina rigida* (Mucina and Rutherford 2006). The coastal dunes are occupied by Southern Cape Dune Fynbos,

primarily *Olea exasperate*, *Phylica litoralis* and a variety of *Searsia* species (Mucina and Rutherford 2006).

Towards the Outeniqua Mountains, patches of Southern Afrotemperate Forest are found in valleys and on the steep, south-facing slopes of the adjacent river catchments. Although the distribution of these forests is fragmented, it represents southern Africa's largest area of Southern Afrotemperate Forest, known as the Knysna Afrotemperate Region (KAR) (Geldenhuys 1993). The forests are dominated by *Podocarpus falcatus* (also now known as *Afrocarpus falcatus*) and *P. latifolius*, *Olea capenisis spp. Marcocarpa* (Oleaceae) and *Ocotea bullata* (Lauraceae) (Midgley et al. 2004; Mucina and Rutherford 2006).

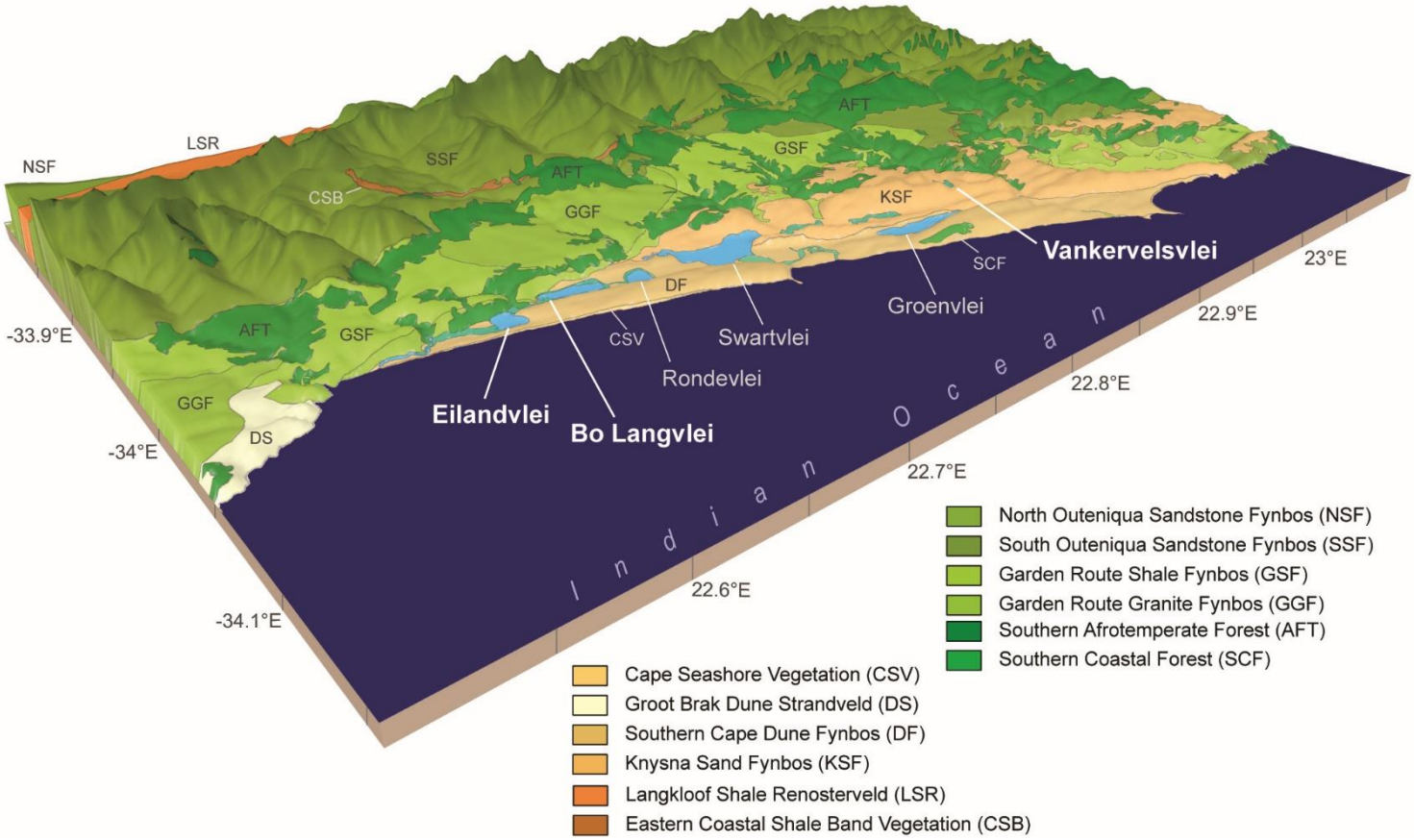

Figure 1-3: The current distribution of the dominant vegetation types in the Wilderness region (Mucina and Rutherford 2006).

Along the lake margins and interconnecting channels, semi-aquatic vegetation is represented by emergent macrophytes, the most common being *Phragmites australis*, generally found together with *Typha latifolia* and *Scirpus littoralis* (Allanson and Whitfield 1983; Russel et al. 2012). *Juncus kraussi* occupies an intermediate zone between semi-aquatic and terrestrial vegetation (Allanson and Whitfield 1983; Russel et al. 2012). Azonal vegetation, specifically along the estuaries is represented by halophytic taxa with *Sarcocornia capensis* and *S. pillansii* (Amaranthaceae), *Chenolea diffusa* (Amaranthaceae) and *Plantago crassifolia* the most prominent (Mucina and Rutherford 2006).

Other prominent taxa in the region include the very diverse Euphorbiaceae family, represented by amongst others *Andrachne ovalis*, *Lachnostylis hirta*, *Clutia spp* and *Euphorbia spp* in drier forest and scrub (Geldenhuys 1993; Von Breitenbach 1972). Asteraceae, also a highly diverse, cosmopolitan family, is, in addition to the genera mentioned above, characterised by especially *Stoebe alopecuroides*, *S. plumose* and *S. capitate* (Mucina and Rutherford 2006).

These natural vegetation types of the larger Wilderness region have been extensively modified, and in some cases even replaced, as a result of human activities, particularly since European colonisation in the 1770's. Today, agriculture and commercial forestry are the major land uses.

1.3.5. Colonisation and forestry: a short history

The rapid utilisation and exploitation of the indigenous forests started in the 1770's with the arrival of European settlers in the southern Cape (Geldenhuys 1991; Phillips 1931; van der Merwe 2009). After extensive exploration of the area, the government of the then Cape Colony established two woodcutter's post – the first at Hoogekraal, near George, in 1776 followed by the second at Plettenberg Bay in 1787 (Geldenhuys 1991; Phillips 1931; van der Merwe 2009). The increasing need for timber led forestry to become an important economic activity. Uncontrolled harvesting practices led to large scale forest destruction, prompting the government to close all forests in 1846 (Geldenhuys 1991; Phillips 1931; van der Merwe 2009). Regrettably, most of the forests were reopened again in 1856 due to a timber shortage; better forest management were however at least attempted with the implementation of a

cyclical harvesting system (Geldenhuys 1991; Phillips 1931; van der Merwe 2009; Von Breitenbach 1972).

After the Great Fire of 1869 ravaged the area, the need for markedly improved land management and conservation practices became abundantly clear (Von Breitenbach 1972). Subsequently, a *Conservator of Forests* was appointed in 1874, imposing additional restrictions on timber harvesting (Geldenhuys 1991; Phillips 1931; van der Merwe 2009). The further appointment of a French forestry officer as *Superintendent of Woods and Forests* in 1880 signalled the first significant progress in forest conservation, followed by the ratification of the Cape Forest Act in 1888 (Geldenhuys 1991; Phillips 1931; van der Merwe 2009). Exploitation of the forests persisted however driving the government to, again, close indigenous forests to all harvesting practices in 1939 (Geldenhuys 1991; Phillips 1931; van der Merwe 2009). In the words of Dr Von Breitenbach (1972, p 39), "What was left … was a battlefield of devastation. It seemed best to leave the healing of the worst wounds to nature". By the early 1960's, the forests have naturally recovered to such a point as to start the active rehabilitation process (Geldenhuys 1991; Von Breitenbach 1972). This led to the establishment of the Indigenous Forest Management Station (IFMS) at Saasveld in 1964 (Geldenhuys 1991; Phillips 1931; van der Merwe 2009). Following intensive research and planning, a multiple-use conservation management system was developed and implemented in 1967 with the reopening of the forests to the timber industry – under the strict control of the IFMS (Geldenhuys 1991; Phillips 1931; van der Merwe 2009; Von Breitenbach 1972).

1.4. Research questions

In order to provide a framework for the research presented here, the preceding sections provided an introduction to the temporal and geographic setting for this study, and an overview of the methodological approach to be undertaken.

In considering these, the following research questions are addressed in this thesis:

- What ecological, environmental and landscape changes have occurred in the Wilderness Embayment during the late Holocene? And what might be the underlying drivers and impacts of these?
- How has climate changed in the region during the late Holocene?
- How does the late Holocene environmental history of the Wilderness Embayment, as inferred from the records presented here, compare to local and regional palaeoenvironmental records, as well as with records from the winter- and summer rainfall zones?

1.5. Aim and objectives

The central aim of this study is to examine vegetation, climatic and landscape dynamics in the Wilderness Embayment during the late Holocene using a multi-proxy approach combining pollen, microscopic charcoal, geochemical and grain size analyses.

The specific objectives related to this aim are:

1. Retrieve sediment cores from the specified study sites within the Wilderness Embayment
2. Sub-sample the cores in order to obtain:
    2.1. High resolution chronologies through radiocarbon and ^{210}Pb dating
    2.2. Palynological records of long term vegetation change, and the associated charcoal records
    2.3. Sediment, elemental- and organic geochemical records to investigate the landscape evolution of the area

3. Assessment of these records in order to reconstruct late Holocene palaeoenvironmental conditions for the study sites
4. Evaluate these findings in the context of local, regional and appropriate broader palaeoenvironmental records

1.6. Thesis Structure

This thesis is presented as standalone chapters with the overarching thread of investigating late Holocene palaeoenvironments of the Wilderness Embayment:

- Chapter 2 presents the pollen and microcharcoal record from Bo Langvlei, exploring vegetation and climate change during the last ~1300 years.
- Bo Langvlei is also the focus of Chapter 3 where we go beyond pollen to understand the dynamics involved in the evolution of this waterbody on a more local scale using a complimentary set of geochemical and sedimentological records encompassing the late Holocene.
- A ~3000 year fossil pollen and microcharcoal record from Eilandvlei is presented in Chapter 4, illustrating the effects of external environmental dynamics on pollen accumulation, and the resultant records, as well as adding to the understanding of vegetation and climate change in the region.
- Chapter 5 provides a ~650 year fossil pollen and microcharcoal record from Vankervelsvlei - the first to cover this time period.
- Lastly, Chapter 6 presents a synthesis of the late Holocene palaeoenvironments of the Wilderness Embayment in which the key findings from this study are placed in context, and reflects on the aims and objectives of the study.

1.7. References

Allanson, B.R. & Whitfield, A.K., 1983. The Limnology of the Touw River Floodplain. *South African National Scientific Programmes Report No. 79*, p.41.

Andrén, E., Klimaschewski, A., Self, A., St Amour, N., Andreev, A., Bennett, K., Conley, D., Edwards, T., Solovieva, N. & Hammarlund, D., 2015. Holocene climate and environmental change in north-eastern Kamchatka (Russian Far East), inferred from a multi-proxy study of lake sediments. *Global and Planetary Change*, 134, pp.41–54.

Balfour, D.A. & Bond, W.J., 1993. Factors Limiting Climber Distribution and Abundance in a Southern African Forest. *Journal of Ecology*, 81(1), pp.93–100.

Bateman, M.D., Holmes, P.J., Carr, A.S., Horton, B.P. & Jaiswal, M.K., 2004. Aeolianite and barrier dune construction spanning the last two glacial–interglacial cycles from the southern Cape coast, South Africa. *Quaternary Science Reviews*, 23(14–15), pp.1681–1698.

Bateman, M.D., Carr, A.S., Dunajko, A.C., Holmes, P.J., Roberts, D.L., McLaren, S.J., Bryant, R.G., Marker, M.E. & Murray-Wallace, C.V., 2011. The evolution of coastal barrier systems: a case study of the Middle-Late Pleistocene Wilderness barriers, South Africa. *Quaternary Science Reviews*, 30(1–2), pp.63–81.

Birks, H.H. & Birks, H.J.B., 2006. Multi-proxy studies in palaeolimnology. *Vegetation History and Archaeobotany*, 15, pp.235–251.

Booth, P., 2011. Stratigraphic, structural and tectonic enigmas associated with the Cape Fold Belt: challenges for future research. *South African Journal of Geology*, 114, pp.235–248.

Von Breitenbach, F., 1972. Indigenous forests of the southern Cape. *Veld & Flora*, 58(1), pp.18–47.

Butzer, K.W. & Helgren, D., 1972. Late Cenozoic evolution of the Cape coast between Knysna and Cape St. Francis, South Africa. *Quaternary Research*, 2, pp.143–169.

Cawthra, H.C., Bateman, M.D., Carr, A.S., Compton, J.S. & Holmes, P.J., 2014. Understanding Late Quaternary change at the land-ocean interface: a synthesis of the evolution of the Wilderness coastline, South Africa. *Quaternary Science Reviews*, 99, pp.210–223.

Chase, B., Chevalier, M., Boom, A. & Carr, A., 2017. The dynamic relationship between temperate and tropical circulation systems across South Africa since the last glacial maximum. *Quaternary Science Reviews*, 174, pp.54–62.

Chase, B.M. & Meadows, M.E., 2007. Late Quaternary dynamics of southern Africa's winter rainfall zone. *Earth-Science Reviews*, 84(3–4), pp.103–138.

Chase, B.M. & Quick, L.J., 2018. Influence of Agulhas forcing of Holocene climate change in South

Africa's southern Cape. *Quaternary Research (United States)*, 90(2), pp.303–309.

Coetzee, J.A., 1967. Pollen analytical studies in East and Southern Africa. *Palaeoecology of Africa*, 3, p.146.

Cohen, A.L. & Tyson, P.D., 1995. Sea-surface temperature fluctuations during the Holocene off the south coast of Africa: implications for terrestrial climate and rainfall. *The Holocene*, 5(3), pp.304–312.

Cohen, K.M., Finney, S.C., Gibbard, P.L. & Fan, J.X., 2020. International Chronostratigraphic Chart.

Conedera, M., Tinner, W., Neff, C., Meurer, M., Dickens, A.F. & Krebs, P., 2009. Reconstructing past fire regimes: methods, applications, and relevance to fire management and conservation. *Quaternary Science Reviews*, 28(5–6), pp.555–576.

Cowling, R.M., 1983. Phytochorology and Vegetation History in the South-Eastern Cape, South Africa. *Journal of Biogeography*, 10(5), pp.393–419.

Cowling, R.M., 1992. *The Ecology of Fynbos: Nutrients, Fire and Diversity*, Cape Town: Oxford University Press.

Cowling, R.M. & Heijinis, C.E., 2001. The identification of broad habitat units as biodiversity entities for systematic conservation planning in the Cape Floristic Region. *South African Journal of Botany*, 67, pp.15–38.

Dellwig, O., Hinrichs, J., Hild, A. & Brumsack, H.J., 2000. Changing sedimentation in tidal flat sediments of the southern North Sea from the Holocene to the present: a geochemical approach. *Journal of Sea Research*, 44(4–3), pp.195–208.

Duffin, K.I. & Bunting, M.J., 2008. Relative pollen productivity and fall speed estimates for southern African savanna taxa. *Vegetation History and Archaeobotany*, 17(5), pp.507–525.

Engelbrecht, C.J., Landman, W.A., Engelbrecht, F.A. & Malherbe, J., 2015. A synoptic decomposition of rainfall over the Cape south coast of South Africa. *Climate Dynamics*, 44(9–10), pp.2589–2607.

Faegri, K. & Iversen, J., 1989. *Textbook of Pollen Analysis*, Chichester: John Wiley & Sons Ltd.

Fijen, A.P.M. & Kapp, J.F., 1995. Wilderness Lakes catchment, Touw and Duiwe Rivers, water management strategy. Volume 1: Present situation. , p.115.

Finch, J.M. & Hill, T.R., 2008. A late Quaternary pollen sequence from Mfabeni Peatland, South Africa: Reconstructing forest history in Maputaland. *Quaternary Research*, 70(3), pp.442–450.

Foster, I. & Walling, D.E., 1994. Using reservoir deposits to reconstruct changing sediment yields and sources in the catchment of the Old Mill Reservoir, South Devon, UK, over the past 50 years.

Hydrological Sciences Journal, 39(4), pp.347–368.

Gayantha, K., Routh, J. & Chandrajith, R., 2017. A multi-proxy reconstruction of the late Holocene climate evolution in Lake Bolgoda, Sri Lanka. *Palaeogeography, Palaeoclimatology, Palaeoecology*, 473, pp.16–25.

Geldenhuys, C.J., 1994. Bergwind fires and the location pattern of forest patches in the southern Cape landscape , South Africa. *Journal of Biogeography*, 21(1), pp.49–62.

Geldenhuys, C.J., 1991. Distribution, size and ownership of forest in the Southern Cape. *South African Forestry Journal*, 158, pp.51–66.

Geldenhuys, C.J., 1993. Floristic composition of the southern Cape forests with an annotated check-list. *South African Journal of Botany*, 59(1), pp.26–44.

Haberzettl, T., Fey, M., Lücke, A., Maidana, N., Mayr, C., Ohlendorf, C., Schäbitz, F., Schleser, G.H., Wille, M. & Zolitschka, B., 2005. Climatically induced lake level changes during the last two millennia as reflected in sediments of Laguna Potrok Aike, southern Patagonia (Santa Cruz, Argentina). *Journal of Paleolimnology*, 33, pp.283–302.

Haberzettl, T., Kirsten, K.L., Kasper, T., Franz, S., Reinwarth, B., Baade, J., Daut, G., Meadows, M.E., Su, Y. & Mäusbacher, R., 2019. Using 210Pb-data and paleomagnetic secular variations to date anthropogenic impact on a lake system in the Western Cape , South Africa. *Quaternary Geochronology*, 51(January), pp.53–63.

Hamilton, A.C., 1972. The interpretation of pollen diagrams from highland Uganda. *Palaeoecology of Africa*, 7, pp.45–149.

Hoffman, S., 1988. Lake sediment geochemistry. *Encyclopedia of Earth Science*.

Hunter, I.T., 1987. *The Weather of the Agulhas Bank and the Cape South Coast*. University of Cape Town.

Illenberger, W.K., 1996. The Geomorphological Evolution of the Wilderness Dune Cordons, South Africa. *Quaternary International*, 33, pp.11–20.

Irving, S.J.E. & Meadows, M.E., 1997. Radiocarbon Chronology and Organic Matter Accumulation at Vankervelsvlei, near Knysa, South Africa. *South African Geographical Journal*, 79(2), pp.101–105.

Jackson, S.T. & Kearsley, J.B., 1998. Quantitative Representation of Local Forest Composition in Forest-Floor Pollen Assemblages. *Journal of Ecology*, 86(3), pp.474–490.

Jackson, S.T. & Williams, J.W., 2004. Modern Analogs in Quaternary Paleoecology: Here Today, Gone Yesterday, Gone Tomorrow? *Annual Review of Earth and Planetary Sciences*, 32(1), pp.495–537.

Jones, P.D., Osborn, T.J. & Briffa, K.R., 2001. The evolution of climate over the last millennium. *Science*, 292(5517), pp.662–667.

Jury, M.R., Valentine, H.R. & Lutjeharms, J.R.E., 1993. Influence of the Agulhas Current on Summer Rainfall along the Southeast Coast of South Africa. *Journal of Applied Meteorology*, 32, pp.1282–1287.

Kasper, T., Haberzettl, T., Doberschütz, S., Daut, G., Wang, J., Zhu, L., Nowaczyk, N. & Mäusbacher, R., 2012. Indian Ocean Summer Monsoon (IOSM)-dynamics within the past 4 ka recorded in the sediments of Lake Nam Co, central Tibetan Plateau (China). *Quaternary Science Reviews*, 39, pp.73–85.

Kirsten, K.L., Haberzettl, T., Wündsch, M., Meschner, S., Smit, A.J., Quick, L.J. & Meadows, M.E., 2018. A multiproxy study of the ocean-atmospheric forcing and the impact of sea-level changes on the southern Cape coast, South Africa during the Holocene. *Palaeogeography, Palaeoclimatology, Palaeoecology*, 496, pp.282–291.

Kylander, M.E., Ampel, L., Wohlfarth, B. & Veres, D., 2011. High-resolution X-ray fluorescence core scanning analysis of Les Echets (France) sedimentary sequence: new insights from chemical proxies. *Journal of Quaternary Science*, 26(1), pp.109–117.

Last, W.M., 2001. Textural Analysis of Lake Sediments. In W. M. Last & J. P. Smol, eds. *Tracking Environmental Change Using Lake Sediments. Volume 2: Physical and Geochemical Methods*. Dodrecht: Kluwer Academic Publishers.

Lotter, A.F., Birks, H.J.B. & Zolitschka, B., 1995. Late-glacial pollen and diatom changes in response to two different environmental perturbations: volcanic eruption and Younger Dryas cooling. *Journal of Paleolimnology*, 14, pp.23–47.

Lowe, J.J. & Walker, M.J.C., 1997. *Reconstructing Quaternary Environments*, London: Longman.

Ma, L., Wu, J., Abuduwaili, J. & Liu, W., 2016. Geochemical Responses to Anthropogenic and Natural Influences in Ebinur Lake Sediments of Arid Northwest China L. Zhu, ed. *PLOS ONE*, 11(5).

MacDonald, G.M., Bennett, K.D., Jackson, S.T., Parducci, L., Smith, F.A., Smol, J.P. & Willis, K.J., 2008. Impacts of climate change on species, populations and communities: palaeobiogeographical insights and frontiers. *Progress in Physical Geography*, 32(2), pp.139–172.

MacDonald, G.M., Larsen, C.P.S., Szeicz, J.M. & Moser, K.A., 1991. The reconstruction of boreal forest fire history from lake sediments: a comparison of charcoal, pollen, sedimentological, and geochemical indices. *Quaternary Science Reviews*, 10, pp.53–71.

von Maltitz, G., Mucina, L., Geldenhuys, C.J., Lawes, M.J., Eeley, H.A.C., Adie, H., Vink, D., Fleming, G. & Bailey, C., 2003. *Classification system for South African indigenous forests: An objective classification for the Department of Water Affairs and Forestry*, Pretoria.

Manders, P.T., 1990. Fire and other variables as determinants of forest / fynbos boundaries in the Cape Province. *Journal of Vegetation Science*, 1(4), pp.483–490.

Manders, P.T. & Richardson, D.M., 1992. Colonization of Cape fynbos communities by forest species. *Forest Ecology and Management*, 48, pp.277–293.

Marker, M.E. & Holmes, P.J., 2002. The distribution and environmental implications of coversand deposits in the Southern Cape, South Africa. *South African Journal of Geology*, 105, pp.135–146.

Marker, M.E. & Holmes, P.J., 2010. The geomorphology of the Coastal Platform in the southern Cape. *South African Geographical Journal*, 92(2), pp.105–116.

Martin, A.R.H., 1962. Evidence relating to the Quaternary history of the Wilderness Lakes. *Transactions of the Geological Society of South Africa*, 65, pp.19–45.

Martin, A.R.H., 1968. Pollen Analysis of Groenvlei Lake Sediments, Knysna (South Africa). *Review of Palaeobotany and Palynology*, 7, pp.107–144.

Martin, A.R.H., 1956. The Ecology and History of Groenvlei. *South African Journal Of Science*, 52(8), pp.187–192.

Matthews, J.A. & Briffa, K.R., 2005. The ' Little Ice Age ': Re-Evaluation of an Evolving Concept. *Geografiska Annaler. Series A, Physical Geography*, 87(1), pp.17–36.

Mayewski, P.A., Rohling, E.E., Stager, J.C., Karlén, W., Maasch, K.A., Meeker, L.D., Meyerson, E.A., Gasse, F., van Kreveld, S., Holmgren, K., Lee-Thorp, J., Rosqvist, G., Rack, F., Staubwasser, M., Schneider, R.R. & Steig, E.J., 2004. Holocene Climate Variability. *Quaternary Research*, 62(3), pp.243–255.

Meadows, M.E., 2012. Quaternary environments : Going forward , looking backwards ? *Progress in Physical Geography*, 36(4), pp.539–547.

Meadows, M.E., 2001. The role of Quaternary environmental change in the evolution of landscapes: case studies from southern Africa. *Catena*, 42(1), pp.39–57.

Meadows, M.E. & Baxter, A.J., 2001. Holocene vegetation history and palaeoenvironments at Klaarfontein Springs, Western Cape, South Africa. *The Holocene*, 11(6), pp.699–706.

Meadows, M.E. & Sugden, J.M., 1991. The application of multiple discriminant analysis to the reconstruction of the vegetation history of Fynbos, southern Africa. *Grana*, 30, pp.325–336.

van der Merwe, I., 2009. *The Knysna and Tsitsikamma forests: Their history, ecology and management* Second. H. Sohnge, ed., Knysna: Tafelberg.

Meyers, P.A., 2003. Application of organic geochemistry to paleolimnological reconstruction: a summary of examples from the Laurention Great Lakes. *Organic Geochemistry*, 34(2), pp.261–289.

Meyers, P.A., 1994. Preservation of elemental and isotopic source identification of sedimentary organic matter. *Chemical Geology*, 114(3–4), pp.289–302.

Meyers, P.A. & Lallier-Vergès, E., 1999. Lacustrine sedimentary organic matter records of Late Quaternary paleoclimates. *Journal of Paleolimnology*, 21(3), pp.345–372.

Midgley, J.J., Cowling, R.M., Seydack, A.H.W. & van Wyk, G.F., 2004. Forest. In R. M. Cowling, D. M. Richardson, & S. M. Pierce, eds. *Vegetation of Southern Africa*. Cambridge: Cambridge University Press, Cambridge, UK, pp. 278–296.

Moberg, A., Sonechkin, D.M., Holmgren, K., Datsenko, N. & Karlén, W., 2005. Highly variable Northern Hemisphere temperatures reconstructed from low- and high-resolution proxy data. *Nature*, 433(10 February), pp.613–618.

Moore, P.D., Webb, J.A. & Collinson, M.E., 1991. *Pollen Analysis* 2nd ed., Oxford: Blackwell Scientific Publications.

Mucina, L. & Rutherford, M.C., 2006. *The vegetation of South Africa, Lesotho and Swaziland*, Pretoria: South African National Biodiveristy Institute, Sterlitzia.

Nash, D.J., Cort, G. De, Chase, B.M., Verschuren, D., Nicholson, S.E., Shanahan, T.M., Asrat, A., Anne-marie, L. & Grab, S.W., 2016. African hydroclimatic variability during the last 2000 years. *Quaternary Science Reviews*, 154, pp.1–22.

Neukom, R., Steiger, N., Gómez-Navarro, J.J.J.J., Wang, J. & Werner, J.P., 2019. No evidence for globally coherent warm and cold periods over the preindustrial Common Era. *Nature*, 571(7766), pp.550–554.

Neumann, F.H., Scott, L., Bousman, C.B. & van As, L., 2010. A Holocene sequence of vegetation change at Lake Eteza, coastal KwaZulu-Natal, South Africa. *Review of Palaeobotany and Palynology*, 162(1), pp.39–53.

Nicholson, S.E., Nash, D.J., Chase, B.M., Grab, S.., Shanahan, T.M., Verschuren, D., Asrat, A., Lezine, A.M. & Umer, M., 2013. Temperature variability over Africa during the last 2000 years. *The Holocene*, 23(8), pp.1085–1094.

Norström, E., Norén, G., Smittenberg, R.H., Massuanganhe, E.A. & Ekblom, A., 2018. Leaf wax δD inferring variable medieval hydroclimate and early initiation of Little Ice Age (LIA) dryness in

southern Mozambique. *Global and Planetary Change*, 170, pp.221–233.

Norström, E., Scott, L., Partridge, T.C., Risberg, J. & Holmgren, K., 2009. Reconstruction of environmental and climate changes at Braamhoek wetland, eastern escarpment South Africa, during the last 16,000 years with emphasis on the Pleistocene–Holocene transition. *Palaeogeography, Palaeoclimatology, Palaeoecology*, 271(3–4), pp.240–258.

PAGES2k, 2013. Continental-scale temperature variability during the past two millennia. *Nature Geoscience*, 6(5), pp.339–346.

Peel, M.C., Finlayson, B.L. & McMahon, T.A., 2007. Updated world map of the Köppen-Geiger climate classification. *Hydrology and Earth System Sciences*, 11, pp.1633–1644.

Phillips, J.F.V., 1931. Forest Succession and Ecology in the Knysna Region. *Botanical Survey South Africa, Memoirs*, 14, pp.99–104.

Quick, L.J., Chase, B.M., Wundsch, M., Kirsten, K.L., Chevalier, M., Mausbacher, R., Meadows, M.E. & Haberzettl, T., 2018. A high-resolution record of Holocene climate and vegetation dynamics from the southern Cape coast of South Africa : pollen and microcharcoal evidence from Eilandvlei. *Journal of Quaternary Science*, 33(5), pp.487–500.

Quick, L.J., Meadows, M.E., Bateman, M.D., Kirsten, K.L., Mäusbacher, R., Haberzettl, T. & Chase, B.M., 2016. Vegetation and climate dynamics during the last glacial period in the fynbos-afrotemperate forest ecotone, southern Cape, South Africa. *Quaternary International*, 404, pp.136–149.

Reinwarth, B., Franz, S., Baade, J., Haberzettl, T., Kasper, T., Daut, G., Helmschrot, J., Kirsten, K.L., Quick, L.J., Meadows, M.E. & Mäusbacher, R., 2013. A 700-year record on the effects of climate and human impact on the southern Cape coast inferred from lake sediments of Eilandvlei, Wilderness Embayment, South Africa. *Geografiska Annaler: Series A, Physical Geography*, 95(4), pp.345–360.

Russel, I.A., Randal, R.M., Cole, N., Kraaij, T. & Kruger, N., 2012. *Garden Route National Park, Wilderness Coastal Section, State of Knowledge*,

Russel, I.A., Randal, R.M., Cole, N., Kraaij, T. & Kruger, N., 2010. *Garden Route National Park, Wilderness Coastal Section, State of Knowledge*,

Schillereff, D.N., Chiverrell, R.C., Macdonald, N. & Hooke, J.M., 2014. Flood stratigraphies in lake sediments: A review. *Earth-Science Reviews*, 135, pp.17–37.

Strobel, P., Kasper, T., Frenzel, P., Schittek, K., Quick, L.J., Meadows, M.E., Mäusbacher, R. & Haberzettl, T., 2019. Late Quaternary palaeoenvironmental change in the year-round rainfall zone of South Africa derived from peat sediments from Vankervelsvlei. *Quaternary Science*

Reviews, 218, pp.200–214.

Tinner, W., Conedera, M., Ammann, B., Gaggeler, H.W., Gedye, S., Jones, R. & Sagesser, B., 1998. Pollen and charcoal in lake sediments compared with historically documented forest fires in southern Switzerland since AD 1920. *The Holocene*, 8(1), pp.31–42.

Tinner, W. & Hu, F.S., 2003. Size parameters, size-class distribution and area-number relationship of microscopic charcoal: relevance for fire reconstruction. *The Holocene*, 13(4), pp.499–505.

Traverse, A., 2008. *Paleopalynology* Second., The Netherlands: Springer.

Tyson, P.D., 1999. Late-Quaternary and Holocene palaeoclimates of southern Africa: A synthesis. *South African Journal of Geology*, 102(4), pp.335–349.

Tyson, P.D., Karlén, W. & Heiss, G.A., 2000. The Little Ice Age and medieval warming in South Africa. *South African Journal Of Science*, 96, pp.121–126.

Tyson, P.D. & Preston-Whyte, R.A., 2000. *The Weather and Climate of Southern Africa*, Cape Town: Oxford University Press.

Walker, M., Gibbard, P., Head, M.J., Berkelhammer, M., Björck, S., Cheng, H., Cwynar, L.C., Fisher, D., Gkinis, V., Long, A., Lowe, J., Newnham, R., Rasmussen, S.O. & Weiss, H., 2019. Formal Subdivision of the Holocene Series/Epoch: A Summary. *Journal of the Geological Society of India*, 93(2), pp.135–141.

Walker, M., Johnsen, S., Rasmussen, S.O., Steffensen, J., Popp, T., Gibbard, P., Hoek, W., Lowe, J., Andrews, J., Björck, S., Cwynar, L., Hughen, K., Kershaw, P., Kromer, B., Litt, T., Lowe, D.J., Nakagawa, T., Newnham, R.M. & Schwander, J., 2008. The Global Stratotype Section and Point (GSSP) for the base of the Holocene Series / Epoch (Quaternary System / Period) in the NGRIP ice core. *Episodes*, 31(2), pp.264–267.

Walker, M.J.C., Berkelhammer, M., Björck, S., Cwynar, L.C., Fisher, D.A., Long, A.J., Lowe, J.J., Newnham, R.M., Rasmussen, S.O. & Weiss, H., 2012. Formal subdivision of the Holocene Series/Epoch: a Discussion Paper by a Working Group of INTIMATE (Integration of ice-core, marine and terrestrial records) and the Subcommission on Quaternary Stratigraphy (International Commission on Stratigraphy). *Journal of Quaternary Science*, 27(7), pp.649–659.

Wanner, H., Beer, J., Bütikofer, J., Crowley, T.J., Cubasch, U., Flückiger, J., Goosse, H., Grosjean, M., Joos, F., Kaplan, J.O., Küttel, M., Müller, S.A., Prentice, I.C., Solomina, O., Stocker, T.F., Tarasov, P., Wagner, M. & Widmann, M., 2008. Mid- to Late Holocene climate change: an overview. *Quaternary Science Reviews*, 27(19–20), pp.1791–1828.

Watling, R., 1977. *Trace metal distribution in the Wilderness lakes. Special report FIS 147*, Pretoria.

Wohlfarth, B., Veres, D., Ampel, L., Lacourse, T., Blaauw, M., Preusser, F., Andrieu-Ponel, V.,

Kéravis, D., Lallier-Vergès, E., Björck, S., Davies, S.M., de Beaulieu, J.L., Risberg, J., Hormes, A., Kasper, H.U., Possnert, G., Reille, M., Thouveny, N. & Zander, A., 2008. Rapid ecosystem response to abrupt climate changes during the last glacial period in western Europe, 40-16 ka. *Geology*, 36(5), pp.407–410.

Wündsch, M., Haberzettl, T., Cawthra, H.C., Kirsten, K.L., Quick, L.J., Zabel, M., Frenzel, P., Hahn, A., Baade, J., Daut, G., Kasper, T., Meadows, M.E. & Mäusbacher, R., 2018. Holocene environmental change along the southern Cape coast of South Africa - Insights from the Eilandvlei sediment record spanning the last 8.9kyr. *Global and Planetary Change*, 163, pp.51–66.

Wündsch, M., Haberzettl, T., Kirsten, K.L., Kasper, T., Zabel, M., Dietze, E., Baade, J., Daut, G., Meschner, S., Meadows, M.E. & Mäusbacher, R., 2016a. Sea level and climate change at the southern Cape coast , South Africa , during the past 4.2 kyr. *Palaeogeography, Palaeoclimatology, Palaeoecology*, 446, pp.295–307.

Wündsch, M., Haberzettl, T., Meadows, M.E., Kirsten, K.L., Kasper, T., Baade, J., Daut, G., Stoner, J.S. & Mäusbacher, R., 2016b. The impact of changing reservoir effects on the 14C chronology of a Holocene sediment record from South Africa. *Quaternary Geochronology*, 36, pp.148–160.

Chapter 2

Vegetation and climate change during the Medieval Climate Anomaly and the Little Ice Age on the southern Cape coast of South Africa: pollen evidence from Bo Langvlei

N du Plessis[1]

BM Chase[1, 2]

LJ Quick[3]

T Haberzettl[4]

T Kasper[5]

ME Meadows[1, 6]

[1]*Department of Environmental and Geographical Science, University of Cape Town, Rondebosch, South Africa*

[2]*Institut des Sciences de l'Evolution-Montpellier (ISEM), University of Montpellier, Centre National de la Recherche Scientifique (CNRS), EPHE, IRD, Montpellier, France*

[3]*African Centre for Coastal Palaeoscience, Nelson Mandela University, Port Elizabeth, South Africa*

[4]*Physical Geography, Institute of Geography and Geology, University of Greifswald, Germany*

[5]*Physical Geography, Institute of Geography, Friedrich-Schiller-University Jena, Germany*

[6]*School of Geographic Sciences, East China Normal University, Shanghai, PR China*

Status: du Plessis, N., Chase, B.M., Quick, L.J., Haberzettl, T., Kasper, T. & Meadows, M.E., 2020. Vegetation and climate change during the Medieval Climate Anomaly and the Little Ice Age on the southern Cape coast of South Africa: Pollen evidence from Bo Langvlei. *The Holocene*, 30(12), pp. 1716-1727

2.1. Abstract

This chapter presents continuous, high resolution fossil pollen and microcharcoal records from Bo Langvlei, a lake in the Wilderness Embayment on South Africa's southern Cape coast. Spanning the past ~1300 years and encompassing the Medieval Climate Anomaly (MCA; c. AD 950 – 1250) and the Little Ice Age (LIA; c. AD 1300 – 1850), these records provide a rare southern African perspective on past temperature, moisture and vegetation change during these much debated periods of the recent geological past. Considered together with other records from the Wilderness Embayment, we conclude that conditions in the region during the MCA chronozone were – in the context of the last 1300 years – likely relatively dry (reduced levels of Afrotemperate forest pollen) and perhaps slightly cooler (increased percentages of *Stoebe*-type pollen) than present. The most significant phase of forest expansion, and more humid conditions, occurred during the transition between the MCA and the most prominent cooling phase of the LIA. The LIA is clearly identified at this locality as a period of cool, dry conditions between c. AD 1600 to c. AD 1850.

The mechanisms driving the changes observed in the Bo Langvlei pollen record appear to be generally linked to changes in temperature, and changes in the influence of tropical circulation systems. During warmer periods, moisture availability was higher at Bo Langvlei, and rainfall was perhaps less seasonal. During colder periods, precipitation resulting from tropical disturbances was more restricted, resulting in drier conditions. While increased precipitation has been reported during the LIA from Verlorenvlei in the Western Cape as a result of an equatorward displacement of the westerly storm-track at this time, the opposing response at Bo Langvlei suggests that any increased influence of westerlies was insufficient to compensate for the concurrent reduction in tropical/local rainfall in the region.

2.2. Introduction

To understand the nature and challenges of climate change in southern Africa it is important to establish an understanding of natural variability in the recent geological past. Two key periods characterize the climate since AD 650: the Medieval Climate Anomaly (MCA; c. AD 950 – 1250) and the Little Ice Age (LIA; c. AD 1300 – 1850) (Jones et al. 2001; Matthews and Briffa 2005). While recognized as not being robust features in proxy records from all regions of the globe (e.g. PAGES2k 2013; Neukom et al. 2019), the study of these periods provides an important context for modern and predicted future climate states.

It is well documented that the South African palaeoenvironmental record is relatively limited in terms of both the quantity and quality of records compared with the mid-latitudes of the Northern Hemisphere (see Chase & Meadows 2007), where the MCA and LIA have been defined. This is mainly due to the region's highly seasonal rainfall regimes and generally arid to semi-arid environments, which are not conducive to the preservation of sedimentary sequences and associated proxy records. Recent reviews by Nicholson et al. (2013), Nash et al. (2016) and Lüning et al. (2017, 2018) survey and synthesize the available data, but conclude that more records are still needed in order to resolve inconsistencies and account for the complexity of spatial and temporal variations.

Recent research initiatives on the southern Cape coast have been directed at addressing this knowledge gap, focusing on sea level, climate and vegetation dynamics during the Holocene (e.g. Haberzettl et al. 2019; Kirsten et al. 2018; Quick et al. 2018; Reinwarth et al. 2013; Strobel et al. 2019; Wündsch et al. 2016b; Wündsch et al. 2016a; Wündsch et al. 2018). The climate along the southern Cape coast is influenced by both tropical and temperate climate systems, and the region hosts a highly diverse vegetation including fynbos and thicket elements and includes the Knysna Afrotemperate Region – the most extensive forest complex in southern Africa (Geldenhuys 1993; Midgley et al. 2004). Studies of the available palaeoenvironmental records have concluded that regional climates have likely been highly dynamic over time (Chase and Meadows 2007), as the mechanisms controlling tropical and temperate systems have responded to changing global boundary conditions (Chase et al. 2017; Chase

and Quick 2018), and that these changes have significantly impacted the regional vegetation mosaic (Martin 1968; Quick et al. 2016; Quick et al. 2018). This apparently highly variable nature of the region's climate and vegetation suggests it is particularly sensitive to climate change, making it an ideal area to evaluate changes in these systems and how they interact over time.

To study vegetation and climate change on the southern Cape coast, we analysed a ~1300-year record of fossil pollen and microcharcoal from Bo Langvlei, one of several coastal lakes in the Wilderness Embayment (Figure 2-1). We present here the first record to come from the region that is sufficiently highly resolved to address questions relating to climate and vegetation change during the last 1000 years (and therefore encompassing the MCA and LIA), and it contributes to the expanding body of work defining a baseline for natural environmental variability along the southern Cape coast.

2.3. Regional setting

A notable feature of the southern Cape coast is the Wilderness Embayment, which includes a series of lakes separated from the coastline by shore parallel dune ridges of Pleistocene age (Bateman et al. 2011; Illenberger 1996) (Figure 2-1). The embayment is underlain by quartzites of the Table Mountain Group as well as Palaeozoic (Ordovician – Silurian) Peninsula Formation sandstones (Bateman et al. 2011; Marker and Holmes 2002; Marker and Holmes 2010).

Today the largest of the three lakes of the Wilderness Lakes system, Bo Langvlei (2.14 km^2; Watling 1977) is connected by a short channel to Rondevlei to the East, and Eilandvlei to the West. Langvlei Spruit, with a catchment size of 8.2 km^2 (Fijen and Kapp 1995), is the main source of freshwater to Bo Langvlei. Additional contributions are received through occasional overflow from Rondevlei and groundwater from non-lithified sandy sediments that border and underlie parts of the Wilderness Embayment (Fijen and Kapp 1995).

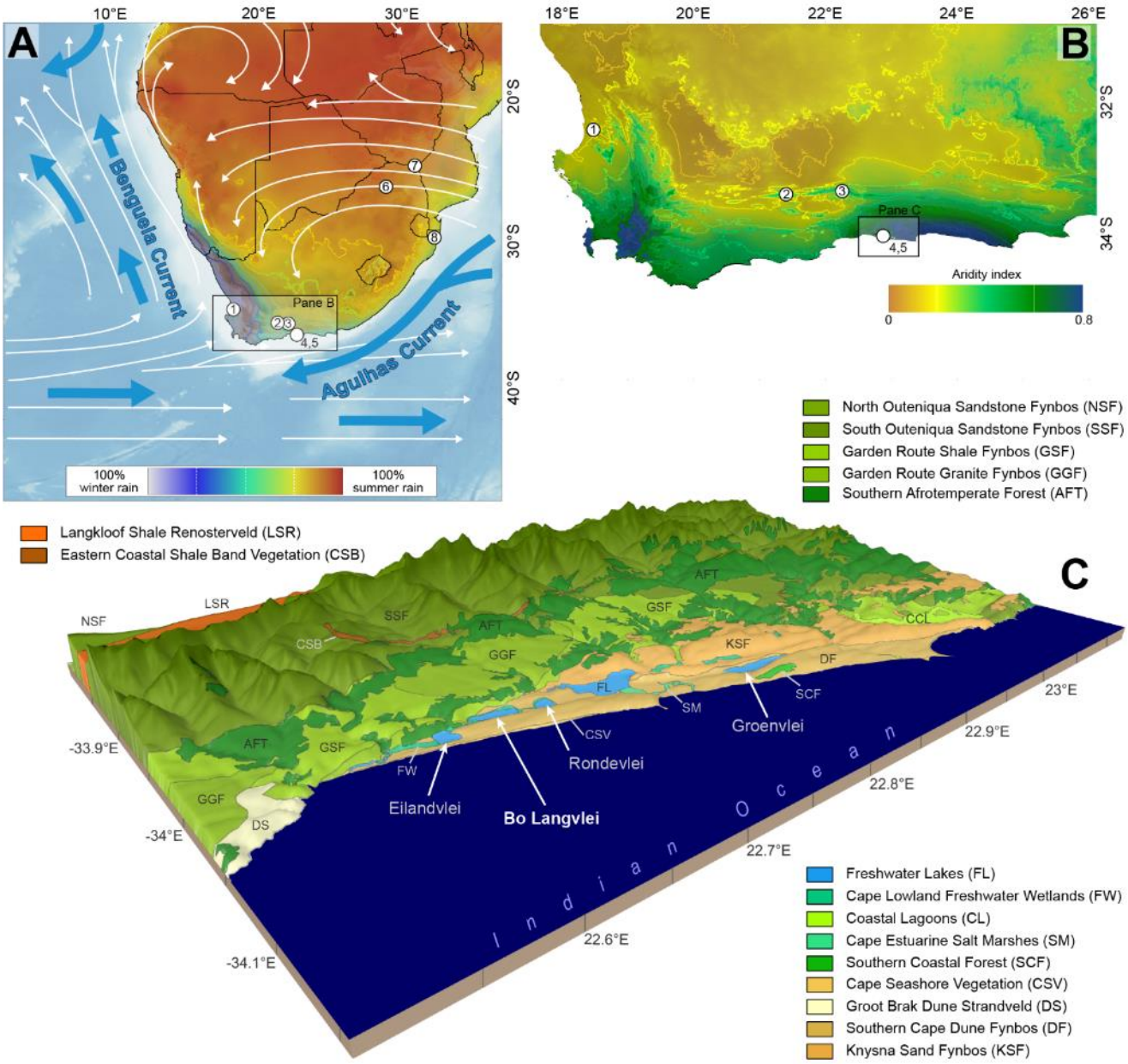

Figure 2-1: A. Map of southern Africa showing seasonality of rainfall and sharp climatic gradients dictated by the zones of summer/tropical (red) and winter/temperate (blue) rainfall dominance. Major atmospheric (white arrows) and oceanic (blue arrows) circulation systems are indicated. Locations of palaeoenvironmental records discussed in this chapter are numbered: 1; Verlorenvlei (Stager et al. 2012), 2; Seweweekspoort (Chase et al. 2013; Chase et al. 2017), 3; Cango Cave (Talma and Vogel 1992), 4; Groenvlei (Martin 1968; Wündsch et al. 2016a) 5; Bo Langvlei (this chapter), 6; Cold Air Cave (Holmgren et al. 1999; Holmgren et al. 2003; Lee-Thorp et al. 2001; Sundqvist et al. 2013), 7; Pafuri (Woodborne et al. 2015) and 8; Lake Sibaya (Neumann et al. 2008; Stager et al. 2013). **B.** Aridity index map of the southwestern Cape (black box in A). Locations of palaeoenvironmental records are numbered as in A. **C.** The Wilderness lakes region, indicating the location of Bo Langvlei and the current distribution of dominant vegetation types (Mucina and Rutherford 2006).

2.3.1. Climate

Located in the modern year round, or aseasonal, rainfall zone (YRZ/ARZ) (*sensu* Chase and Meadows 2007), the contemporary climate of the Wilderness region can be described as temperate oceanic ("Cfb"; Peel et al. 2007) with 800 to 1000 mm of mean annual rainfall distributed largely uniformly throughout the year (Allanson and Whitfield 1983; Russel et al. 2012). Winter rainfall along the coast is brought about by frontal depressions embedded in the mid-latitude westerlies, with ridging anticyclones and cut off lows responsible for the majority of the rainfall events (Engelbrecht et al. 2015; Engelbrecht and Landman 2016; Tyson and Preston-Whyte 2000). Summer rainfall results from the association of warmer sea surface temperatures in the Indian Ocean and enhanced easterly flow, as well as tropical-temperate trough cloud bands (Engelbrecht et al. 2015; Tyson and Preston-Whyte 2000). The Agulhas Current also has a major influence on local climatic conditions along the coast, as its warm waters provide a source of moisture, generating increased humidity (Jury et al. 1993).

2.3.2. Contemporary vegetation

Vegetation in the Wilderness region consists of a mosaic of fynbos and thicket elements with pockets of Knysna Afrotemperate forest also present (Cowling and Heijinis 2001). In the immediate vicinity of the lakes, including the interconnecting channels, semi-aquatic vegetation is represented by bulrushes (*Typha latifolia*), reeds (*Phragmites australis*) and sedges (*Scirpus littoralis*) (Allanson and Whitfield 1983; Russel et al. 2012). The area inundated during extremely high water levels represents an intermediate zone between the semi-aquatic and terrestrial environments and is occupied by rushes such as *Juncus kraussi* (Allanson and Whitfield 1983; Russel et al. 2012). Azonal vegetation specifically along the estuaries is represented by halophytic taxa with *Sarcocornia capensis* and *S. pillansii* (Amaranthaceae), *Chenolea diffusa* (Amaranthaceae) and *Plantago crassifolia* being most prominent (Mucina and Rutherford 2006; Quick et al. 2018).

North of the lakes, the coastal plains are occupied by Knysna Sand Fynbos which is characterised by dense, moderately tall micropyllous shrublands (predominantly *Erica curvifolia*,

Metalasia densa (Asteraceae) and *Passerina rigida* (Mucina and Rutherford 2006; Quick et al. 2018). Southern Cape Dune Fynbos (mainly *Olea exasperata*, *Phylica litoralis* and a variety of *Searsia* species) is found on the seaward barrier dune, as termed by Illenberger (1996), separating Bo Langvlei from the coastline (Mucina and Rutherford 2006; Quick et al. 2018). Patches of Southern Afrotemperate Forest are typically found on the south-facing slopes of the adjacent river catchments and valleys, generally comprising *Afrocarpus falcatus* and *Podocarpus latifolius* (in the pollen record we cannot differentiate between these species, as such these are all labelled *Podocarpus* for the purpose of this chapter), *Ocotea bullata* (Lauraceae) and *Olea capensis ssp. marcocarpa* (Oleaceae) (Midgley et al. 2004; Quick et al. 2018). Garden Route Shale Fynbos occupies the boundary between Afrotemperate forest and fynbos, it is dispersed along the coastal plateau and defined by ericaceous and tall dense proteoid fynbos (Mucina and Rutherford 2006; Quick et al. 2018).

2.4. Material and Methods

2.4.1. Core extraction and sampling

Coring was undertaken at Bo Langvlei during October 2013 as part of the first fieldwork campaign for the RAiN project (Haberzettl et al. 2014). The core, BoLa 13.2 (33°59'12.54''S, 22°40'44.46''E), was retrieved using a modified ETH-gravity corer (Kelts et al. 1986), and measures 178.5 cm in length. BoLa 13.2 was opened at the Institute of Geography at Friedrich Schiller University Jena, Germany where it was photographed, lithologically described and sampled. The core was continuously sub-sampled in a closed laboratory setting at a resolution of 1 cm for both pollen and microcharcoal analysis.

2.4.2. Chronology

The BoLa 13.2 age-depth model was established using both ^{210}Pb and ^{14}C ages (Table 2-1, 2-2). 24 bulk samples from the top 12 cm of the core (at 0.5 cm intervals) were sent to the Radiochronology Laboratory (Centre for Northern Studies, Laval University, Quebec, Canada) for ^{210}Pb-dating. For AMS-^{14}C dating, five organic sediment samples were sent to Beta Analytic Inc. (Miami, Florida, USA).

Table 2-1: Radiocarbon ages and calibration details. Ages are presented as both cal BP and AD where relevant.

Lab code Beta -	Depth (cm)	Conventional ^{14}C age [BP]	1σ error	Calibration data	ΔR	2σ cal age range [cal BP/AD]	Median probability [cal BP]	Age [AD]
369745	0	(105.5 ± 0.3 pMC)	-	-	-	-	-	2013 (year of coring)
369746	45.5	660	30	SHCal13	-	670-630 cal BP 1280-1320 AD 600-650 cal BP 1350-1390 AD	660	1290
369748	98.5	1790	30	Marine13	148 ± 27	1820-1690 cal BP 130-260 AD 1670-1620 cal BP 280-330 AD	1710	240
369749	137.5	3470	30	Marine13	148 ± 27	3830 - 3680 cal BP 3660 – 3640 cal BP	3720	-
369744	178.5	4270	30	Marine13	148 ± 27	4860 – 4830 cal BP	4840	-

The ^{14}C age for the sample at 45.5 cm was calibrated using the SHcal13 curve (Hogg et al. 2013) as the radiocarbon content of the uppermost sample showed 105.5±0.3 pMC indicating the absence of a reservoir effect in the lacustrine facies of the sediment. The Marine13 data set (Reimer et al. 2013) was applied for the samples at 98.5 cm, 137.5 cm and 178.5 cm, respectively as the lithology indicated that sediment in these depths is of marine origin. A marine reservoir correction of ΔR = 148 ± 27 was applied here in reference to recent studies by Wündsch et al. (2016a) and Haberzettl et al. (2019). The CRS (constant rate of ^{210}Pb supply) model (Appleby and Oldfield 1978; Appleby 2008) was applied to the ^{210}Pb results to obtain the ages. The age-depth model was subsequently developed using the R software package Bacon (v2.2) (Blaauw and Christen 2011).

Table 2-2: ^{210}Pb data and age estimates

Depth (cm)	^{210}Pb activity (Bq g^{-1}) unsupported	CRS	Age (AD)
0.5	0.129462675	8.45713091	2005
1	0.089934642	9.27115037	2004
1.5	0.11267076	9.93547901	2003
2	0.113936	10.9153558	2002
2.5	0.088817176	12.1245561	2001
3	0.072538177	13.2705585	2000
3.5	0.053182181	14.3806752	1999
4	0.058556788	15.320281	1998
4.5	0.037472791	16.507877	1996
5	0.055113512	17.3695226	1996
5.5	0.087106133	18.8138195	1994
6	0.072051752	21.6604169	1991
6.5	0.071103802	24.7591211	1988
7	0.045781601	28.8291055	1984
7.5	0.054150798	32.2416027	1981
8	0.054310576	37.4906148	1976
8.5	0.021339275	44.8067948	1968
9	0.017892135	48.527683	1964
9.5	0.035545938	52.1594525	1961
10	0.013712608	61.2690128	1952
10.5	0.031668121	65.6951819	1947
11	0.05203818	78.8502255	1934
11.5	0.039863802	117.519829	1895
12	0.066245955	188.237915	1825

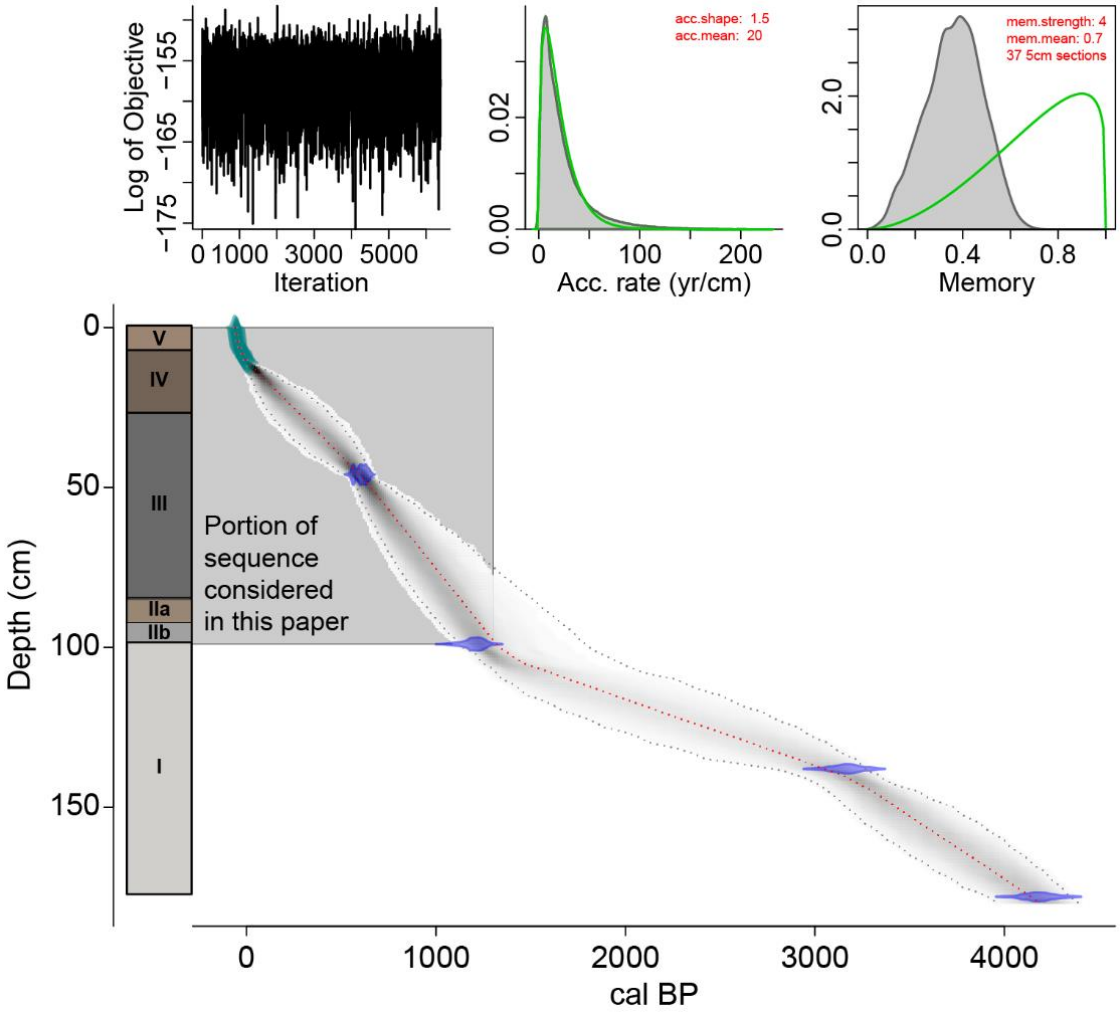

Figure 2-2: The BoLa 13.2 lithology and age-depth model. The age-depth model was developed using the R software package Bacon (V2.2) (Blaauw and Christen 2011). The 2σ probability distribution of calibrated ^{14}C ages is presented in blue and the 95% confidence intervals are represented by the grey dotted line. ^{210}Pb ages are represented by the turquoise area and the red line represents the best model according to the weighted mean age at each depth. BoLa 13.2 is divided into four lithological units. Unit I (178 – 100 cm) predominantly consists of silty sand and is characterized by an abundance of marine shell fragments. A gradual coarsening of sediment is observed in Unit II-a (100 – 94 cm), changing to finer silty clay in Unit II-b (94 – 86 cm). Marine shell fragments appear less frequently upwards of 94 cm. Unit III (86 – 27 cm) is mainly composed of clayey silt. Units IV (27 – 6 cm) and V (6 – 0 cm) consists of the similar fine-grained sediment as Unit III. Unit IV is characterized by the presence of filamentous plant material, while marine shell fragments are present again in Unit V.

2.4.3. Pollen and microcharcoal analyses

In total, 84 samples were processed for pollen and microscopic charcoal analyses. Samples from the basal 78.5 cm of the core yielded insufficient pollen concentrations for analysis. Standard palynological methods were employed as per Faegri & Iversen (1989) and Moore et al. (1991) with particular adaptations for dense media separation (Nakagawa et al. 1998) in order to extract palynomorphs. These adaptations included the removal of carbonates and humic acids using 30% HCl and 10% KOH, respectively. This was followed by heavy liquid separation, through the use of $ZnCl_2$, in order to separate pollen grains from the non-pollen matrix (Faegri and Iversen 1989; Moore et al. 1991; Nakagawa et al. 1998). Acetolysis was further applied to remove any cellulose and/or organic matter still present in the sample, after which the samples were mounted on slides using the aqueous mounting agent Aquatex. Three slides were produced per sample and 0.5 ml of LacCore's polystaene microsphere pollen spike was added to each sample to determine pollen concentrations and absolute counts.

Counts of 300 pollen grains (Birks and Birks 1980) were performed using a Zeiss Axiostar Plus microscope with magnifications from 400x to 1000x. Three samples exhibited lower pollen concentrations, and from these only 222 (AD 1965), 280 (AD 740) and 299 (AD 760) grains were observed. To aid in identification, the pollen reference collection from the Environmental and Geographical Science department at the University of Cape Town was used, as was reference material from Van Zinderen Bakker (1953, 1976), Van Zinderen Bakker and Coetzee (1959), Welman and Kuhn, (1970) and Scott (1982). The counting process was aided by the use of the software program Polycounter, version 2.5.3 (Nakagawa 2007).

Charcoal particles were counted in conjunction with pollen grains. Particle number was recorded according to the guidelines of Tinner & Hu (2003) with only black, opaque and angular fragments >75 μm^2, or ~10 µm in length, being counted. These fragments were classified into two groups according to size: 10 – 100 µm and >100 µm (Tinner and Hu 2003). Charcoal concentrations were calculated using the microsphere spike, as with the pollen concentrations.

The results obtained through pollen and charcoal analysis are presented using the software package Tilia (version 1.7.16) (Grimm 2011). Zonation of the diagrams was achieved using the CONISS (Constrained Incremental Sum of Squares) module of the same software using stratigraphically constrained analysis and square root transformation of the data (Grimm 1987).

2.4.4. TRaCE21ka climate model

To compare our results with general circulation model simulations, we use data from the TRaCE21ka experiment (He et al. 2013; Liu et al. 2009; Otto-Bliesner et al. 2014). TRaCE21ka used the Community Climate System Model ver. 3; (Collins 2006) a global coupled atmosphere – ocean – sea ice – land general circulation model that has a latitude – longitude resolution of ~3.75° in the atmosphere and ~3° in the ocean and includes a dynamic global vegetation module. The simulation includes transient orbitally forced insolation changes and changes in the atmospheric concentrations of carbon dioxide, methane and nitrous oxide, as well as the evolution of ice sheets and their meltwater contributions to the ocean. The climate data have been regridded using bilinear interpolation to a spatial resolution of 2.5° x 2.5° (latitude/longitude) (Fordham et al. 2017).

2.5. Results

2.5.1. Chronology

The ^{14}C ages (Table 2-1) indicate that BoLa13.2 has a basal age of 4140 $^{+185}/_{-220}$ cal BP (Figure 2-2). The results from the CRS-model of ^{210}Pb activity (Table 2-2) provide ages for the top 12 cm of the core ranging from AD 1825 to present. The age-depth model suggests continuous deposition and an average sedimentation rate of 0.07 cm y^{-1}.

2.5.2. Pollen and microcharcoal analyses

Due to the sandy nature of the sediment in Unit I, as well as the presence of marine shells, it was inferred that this unit represents marine conditions within the lake. Accordingly, it is suggested that this marine environment was not conducive to the preservation of organic matter hence the inadequate pollen preservation below 100 cm. As such, the pollen record encompasses the time period from AD 680 $^{+530}/_{-110}$ to present.

The BoLa13.2 pollen assemblage are summarized by ecological affinity based on the primary vegetation types present in the region today, of which the main contributor is the fynbos vegetation group, with Ericaceae, Restionaceae and *Stoebe*-type pollen being most prevalent. Succulent and/or drought resistant taxa are mainly represented by *Euphorbia* with lesser contributions from Aizoaceae and *Crassula*, while *Olea* is the main constituent of the coastal thicket group. *Podocarpus* dominates the Afrotemperate forest group with the other taxa in this group making negligible contributions. Cyperaceae, Juncaceae and *Typha* were deemed to form part of the local wetland taxa, and Amaranthaceae is also included in this group as it is an indicator of salt marsh conditions. These local wetland taxa were excluded from the total pollen sum. From the cluster analysis results, the pollen and charcoal diagrams were divided into six pollen assemblage zones – BoLa13.2-A to BoLa13.2-F.

Zone BoLa13.2-A represents the oldest part of the pollen sequence, c. AD 650 to 750. As for much of the record, fynbos taxa dominate this zone, exhibiting increasing percentages towards the top of the zone, with a concomitant peak in the charcoal concentration. Relative to mean values for the whole of the record, succulent/drought resistant taxa are more prevalent in this zone, most notably *Euphorbia*. Coastal thicket is present throughout this period, since taxa from this group are relatively abundant. Afrotemperate forest (predominantly *Podocarpus*) pollen is relatively low during this period.

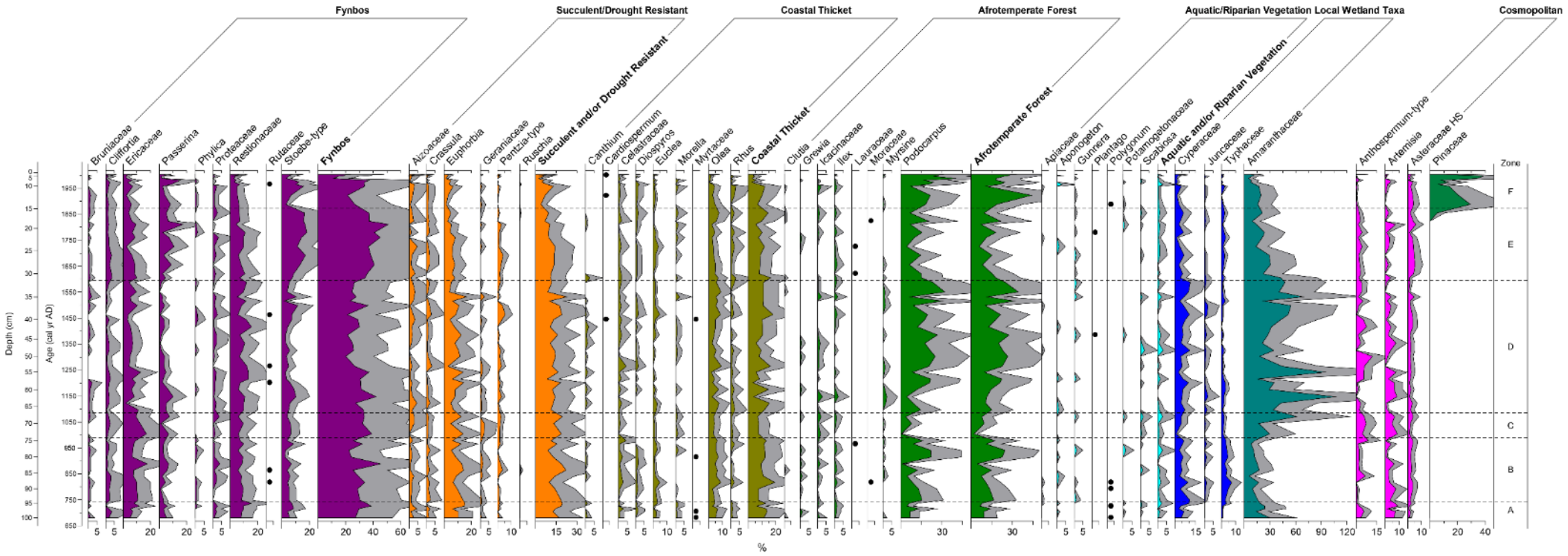

Figure 2-3: Relative pollen percentage diagram for BoLa13.2 organized according to ecological affinity. Pollen taxa occurring at less than 1% are shown only as presence points. Exaggeration curves are 4x for taxa present between 5 and 2% and 2x for those above 5%. Zonation of the diagram is based on cluster analysis results from CONISS.

Both the succulent/drought resistant and coastal thicket groups reach maximum levels in zone BoLa13.2-B (c. AD 750 to 1000). A prominent increase in coastal thicket (*Olea*, *Euclea* and Celastraceae) is noted ~AD 820 after which values remain consistently elevated throughout the rest of the zone. Afrotemperate forest pollen is notably more abundant during this period. There is, however, a sharp decline ~AD 900, a point where the fynbos elements Ericaceae and *Passerina* reach maximum percentages. Additionally, (non-local) aquatic vegetation is completely absent, while the pollen concentration is at a minimum (1.4 x 10^3 grains g^{-1}). Towards the end of the zone, a marked peak in charcoal concentration is evident ~AD 980 along with slightly elevated values noted for fynbos (mostly *Stoebe*-type) and *Euphorbia*.

BoLa13.2-C (c. AD 1000 to 1100) is the shortest of the pollen assemblage zones, including only three samples. *Podocarpus* is present at a minimum ~AD 1000, with *Icacinaceae* the only other forest element present here. Simultaneously, Ericaceae representation is notably elevated (17%) and *Cyperaceae*, representing local wetland vegetation, occurs minimally. At the top of the zone significantly higher levels of Amaranthaceae are noted, accompanied by increased representation of the fynbos elements *Passerina* and *Protea*. Coastal thicket is present at lower values than in the previous zones while succulent/drought resistant taxa remain present at higher levels throughout the zone.

The longest of the pollen assemblage zones, BoLa13.2-D (c. AD 1100 to 1600), is dominated by the halophytic element Amaranthaceae which achieves maximum values ~AD 1150. The fynbos taxa *Passerina* and *Stoebe*-type exhibit relatively high percentages at the beginning of the period, and then decline between ~AD 1230 and AD 1410. The inverse of this pattern is observed in *Podocarpus*, which increases from the beginning of the period, and maintains high levels until ~AD 1550. Succulent/drought resistant taxa remain generally constant throughout the zone. Towards the top of the zone, ~AD 1550, both pollen- (13.89 x 10^3 grains g^{-1}) and charcoal (5.27 x 10^4 fragments g^{-1}) concentrations are at their highest.

The beginning of zone BoLa13.2-E (c. AD 1600 to 1900) is marked by a sharp decline in both Amaranthaceae and *Podocarpus*, and an increase in fynbos taxa, particularly *Stoebe*-type. This latter remains abundant throughout the zone, reaching maximum representation ~AD 1800. Charcoal

concentrations are close to their lowest values at this point. Pinaceae also appears for the first time towards the top of the zone, ~AD 1850. *Podocarpus* percentages are variable but notably lower than in zone BoLa13.2-D. Succulent/drought resistant taxa show a similar, but subtler pattern, declining after ~AD 1750 towards the top of the zone.

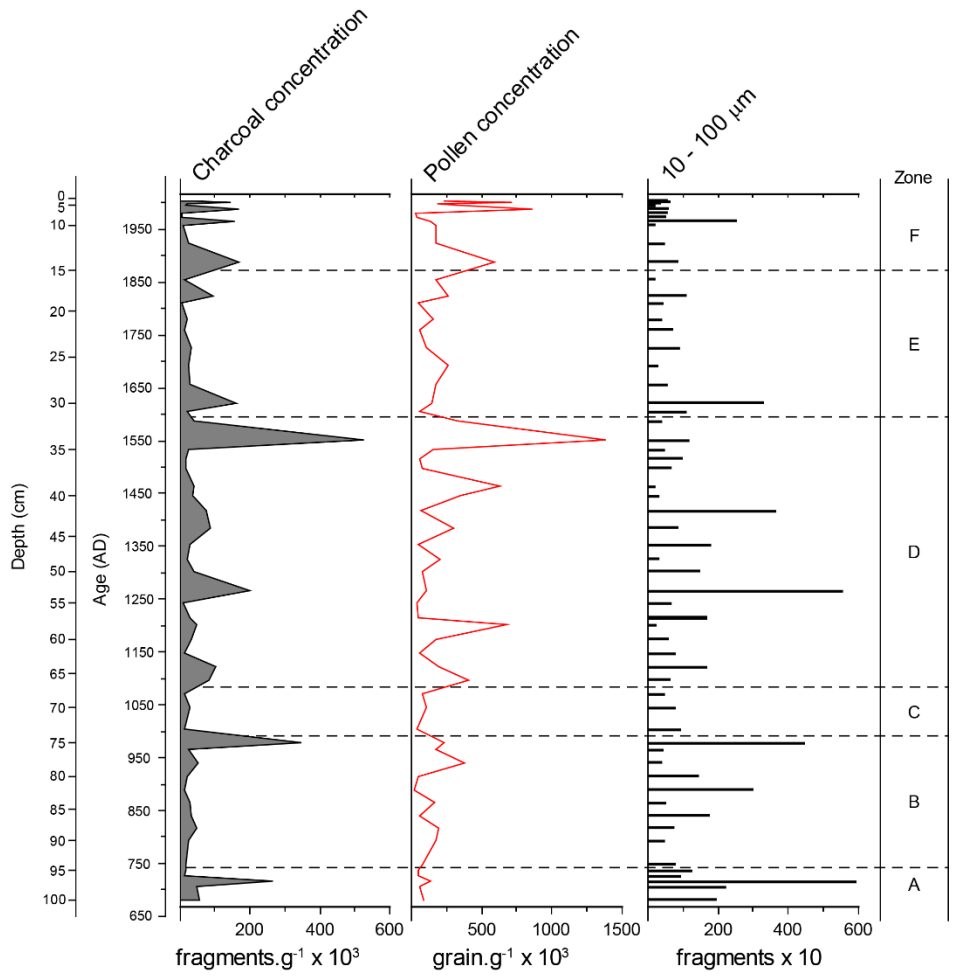

Figure 2-4: Charcoal and pollen concentrations for BoLa13.2. Only charcoal fragments smaller than 100 µm were present. Charcoal and pollen concentrations were calculated in the same manner using microsphere counts. The zonation of the diagram is the same as for the pollen diagram.

Zone BoLa13.2-F represents the top of the core, extending from ~AD 1900 to the top of the record. Fynbos generally declines across this zone apart from a peak between ~AD 1950 and 1980. Both coastal thicket and succulent/drought resistant taxa follow a similar pattern in this zone with percentages increasing until ~AD 1960, after which both decline. *Podocarpus* continues to exhibit an inverse relationship to *Stoebe*-type pollen during this period, with a peak ~AD 1920, a sharp decline ~AD 1960, followed by a period of increasing values until ~AD 1990, when it reaches its highest levels. Charcoal concentrations are at their lowest for the whole assemblage at this point.

2.6. Discussion

Climate and environmental change during the last ~1300 years at Bo Langvlei

Despite the diversity of vegetation types present in the Wilderness Embayment region, and observed in the Bo Langvlei record, there are several primary patterns in the fossil record that can be used to infer past environmental changes. Foremost among these is the variability observed in the 1) Afrotemperate forest pollen record (dominated by *Podocarpus*) and 2) *Stoebe*-type pollen, which is one of the most prevalent fynbos taxa. Afrotemperate forests, and *Podocarpus* in particular, are sensitive to drought, and in the fossil record related pollen types have been shown to be valuable indicators of aridity/humidity in the region (e.g. Quick et al. 2018) (with aridity/humidity being distinct from rainfall amount per se [see Chevalier & Chase 2016]). *Stoebe*-type pollen is most clearly associated with cooler temperatures, making it an important indicator of past temperature change at many sites in South Africa (Scott 1982; Scott et al. 2012; Quick et al. 2016). Considering these elements of the pollen record, it is possible to infer general changes in – and relationships between - moisture and temperature at Bo Langvlei.

In this chapter, we limit the contextualization of these results to records within the southern Cape, and select keystone records from more distant regions that can be used to infer mechanistic relationships with southern Cape climates. This selection was made on the basis of a record's resolution, age control, and the extent to which the proxy can be reasonably interpreted in terms of changes in

temperature and/or hydroclimate. Other records spanning the last 1300 years do exist in southern Africa (e.g. Norström et al., 2018; Scott, 1996; Stager et al., 2013), but we defer detailed inter-regional consideration of these records for a fuller synthetic study.

From c. AD 650 to 900 the landscape around Bo Langvlei was generally characterized by open scrub vegetation, dominated by ericoid/restioid fynbos (Figure 2-3). Despite the prevalence of fynbos vegetation, relatively low levels of *Stoebe*-type and *Passerina* pollen imply that conditions were not significantly cooler than present. Levels of Afrotemperate forest pollen are low during this period, while succulent/drought-resistant taxa and coastal thicket vegetation is relatively abundant, indicating drier conditions and a diverse mosaic of vegetation in the Wilderness Embayment during this period.

The period from AD 900 to AD 1300 – broadly consistent with the Medieval Climate Anomaly (MCA; AD 950 – 1250, Jones et al. 2001) – begins with a peak in Afrotemperate forest pollen from c. AD 900 to AD 950, followed by a decline to minimum values ~AD 980, indicating dry conditions, and a subsequent progressive increase until ~AD 1300 (Figure 2-3, 2-5). At Groenvlei, 20 km to the east of Bo Langvlei in the Wilderness Embayment, changes in terrigenous sediment fluxes (e.g., grain size percentages, Ti and Fe counts) have been interpreted as – in part – indicators of rainfall amount/intensity (Wündsch et al. 2016a). These records show similar patterns to the Bo Langvlei Afrotemperate forest pollen record at multi-centennial timescales (Figure 2-5) and indicate that the MCA was a relatively arid phase in the context of the last 1300 years. This may also be reflected in the strongly variable nature of Amaranthaceae pollen frequencies. Quick et al. (2018), noted that in this setting Amaranthaceae most likely represents halophytic species like *Salicornia* (Slenzka et al. 2013); however, the presence of Amaranthaceae could also be related to drier and more evaporative conditions. The strong negative correlation between Amaranthaceae and Afrotemperate forest taxa during this period suggests that it may have been a time of greater climatic variability and lower moisture availability.

In terms of temperature, *Stoebe*-type pollen is present at minimum values from c. AD 900 to AD 950, increases slightly until ~AD 1180, and then declines as Afrotemperate forest pollen increases in abundance. This potential indication of slightly cooler conditions around this time runs counter to some other studies (Tyson et al. 2000; Lüning et al. 2017; Tyson and Lindesay 1992), but the existing

evidence from southern Africa does not unequivocally indicate warmer conditions during the MCA (see Nicholson et al. 2013; Figure 2-5). The Cango Cave speleothem palaeotemperature record – the closest temperature record to Bo Langvlei – indicates only a slight warming during the MCA, while the Cold Air Cave speleothem records indicate cooler conditions (Lee-Thorp et al. 2001; Holmgren et al. 2003) according to the $\delta^{18}O$ interpretation of Sundqvist et al. (2013) (lower values indicating cooler conditions). When considered with the $\delta^{13}C$ (lower values indicating less shallow-rooting grass and thus drier conditions) and grey-scale records from Cold Air Cave (Lee-Thorp et al. 2001; Holmgren et al. 2003), this cooling may be associated with weakened tropical influence in eastern South Africa and the southern Cape. Concurrent indications of increased precipitation at Verlorenvlei in the Western Cape (Stager et al. 2012) and more humid conditions at nearby Seweweekspoort (Chase et al. 2013; Chase et al. 2017) may suggest the increased influence of temperate circulation systems at this time, supporting the model of an coeval inverse relationship between temperate and tropical circulation systems in South Africa (Van Zinderen Bakker 1976; Cockroft et al. 1987). While simulations of seasonal precipitation in the Bo Langvlei region are complex during the MCA, precipitation seasonality is generally higher (Figure 2-6) (He et al. 2013; Liu et al. 2009). This is consistent with a decrease in Afrotemperate forest pollen, which favours regular rainfall and low seasonality.

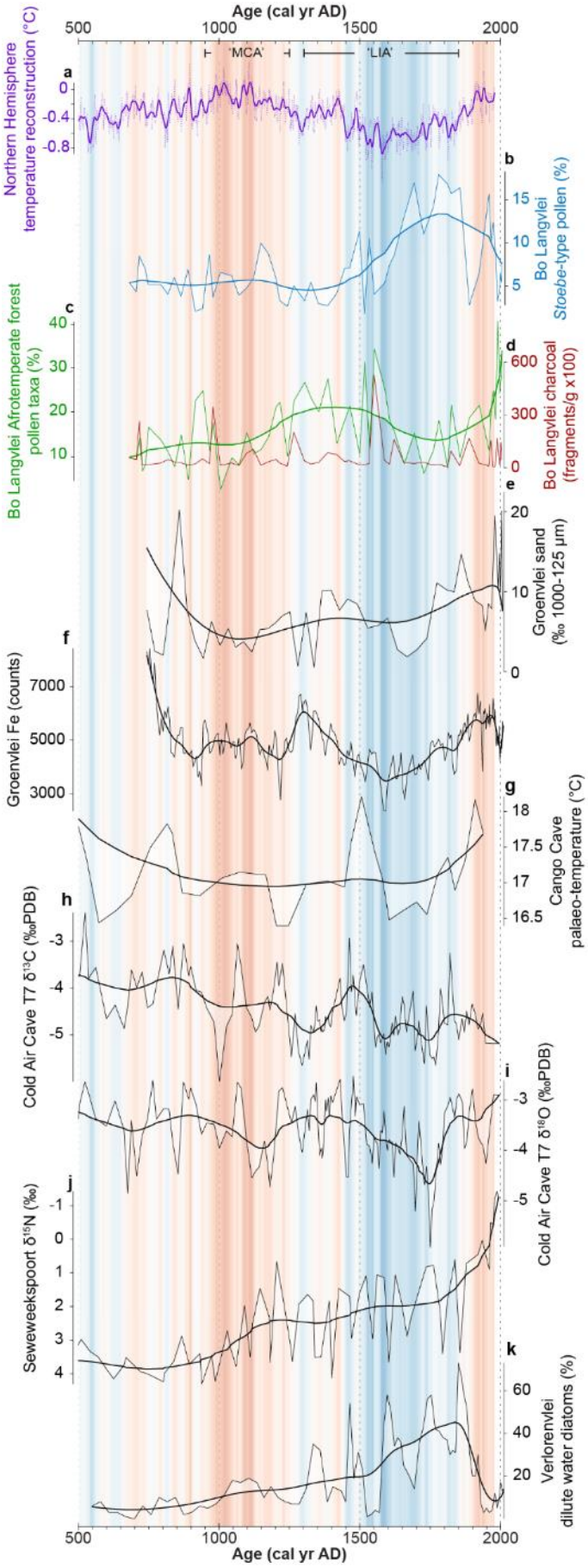

Figure 2-5: Comparison of **a.** Northern Hemisphere temperature reconstruction (Moberg et al. 2005) with percentages of **b.** *Stoebe*-type (cold indicator) and **c.** Afrotemperate forest (humidity indicator) pollen from Bo Langvlei and key palaeoclimate records in southern Africa; **e** and **f**: Groenvlei Fe and sand percentages (Wündsch et al. 2016a), **g.** Cango Cave palaeo-temperature record (Talma & Vogel 1992), **h** and **i**: Cold Air Cave $\delta^{13}C$ and $\delta^{18}O$ records (Lee-Thorp et al. 2001; Holmgren et al. 2003), **j.** Seweweekspoort $\delta^{15}N$ record (Chase et al. 2013, Chase et al. 2017), **k.** Verlorenvlei percentage dilute water diatoms (Stager et al. 2013) (location of sites indicated in Figure 1). The Medieval Climate Anomaly (MCA) and Little Ice Age (LIA) are indicated by red and blue shading, respectively, with the degree of shading within these periods indicating the strength of the reconstructed Northern Hemisphere temperature anomaly (Moberg et al. 2005) relative to the average temperatures between AD 500 and 1979.

Along with climate, fire should also be considered as a factor driving vegetation change when interpreting the Bo Langvlei record. Major peaks in charcoal concentration (Figure 2-4) are observed at AD 715 $^{+500}/_{-130}$, AD 980 $^{+330}/_{-180}$, AD 1265 $^{+150}/_{-95}$ and AD 1550 $^{+140}/_{-160}$, indicative of discrete periods of increased fire activity and/or large fire events. These episodes are often followed by declines in forest pollen and increases in fynbos representation (Figure 2-5), which might be expected considering the fire-adapted nature of fynbos (Cowling et al. 2004). Afrotemperate forest percentages and charcoal concentrations exhibit a generally positive relationship for these major peaks, which may appear contradictory, as fires are associated with more seasonal rainfall or drier conditions. In absence of other charcoal records that may help elucidate the regional significance of these data, we propose that the relationship with forest pollen may relate to increases in biomass, which would result in a larger charcoal flux, and/or the warmer conditions that appear to foster forest expansion. Under warmer conditions, periods of increased seasonality or anomalously dry years or decades may occur that provide favorable conditions for ignition, and the accumulation of forest biomass may result in larger fires. Moreover, the occurrence of periodically more extreme berg wind conditions can have a desiccating effect on vegetation, increasing the flammability of habitually moist vegetation, such as forests (Geldenhuys 1994). A more detailed study of long-term fire ecology in the Wilderness region and Afrotemperate Forest Biome is clearly warranted.

In general, the palaeoenvironmental data described above appear to support climatic factors as being the primary determinant of the Bo Langvlei pollen record. However, as declines in Afrotemperate forest pollen systematically follow the major charcoal peaks in the record, the sensitivity of this vegetation type to fire, and its recovery time follow major burning events/phases may also influence the record, perhaps amplifying declines in Afrotemperate forest pollen at the beginning of more arid phases and contributing to the pattern of progressive increases in this pollen type during these periods.

Towards the end of the MCA interval the landscape appears to have become progressively more forested, as Afrotemperate forest percentages increase significantly after ~AD 1200. Although of lower resolution, a similar expansion of forest is noted in the Groenvlei (Martin 1968) and Eilandvlei (Quick et al. 2018) pollen records, with wetter than present conditions inferred for the region from c. AD 1250

to 1350 (Wündsch et al. 2016a). The Bo Langvlei record indicates that the period from c. AD 1200 to 1400, spanning the transition from the MCA to the LIA is characterized by relatively warm (low levels of *Stoebe*-type pollen) and humid (increased Afrotemperate forest pollen) conditions (Figure 2-5). These findings are supported by the palaeotemperature records from Cango Cave (Talma and Vogel 1992) and Cold Air Cave (Lee-Thorp et al. 2001; Holmgren et al. 2003), records of terrestrial sediment flux at nearby Groenvlei (Wündsch et al. 2016a), and reductions in simulated precipitation seasonality (He et al. 2013; Liu et al. 2009).

After ~AD 1400, broadly coincident with the onset of Northern Hemisphere Little Ice Age cooling, percentages of *Stoebe*-type pollen begin to increase significantly, indicating cooling in the Wilderness Embayment region (Figure 2-5). This cooling coincides with a period of forest retreat and drier conditions (declining Afrotemperate forest percentages and reduced terrestrial sediment flux at Groenvlei (Wündsch et al. 2016a)), with the period from c. AD 1400 to 1600 exhibiting marked environmental variability, with strong shifts between warm-wet and cool-dry conditions. The Cold Air Cave speleothem records indicate a cooling and drying trend in the northern summer rainfall zone at this time (Lee-Thorp et al. 2001; Holmgren et al. 2003), while the lower resolution Cango Cave speleothem records a strong increase in temperature (Talma and Vogel 1992). The Verlorenvlei diatom record has been interpreted as indicating increased – but variable – precipitation in the winter rainfall zone (Stager et al. 2012). Based on simulations of winter rainfall amount in the region, these findings cannot be easily extrapolated to the Wilderness Embayment, but patterns in simulated rainfall seasonality are consistent with expectations based on Afrotemperate forest pollen (Figure 2-6). The challenges in determining the influence of tropical versus temperate circulation systems on winter and summer rainfall regimes in the southern Cape has become increasingly recognized in recent years (Chase et al. 2017; Chase and Quick 2018; Chase et al. 2020), and further data from both terrestrial and marine archives is required to adequately address these questions.

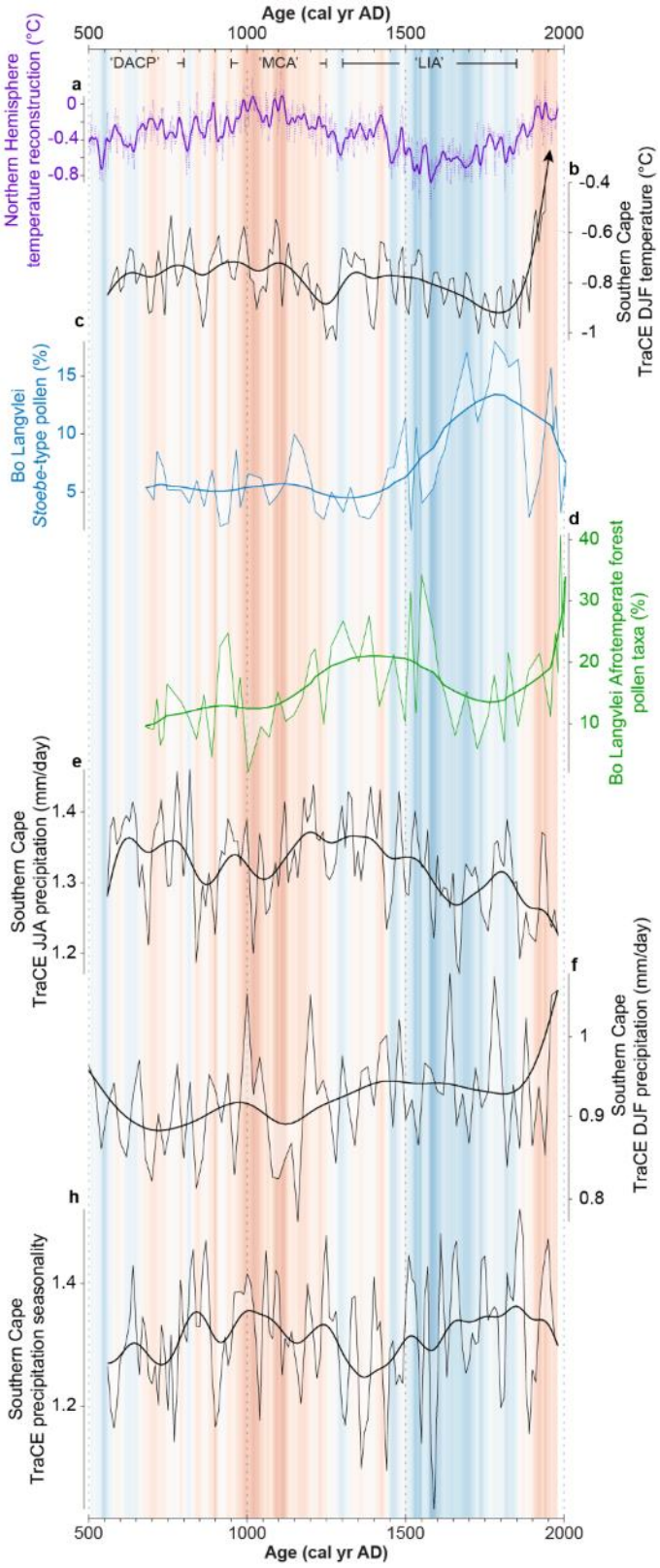

Figure 2-6: Comparison of **a.** Northern Hemisphere temperature reconstruction (Moberg et al. 2005) with percentages of **c.** *Stoebe*-type (cold indicator) and **d.** Afrotemperate forest (humidity indicator) pollen and climatic parameters (**b.** Southern Cape DJF temperature; **e.** Southern Cape JJA precipitation; **f.** Southern Cape DJF precipitation; **g.** Southern Cape precipitation seasonality) for the Wilderness region obtained from the TraCE-21k transient climate model simulation (He et al. 2013; Liu et al. 2009). The Medieval Climate Anomaly (MCA) and Little Ice Age (LIA) are indicated by red and blue shading, respectively, with the degree of shading within these periods indicating the strength of the reconstructed Northern Hemisphere temperature anomaly (Moberg et al. 2005) relative to the average temperatures between AD 500 and 1979.

From around c. AD 1600 to 1850 – the coldest portion of the LIA (Matthews & Briffa 2005) – fynbos elements dominate the landscape, most notably *Stoebe*-type and the cryophilic element *Passerina*, clearly indicating cooler conditions at Bo Langvlei at this time. A strong decline in Afrotemperate forest pollen is also observed, signaling substantially drier conditions (Figure 2-5). This is further supported by increased Asteraceae pollen, suggestive of drier, more asteraceous fynbos. These findings are consistent with Cango Cave palaeotemperature reconstructions (Talma and Vogel 1992) and inferences of drier conditions at Groenvlei (Wündsch et al. 2016a). The Cold Air Cave record also indicates cool, dry conditions in the northern summer rainfall zone during this period (Lee-Thorp et al. 2001; Holmgren et al. 2003), as does the Parfuri baobab tree-ring record (Woodborne et al. 2015). In contrast, the Seweweekspoort (Chase et al. 2013; Chase et al. 2017) and Verlorenvlei (Stager et al. 2012) records suggest increased temperate influence/winter rain, respectively. Considering the opposing trends between Verlorenvlei and Bo Langvlei, it can be hypothesised that the influence of the frontal systems associated with the westerly storm-track was not sufficient along the southern Cape coast to compensate for the concurrent reduction in tropical/local rainfall in the region.

After ~AD 1850, fynbos pollen – and *Stoebe*-type pollen in particular – decreases sharply, and there are marked increases in *Podocarpus* pollen, consistent with warmer, more humid conditions at Groenvlei (Wündsch et al. 2016a). It seems that the LIA was followed by a period of increasing temperatures and moisture availability and the establishment of the current aseasonal rainfall pattern in the Wilderness area. This trend is also observed at Eilandvlei (Quick et al. 2018) and Cango Cave (Talma and Vogel 1992), and thus seems to be a well-defined response in at least this portion of the southern Cape. It should be noted that this period is one of increasing colonial human impact in the region, with *Pinus* appearing in the Bo Langvlei record from ~AD 1850. As *Stoebe*-type pollen has in some cases been related to disturbance (Meadows et al. 1996) it may be that some of the variability observed in the most recent portion of the record may be related to non-climatic influences.

2.7. Conclusion

The Bo Langvlei pollen record provides valuable information regarding past temperature, moisture and vegetation change from the southern Cape Coast during the past 1300 years. Consideration of this period is often framed in terms of the Medieval Climate Anomaly (MCA; c. AD 950 – 1250) and the Little Ice Age (LIA; c. AD 1300 – 1850) (Jones et al. 2001; Matthews & Briffa 2005; PAGES2k 2013), which have largely been defined based on evidence from the Northern Hemisphere. Syntheses of palaeoenvironmental records from southern Africa have sometimes concluded that regional patterns have been coherent with these periods of warmer and cooler climates (e.g. Lüning et al., 2017; Tyson et al., 2000; Tyson and Lindesay, 1992), but other works have highlighted a more complex spatio-temporal patterning of climate anomalies (e.g., Nicholson et al. 2013; Nash et al. 2016).

The data presented in this chapter – together with other records from the Wilderness Embayment – indicate that conditions in the region during the MCA chronozone were relatively dry and perhaps slightly cooler than present. The most durable phase of forest expansion, and likely more humid conditions, occurred during the transition between the MCA and core cooling of the LIA. Data from the TraCE-21ka transient simulation (He et al. 2013; Liu et al. 2009) indicate that this was a period of reduced rainfall seasonality, which would be consistent with the expansion of drought-sensitive forest taxa like *Podocarpus*. The strongest signal preserved in the Bo Langvlei pollen record is the period of cool, dry conditions that occurred during the LIA, most notably from c. AD 1600 to 1850. Post-LIA warming occurred rapidly after ~AD 1850, but some of the subsequent variability observed may be related to non-climatic factors such as intensifying colonial land use.

The mechanisms driving the changes observed in the Bo Langvlei pollen record appear to be generally linked to changes in temperature, and changes in the influence of tropical systems, perhaps transmitted at least in part via the Agulhas Current and the development of localized precipitation systems (cf. Chase and Quick, 2018). During relatively warmer periods, moisture availability was apparently higher, and rainfall was perhaps less seasonal, fostering the development and expansion of Afrotemperate forests. During colder periods, precipitation resulting from tropical disturbances or

relating to higher Agulhas Current sea-surface temperatures was more restricted, resulting in drier conditions, and possibly greater seasonal contrasts in rainfall. Records from Seweweekspoort (Chase et al. 2013; Chase et al. 2017) and Verlorenvlei (Stager et al. 2012), which have been associated with temperate circulation system controls, indicate wetter conditions during the LIA. This supports to a degree the commonly cited coeval inverse relationship between tropical and temperate moisture-bearing systems, and increased westerly influence under globally cooler conditions (see Chase and Meadows, 2007; Tyson, 1999; Van Zinderen Bakker, 1976). The limited impact of increased frontal systems on the Bo Langvlei record during the LIA reinforces the proposed importance of summer rainfall in regulating moisture availability along the southern Cape coast, as suggested by Quick et al. (2018).

Data from the TraCE-21ka transient climate simulation (He et al. 2013; Liu et al. 2009) indicate that both the MCA and LIA were periods of higher rainfall seasonality, which is consistent with trends in Afrotemperate forest pollen. However, the drying trend during the LIA is simulated as resulting from a decline in winter rainfall, in apparent contradiction with the above-mentioned inferences and conceptual models. Whether this is due to insensitivity or inaccuracy in the models at these spatio-temporal scales during the late Holocene, or the need for refinement of interpretive paradigms, as has been recently suggested (e.g., Chase et al. 2017; Chase & Quick 2018) remains unclear. More data along transects encompassing the climate gradients of the southern Cape region are required to develop a more comprehensive understanding of regional climate dynamics, drivers and the impact of climate change on regional environments.

2.8. Acknowledgements

This study was funded by the German Federal Ministry of Education and Research (BMBF). The investigations were conducted within the collaborative project ‘Regional Archives for Integrated Investigations’ (RAiN), which is embedded in the international research program SPACES (Science Partnership for the Assessment of Complex Earth System Processes). We also wish to thank Thomas Leser for his help in the field as well as in the laboratory, and to thank two anonymous reviewers and Vivienne Jones for their constructive comments.

2.9. References

Allanson, B.R. & Whitfield, A.K., 1983. The Limnology of the Touw River Floodplain. *South African National Scientific Programmes Report No. 79*, p.41.

Appleby, P.G., 2008. Three decades of dating recent sediments by fallout radionuclides: a review. *The Holocene*, 18(1), pp.83–93.

Appleby, P.G. & Oldfield, F., 1978. The calculation of lead-210 dates assuming a constant rate of supply of unsupported 210Pb to the sediment. *CATENA*, 5(1), pp.1–8.

Bateman, M.D., Carr, A.S., Dunajko, A.C., Holmes, P.J., Roberts, D.L., McLaren, S.J., Bryant, R.G., Marker, M.E. & Murray-Wallace, C.V., 2011. The evolution of coastal barrier systems: a case study of the Middle-Late Pleistocene Wilderness barriers, South Africa. *Quaternary Science Reviews*, 30(1–2), pp.63–81.

Birks, H.J.B. & Birks, H.H., 1980. *Quaternary Palaeoecology*, London: Arnold.

Blaauw, M. & Christen, J.A., 2011. Flexible paleoclimate age-depth models using an autoregressive gamma process. *Bayesian Analysis*, 6(3), pp.457–474.

Chase, B., Chevalier, M., Boom, A. & Carr, A., 2017. The dynamic relationship between temperate and tropical circulation systems across South Africa since the last glacial maximum. *Quaternary Science Reviews*, 174, pp.54–62.

Chase, B.M., Boom, A., Carr, A.S., Quick, L.J. & Reimer, P.J., 2020. High-resolution record of Holocene climate change dynamics from southern Africa's temperate-tropical boundary, Baviaanskloof, South Africa. *Palaeogeography, Palaeoclimatology, Palaeoecology*, 539(October 2019), p.109518.

Chase, B.M., Boom, A., Carr, A.S., Meadows, M.E. & Reimer, P.J., 2013. Holocene climate change in southernmost South Africa : rock hyrax middens record shifts in the southern westerlies. *Quaternary Science Reviews*, 82, pp.199–205.

Chase, B.M. & Meadows, M.E., 2007. Late Quaternary dynamics of southern Africa's winter rainfall zone. *Earth-Science Reviews*, 84(3–4), pp.103–138.

Chase, B.M. & Quick, L.J., 2018. Influence of Agulhas forcing of Holocene climate change in South Africa's southern Cape. *Quaternary Research (United States)*, 90(2), pp.303–309.

Chevalier, M. & Chase, B.M., 2016. Determining the drivers of long-term aridity variability: A southern African case study. *Journal of Quaternary Science*, 31(2), pp.143–151.

Cockroft, M.J., Wilkinson, M.J. & Tyson, P.D., 1987. The application of a present-day climate model to the late Quaternary in southern Africa. *Climatic Change*, 10, pp.161–181.

Collins, W., 2006. The Community Climate System Model version 3 (CCSM3). *Journal of Climate*, 19, pp.2122–2143.

Cowling, R.M. & Heijinis, C.E., 2001. The identification of broad habitat units as biodiversity entities for systematic conservation planning in the Cape Floristic Region. *South African Journal of Botany*, 67, pp.15–38.

Cowling, R.M., Richardson, D.M. & Mustart, P.J., 2004. Fynbos. In R. M. Cowling, D. M. Richardson, & S. M. Pierce, eds. *Vegetation of Southern Africa*. Cambridge: Cambridge University Press, Cambridge, UK, pp. 99–123.

Engelbrecht, C.J., Landman, W.A., Engelbrecht, F.A. & Malherbe, J., 2015. A synoptic decomposition of rainfall over the Cape south coast of South Africa. *Climate Dynamics*, 44(9–10), pp.2589–2607.

Engelbrecht, C.J. & Landman, W.A., 2016. Interannual variability of seasonal rainfall over the Cape south coast of South Africa and synoptic type association. *Climate Dynamics*, 47(1–2), pp.295–313.

Faegri, K. & Iversen, J., 1989. *Textbook of Pollen Analysis*, Chichester: John Wiley & Sons Ltd.

Fijen, A.P.M. & Kapp, J.F., 1995. Wilderness Lakes catchment, Touw and Duiwe Rivers, water management strategy. Volume 1: Present situation. , p.115.

Fordham, D.A., Saltré, F., Haythorne, S., Wigley, T.M.L., Otto-Bliesner, B., Chan, K.C. & Brook, B.W., 2017. PaleoView: a tool for generating continuous climate projections spanning the last 21 000 years at regional and global scales. *Ecography*, 40, pp.1348–1358.

Geldenhuys, C.J., 1994. Bergwind fires and the location pattern of forest patches in the southern Cape landscape , South Africa. *Journal of Biogeography*, 21(1), pp.49–62.

Geldenhuys, C.J., 1993. Floristic composition of the southern Cape forests with an annotated check-list. *South African Journal of Botany*, 59(1), pp.26–44.

Grimm, E.C., 1987. CONISS: A Fortran 77 program for stratigraphically constrained cluster analysis by the method of incremental sum of squares. *Computers & Geosciences*, 13, pp.13–35.

Grimm, E.C., 2011. Tilia 1.7.16.

Haberzettl, T., Baade, J., Compton, J., Daut, G., Dupont, L., Finch, J., Frenzel, P., Green, A., Hahn, A., Hebbeln, D., Helmschrot, J., Humphries, M., Kasper, T., Kirsten, K., Mäusbacher, R.,

Meadows, M., Meschner, S., Quick, L., Schefuß, E., Wündsch, M. & Zabel, M., 2014. Paleoenvironmental investigations using a combination of terrestrial and marine sediments from South Africa - The RAIN (Regional Archives for Integrated iNvestigations) approach. *Zentralblatt für Geologie und Paläontologie, Teil I*, 2014(1), pp.55–73.

Haberzettl, T., Kirsten, K.L., Kasper, T., Franz, S., Reinwarth, B., Baade, J., Daut, G., Meadows, M.E., Su, Y. & Mäusbacher, R., 2019. Using 210Pb-data and paleomagnetic secular variations to date anthropogenic impact on a lake system in the Western Cape , South Africa. *Quaternary Geochronology*, 51(January), pp.53–63.

He, F., Shakun, J., PU, C., Carlson, A., Liu, Z., Otto-Bliesner, B. & Kutzbach, J., 2013. Northern Hemisphere forcing of Southern Hemisphere climate during the last deglaciation. *Nature*, 494, pp.81–85.

Hogg, A.G., Hua, Q., Blackwell, P.G., Niu, M., Buck, C.E., Guilderson, T.P., Heaton, T.J., Palmer, J.G., Reimer, P.J., Reimer, R.W., Turney, C.S.M. & Zimmerman, S.R.H., 2013. SHCal13 Southern Hemisphere Calibration, 0–50 000 Years Cal BP. *Radiocarbon*, 55(4), pp.1889–1903.

Holmgren, K., Karlen, W., Lauritzen, S.E., Lee-Thorp, J.A., Partridge, T.C., Piketh, S., Repinski, P., Stevenson, C., Svanered, O. & Tyson, P.D., 1999. A 3000-year high-resolution stalagmite-based record of palaeoclimate for northeastern South Africa. *The Holocene*, 9(3), pp.295–309.

Holmgren, K., Lee-Thorp, J.A., Cooper, G.R.J., Lundblad, K., Partridge, T.C., Scott, L., Sithaldeen, R., Siep Talma, A. & Tyson, P.D., 2003. Persistent millennial-scale climatic variability over the past 25,000 years in Southern Africa. *Quaternary Science Reviews*, 22(21–22), pp.2311–2326.

Illenberger, W.K., 1996. The Geomorphological Evolution of the Wilderness Dune Cordons, South Africa. *Quaternary International*, 33, pp.11–20.

Jones, P.D., Osborn, T.J. & Briffa, K.R., 2001. The evolution of climate over the last millennium. *Science*, 292(5517), pp.662–667.

Jury, M.R., Valentine, H.R. & Lutjeharms, J.R.E., 1993. Influence of the Agulhas Current on Summer Rainfall along the Southeast Coast of South Africa. *Journal of Applied Meteorology*, 32, pp.1282–1287.

Kelts, K., Briegel, U., Ghilardi, K. & Hsu, K., 1986. The limnogeology-ETH coring system. *Swiss Journal of Hydrology*, 48(1), pp.104–115.

Kirsten, K.L., Haberzettl, T., Wündsch, M., Meschner, S., Smit, A.J., Quick, L.J. & Meadows, M.E., 2018. A multiproxy study of the ocean-atmospheric forcing and the impact of sea-level changes on the southern Cape coast, South Africa during the Holocene. *Palaeogeography,*

Palaeoclimatology, Palaeoecology, 496, pp.282–291.

Lee-Thorp, J.A., Holmgren, K., Lauritzen, S.E., Linge, H., Moberg, A., Partridge, T.C., Stevenson, C. & Tyson, P.D., 2001. Rapid climate shifts in the southern African interior throughout the mid to late Holocene. *Geophysical Research Letters*, 28(23), pp.4507–4510.

Liu, Z., Otto-Bliesner, B., He, F., Brady, E., Tomas, R., Clark, P., Carlson, A., Lynch-Stieglitz, J., Curry, W., Brook, E., Erickson, D., Jacob, R., Kutzbach, J. & Cheng, J., 2009. Transient simulation of last deglaciation with a new mechanism for Bølling-Allerød warming. *Science*, 325, pp.310–314.

Lüning, S., Ga, M., Danladi, I.B., Adagunodo, T.A. & Vahrenholt, F., 2018. Hydroclimate in Africa during the Medieval Climate Anomaly. *Palaeogeography, Palaeoclimatology, Palaeoecology*, 495(January), pp.309–322.

Lüning, S., Galka, M. & Vahrenholt, F., 2017. Warming and Cooling: The Medieval Climate Anomaly in Africa and Arabia. *Paleooceanography*, 32, pp.1219–1235.

Marker, M.E. & Holmes, P.J., 2002. The distribution and environmental implications of coversand deposits in the Southern Cape, South Africa. *South African Journal of Geology*, 105, pp.135–146.

Marker, M.E. & Holmes, P.J., 2010. The geomorphology of the Coastal Platform in the southern Cape. *South African Geographical Journal*, 92(2), pp.105–116.

Martin, A.R.H., 1968. Pollen Analysis of Groenvlei Lake Sediments, Knysna (South Africa). *Review of Palaeobotany and Palynology*, 7, pp.107–144.

Matthews, J.A. & Briffa, K.R., 2005. The ' Little Ice Age ': Re-Evaluation of an Evolving Concept. *Geografiska Annaler. Series A, Physical Geography*, 87(1), pp.17–36.

Meadows, M.E., Baxter, A.J. & Parkington, J., 1996. Late Holocene Environments at Verlorenvlei, Western Cape Province, South Africa. *Quaternary International*, 33, pp.81–95.

Midgley, J.J., Cowling, R.M., Seydack, A.H.W. & van Wyk, G.F., 2004. Forest. In R. M. Cowling, D. M. Richardson, & S. M. Pierce, eds. *Vegetation of Southern Africa*. Cambridge: Cambridge University Press, Cambridge, UK, pp. 278–296.

Moberg, A., Sonechkin, D.M., Holmgren, K., Datsenko, N. & Karlén, W., 2005. Highly variable Northern Hemisphere temperatures reconstructed from low- and high-resolution proxy data. *Nature*, 433(10 February), pp.613–618.

Moore, P.D., Webb, J.A. & Collinson, M.E., 1991. *Pollen Analysis* 2nd ed., Oxford: Blackwell Scientific Publications.

Mucina, L. & Rutherford, M.C., 2006. *The vegetation of South Africa, Lesotho and Swaziland*, Pretoria: South African National Biodiveristy Institute, Sterlitzia.

Nakagawa, T., Brugiapaglia, E., Digerfeldt, G., Reille, M., De Beaulieu, J.-L. & Yasuda, Y., 1998. Dense media separation as a more efficient pollen extraction method for use with organic sediment/deposit samples: comparison with the conventional method. *Boreas*, 27, pp.15–24.

Nakagawa, T., 2007. PolyCounter ver.1.0 & Ergodex DX-1: a cheap and very ergonomic counter board system. *Quaternary International*, 167–668(Supplement), pp.3–486.

Nash, D.J., Cort, G. De, Chase, B.M., Verschuren, D., Nicholson, S.E., Shanahan, T.M., Asrat, A., Anne-marie, L. & Grab, S.W., 2016. African hydroclimatic variability during the last 2000 years. *Quaternary Science Reviews*, 154, pp.1–22.

Neukom, R., Steiger, N., Gómez-Navarro, J.J.J.J., Wang, J. & Werner, J.P., 2019. No evidence for globally coherent warm and cold periods over the preindustrial Common Era. *Nature*, 571(7766), pp.550–554.

Neumann, F.H., Stager, J.C., Scott, L., Venter, H.J.T. & Weyhenmeyer, C., 2008. Holocene vegetation and climate records from Lake Sibaya, KwaZulu-Natal (South Africa). *Review of Palaeobotany and Palynology*, 152(3–4), pp.113–128.

Nicholson, S.E., Nash, D.J., Chase, B.M., Grab, S.., Shanahan, T.M., Verschuren, D., Asrat, A., Lezine, A.M. & Umer, M., 2013. Temperature variability over Africa during the last 2000 years. *The Holocene*, 23(8), pp.1085–1094.

Norström, E., Norén, G., Smittenberg, R.H., Massuanganhe, E. & Ekblom, A., 2018. Leaf wax δD inferring variable medieval hydroclimate and early initiation of Little Ice Age (LIA) dryness in southern Mozambique. *Global and Planetary Change*, 170, pp.221–233.

Otto-Bliesner, B., Russell, J.M., Clark, P., Liu, Z., Overpeck, J., Konecky, B., Demenocal, P.B., Nicholson, S.E., He, F. & Lu, Z., 2014. Coherent changes of southeastern equatorial and northern African rainfall during the last deglaciation. *Science*, 346(6214), pp.1223–1227.

PAGES2k, 2013. Continental-scale temperature variability during the past two millennia. *Nature Geoscience*, 6(5), pp.339–346.

Peel, M.C., Finlayson, B.L. & McMahon, T.A., 2007. Updated world map of the Köppen-Geiger climate classification. *Hydrology and Earth System Sciences*, 11, pp.1633–1644.

Quick, L.J., Chase, B.M., Wundsch, M., Kirsten, K.L., Chevalier, M., Mausbacher, R., Meadows, M.E. & Haberzettl, T., 2018. A high-resolution record of Holocene climate and vegetation dynamics from the southern Cape coast of South Africa : pollen and microcharcoal evidence

from Eilandvlei. *Journal of Quaternary Science*, 33(5), pp.487–500.

Quick, L.J., Meadows, M.E., Bateman, M.D., Kirsten, K.L., Mäusbacher, R., Haberzettl, T. & Chase, B.M., 2016. Vegetation and climate dynamics during the last glacial period in the fynbos-afrotemperate forest ecotone, southern Cape, South Africa. *Quaternary International*, 404, pp.136–149.

Reimer, P.J., Bard, E., Bayliss, A., Beck, J.W., Blackwell, P.G., Ramsey, C.B., Buck, C.E., Cheng, H., Edwards, R.L., Friedrich, M., Grootes, P.M., Guilderson, T.P., Haflidason, H., Hajdas, I., Hatté, C., Heaton, T.J., Hoffmann, D.L., Hogg, A.G., Hughen, K.A., Kaiser, K.F., Kromer, B., Manning, S.W., Niu, M., Reimer, R.W., Richards, D.A., Scott, E.M., Southon, J.R., Staff, R.A., Turney, C.S.M. & van der Plicht, J., 2013. IntCal13 and Marine13 Radiocarbon Age Calibration Curves 0–50,000 Years cal BP. *Radiocarbon*, 55(04), pp.1869–1887.

Reinwarth, B., Franz, S., Baade, J., Haberzettl, T., Kasper, T., Daut, G., Helmschrot, J., Kirsten, K.L., Quick, L.J., Meadows, M.E. & Mäusbacher, R., 2013. A 700-year record on the effects of climate and human impact on the southern Cape coast inferred from lake sediments of Eilandvlei, Wilderness Embayment, South Africa. *Geografiska Annaler: Series A, Physical Geography*, 95(4), pp.345–360.

Russel, I.A., Randal, R.M., Cole, N., Kraaij, T. & Kruger, N., 2012. *Garden Route National Park, Wilderness Coastal Section, State of Knowledge*,

Scott, L., 1982. Late quaternary fossil pollen grains from the Transvaal, South Africa. *Review of Palaeobotany and Palynology*, 36(3–4), pp.241–278.

Scott, L., 1996. Palynology of hyrax middens: 2000 years of palaeoenvironmental history in Namibia. *Quaternary International*, 33, pp.73–79.

Scott, L., Neumann, F.H., Brook, G.A., Bousman, C.B., Norström, E. & Metwally, A.A., 2012. Terrestrial fossil-pollen evidence of climate change during the last 26 thousand years in Southern Africa. *Quaternary Science Reviews*, 32, pp.100–118.

Slenzka, A., Mucina, L. & Kadereit, G., 2013. Salicornia L. (Amaranthaceae) in South Africa and Namibia: rapid spread and ecological diversification of cryptic species. *Botanical Journal of the Linnean Society*, 172, pp.175–186.

Stager, J.C., Ryves, D.B., King, C., Madson, J., Hazzard, M., Neumann, F.H. & Maud, R., 2013. Late Holocene precipitation variability in the summer rainfall region of South Africa. *Quaternary Science Reviews*, 67, pp.105–120.

Stager, J.C., Mayewski, P.A., White, J., Chase, B.M., Neumann, F.H., Meadows, M.E., King, C.D. &

Dixon, D.A., 2012. Precipitation variability in the winter rainfall zone of South Africa during the last 1400 yr linked to the austral westerlies. *Climate of the Past*, 8(3), pp.877–887.

Strobel, P., Kasper, T., Frenzel, P., Schittek, K., Quick, L.J., Meadows, M.E., Mäusbacher, R. & Haberzettl, T., 2019. Late Quaternary palaeoenvironmental change in the year-round rainfall zone of South Africa derived from peat sediments from Vankervelsvlei. *Quaternary Science Reviews*, 218, pp.200–214.

Sundqvist, H.S., Holmgren, K. & Zhang, Q., 2013. Evidence of a large cooling between 1690 and 1740 AD in southern Africa. *Scientific Reports*, 3.

Talma, A.S. & Vogel, J.C., 1992. Late Quaternary paleotemperatures derived from a Speleothem from Cango Caves, Cape Province, South Africa. *Quaternary Research*, 37, pp.203–213.

Tinner, W. & Hu, F.S., 2003. Size parameters, size-class distribution and area-number relationship of microscopic charcoal: relevance for fire reconstruction. *The Holocene*, 13(4), pp.499–505.

Tyson, P.D., 1999. Atmospheric circulation changes and palaeoclimates of southern Africa. *South African Journal of Geology*, 95, pp.194–201.

Tyson, P.D., Karlén, W. & Heiss, G.A., 2000. The Little Ice Age and medieval warming in South Africa. *South African Journal Of Science*, 96, pp.121–126.

Tyson, P.D. & Lindesay, J.A., 1992. The climate of the last 2000 years in southern Africa. *The Holocene*, 2, pp.271–278.

Tyson, P.D. & Preston-Whyte, R.A., 2000. *The Weather and Climate of Southern Africa*, Cape Town: Oxford University Press.

Watling, R., 1977. *Trace metal distribution in the Wilderness lakes. Special report FIS 147*, Pretoria.

Welman, W.G. & Kuhn, L., 1970. *South African pollen grains and spores, Volume VI*, Amsterdam-Cape Town: Balkema.

Woodborne, S., Hall, G., Robertson, I., Patrut, A., Rouault, M., Loader, N.J. & Hofmeyr, M., 2015. A 1000-Year Carbon Isotope Rainfall Proxy Record from South African Baobab Trees (Adansonia digitata L .). *PLoS ONE*, 10(5).

Wündsch, M., Haberzettl, T., Cawthra, H.C., Kirsten, K.L., Quick, L.J., Zabel, M., Frenzel, P., Hahn, A., Baade, J., Daut, G., Kasper, T., Meadows, M.E. & Mäusbacher, R., 2018. Holocene environmental change along the southern Cape coast of South Africa - Insights from the Eilandvlei sediment record spanning the last 8.9kyr. *Global and Planetary Change*, 163, pp.51–66.

Wündsch, M., Haberzettl, T., Kirsten, K.L., Kasper, T., Zabel, M., Dietze, E., Baade, J., Daut, G., Meschner, S., Meadows, M.E. & Mäusbacher, R., 2016a. Sea level and climate change at the southern Cape coast , South Africa , during the past 4.2 kyr. *Palaeogeography, Palaeoclimatology, Palaeoecology*, 446, pp.295–307.

Wündsch, M., Haberzettl, T., Meadows, M.E., Kirsten, K.L., Kasper, T., Baade, J., Daut, G., Stoner, J.S. & Mäusbacher, R., 2016b. The impact of changing reservoir effects on the 14C chronology of a Holocene sediment record from South Africa. *Quaternary Geochronology*, 36, pp.148–160.

Van Zinderen Bakker, E.M., 1953. *South African Pollen Grains and Spores, Volume I*, AA Balkema.

Van Zinderen Bakker, E.M., 1976. The evolution of late Quaternary paleoclimates of Southern Africa: Palaeoecology of Africa, v 9. , pp.160–202.

Van Zinderen Bakker, E.M. & Coetzee, J.A., 1959. *South African Pollen Grains and Spores, Volume III*, Cape Town: AA Balkema.

Chapter 3

Geochemical perspectives on the Late Holocene evolution of Bo Langvlei, southern Cape coast, South Africa

---

Nadia du Plessis[1]

Michael E. Meadows[1, 2, 5]

Thomas Kasper[3]

Torsten Haberzettl[4]

[1] *Department of Environment and Geographical Science, University of Cape Town, Rondebosch, South Africa*

[2] *School of Geographic Sciences, East China Normal University, Shanghai, PR China*

[3]*Physical Geography, Institute of Geography, Friedrich Schiller University Jena, Germany*

[4]*Institute of Geography and Geology, University of Greifswald, Germany*

[5]*College of Geography and Environmental Sciences, Zhejiang Normal University, China*

Status: Final draft with co-authors in preparation for submission to peer reviewed journal

3.1. Introduction

Permanent lakes, particularly along the south coast of South Africa, are typically of estuarine origin resulting from sea level oscillations during the Pleistocene and Holocene (Martin 1956; Whitfield et al. 2017). Indeed, it has been proposed that the geomorphic evolution of the Wilderness Embayment can largely be ascribed to a series of sea level regressions and transgressions (Bateman et al. 2011; Birch et al. 1978; Illenberger 1996; Martin 1962).

Due to its coastal setting, the lakes contained within the Wilderness Embayment (Figure 3-1) offer a perfect setting for reconstructing environmental change as it has preserved evidence of both past marine inundations and climatic influences in the region and how these have shaped the embayment over time. Records from several waterbodies in the area are available, e.g. Groenvlei (Martin 1956; 1959; 1960; 1968; Wündsch et al. 2016a), Swartvlei (Birch et al. 1978; Haberzettl et al. 2019), Eilandvlei (Kirsten et al. 2018; Quick et al. 2018; Reinwarth et al. 2013; Wündsch et al. 2018) and Vankervelsvlei (Quick et al. 2016; Strobel et al. 2019), exploring these dynamics to varying degrees, with the most recent evidence from Eilandvlei demonstrating the role of Holocene sea level fluctuations in its development from a marine dominated system to a freshwater lake (Kirsten et al. 2018; Wündsch et al. 2018). Absent from this list however is Bo Langvlei, which today is connected to Eilandvlei only by a reed choked channel.

In analysing the geochemical and sedimentological characteristics of late Holocene sediments from Bo Langvlei, we aim to investigate the effects of sea level variations and inter-basin dynamics on the development of this waterbody in order to gain further insight into the evolution of the Wilderness Lakes system during this time period.

3.2. Regional setting

Geomorphologically, the Wilderness region is characterised by three elements: the Outeniqua Mountains in the north, the coastal plateau, and the coastal embayment (Figure 3-1). The Outeniqua Mountains are primarily composed of quartzites and sandstones of the Table Mountain Group (Balfour and Bond 1993; Booth 2011), while the coastal plateau represents the old sea floor of Tertiary origin, comprised of Table Mountain sandstones, pre-Cape granite and Kaaiman Group sediments (Bateman et al. 2011; Illenberger 1996; Marker and Holmes 2002; 2010; Martin 1962). The coastal embayment dates from the Pleistocene and predominantly consists of dune deposits, forming a series of shore parallel dune cordons (Bateman et al. 2004; 2011; Illenberger 1996; Martin 1962).

The lakes within the Wilderness Embayment can essentially be divided into three units: the Wilderness Lakes system or complex, Swartvlei, and Groenvlei (Figure 3-1). Three interconnected lakes define the Wilderness Lakes system - Eilandvlei, Bo Langvlei and Rondevlei. These are further connected to the Touw River and its estuary through the Serpentine channel, which acts as a conduit between the marine dominated Touw River estuary and Eilandvlei, although marine inputs into the lake are today relatively minimal (Russell 2003). Bo Langvlei (2.14 km^2; Watling 1977), the largest of the three lakes, mainly receives its freshwater from Langvlei Spruit (catchment size 8.2 km^2; Fijen and Kapp, 1995), with occasional overflow from Rondevlei (Fijen and Kapp 1995). The narrow channel between Eilandvlei and Bo Langvlei is usually obstructed by macrophytes, although Bo Langvlei does at times receive runoff from the Duiwe River (catchment size 42.1 km^2; Fijen and Kapp, 1995) via this connection as well as direct precipitation inputs. The Wilderness Lakes system typically drains in a westerly direction via the Serpentine Channel, the the Touw River and ultimately via its estuary, into the ocean (Watling 1977). The flow direction is however reversed at times, usually when the Touw River mouth is closed by a sandbar, resulting in the back ponding of discharge from the river back into the lakes (Martin 1962; Russel et al. 2010).

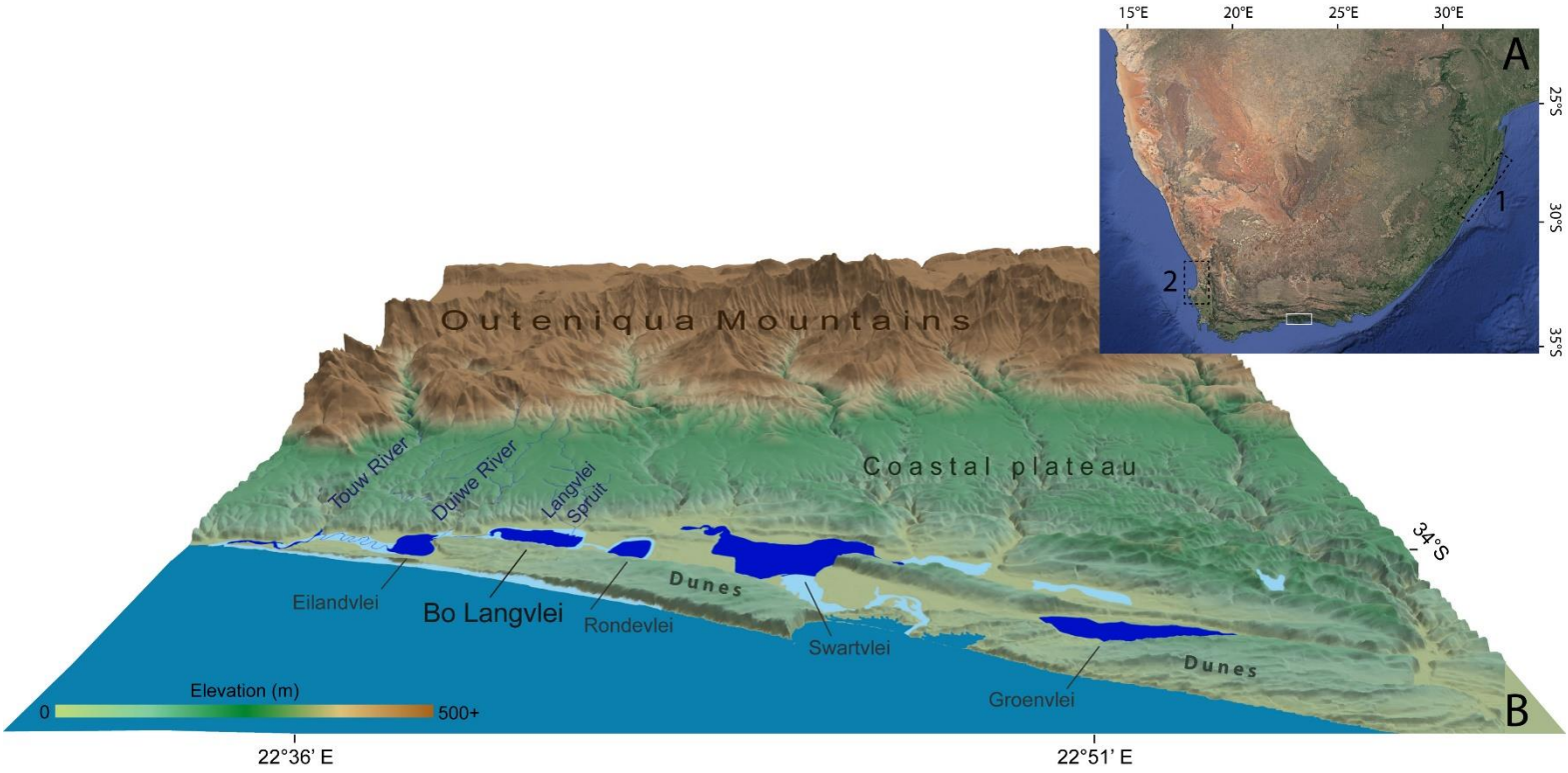

Figure 3-1: A. Map of southern Africa indicating the approximate location of the Wilderness Embayment (white box), and the location of records outside of the Wilderness Embayment mentioned in this chapter: *1.* East Coast: Cooper et al. (2018), Miller et al. (1995) and Ramsay (1995); *2.* West Coast: Baxter and Meadows (1999), Carr et al. 2015) and Compton (2001; 2006). **B.** The Wilderness Embayment indicating the location of Bo Langvlei and the lakes referred to in the text.

Vegetation in the region is characterised by Knysna Afrotemperate forest and a mosaic of fynbos and thicket elements (Cowling and Heijinis 2001). Various fynbos types are found in the region, including Garden Route Shale Fynbos, Southern Cape Dune Fynbos and Knysna Sand Fynbos (Mucina and Rutherford 2006; Quick et al. 2018). Patches of Southern Afrotemperate Forest are located in the river valleys and kloofs of the Outeniqua mountains (Mucina and Rutherford 2006; Quick et al. 2018). The lake margins and interconnecting channels are vegetated by semi-aquatic emergent macrophytes – predominantly *Phragmites australis* (Poaceae) with *Typha latifolia* and *Scirpus littoralis* also present (Cyperaceae) – and together with aquatic plants and algae, are the primary components of biomass in the lakes (Allanson and Whitfield 1983; Howard-Williams 1980; Russel et al. 2012). Mainly found

along the estuaries, azonal vegetation is represented by various species of the halophytic taxon Amaranthaceae (Mucina and Rutherford 2006).

3.3. Material and methods

3.3.1. Core extraction and sampling

As part of the first fieldwork campaign for the RAiN project (Haberzettl et al. 2014) in October 2013, a sediment core was retrieved from Bo Langvlei using a modified ETH-gravity corer (Kelts et al. 1986). Sediment core BoLa 13.2 (33°59'12.54''S, 22°40'44.46''E) measures 178.5 cm in length and was opened at the Institute of Geography at Friedrich Schiller University Jena, Germany where it was photographed, lithologically described and sampled according to standard protocols. The core was continuously sub-sampled at a resolution of 0.5 cm for elemental analyses and 1 cm for grain size and CNS analysis.

3.3.2. Chronology

The BoLa 13.2 age-depth model was established using both ^{14}C (Table 3-1) and ^{210}Pb (Table 3-2) ages. 24 bulk samples from the top 12 cm of the core (at 0.5 cm intervals) were sent to the Radiochronology Laboratory (Centre for Northern Studies, Laval University, Quebec, Canada) for ^{210}Pb-dating. For AMS ^{14}C dating, five organic sediment samples were sent to Beta Analytic Inc. (Miami, Florida, USA). From the modern age of the sediment water interface it can be inferred that no reservoir effect has to be taken into account for sediments similar to the present ones, i.e., down to a sediment depth of 94 cm. Hence the SHCal13 calibration curve (Hogg et al. 2013) was used for calibration of the radiocarbon age at 45.5 cm sediment depth. According to the lithology, the lower part experienced a marine influence (which will be confirmed later in the geochemical results). For this reason the Marine13 calibration curve (Reimer et al. 2013) was used for the samples at 98.5 cm, 137.5 cm and 178.5 cm sediment depth, respectively. A marine reservoir correction of $\Delta R = 148 \pm 27$ was applied here in reference to recent studies by Wündsch et al. (2016) and Haberzettl et al. (2019). The CRS (constant rate of ^{210}Pb supply) model (Appleby and Oldfield 1978; Appleby 2008) was applied to the ^{210}Pb results to obtain the ages.

The age-depth model was subsequently developed using the R software package Bacon (v2.2) (Blaauw and Christen 2011).

Table 3-1: Radiocarbon ages and calibration details. Ages are presented as both cal yr BP and AD where relevant.

Lab code Beta -	Depth (cm)	Conventional ^{14}C age [BP]	1σ error	Calibration data	ΔR	2σ cal age range [cal BP/AD]	Median probability [cal BP]	Age [AD]
369745	0	(105.5 ± 0.3 pMC)	-	-	-	-	-	2013 (year of coring)
369746	45.5	660	30	SHCal13	-	670-630 cal BP 1280-1320 AD 600-650 cal BP 1350-1390 AD	660	1290
369748	98.5	1790	30	Marine13	148 ± 27	1820-1690 cal BP 130-260 AD 1670-1620 cal BP 280-330 AD	1710	240
369749	137.5	3470	30	Marine13	148 ± 27	3830 - 3680 cal BP 3660 – 3640 cal BP	3720	-
369744	178.5	4270	30	Marine13	148 ± 27	4860 – 4830 cal BP	4840	-

Table 3-2: ^{210}Pb data and age estimates

Depth (cm)	^{210}Pb activity (Bq g^{-1}) unsupported	CRS	Age (AD)
0.5	0.129462675	8.45713091	2005
1	0.089934642	9.27115037	2004
1.5	0.11267076	9.93547901	2003
2	0.113936	10.9153558	2002
2.5	0.088817176	12.1245561	2001
3	0.072538177	13.2705585	2000
3.5	0.053182181	14.3806752	1999
4	0.058556788	15.320281	1998
4.5	0.037472791	16.507877	1996
5	0.055113512	17.3695226	1996
5.5	0.087106133	18.8138195	1994
6	0.072051752	21.6604169	1991
6.5	0.071103802	24.7591211	1988
7	0.045781601	28.8291055	1984
7.5	0.054150798	32.2416027	1981
8	0.054310576	37.4906148	1976
8.5	0.021339275	44.8067948	1968
9	0.017892135	48.527683	1964
9.5	0.035545938	52.1594525	1961
10	0.013712608	61.2690128	1952
10.5	0.031668121	65.6951819	1947
11	0.05203818	78.8502255	1934
11.5	0.039863802	117.519829	1895
12	0.066245955	188.237915	1825

3.3.3. Geochemical analyses

X-Ray fluorescence (XRF) scanning was conducted at Marum (University of Bremen, Germany) using an Avaatech XRF-scanner, at a resolution of 5mm. Two runs were performed at 10 kV and 30 kV, respectively, with a 20 second detection time per depth step for each run. Elemental count values were obtained for Al, Si, P, S, Cl, K, Ca, Ti, Cr, Mn, Fe, Rh, Ni, Cu, Zn, Ga, Br, Rb, Sr, Zr, Nb, Mo, Pb and Bi; only elements with values > 100 pa (peak area) were evaluated. The total carbon (TC) and total

nitrogen (TN) content were measured using a CNS elemental analyser (VarioEL Cube, Elementar). Following this, samples were treated with 10% and 30% HCl consecutively, in order to remove carbonates after which the samples were analysed again to determine the total organic carbon (TOC) content. Principal component analysis (PCA) was performed with the z-standardised XRF and CNS data with the purpose of identifying patterns in the dataset.

3.3.4. Grain size analysis

For grain size analysis, samples were treated with 30% H_2O_2 and 10% HCl in order to remove organic matter and carbonates. $Na_4P_2O_7$ was used as a dispersion medium while the samples were shaken for two hours. The grain size distribution was then measured using a Laser Diffraction Particle Size Analyzer (Beckman Coulter LS 13320, Fraunhofer optical model) at Friedrich Schiller University Jena. The samples were measured several times until a reproducible signal was obtained. The first of these was used for further statistical processing with a modified version of Gradistat 4.2 (Blott and Pye 2001).

3.4. Results and interpretation

3.4.1. Lithology

BoLa13.2 is divided into five lithological units according to changes in colour and grain size (Figure 3-2). Unit I (178 – 100 cm) represents the base of the core and is uniformly light grey in colour. It consists predominantly of silty sand and is characterised by an abundance of marine shell fragments. Unit II (100 – 86 cm) is identified as a transitional zone. From 100 to 94 cm (Unit II-a) a gradual coarsening of sediment is observed while the colour is darker grey in comparison to the unit below. The colour changes to brownish grey between 94 and 86 cm (Unit II-b) with a change to finer silty clay. Shell fragments also appear less frequently from 94 cm. Upward of 86 cm, Unit III (86 – 27 cm) appears lighter brownish grey than Unit II. The sediment also becomes finer, mainly composed of clayey silt. Filamentous plant material is present from 37 cm to the top of Unit IV (27 – 6 cm). The sediment in Unit IV is similar to that of Unit III and brownish grey in colour. At the top of the core, Unit V (6 – 0

cm) shell fragments are present again. This unit is slightly darker brownish grey than the unit below and consists of the similar finer sediment as Units III and IV.

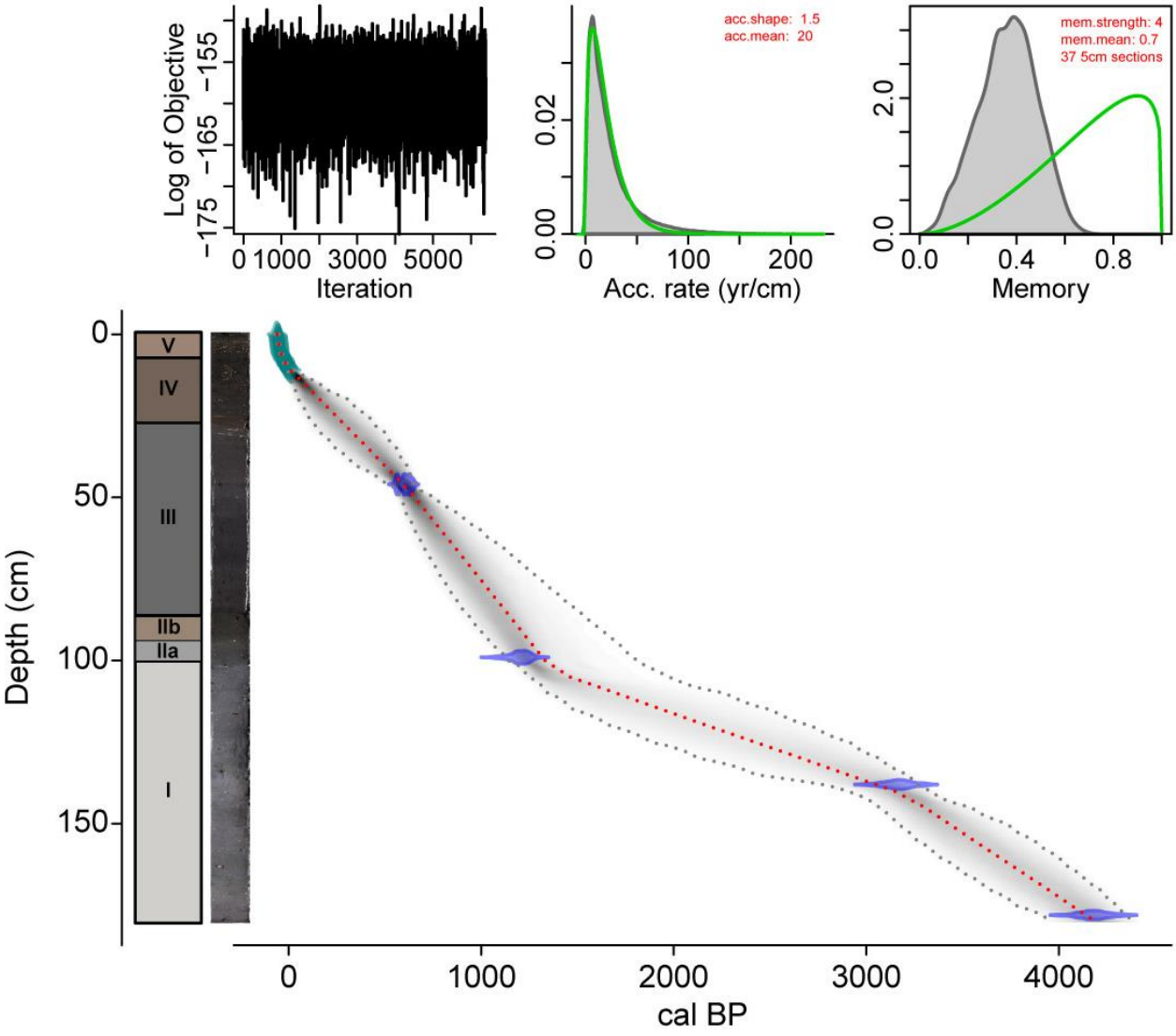

Figure 3-2: Core picture of BoLa 13.2 with an illustration of the defined lithological units on the left, and the age-depth model on the right. The age-depth model was developed using the R software package Bacon (V2.2) (Blaauw and Christen 2011). The 2σ probability distribution of calibrated ^{14}C ages is presented in blue and the 95% confidence intervals are represented by the grey dotted line. ^{210}Pb ages are represented by the turquoise area and the red line represents the best model according to the weighted mean age at each depth.

3.4.2. Chronology

According to the ^{14}C dating results (Table 3-1) and the resulting age-depth model (Figure 3-2) BoLa13.2 has a basal age of 4140 $^{+185}/_{-220}$ cal yr BP. The results from the CRS-model of ^{210}Pb activity (Table 3-2) provides ages for the top 12 cm of the core ranging from AD 1825 to present. The lithology and age-depth model show no obvious signs of a hiatus indicating continuous deposition.

Sedimentation rates are lowest in Unit I, at an average of 0.03 cm y^{-1}, increasing sharply to an average rate of 0.08 cm y^{-1} in Unit II. There are no significant changes in the sedimentation rates for Units III (average = 0.08 cm y^{-1}) and IV (average = 0.07 cm y^{-1}) in comparison to Unit II below. A very distinct acceleration in deposition is evident towards the top of core BoLa 13.2 with an average sedimentation rate of 0.30 cm y^{-1} and a maximum of 0.4 cm y^{-1} for Unit V. This change in sedimentation rate is at the point where dating methods change which warrants further investigation.

3.4.3. Palaeoenvironmental implications of sedimentology and geochemistry

Results from the principal component analysis (PCA) of the standardised XRF and CNS data (Figure 3-3) show that PC1 accounts for 61.3 % and PC2 for 18.8 % of the total variance. The results further reveal three very distinct groups. The first has high positive loadings for PC1 and contains elements that mainly reflect minerogenic sediment input from the catchment, i.e. K, Ti, Si, Al, Zr (Haberzettl et al. 2005; Kasper et al. 2012). The second group – TOC, TN and Br – exhibits high negative loadings for PC1, and hence is negatively correlated with minerogenic input and can be representative of organic input into the lake and/or bioproductivity within the lake. The third group, with high negative loadings for PC2, includes elements that are commonly used as marine indicators in lacustrine environments, i.e. Ca, Sr, TIC (Haberzettl et al. 2019; Watling 1977; Wündsch et al. 2018). Accordingly, in interpreting the geochemical and sedimentological results, PC1 is used as an indicator of minerogenic input from the catchment and TOC, representing the second group, as proxy for internal bioproductivity and/or organic input into the lake. Ca, and to a lesser degree Sr, are applied as marine indicators.

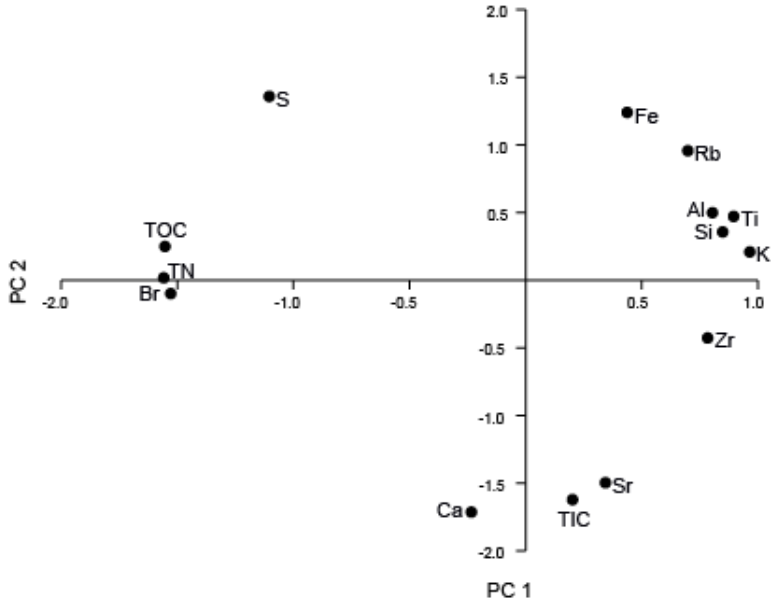

Figure 3-3: Vector plot of the z-standardized XRF and CNS data PCA.

Unit I: 4140 – 1270 cal yr BP

High Ca and Sr values (Figure 3-4) in Unit I are consistent with the presence of marine shell debris. These were likely deposited during periods of higher sea level indicating a greater marine influence on the lake. This stronger marine signal is present until c. 2590 cal yr BP after which a period of consistently lower values in the marine proxies are observed. Most evident for Sr, this could be indicative of a period of lower sea levels extending to c. 2000 cal yr BP. Following this lowstand, a rapid rise in the marine indicators are displayed, likely related to a brief return to higher sea levels, after which this marine influence appears to diminish.

At the same time, TOC (Figure 3-4) values remain very low throughout Unit I indicating either a reduced supply of allochthonous organic matter into the lake or the poor preservation of such matter within the lake. Additionally, this also points towards low bioproductivity within the lake. Molar TOC/TN ratios designate the source of organic matter – ratios between four and ten are typically associated with algal organic matter while higher values (>20) are generally related to organic matter derived from vascular terrestrial vegetation (Haberzettl et al. 2005; Meyers and Ishiwatari 1993; Meyers 1994). The C/N ratios (Figure 3-4) range between 7.8 and 22.8 with an average of 11.1 for this unit,

suggesting that autochthonous aquatic biomass makes up the majority of the deposited organic matter. Notably higher C/N ratios between c. 4000 and 3600 cal yr BP, and especially around c. 2040 cal yr BP, point towards brief episodes where terrestrial organic matter entered the lake.

Unit I is also characterised by markedly higher values for PC1 (Figure 3-4) in comparison to the units above, signifying a period of greater minerogenic input. This enhanced sediment delivery to Bo Langvlei could be related to increased surface runoff and/or intensified fluvial activity generally associated with increased precipitation.

The sediments in Unit I are coarser than those above, dominated mainly by the sand fraction (Figure 3-4). This sandy sediment is likely of marine origin considering the co-occurrence of marine shell debris and higher values for the marine proxies at this time. These larger grain sizes additionally indicate deposition under high energy conditions (Humphries et al. 2016). This turbulent depositional environment could further be responsible for the poor preservation of organic matter in this unit. A distinct increase in grain size is evident between c. 3710 and 3610 cal yr BP and from c. 2440 to 2340 cal yr BP which could suggest high energy depositional episodes possibly related to fluctuating sea levels and/or heavy rainfall events.

Unit II: 1270 – 1110 cal yr BP

Unit II is identified as a transitional phase with two distinct stages displaying largely contrasting trends. The first phase, c. 1270 to 1200 cal yr BP (Unit II-a), still reflects a minor marine influence, terminating around c. 1210 cal yr BP. A marked increase in grain size (maximum mean grain size) at this time suggests a major depositional episode. This likely represents a large flood event as flood deposits are typically identified by coarser grain sizes than the surrounding matrix (Schillereff et al. 2014; Wilhelm et al. 2019). Preceding this depositional event, a prominent peak in PC1 at c. 1230 cal yr BP points towards a sudden influx of minerogenic sediment into the lake, probably reflecting heavy rainfall which would further substantiate flood conditions. Unit II-b (1200 – 1110 cal yr BP), representing the second stage, is marked by a distinctive increase in TOC and a rapid decline in PC1. The average C/N ratio for

the unit as a whole is slightly higher (11.9) in comparison to Unit I but does not reflect a significant change in the source of organic matter.

Unit III: 1110 – 275 cal yr BP

The trend of higher TOC and lower PC1 values identified in Unit II-b continue in Unit III which possibly suggest constraining the transitional phase to the period c. 1270 - 1200 cal yr BP; alternatively the flood event at c. 1210 cal yr BP may mark the end of this phase. This trend extends to c. 820 cal yr BP indicating a period of enhanced internal lake productivity and/or increased organic matter supply, and reduced minerogenic input, possibly reflecting decreased fluvial runoff related to drier conditions in the catchment.

After c. 820 cal yr BP a reversal of this trend is observed, i.e. lower TOC percentages concomitant with increased PC1 values. The increase in minerogenic input is likely related to increased rainfall while the reduced amount of organic matter could result from higher energy lacustrine process, associated with enhanced fluvial activity, prohibiting the deposition of organic matter. In addition, a peak in mean grain size at c. 650 cal yr BP could further suggest high energy conditions in Bo Langvlei.

From around c. 560 until 400 cal yr BP the opposite (i.e. higher TOC, lower PC1) is noted in the record again, with a change to higher PC1 and lower TOC percentages after c. 400 cal yr BP.

A further period of higher energy lacustrine processes are identified from around c. 310 to 260 cal yr BP which may suggests a series of flood events. The mean grain size indicates that the sediment deposited over this time is not as coarse as those from the c. 1210 cal yr BP event possibly suggesting a different sediment source. A very sharp decline in minerogenic input is also noted at this time, as well as an abrupt increase in TOC.

In general, the sediments in Unit III are finer in comparison to Units I and II which may indicate a change in sediment provenance. The C/N ratio ranges from 10.3 to 12.7 with an average of 11.8, generally similar to Unit II, indicating that the bulk of the organic matter still consists predominantly of autochthonous aquatic biomass.

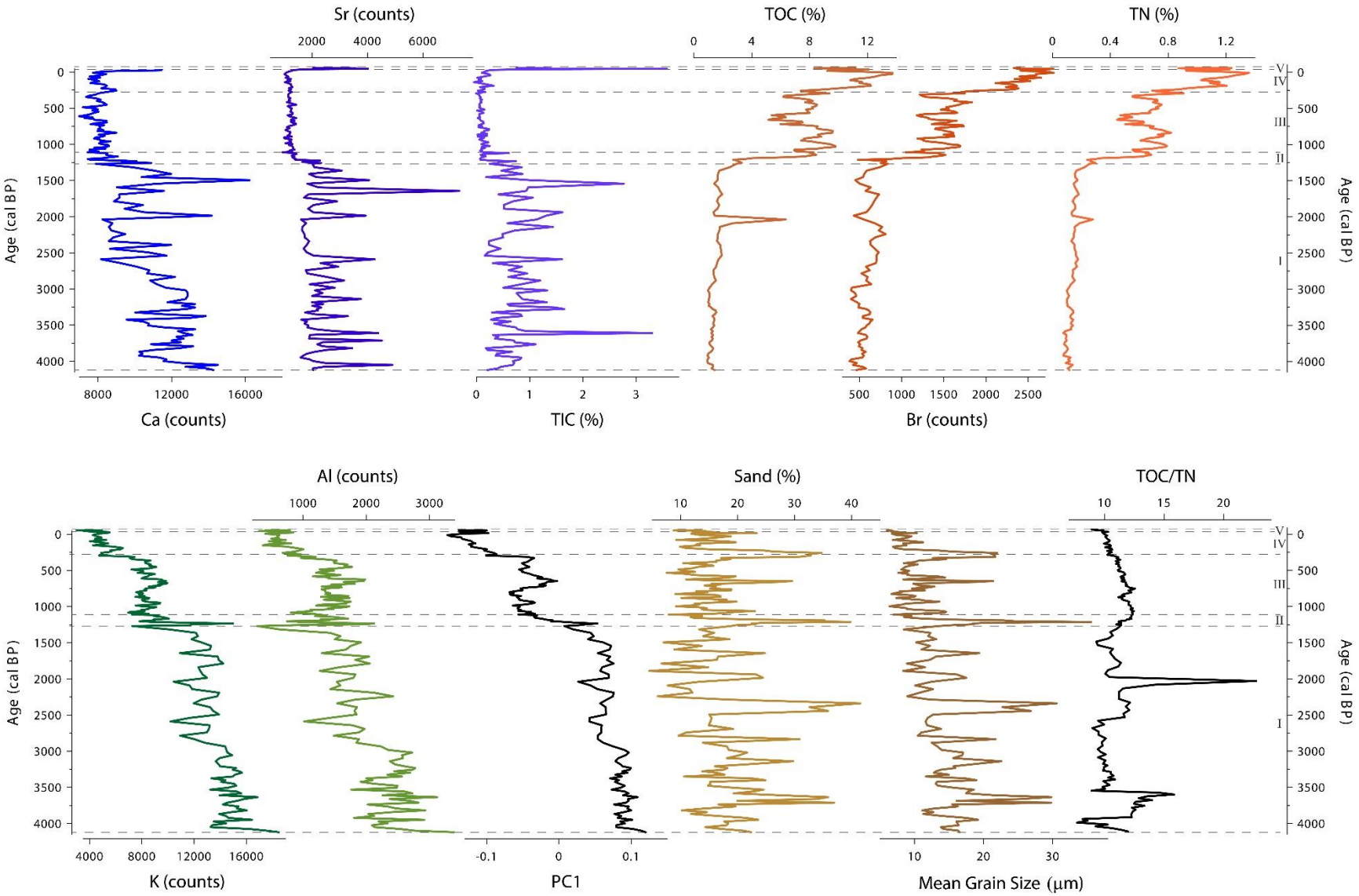

Figure 3-4: Selected XRF, CNS and grain size results from the BoLa 13.2 record. Lithological units are indicated on the right.

Unit IV: 275 to -40 cal yr BP/AD 1675 – 1990

After the depositional event at c. 310 cal yr BP, organic matter content increases rapidly until c. AD 1920 (c. 30 cal yr BP) with a very sharp decline in minerogenic input. This is similar to the trends observed after the event at 1210 cal yr BP. The C/N ratios vary between 9.9 and 11.8 around an average of 10.3 – somewhat lower than in Unit III.

Unit V: AD 1990 – present

Unit V represents the shortest, most recent section of the record. The presence of marine shell fragments together with very high Ca, Sr and TIC values reflect a possible marine influence in the system. Maximum sedimentation rates are further observed in this unit.

3.5. Discussion

The late Holocene evolution of Bo Langvlei can essentially be divided into three phases: a marine or lagoonal phase, a transitional phase and the more recent lacustrine phase.

Marine/Lagoon phase: 4140 – 1270 cal yr BP

Analogous marine conditions as found in Bo Langvlei during this phase were also recorded at adjacent Eilandvlei (Kirsten et al. 2018; Wündsch et al. 2018) and nearby Groenvlei (Wündsch et al. 2016a), indicating that, although fluctuating, sea level was still elevated in relation to present day conditions. These results postdate records along the South African coast (e.g. Baxter & Meadows 1999; Compton 2001, 2006; Miller et al. 1995; Ramsay 1995) which exhibit a succession of marine regressions and transgressions throughout the Holocene and a mid-Holocene sea level highstand. The timing of this highstand does seem to vary geographically with maximum Holocene sea levels recorded along the south coast between c. 6400 and 4700 cal yr BP (Martin 1962; Martin 1968; Wündsch et al. 2018), evidence from the west coast puts this highstand at c. 7300 to 5900 cal yr BP (Compton 2001, 2006) while for the east coast this peak is suggested to be around c. 5100 cal yr BP (Cooper et al. 2018;

Ramsay 1995) (Figure 3-5). Unfortunately, our record does not cover this period but evidences that the marine impact lasted much longer in the Wilderness embayment than only the marine maximum. This was similarly found along the west coast with marine conditions likely extending until c. 2500 cal yr BP in the region (Carr et al. 2015; Compton 2001; 2006). After c. 2600 cal yr BP, a period of lower sea levels were inferred at Bo Langvlei, consistent with a sea level lowstand along the west coast between c. 2500 and 1800 cal yr BP (Baxter and Meadows 1999; Compton 2001; 2006). Lower sea levels were also indicated at Groenvlei at this time (Deevey et al. 1959; Martin 1968) (Figure 3-5).

From the evidence above it is proposed that Bo Langvlei and Eilandvlei were connected by a much wider channel than today facilitating the transfer of marine sediment into Bo Langvlei, especially when sea levels were elevated, propagating the marine signal via Eilandvlei into Bo Langvlei. After c. 2000 cal yr BP however, indications of a minor sea level highstand, as recorded along the west coast (Baxter and Meadows 1999; Compton 2001; 2006), is much more pronounced at Bo Langvlei (Figure 3-5). This could potentially suggest that there was another inflow, directly from the ocean, closer to Bo Langvlei. Bateman et al. (2011) identified a possible offshore palaeoestuary for both the Touw and Swart Rivers but Birch et al. (1978) found no such evidence (Cawthra et al. 2014), as such this remains a speculative hypothesis.

Distinctly higher minerogenic input (Figure 3-4; 3-6) is further reflected in the Bo Langvlei record during this phase. As Langvlei Spruit is the main source of fresh water, and thus sediment, into Bo Langvlei, it is proposed that this terrestrial signal is amplified due to the inwash of sediment from Langvlei Spruit, Eilandvlei and the Duiwe River. Particularly during periods of increased rainfall when fluvial runoff to the sea (via the Touw River estuary) is blocked by the intruding ocean, large quantities of sediment would be transported back and deposited in Bo Langvlei. This would be similar to the effect today when the Touw River estuary mouth is blocked by a sandbar, reversing the flow of the system.

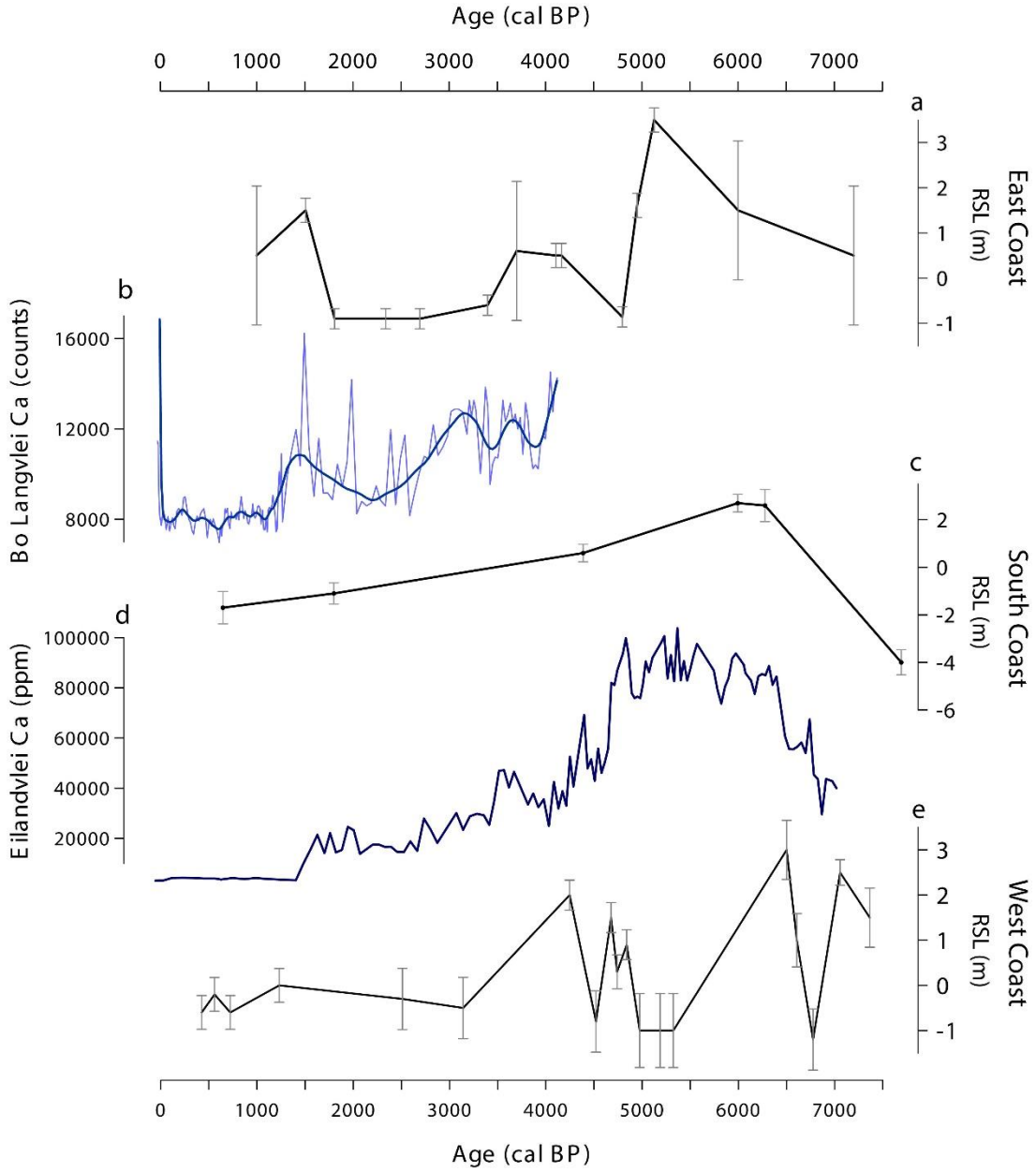

Figure 3-5: Comparison of Ca data from Bo Langvlei with that of Eilandvlei and Holocene sea level reconstructions for the east, south and west coasts of South Africa: **a)** Sea level reconstruction from several sites along the east coast (Cooper et al. 2018); **b)** Bo Langvlei Ca data; **c)** Sea level reconstruction for the south coast using sea level indicators from several sites along the south coast, including Groenvlei (Deevey et al. 1959; Martin 1968); **d)** Eilandvlei Ca data (Wündsch et al. 2018); **e)** Sea level reconstruction for the west coast (Compton 2001; 2006) . Data for sea level curves from Cooper et al. (2018).

Transitional phase: 1270 – 1200 cal yr BP

This short period represents an important phase in the development of Bo Langvlei and the Wilderness Lakes system as a whole, marking the shift from marine/lagoonal conditions towards a lacustrine system. The marine influence in Bo Langvlei is starting to dissipate, coming to an end around c. 1210 cal yr BP (Figure 3-5; 3-6). This transition is similarly seen at Eilandvlei (Kirsten et al. 2018; Wündsch et al. 2018) and Groenvlei (Martin 1968; Wündsch et al. 2016a), ascribed to receding sea levels and dune accretion, resulting in the progressive isolation of the lakes from the ocean (Wündsch et al. 2018).

The inference of the c. 1210 cal yr BP event as a flood episode can be substantiated by evidence from Groenvlei where a distinctive sand layer, dated between c. 2710 and 1210 cal yr BP, has been interpreted to represent a heavy rainfall event (Wündsch et al. 2016a). This flood event further signals either a distinct narrowing of the connection between Bo Langvlei and Eilandvlei, or a complete cut off between the two. In the case of a narrowed connection, some water exchange would still occur between the two waterbodies but not of the magnitude seen previously.

Lacustrine phase: 1200 cal yr BP to present

In the present day, Bo Langvlei is largely separated from Eilandvlei and mainly receives runoff from the small catchment of Langvlei Spruit (MAR ~1.5 x 10^6 m^3; CSIR 1981). Therefore, it is suggested that the environmental proxies preserved in the Bo Langvlei sediments after c. 1200 cal yr BP represents a more accurate reflection of changes, both across the catchment and within the lake itself, in comparison to the preceding ~3000 years of the record as it was largely over printed by a marine signal. The strong negative correlation between minerogenic input and organic matter is also more prominent in this part of the record. Two scenarios are put forward to explain this interrelationship:

During drier periods, associated with reduced runoff and less allochthonous minerogenic input, conditions within the lake would become more stagnant with limited oxygen availability inhibiting organic matter decomposition. These more tranquil conditions would further promote the accumulation and preservation of organic matter.

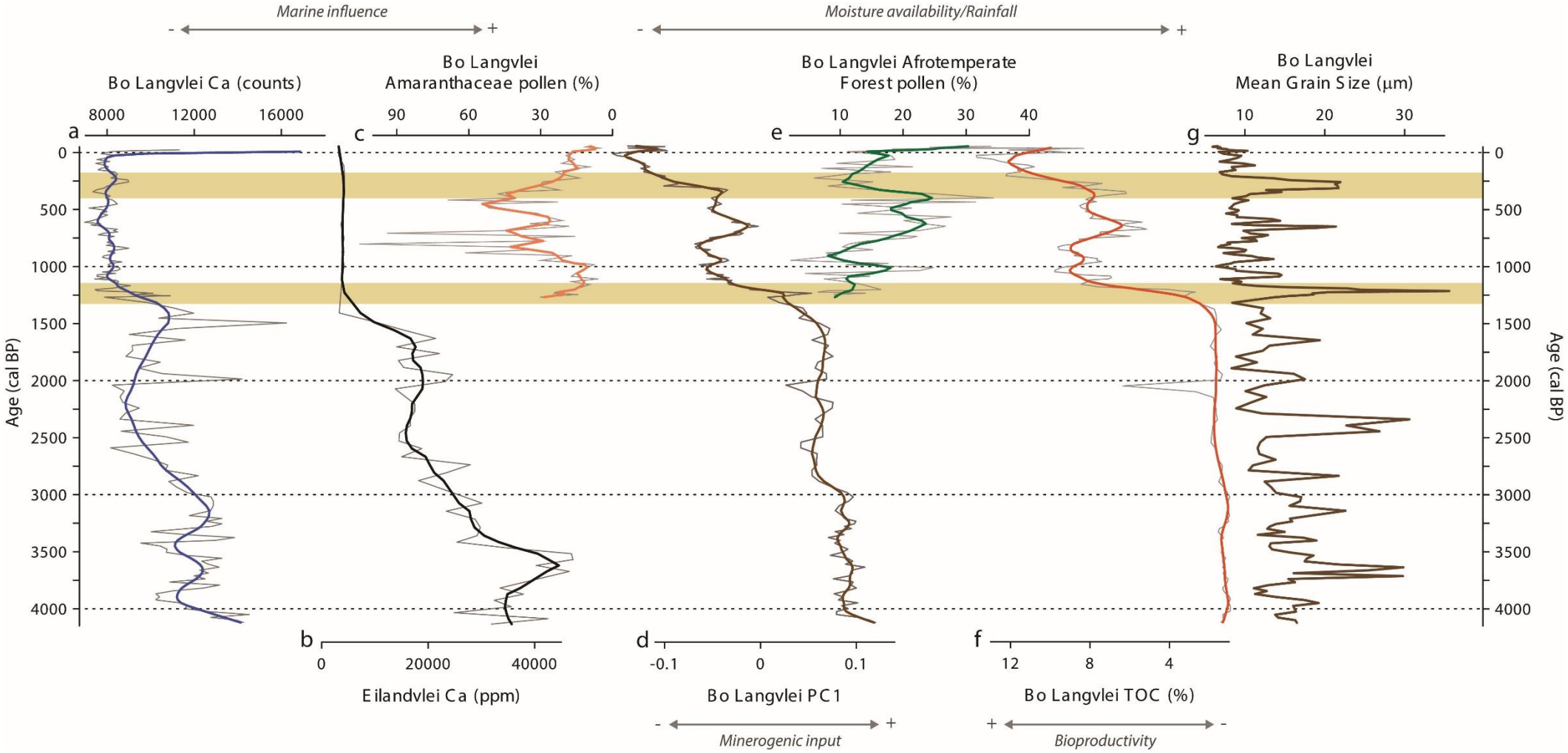

Figure 3-6: Summary of the late Holocene evolution of Bo Langvlei: **a)** Bo Langvlei Ca data; **b)** Eilandvlei Ca data (Wündsch et al. 2018); **c)** Bo Langvlei Amaranthaceae pollen percentages (axis reversed); **d)** Bo Langvlei PC1; **e)** Bo Langvlei Afrotemperate forest pollen percentages; **f)** Bo Langvlei TOC (%) (axis reversed); **g)** Bo Langvlei mean grain size. The brown shading indicates the two flood events, at ~1210 and ~310 cal yr BP respectively, as identified in the BoLa 13.2 record.

In contrast, minerogenic input into Bo Langvlei would be greater during periods of increased rainfall due to both surface and fluvial runoff. Furthermore, in addition to runoff from Langvlei Spruit, intensified fluvial activity may result in the rejuvenation of the channel between Eilandvlei and Bo Langvlei, transporting sediment-laden water from both Eilandvlei and the Duiwe River into Bo Langvlei. This input of freshwater and increased mixing would accelerate the decomposition of organic matter, and in the event of particularly heavy rainfall events, possibly even flush organic matter out of the system (Bally et al. 1985).

In considering these dynamics, enhanced bioproductivity/organic matter accumulation and reduced minerogenic input reflected in the record between c. 1200 and 820 cal yr BP (Figure 3-6) suggest drier conditions in the catchment with reduced fluvial runoff. This is consistent with a period of increased rainfall seasonality and a drier environment (lower Afrotemperate forest pollen percentages; Figure 3-6) as inferred from the Bo Langvlei pollen record (this thesis). Towards the end of this drier period, from around c. 880 cal yr BP, an increase in the representation of pollen from the halophytic taxon Amaranthaceae (Figure 3-6; 3-7) is further displayed in the record. This may suggest a slightly delayed vegetation response to increased salinity in Bo Langvlei resulting from reduced rainfall at this time. Such drier conditions would further result in lower lake water levels (Olds et al. 2016), exposing the mudflats along the shoreline which species of the family Amaranthaceae, such as *Sarcocornia capensis* and *S. pillansii*, then colonise, as seen in the modern Swartvlei estuary nearby.

A further consequence of increased salinity and lower water levels is the die-back of emergent and submerged aquatic vegetation (Russel 2003; Olds et al. 2016). Macrophyte detritus would then further contribute to the high organic matter content seen in the record at this time (Figure 3-7). Moreover, in the absence of aquatic macrophytes, especially in shallow lakes, conditions within the lake would become more turbid, dominated by phytoplankton (Hupfer and Hilt 2008).

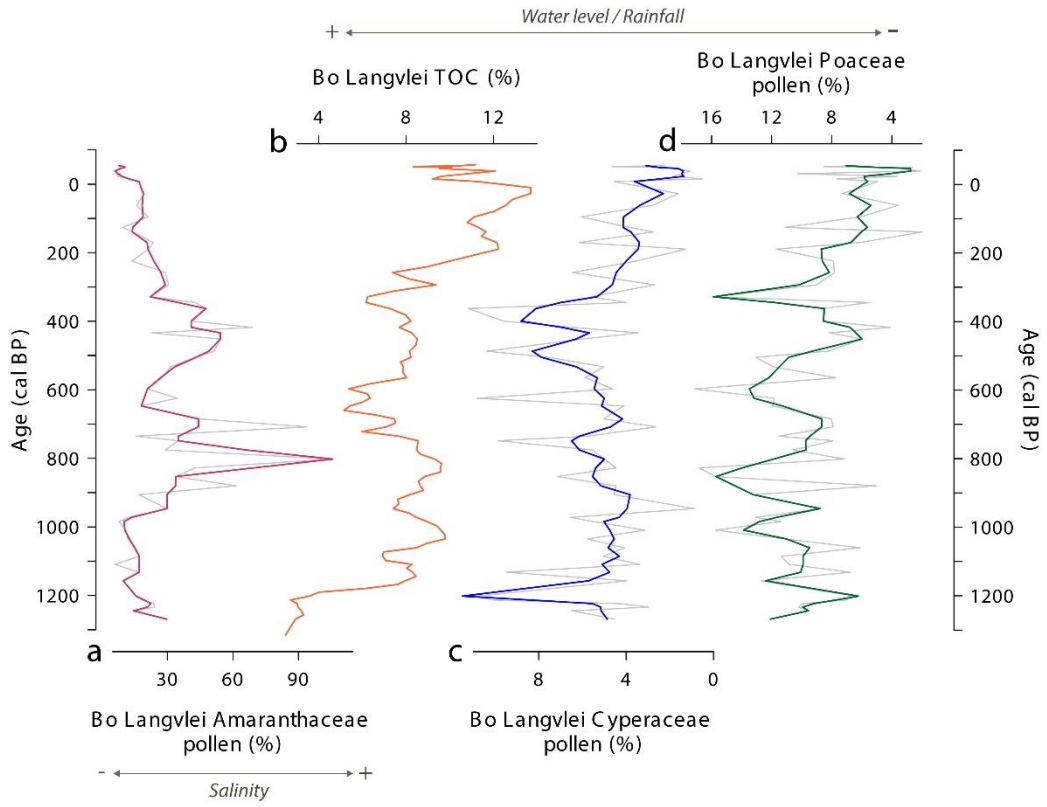

Figure 3-7: Illustration of the relationship between organic matter accumulation/bioproductivity, salinity and the presence of wetland taxa during the last ~1200 years in Bo Langvlei: **a)** Amaranthaceae pollen percentages; **b)** percentage of TOC in the sediment; **c)** Cyperaceae pollen percentages (axis reversed); **d)** Poaceae (likely *Phragmites australis*) pollen percentages (axis reversed).

After c. 820 cal yr BP, a more mesic environment, with reduced rainfall seasonality as evidenced by the increase in pollen from Afrotemperate forest taxa in the Bo Langvlei pollen record (this thesis), supports the suggested increased minerogenic input, consequent on increased rainfall in the catchment and increased fluvial activity and runoff into the lake. This input of freshwater, in turn, could possibly lead to dilution of nutrients, lower internal lake productivity and an increase in emergent macrophyte development along the lake margins which stabilise and capture detritus matter preventing deposition into the lake.

Following this wetter period, a return to drier conditions are inferred from the increase in organic matter and decline in minerogenic input observed in the record from c. 560 until around 400

cal yr BP. A cool and dry period, with enhanced rainfall seasonality is similarly observed in the Bo Langvlei pollen record (this thesis), with drier conditions and lower lake water levels at Groenvlei during this time (Wündsch et al. 2016a). Between c. 310 and 260 cal yr BP a series of high energy flood events triggered another change in the system, with similar results as after the c. 1210 cal yr BP flood event. Accordingly, the evidence suggests that although drier conditions prevailed, heavy rainfall events did occur. In addition, as forest cover declined during this period – as evidence in the Bo Langvlei pollen record (this thesis) – erosion rates during such rainfall events would increase markedly due to less dense vegetation cover, resulting in the increased deposition of fluvial sediment from the catchment in Bo Langvlei.

3.6. Conclusion

The ~4200 year geochemical and sedimentary record from Bo Langvlei provides unique insights into the late Holocene evolution of the Wilderness Embayment. The evidence indicates that, from the onset of the record, the Wilderness lakes were largely a marine dominated system, transitioning towards lagoonal conditions as sea levels regressed and the embayment became increasingly isolated from the ocean. A large flood event around c. 1210 cal yr BP likely severed, or at least narrowed, the connection between Bo Langvlei and Eilandvlei, initiating the onset of the lacustrine phase as the lakes developed conditions broadly consistent with the contemporary scenario.

The data further indicate a negative correlation between organic matter accumulation/bioproductivity and minerogenic input, suggesting enhanced deposition and preservation of organic matter in the lake during drier periods, and more turbulent conditions within the lake during periods of increased rainfall, inhibiting the accumulation of such matter.

In addition, the records presented here show good agreement with the pollen record from Bo Langvlei, supporting inferences with regard to minerogenic input and increased fluvial activity due to increased precipitation. Together these records further illustrate the relationship between organic matter content and the presence of macrophyte pollen in the sediment, suggesting that, in conjunction,

geochemical and pollen records can provide a better understanding of internal lake dynamics, especially in the context of the deposition and accumulation of organic matter.

3.7. Acknowledgements

This study was funded by the German Federal Ministry of Education and Research (BMBF). The investigations were conducted within the collaborative project 'Regional Archives for Integrated Investigations' (RAiN), which is embedded in the international research program SPACES (Science Partnership for the Assessment of Complex Earth System Processes). We also wish to thank Thomas Leser for his help in the field as well as in the laboratory.

3.8. References

Allanson, B.R. & Whitfield, A.K., 1983. The Limnology of the Touw River Floodplain. *South African National Scientific Programmes Report No. 79*, p.41.

Appleby, P.G., 2008. Three decades of dating recent sediments by fallout radionuclides: a review. *The Holocene*, 18(1), pp.83–93.

Appleby, P.G. & Oldfield, F., 1978. The calculation of lead-210 dates assuming a constant rate of supply of unsupported 210Pb to the sediment. *CATENA*, 5(1), pp.1–8.

Balfour, D.A. & Bond, W.J., 1993. Factors Limiting Climber Distribution and Abundance in a Southern African Forest. *Journal of Ecology*, 81(1), pp.93–100.

Bally, R., McQuaid, C.D. & Pierce, S.M., 1985. Primary productivity of the Bot River estuary, South Africa. *Transactions of the Royal Society of South Africa*, 45(3–4), pp.333–345.

Bateman, M.D., Holmes, P.J., Carr, A.S., Horton, B.P. & Jaiswal, M.K., 2004. Aeolianite and barrier dune construction spanning the last two glacial–interglacial cycles from the southern Cape coast, South Africa. *Quaternary Science Reviews*, 23(14–15), pp.1681–1698.

Bateman, M.D., Carr, A.S., Dunajko, A.C., Holmes, P.J., Roberts, D.L., McLaren, S.J., Bryant, R.G., Marker, M.E. & Murray-Wallace, C.V., 2011. The evolution of coastal barrier systems: a case study of the Middle-Late Pleistocene Wilderness barriers, South Africa. *Quaternary Science Reviews*, 30(1–2), pp.63–81.

Baxter, A.J. & Meadows, M.E., 1999. Evidence for Holocene sea level change at Verlorenvlei, Western Cape, South Africa. *Quaternary International*, 56(1), pp.193–206.

Birch, G.F., Du Plessis, A. & Willis, J.P., 1978. Offshore and onland geological and geophysical investigations in the Wilderness Lakes region. *Transactions of the Geological Society of South Africa*, 81, pp.339–352.

Blaauw, M. & Christen, J.A., 2011. Flexible paleoclimate age-depth models using an autoregressive gamma process. *Bayesian Analysis*, 6(3), pp.457–474.

Blott, S.J. & Pye, K., 2001. GRADISTAT: A Grain Size Distribution and Statistics Package for the Analysis of Unconsolidated Sediments. *Earth Surface Processes and Landforms*, 26, pp.1237–1248.

Booth, P., 2011. Stratigraphic, structural and tectonic enigmas associated with the Cape Fold Belt: challenges for future research. *South African Journal of Geology*, 114, pp.235–248.

Carr, A.S., Boom, A., Chase, B.M., Meadows, M.E. & Grimes, H.L., 2015. *Holocene sea level and environmental change on the west coast of South Africa: evidence from plant biomarkers, stable isotopes and pollen*,

Cawthra, H.C., Bateman, M.D., Carr, A.S., Compton, J.S. & Holmes, P.J., 2014. Understanding Late Quaternary change at the land-ocean interface: a synthesis of the evolution of the Wilderness coastline, South Africa. *Quaternary Science Reviews*, 99, pp.210–223.

Compton, J.S., 2001. Holocene sea-level fluctuations inferred from the evolution of depositional environments of the southern Langebaan Lagoon salt marsh, South Africa. *The Holocene*, 11(4), pp.395–405.

Compton, J.S., 2006. The mid-Holocene sea-level highstand at Bogenfels Pan on the southwest coast of Namibia. *Quaternary Research*, 66(2), pp.303–310.

Cooper, J.A.G., Green, A.N. & Compton, J.S., 2018. Sea-level change in southern Africa since the Last Glacial Maximum. *Quaternary Science Reviews*, 201, pp.303–318.

Cowling, R.M. & Heijinis, C.E., 2001. The identification of broad habitat units as biodiversity entities for systematic conservation planning in the Cape Floristic Region. *South African Journal of Botany*, 67, pp.15–38.

CSIR, 1981. *Evaluation of prototype data and the application of a numerical model to the Wilderness Lakes and Touw River flood plain. CSIR Report No. C/SEA 8113*, Stellenbosch, South Africa.

Deevey, E.S., Gralenski, L.J. & Hoffren, V., 1959. Yale natural radiocarbon measurements IV. *Radiocarbon*, 1, pp.144–159.

Fijen, A.P.M. & Kapp, J.F., 1995. Wilderness Lakes catchment, Touw and Duiwe Rivers, water management strategy. Volume 1: Present situation. , p.115.

Haberzettl, T., Fey, M., Lücke, A., Maidana, N., Mayr, C., Ohlendorf, C., Schäbitz, F., Schleser, G.H., Wille, M. & Zolitschka, B., 2005. Climatically induced lake level changes during the last two millennia as reflected in sediments of Laguna Potrok Aike, southern Patagonia (Santa Cruz, Argentina). *Journal of Paleolimnology*, 33, pp.283–302.

Haberzettl, T., Baade, J., Compton, J., Daut, G., Dupont, L., Finch, J., Frenzel, P., Green, A., Hahn, A., Hebbeln, D., Helmschrot, J., Humphries, M., Kasper, T., Kirsten, K., Mäusbacher, R., Meadows, M., Meschner, S., Quick, L., Schefuß, E., Wündsch, M. & Zabel, M., 2014. Paleoenvironmental investigations using a combination of terrestrial and marine sediments from South Africa - The RAIN (Regional Archives for Integrated iNvestigations) approach. *Zentralblatt für Geologie und Paläontologie, Teil I*, 2014(1), pp.55–73.

Haberzettl, T., Kirsten, K.L., Kasper, T., Franz, S., Reinwarth, B., Baade, J., Daut, G., Meadows, M.E., Su, Y. & Mäusbacher, R., 2019. Using 210Pb-data and paleomagnetic secular variations to date anthropogenic impact on a lake system in the Western Cape , South Africa. *Quaternary Geochronology*, 51(January), pp.53–63.

Hogg, A.G., Hua, Q., Blackwell, P.G., Niu, M., Buck, C.E., Guilderson, T.P., Heaton, T.J., Palmer, J.G., Reimer, P.J., Reimer, R.W., Turney, C.S.M. & Zimmerman, S.R.H., 2013. SHCal13 Southern Hemisphere Calibration, 0–50 000 Years Cal BP. *Radiocarbon*, 55(4), pp.1889–1903.

Howard-Williams, C., 1980. Aquatic macrophyte communities of the Wilderness lakes: community structure and associated environmental conditions. *Journal of the Limnological Society of Southern Africa*, 6, pp.85–92.

Humphries, M.S., Green, A.N. & Finch, J.M., 2016. Evidence of El Niño driven desiccation cycles in a shallow estuarine lake: The evolution and fate of Africa's largest estuarine system, Lake St Lucia. *Global and Planetary Change*, 147, pp.97–105.

Hupfer, M. & Hilt, S., 2008. Lake Restoration. In S. E. Jørgensen & B. D. Fath, eds. *Encyclopedia of Ecology*. Academic Press, pp. 2080–2093.

Illenberger, W.K., 1996. The Geomorphological Evolution of the Wilderness Dune Cordons, South Africa. *Quaternary International*, 33, pp.11–20.

Kasper, T., Haberzettl, T., Doberschütz, S., Daut, G., Wang, J., Zhu, L., Nowaczyk, N. & Mäusbacher, R., 2012. Indian Ocean Summer Monsoon (IOSM)-dynamics within the past 4 ka recorded in the sediments of Lake Nam Co, central Tibetan Plateau (China). *Quaternary Science Reviews*, 39, pp.73–85.

Kelts, K., Briegel, U., Ghilardi, K. & Hsu, K., 1986. The limnogeology-ETH coring system. *Swiss Journal of Hydrology*, 48(1), pp.104–115.

Kirsten, K.L., Haberzettl, T., Wündsch, M., Meschner, S., Smit, A.J., Quick, L.J. & Meadows, M.E., 2018. A multiproxy study of the ocean-atmospheric forcing and the impact of sea-level changes on the southern Cape coast, South Africa during the Holocene. *Palaeogeography, Palaeoclimatology, Palaeoecology*, 496, pp.282–291.

Marker, M.E. & Holmes, P.J., 2002. The distribution and environmental implications of coversand deposits in the Southern Cape, South Africa. *South African Journal of Geology*, 105, pp.135–146.

Marker, M.E. & Holmes, P.J., 2010. The geomorphology of the Coastal Platform in the southern Cape. *South African Geographical Journal*, 92(2), pp.105–116.

Martin, A.R.H., 1962. Evidence relating to the Quaternary history of the Wilderness Lakes. *Transactions of the Geological Society of South Africa*, 65, pp.19–45.

Martin, A.R.H., 1968. Pollen Analysis of Groenvlei Lake Sediments, Knysna (South Africa). *Review of Palaeobotany and Palynology*, 7, pp.107–144.

Martin, A.R.H., 1956. The Ecology and History of Groenvlei. *South African Journal Of Science*, 52(8), pp.187–192.

Martin, A.R.H., 1960. The Ecology of Groenvlei, A South African Fen: Part II. The Secondary Communities. *Journal of Ecology*, 48(1), pp.55–71.

Martin, A.R.H., 1959. The Stratigraphy and History of Groenvlei, a South African Coastal Fen. *Australian Journal of Botany*.

Meyers, P.A., 1994. Preservation of elemental and isotopic source identification of sedimentary organic matter. *Chemical Geology*, 114(3–4), pp.289–302.

Meyers, P.A. & Ishiwatari, R., 1993. Lacustrine organic geochemistry - an overview of indicators of organic matter sources and diagenesis in lake sediments. *Organic Geochemistry*, 20, pp.867–900.

Miller, D.E., Yates, R.J., Jerardino, A. & Parkington, J.E., 1995. Late Holocene Coastal Change in the Southwestern Cape, South Africa. *Quaternary International*, 29/30, pp.3–10.

Mucina, L. & Rutherford, M.C., 2006. *The vegetation of South Africa, Lesotho and Swaziland*, Pretoria: South African National Biodiveristy Institute, Sterlitzia.

Olds, A.A., James, N.C., Smith, M.K.S. & Weyl, O.L.F., 2016. Fish communities of the wilderness

lakes system in the southern Cape, South Africa. *Koedoe*, 58(1), pp.1–10.

Quick, L.J., Chase, B.M., Wundsch, M., Kirsten, K.L., Chevalier, M., Mausbacher, R., Meadows, M.E. & Haberzettl, T., 2018. A high-resolution record of Holocene climate and vegetation dynamics from the southern Cape coast of South Africa : pollen and microcharcoal evidence from Eilandvlei. *Journal of Quaternary Science*, 33(5), pp.487–500.

Quick, L.J., Meadows, M.E., Bateman, M.D., Kirsten, K.L., Mäusbacher, R., Haberzettl, T. & Chase, B.M., 2016. Vegetation and climate dynamics during the last glacial period in the fynbos-afrotemperate forest ecotone, southern Cape, South Africa. *Quaternary International*, 404, pp.136–149.

Ramsay, P.J., 1995. 9000 years of sea-level change along the southern African coastline. *Quaternary International*, 31(1989), pp.71–75.

Reimer, P.J., Bard, E., Bayliss, A., Beck, J.W., Blackwell, P.G., Ramsey, C.B., Buck, C.E., Cheng, H., Edwards, R.L., Friedrich, M., Grootes, P.M., Guilderson, T.P., Haflidason, H., Hajdas, I., Hatté, C., Heaton, T.J., Hoffmann, D.L., Hogg, A.G., Hughen, K.A., Kaiser, K.F., Kromer, B., Manning, S.W., Niu, M., Reimer, R.W., Richards, D.A., Scott, E.M., Southon, J.R., Staff, R.A., Turney, C.S.M. & van der Plicht, J., 2013. IntCal13 and Marine13 Radiocarbon Age Calibration Curves 0–50,000 Years cal BP. *Radiocarbon*, 55(04), pp.1869–1887.

Reinwarth, B., Franz, S., Baade, J., Haberzettl, T., Kasper, T., Daut, G., Helmschrot, J., Kirsten, K.L., Quick, L.J., Meadows, M.E. & Mäusbacher, R., 2013. A 700-year record on the effects of climate and human impact on the southern Cape coast inferred from lake sediments of Eilandvlei, Wilderness Embayment, South Africa. *Geografiska Annaler: Series A, Physical Geography*, 95(4), pp.345–360.

Russel, I.A., 2003. Changes in the distribution of emergent aquatic plants in a brackish South African estuarine-lake system. *African Journal of Aquatic Science*, 28(2), pp.103–122.

Russel, I.A., Randal, R.M., Cole, N., Kraaij, T. & Kruger, N., 2012. *Garden Route National Park, Wilderness Coastal Section, State of Knowledge*,

Russel, I.A., Randal, R.M., Cole, N., Kraaij, T. & Kruger, N., 2010. *Garden Route National Park, Wilderness Coastal Section, State of Knowledge*,

Russell, I.A., 2003. Changes in the distribution of emergent aquatic plants in a brackish South African estuarine-lake system. *African Journal of Aquatic Science*, 28(2), pp.103–122.

Schillereff, D.N., Chiverrell, R.C., Macdonald, N. & Hooke, J.M., 2014. Flood stratigraphies in lake sediments: A review. *Earth-Science Reviews*, 135, pp.17–37.

Strobel, P., Kasper, T., Frenzel, P., Schittek, K., Quick, L.J., Meadows, M.E., Mäusbacher, R. & Haberzettl, T., 2019. Late Quaternary palaeoenvironmental change in the year-round rainfall zone of South Africa derived from peat sediments from Vankervelsvlei. *Quaternary Science Reviews*, 218, pp.200–214.

Watling, R., 1977. *Trace metal distribution in the Wilderness lakes. Special report FIS 147*, Pretoria.

Whitfield, A.K., Weerts, S.P. & Weyl, O.L.F., 2017. A review of the influence of biogeography, riverine linkages, and marine connectivity on fish assemblages in evolving lagoons and lakes of coastal southern Africa. *Ecology and Evolution*, 7(18), pp.7382–7398.

Wilhelm, B., Ballesteros Cánovas, J.A., Macdonald, N., Toonen, W.H.J., Baker, V., Barriendos, M., Benito, G., Brauer, A., Corella, J.P., Denniston, R., Glaser, R., Ionita, M., Kahle, M., Liu, T., Luetscher, M., Macklin, M., Mudelsee, M., Munoz, S., Schulte, L., St. George, S., Stoffel, M. & Wetter, O., 2019. Interpreting historical, botanical, and geological evidence to aid preparations for future floods. *Wiley Interdisciplinary Reviews: Water*, 6(1).

Wündsch, M., Haberzettl, T., Cawthra, H.C., Kirsten, K.L., Quick, L.J., Zabel, M., Frenzel, P., Hahn, A., Baade, J., Daut, G., Kasper, T., Meadows, M.E. & Mäusbacher, R., 2018. Holocene environmental change along the southern Cape coast of South Africa - Insights from the Eilandvlei sediment record spanning the last 8.9kyr. *Global and Planetary Change*, 163, pp.51–66.

Wündsch, M., Haberzettl, T., Kirsten, K.L., Kasper, T., Zabel, M., Dietze, E., Baade, J., Daut, G., Meschner, S., Meadows, M.E. & Mäusbacher, R., 2016a. Sea level and climate change at the southern Cape coast , South Africa , during the past 4.2 kyr. *Palaeogeography, Palaeoclimatology, Palaeoecology*, 446, pp.295–307.

Wündsch, M., Haberzettl, T., Meadows, M.E., Kirsten, K.L., Kasper, T., Baade, J., Daut, G., Stoner, J.S. & Mäusbacher, R., 2016b. The impact of changing reservoir effects on the 14C chronology of a Holocene sediment record from South Africa. *Quaternary Geochronology*, 36, pp.148–160.

Chapter 4

A late Holocene pollen and microcharcoal record from Eilandvlei, southern Cape coast, South Africa

---

N du Plessis[1]

BM Chase[1, 2]

LJ Quick[3]

ME Meadows[1, 4, 5]

[1]*Department of Environmental and Geographical Science, University of Cape Town, Rondebosch, South Africa*

[2]*Centre National de la Recherche Scientifique, Institut des Sciences de l'Evolution-Montpellier, Université Montpellier, Montpellier, France*

[3]*African Centre for Coastal Palaeoscience, Nelson Mandela University, Port Elizabeth, South Africa*

[4]*School of Geographic Sciences, East China Normal University, Shanghai, China*

[5]*College of Geography and Environmental Sciences, Zhejiang Normal University, China*

Status: Accepted: *Palaeoecology of Africa Volume 35: Quaternary Vegetation Dynamics. Special Edition: Contributions to the African Pollen Database*

4.1. Introduction

The Wilderness Embayment has been the focus of multiple studies over the last few years, with recent work from Quick et al. (2018) (pollen), Wündsch et al. (2018) (geochemistry) and Kirsten et al. (2018) (diatoms) producing multi proxy records for Eilandvlei from a longer sequence (EV13) spanning the last ~8900 years. Although of apposite resolution to offer insights on broader climatic and environmental trends during the Holocene, there is a lack of specific focus on the late Holocene. To fill this gap, a shorter sediment core from Eilandvlei (EV11) was analysed for fossil pollen and microcharcoal with the aim of exploring these dynamics on a shorter time scale. This time frame further represents a period of great physiographic change in the Wilderness region, as illustrated in Chapter 3.

This chapter begins with an introduction to Eilandvlei, followed by a description of sediment core EV11. The radiocarbon dating results and age model are then presented, followed by a description and interpretation of the results from the ~3000 year fossil pollen and microcharcoal record from EV11[1]. This record is then discussed in relation to local and regional records to provide a fuller contextualization of the research.

4.2. Site details

Eilandvlei forms part of the Wilderness Lakes system found along the southern Cape coast of South Africa (Figure 4-1). These lakes are located behind Pleistocene dune ridges that run parallel along the coastline. Situated within South Africa's aseasonal rainfall zone, climate is influenced by both temperate and tropical circulation systems.

The regional vegetation is most noteworthy for the extensive development of Southern Afrotemperate Forest (generally *Afrocarpus falcatus* and *Podocarpus latifolius* [in the pollen record we cannot differentiate between these species, as such these are all labelled *Podocarpus* for the purpose of

[1] The data in this chapter have been submitted to Palaeoecology of Africa Volume 35: Quaternary Vegetation Dynamics. Special Edition: Contributions to the African Pollen Database as a data paper, and will broadly follow that format from section 4.2 to 4.5.

this chapter], *Ocotea bullata* (Lauraceae) and *Olea capensis ssp. marcocarpa* (Oleaceae)), which is found in valleys and on the south-facing slopes of the adjacent river catchments (Midgley et al. 2004). A variety of fynbos types also occupy this region including Garden Route Shale Fynbos (distinguished by ericaceous and tall dense proteoid fynbos), Knysna Sand Fynbos (primarily *Erica curvifolia*, *Metalasia densa* (Asteraceae) and *Passerina rigida*) and Southern Cape Dune Fynbos (largely *Olea exasperata*, *Phylica litoralis* and a variety of *Searsia* species) (Mucina and Rutherford 2006; Quick et al. 2018).

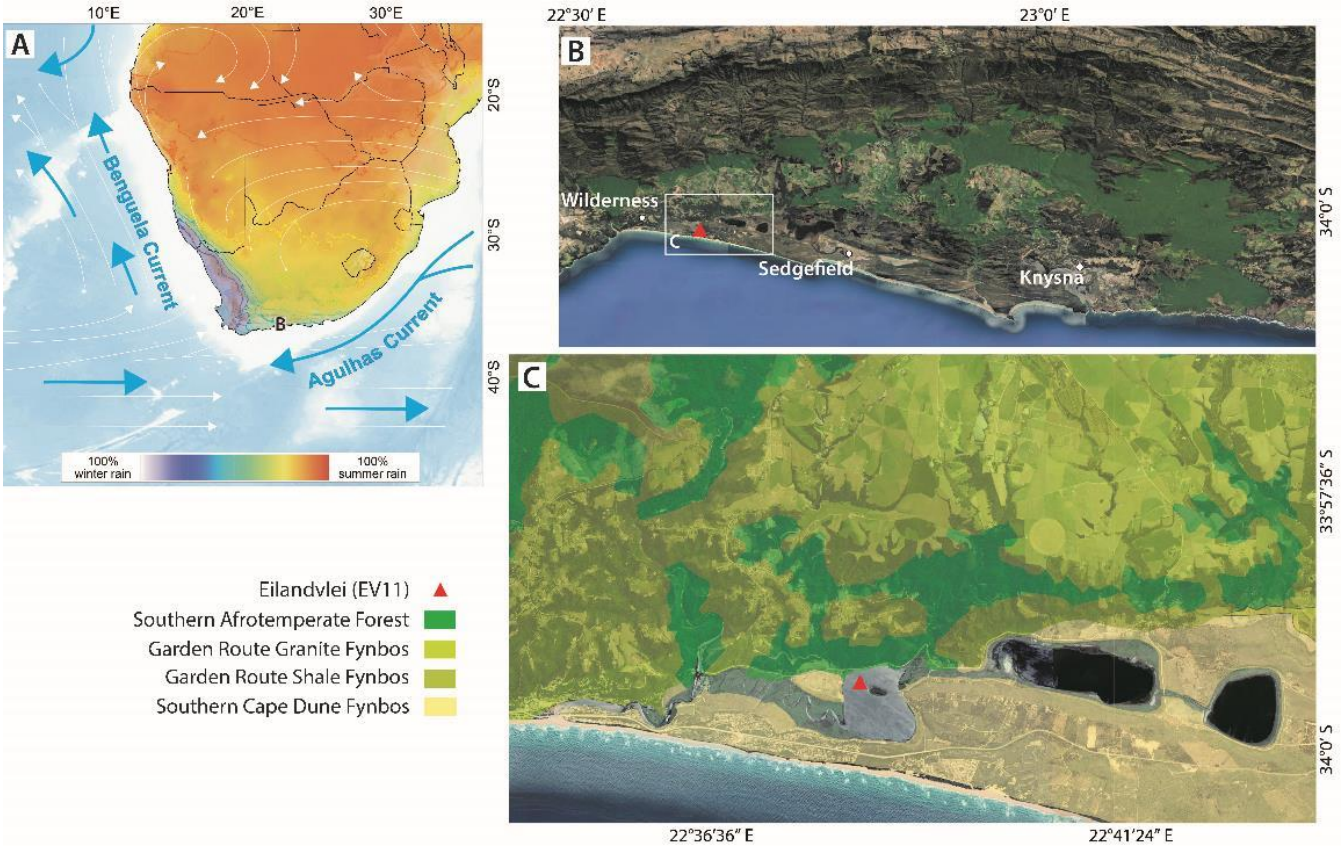

Figure 4-1: A. Map of southern Africa showing seasonality of rainfall and sharp climatic gradients dictated by the zones of summer/tropical (red) and winter/temperate (blue) rainfall dominance. Major atmospheric (white arrows) and oceanic (blue arrows) circulation systems are indicated. **B.** A section of the southern Cape coast between the towns of Wilderness and Knysna indicating the location of Eilandvlei and the current extent of Afrotemperate forest in the region. **C.** The location of EV11 and the contemporary distribution of the dominant vegetation types (Mucina and Rutherford 2006).

4.3. Sediment description and methods

EV11 (33°59’23.10” S, 22°38’17.60” E) (Figure 4-1) was retrieved using a portable vibracorer mounted on a floating platform. The final core length measured ~1.54 m. The stratigraphy of EV11 (Figure 4-2) is relatively uniform primarily comprising of fine to coarse silts, with the top 14 cm consisting of distinctly darker sandy clay.

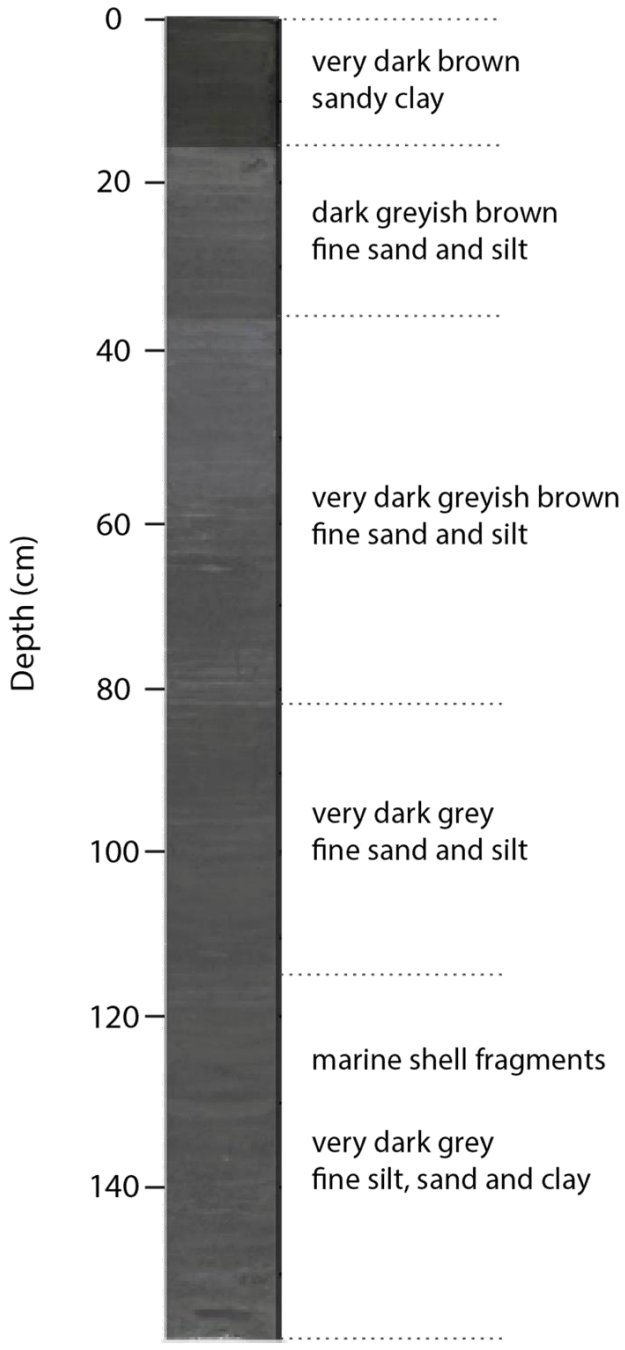

Figure 4-2: Core image and sediment description for EV11

Forty-seven subsamples, with a minimum weight of 2 g, were analysed using standard palynological methods as per Faegri and Iversen (1989) and Moore *et al.* (1991) with adaptations for dense media separation (Nakagawa *et al.* 1998). Pollen grains were examined and counted using a Zeiss Axiostar Plus microscope. Identifications were achieved through comparison with reference material from the Environmental and Geographical Science department at the University of Cape Town and published material (Van Zinderen Bakker 1953, Van Zinderen Bakker and Coetzee 1959, Welman and Kuhn 1970 and Scott 1982). Charcoal particles were counted together with the pollen grains using the particle count method (Tinner and Hu 2003). Fragments were classified according to size: 10 – 50 µm and 50 – 100 µm. The exotic marker *Lycopodium* was added during preparation to enable pollen and charcoal concentrations to be calculated (one tablet per sample; Lund University, Batch # 483216, 18583±1708 spores per tablet). Two samples were omitted due to insufficient pollen concentrations; depths 80 and 138 cm. A total pollen sum of 500 grains, or three slides, was achieved for each sample. On considering the results, it was deemed appropriate to remove the local aquatic components and Amaranthaceae from the pollen sum. Pollen assemblage zones were determined by the use of cluster analysis by the application of CONISS (Constrained Incremental Sum of Squares) (Grimm 1987) – all identified taxa were included in this analysis.

4.4. Dating

Seven organic bulk sediment samples were selected for AMS-^{14}C dating (Table 4-1). The two top samples returned pre-bomb ages and were calibrated using CALIBomb (Reimer et al. 2004). The remainder of the samples were calibrated with the Marine13 data set (Reimer et al. 2013) with a marine reservoir correction of $\Delta R = 252 \pm 64$ (Wündsch et al. 2016b). The age-depth model (Figure 4-3) was developed with the R software package Bacon (v2.2) (Blaauw and Christen 2011).

EV11 has a median basal age of 3165 $^{+195}/_{-260}$ cal BP as determined from the ^{14}C results (Table 4-1). The age-depth model (Figure 4-3) suggests continuous deposition with the sedimentation rate ranging from 0.02 to 0.48 cm y^{-1} and an average of 0.09 cm y^{-1}.

Table 4-1: Radiocarbon and calibration details for EV11

Sample	Depth (cm)	^{14}C age [yr BP]	cal BP	1 σ error	Calibration data set	ΔR	2σ cal age range [cal BP]	Median probability [cal BP]
EV11-1	0	-	-58.9	-	CALIBomb	-	-	-
EV11-2	20	-	-5.6	-	CALIBomb	-	-	-
EV11-3	40	470	-	30	Marine13	252 ± 64	340 - 352 451 - 526	497
EV11-7	78	1290	-	30	Marine13	252 ± 64	1072 - 1192 1206 - 1268	1171
EV11-4	102	2140	-	30	Marine13	252 ± 64	2002 - 2154 2276 - 2287	2074
EV11-6	134	3300	-	30	Marine13	252 ± 64	3397 - 3568	3485
EV11-5	151	3620	-	30	Marine13	252 ± 64	3726 - 3751 3791 - 3794 3820 - 3980	3880

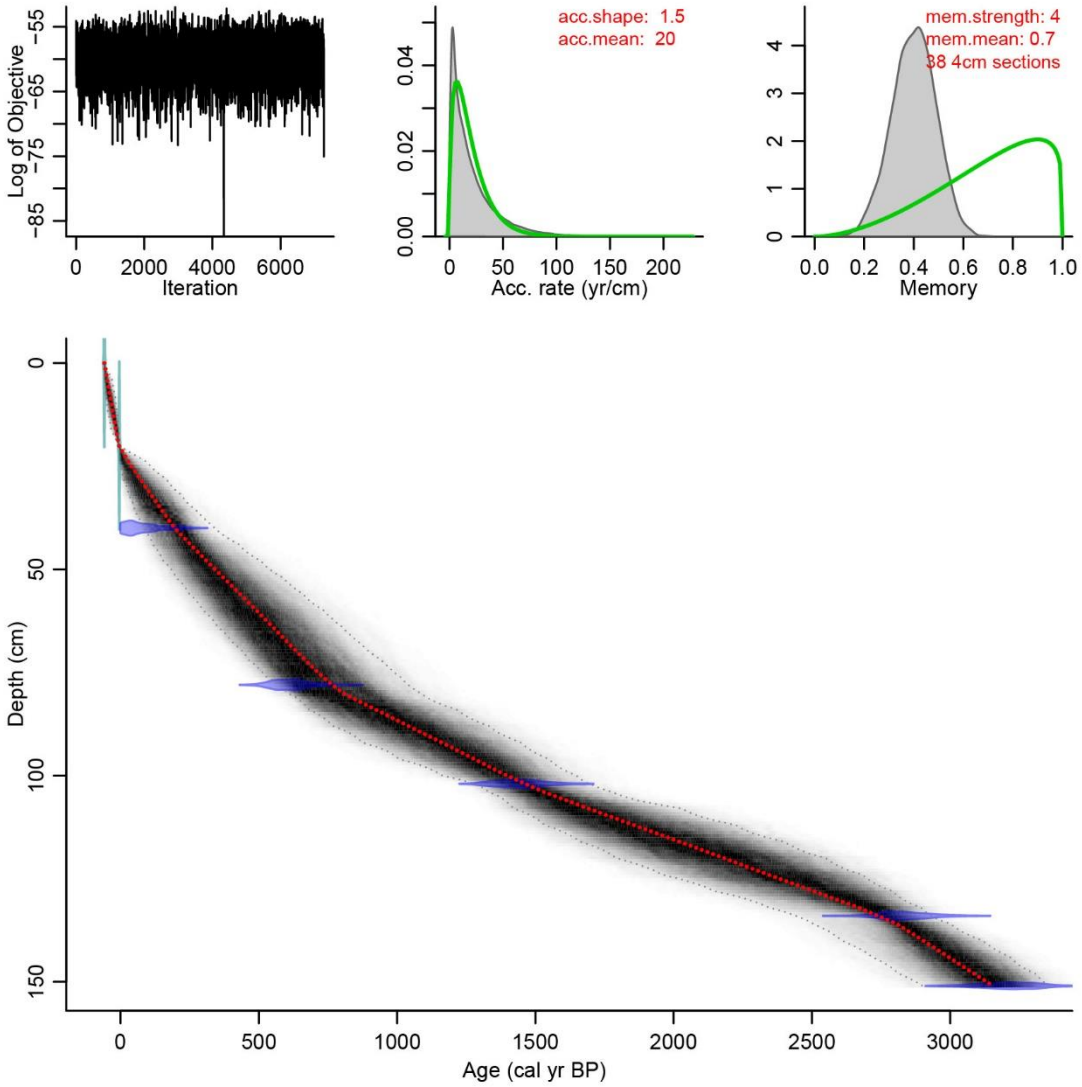

Figure 4-3: The EV11 age-depth model. The 2σ probability distribution of calibrated ^{14}C ages is presented in blue and the 95% confidence intervals are represented by the grey dotted line. The red line represents the best model according to the weighted mean age at each depth.

4.5. Results and interpretation

In total 65 taxa were identified. Pollen concentrations range from 6.26 x 103 grains.g-1 near the base, to a maximum of 7.86 x 104 grains.g-1 around the top of the assemblage, with an average of 2.72 x 104 grains.g-1. The EV11 record extends from c. 3100 cal yr BP to present. The sequence is divided into five pollen zones labelled EV11-A to E.

The EV11 pollen assemblage (Figure 4-4) is summarised according to ecological affinity focusing on the predominant vegetation types found in the region today. Fynbos dominates the EV11 assemblage with the coastal lowland elements Ericaceae, Restionaceae and *Stoebe*-type most common. The coastal thicket group is largely represented by *Euclea*, *Olea* and *Rhus*, with *Euphorbia* the largest contributor to the succulent and/or drought resistant group. *Podocarpus* is the main constituent of the Aftrotemperate forest group. The limited presence of other forest taxa in this group is likely related to the low pollen productivity and differential pollen dispersal methods of some forest taxa (Jackson and Kearsley 1998; Jackson and Williams 2004; Lowe and Walker 1997). *Podocarpus* pollen is very successfully dispersed through wind, and as such its presence in the assemblage could rather be a reflection of more regional conditions due to long-distance transport - this could additionally result in *Podocarpus* being overrepresented in the pollen record (Jackson and Kearsley 1998; Jackson and Williams 2004; Roy et al. 2018). These considerations aside, it has been illustrated that *Podocarpus* is an effective indicator of aridity/humidity the region (e.g. du Plessis et al. 2020 (this thesis); Martin 1968; Quick et al. 2018) (with aridity/humidity being distinct from rainfall amount per se [see Chevalier & Chase 2016]).

EV11-A *(c. 3100 – 2560 cal yr BP)*

Elevated levels of drought resistant taxa (i.e. Aizoaceae, *Pentzia*-type and *Euphorbia*) are seen at the onset of record with *Euphorbia* present throughout the zone. *Stoebe*-type percentages are similarly increased, though decline towards the top of zone. Ericaceae pollen percentages are somewhat higher in comparison to the zone above. Afrotemperate forest pollen (primarily *Podocarpus*) increase after c.

3000 cal yr BP, with coastal thicket taxa (mostly *Olea, Searsia* and *Euclea*) well represented from the start of the record. Significant peaks in charcoal concentration is noted at c. 2910 and 2600 cal yr BP, with maximum counts of the large charcoal fragments (50 – 100 µm) coinciding with the second peak at c. 2600 cal yr BP (Figure 4-5). Taken together, these trends suggest that moisture availability was fairly limited with large fire events likely related to these drier conditions. Rainfall seasonality was however gradually declining over this period, allowing for the increasing presence of Afrotemperate forest.

EV11-B *(c. 2560 – 1560 cal yr BP)*

Zone B is strongly dominated by the halophytic taxon Amaranthaceae with a distinct increase after c. 2600 cal yr BP. This could be representative of expanding salt marsh vegetation in response to lower sea levels. Fluctuating Afrotemperate forest pollen percentages are noted from around c. 2400 cal yr BP until c.1600 cal yr BP with maximum charcoal concentrations (Figure 4-5) concomitant with the increased presence of *Podocarpus* at c. 2260 cal yr BP. Restionaceae is more prominent in this zone than elsewhere in the record.

EV11-C *(c. 1560 – 670 cal yr BP)*

Podocarpus pollen is more prominent here in comparison to the zones below, with sporadic appearances of other wet forest elements, i.e. *Cunonia,* Icacinaceae and *Ilex*, likely representing a phase of forest expansion. At the same time, fynbos (largely Ericaceae) show a moderate decline towards the top of the zone. This could indicate a shift towards a more mesic environment with reduce rainfall seasonality, promoting the growth of Afrotemperate forest taxa.

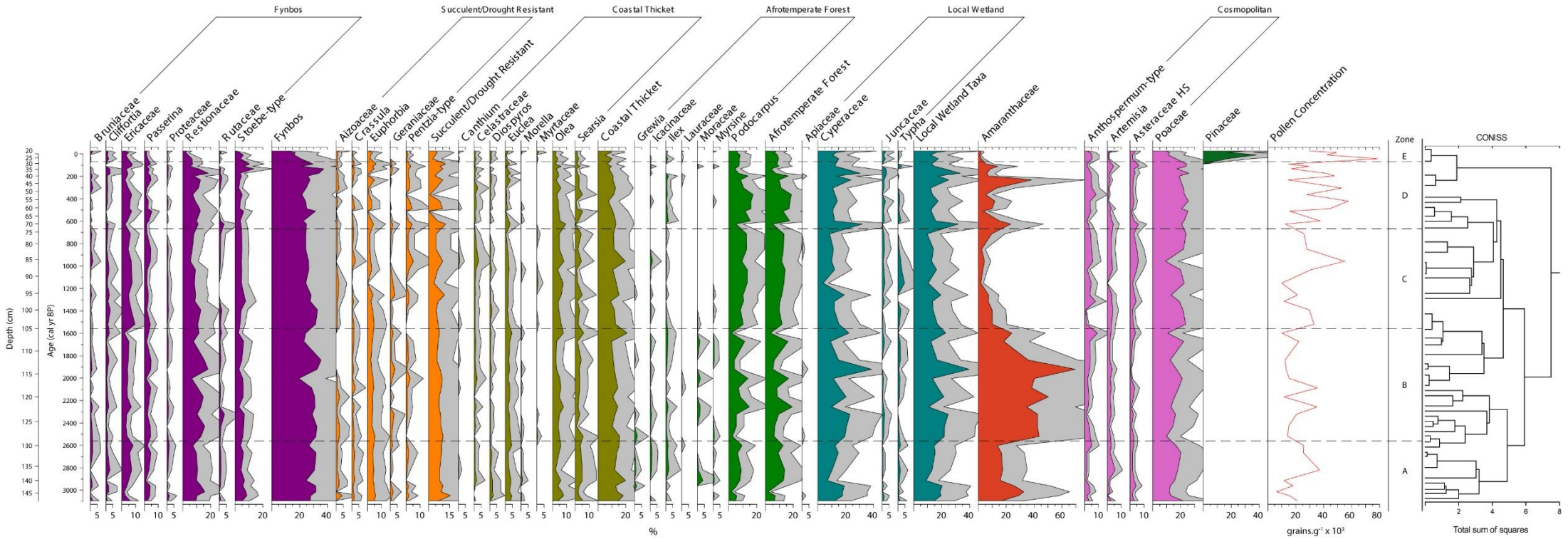

Figure 4-4: Relative pollen percentage diagram for EV11 organized according to ecological affinity. Exaggeration curves are 4x for taxa present between 5 and 2%, and 2x for those above 5%. Zonation of the diagram is based on cluster analysis results from CONISS.

EV11-D *(670 – 70 cal yr BP/AD 1880)*

Forest development continues until c. 360 cal yr BP, with a sudden break in this trend around 620 cal yr BP. After c. 360 cal yr BP a rather abrupt decline in Afrotemperate forest pollen is noted. Drought resistant taxa (mostly *Euphorbia*) become more prevalent from this point with a rapid increase in *Stoebe*-type pollen around 130 cal yr BP. These vegetation responses are likely a result of the cooler and drier conditions experienced in the region during the latter part of the Little Ice Age (LIA).

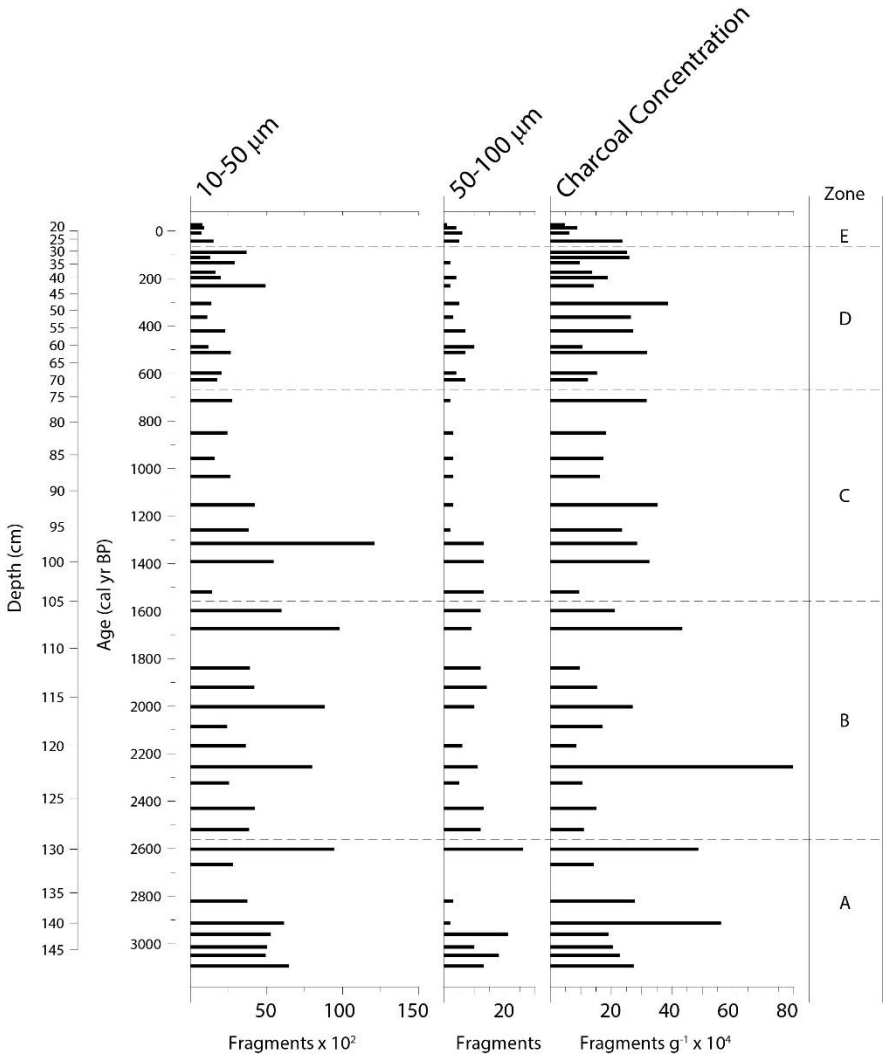

Figure 4-5: Charcoal counts and concentration for EV11. Charcoal and pollen concentrations were calculated in the same manner using Lycopodium spore counts. The zonation of the diagram is the same as for the pollen diagram.

EV11-E *(c. 70 to -30 cal yr BP/c. AD 1880 to 1980)*

The most recent part of the record is characterised by the appearance of *Pinus* pollen c. AD 1910 marking the onset of the anthropogenic influence in the region.

4.6. Reconstruction of Late Holocene environments inferred from the EV11 record

Having identified the main trends in pollen and, accordingly, vegetation, these are now discussed in the context of the key climatic, and geomorphic, mechanisms that are interpreted as underlying the observed changes and compared with other appropriate local and regional records.

Prior to ~3000 cal yr BP, the Wilderness region experienced seasonal and relatively arid conditions, likely accompanied by the increased prevalence of periods of summer drought (Quick et al. 2018; Wündsch et al. 2016a; Wündsch et al. 2018). A comparatively dry environment can be inferred from the first ~100 years of the EV11 record by the prevalence of succulent/drought resistant taxa as well as the dry heath elements *Stoebe*-type and *Passerina*. A significant peak in charcoal concentration is further noted at c. 2900 cal yr BP, signifying a large fire event, likely resulting from these drier conditions.

This phase appears to have been followed by a gradual trend towards reduced rainfall seasonality as inferred in the EV11 record (increasing Afrotemperate forest pollen; Figure 4-4, 4-8) which may also be related to a decline in the incidence of summer drought resulting from the increasing influence of tropical circulation systems along the south coast. This is also seen in the EV13 record (Quick et al. 2018; Wündsch et al. 2018) with similar conditions recorded at nearby Groenvlei (Wündsch et al. 2016a).

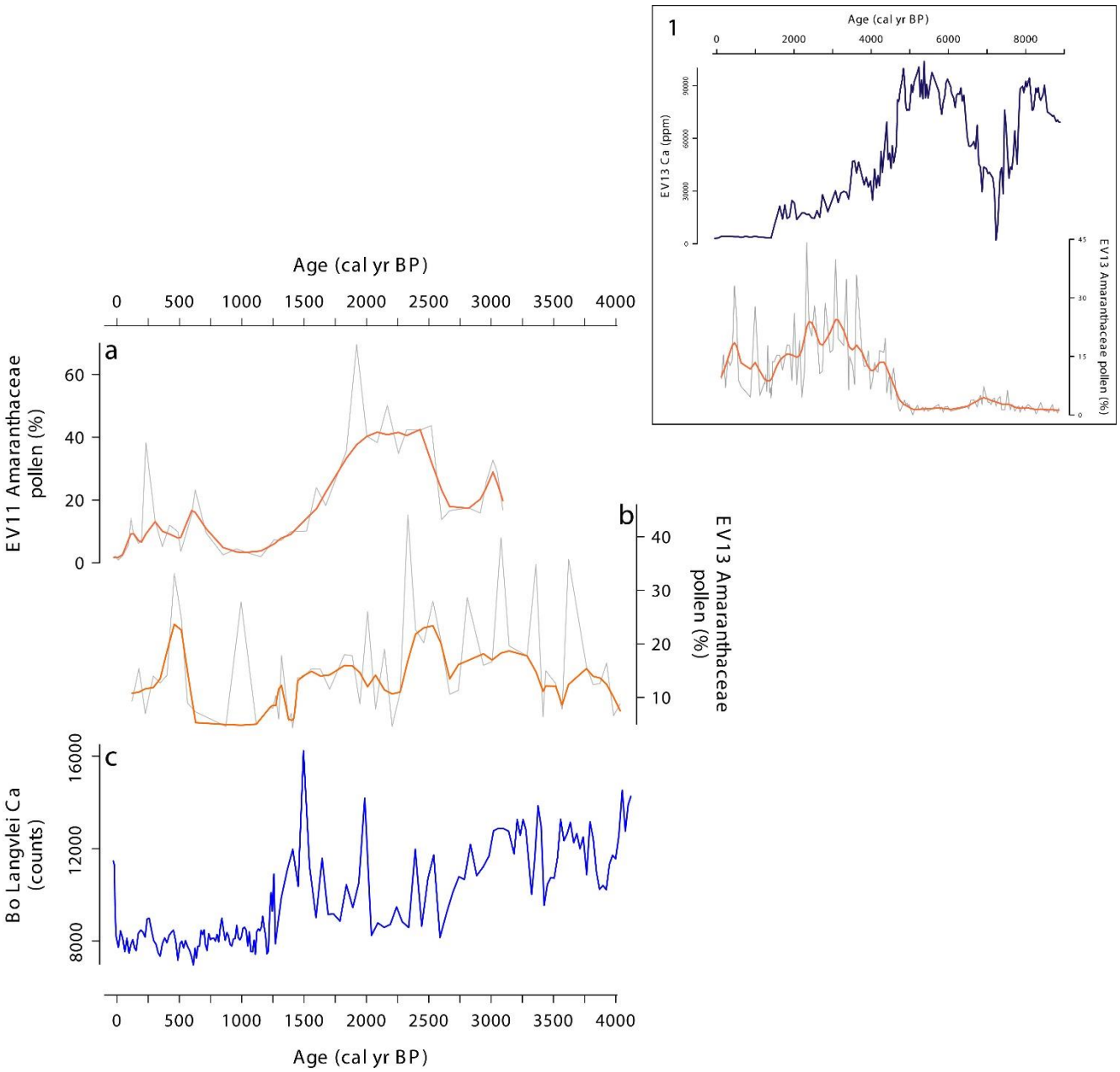

Figure 4-6: Comparison of Amaranthaceae pollen and geochemical marine indicators illustrating the relationship between sea level and salt marsh vegetation. Increased Ca values equate to elevated sea levels: **Inset 1:** The complete EV13 Amaranthaceae pollen (Quick et al. 2018) and Ca (Wündsch et al. 2018) records; **a)** EV11 Amaranthaceae pollen percentages; **b)** shortened EV13 Amaranthaceae pollen record; **c)** Bo Langvlei Ca record (this thesis).

Between c. 2600 and 1900 cal yr BP, the overriding feature in the EV11 record is the expansion of salt marsh vegetation (Figure 4-4). A sea level lowstand is reported along the West Coast at this time (Compton 2001; 2006), this signal is also present in adjacent Bo Langvlei (this thesis; Figure 4-6).

Indications are thus that as lake water levels declined in response to retreating sea levels, halophytic vegetation, as indicated by the frequencies of Amaranthaceae pollen, was able to occupy the newly exposed mud flats. Interestingly, the highest Amaranthaceae percentages in the EV13 record are present earlier, from c. 3700 to 2300 cal yr BP (Quick et al. 2018; Figure 4-6). It is proposed that this offset could be related to the different locations of the two cores (Figure 4-7) – with the coring site of EV13 closer to the coast, the area around EV13 may have been colonised by Amaranthaceae before that of EV11. In addition, the presence of the island in the lake may influence hydrodynamics and sedimentation, hence pollen accumulation, within the lake (Barreto et al. 2012; Luz et al. 2005).

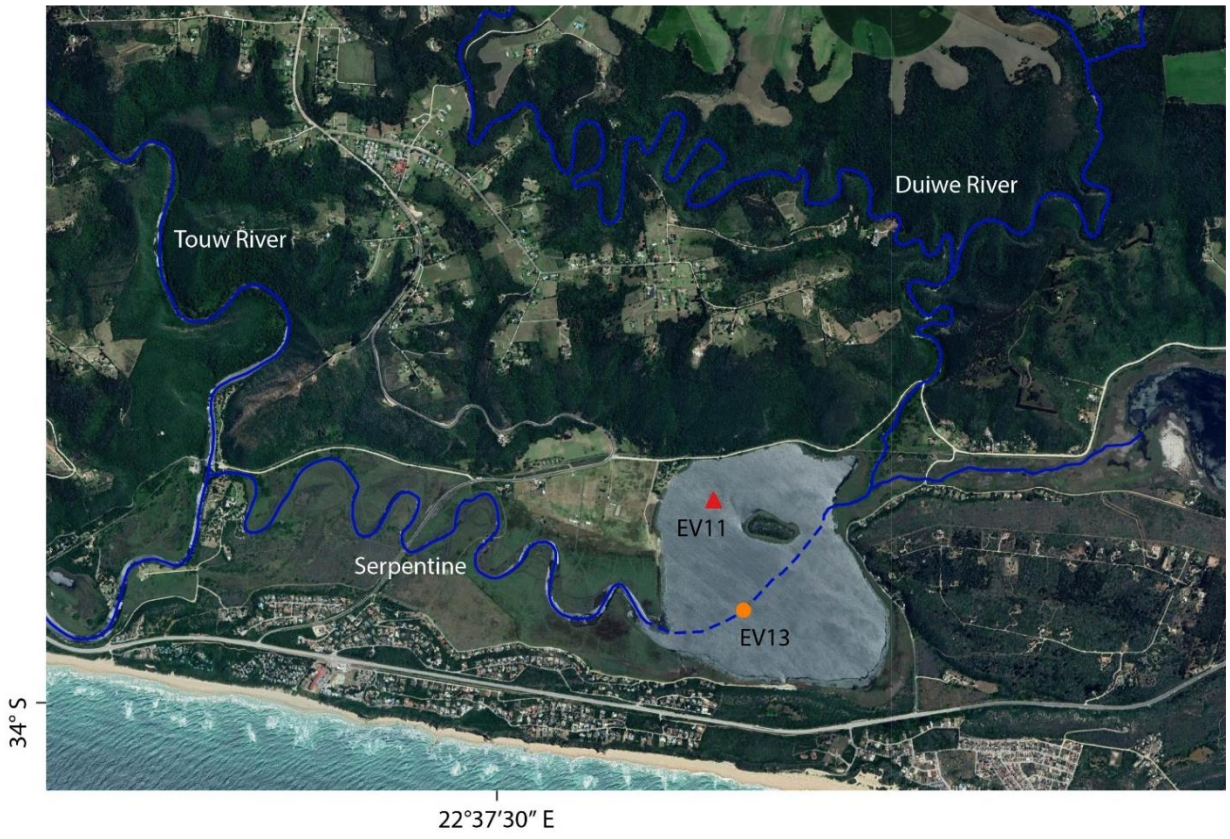

Figure 4-7: The coring locations of EV11 and EV13

No obvious trends with regard to climate are further evident during this period but significant variability in Afrotemperate forest pollen percentages between c. 2600 and 1600 cal yr BP (Figure 4-8), and the prominence of Restionaceae is noteworthy. This variability is also seen in the EV13 pollen

record at this time (Quick et al. 2018) (Figure 4-8). A phase of widespread aeolian deposition and dune mobility has been identified in the Wilderness region between c. 3700 and 2400 cal yr BP, possibly extending to around 1300 cal yr BP (Martin 1962, 1968; Bateman et al. 2011). Taken together with sea level fluctuations, it is suggested that environmental conditions at this time were highly dynamic and that, although the variability observed in the pollen assemblage might be related to climatic factors, it is rather a reflection of the changing landscape dynamics in the Wilderness Embayment as a whole. Additionally, the increased prevalence of Restionaceae, likely *Restio eleocharis* (Martin 1968), is consistent with the spread of pioneer scrub vegetation on the dunes (Martin 1968).

A period of more extensive forest development is evident after c. 1600 cal yr BP extending to c. 710 cal yr BP, consistent with Martin's (1968) 'last phase of forest expansion*'* as recorded at nearby Groenvlei (Figure 4-8). Similar trends are present in the pollen sequences from EV13 (Quick et al. 2018) and Bo Langvlei (this thesis) although the onset of this "phase" is indicated to be later in both – from c. 950 cal yr BP in EV13 and at Bo Langvlei this phase is evident between c. 750 and 550 cal yr BP (Figure 4-8). A further period of increased Afrotemperate forest pollen percentages is seen in the EV11 record between c. 600 and 360 cal yr BP. A resurgence in dune activity was proposed at this time (Bateman et al. 2011) which could explain the offsets in the records.

A strong LIA signal is evident in the rapid increase in *Stoebe*-type pollen c. 130 cal yr BP and the sharp decline in Afrotemperate forest pollen after c. 360 cal yr BP, suggesting cold and dry climatic conditions, as in adjacent Bo Langvlei (this thesis). The high *Stoebe*-type percentages are however also concomitant with the arrival of European settlers in the area. Although *Pinus* is only present in the record from ~AD 1910 (c. 40 cal yr BP), the increased representation of *Stoebe*-type could indeed be the first signal of anthropogenically related disturbances in the region (Meadows et al. 1996). This pattern is similarly recorded in the Bo Langvlei pollen record where *Pinus* appears for the first time around ~AD 1850 (c. 100 cal yr BP).

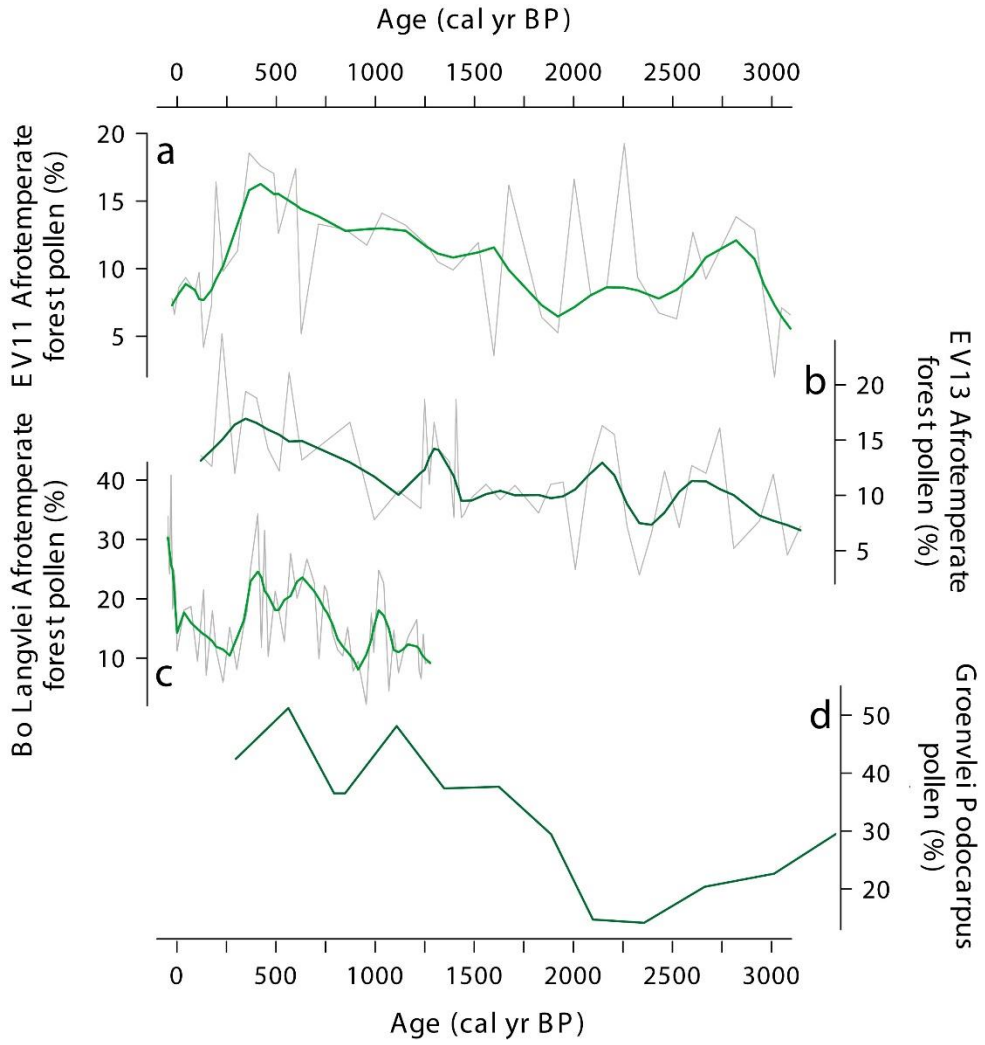

Figure 4-8: Comparison of local Afrotemperate forest pollen records: **a)** EV11 Afrotemperate forest pollen percentages; **b)** EV13 Afrotemperate forest pollen percentages (Quick et al. 2018); **c)** Bo Langvlei Afrotemperate forest percentages (this thesis); **d)** Groenvlei *Podocarpus* pollen percentages (Martin 1968).

4.7. Conclusion

This chapter presented palynological and microcharcoal records from EV11 and the main trends reflected therein. The key findings indicate a gradual shift towards more aseasonal conditions after c. 3000 cal yr BP. A period of great geomorphic instability from ~2600 cal yr BP to around 1600 cal yr BP largely overshadow any climatic signals that would be apparent in the record here. It would seem that receding sea levels and dune accretion are the major drivers of landscape change at this time. A

prominent phase of forest expansion was identified between c. 1600 and 360 cal yr BP followed by abrupt cooling and aridity typifying the LIA.

In general, the EV11 record shows good agreement with other prominent palynological records from the Wilderness. It is however interesting to note that, although the broader trends in the EV11 and EV13 pollen records agree, finer-scale differences are apparent. These may be a result of internal lake dynamics and sediment deposition while the possible impact of the different coring locations on the results cannot be ignored. In addition, while the EV11 record is shorter, it is of higher temporal resolution which could further account for some of the discrepancies observed between the two records.

4.8. Acknowledgements

This study was funded in part by the German Federal Ministry of Education and Research (BMBF). The investigations were conducted as part of a pilot study for the collaborative project 'Regional Archives for Integrated Investigations' (RAiN), embedded in the international research program SPACES (Science Partnership for the Assessment of Complex Earth System Processes).

4.9. References

Barreto, C.F., Vilela, C.G., Baptista-Neto, J.A. & Barth, O.M., 2012. Spatial distribution of pollen grains and spores in surface sediments of Guanabara Bay, Rio de Janeiro, Brazil. *Anais da Academia Brasileira de Ciencias*, 84(3), pp.627–643.

Bateman, M.D., Carr, A.S., Dunajko, A.C., Holmes, P.J., Roberts, D.L., McLaren, S.J., Bryant, R.G., Marker, M.E. & Murray-Wallace, C.V., 2011. The evolution of coastal barrier systems: a case study of the Middle-Late Pleistocene Wilderness barriers, South Africa. *Quaternary Science Reviews*, 30(1–2), pp.63–81.

Blaauw, M. & Christen, J.A., 2011. Flexible paleoclimate age-depth models using an autoregressive gamma process. *Bayesian Analysis*, 6(3), pp.457–474.

Chevalier, M. & Chase, B.M., 2016. Determining the drivers of long-term aridity variability: A southern African case study. *Journal of Quaternary Science*, 31(2), pp.143–151.

Compton, J.S., 2001. Holocene sea-level fluctuations inferred from the evolution of depositional

environments of the southern Langebaan Lagoon salt marsh, South Africa. *The Holocene*, 11(4), pp.395–405.

Compton, J.S., 2006. The mid-Holocene sea-level highstand at Bogenfels Pan on the southwest coast of Namibia. *Quaternary Research*, 66(2), pp.303–310.

Faegri, K. & Iversen, J., 1989. *Textbook of Pollen Analysis*, Chichester: John Wiley & Sons Ltd.

Grimm, E.C., 1987. CONISS: A Fortran 77 program for stratigraphically constrained cluster analysis by the method of incremental sum of squares. *Computers & Geosciences*, 13, pp.13–35.

Jackson, S.T. & Kearsley, J.B., 1998. Quantitative Representation of Local Forest Composition in Forest-Floor Pollen Assemblages. *Journal of Ecology*, 86(3), pp.474–490.

Jackson, S.T. & Williams, J.W., 2004. Modern Analogs in Quaternary Paleoecology: Here Today, Gone Yesterday, Gone Tomorrow? *Annual Review of Earth and Planetary Sciences*, 32(1), pp.495–537.

Kirsten, K.L., Haberzettl, T., Wündsch, M., Meschner, S., Smit, A.J., Quick, L.J. & Meadows, M.E., 2018. A multiproxy study of the ocean-atmospheric forcing and the impact of sea-level changes on the southern Cape coast, South Africa during the Holocene. *Palaeogeography, Palaeoclimatology, Palaeoecology*, 496, pp.282–291.

Lowe, J.J. & Walker, M.J.C., 1997. *Reconstructing Quaternary Environments*, London: Longman.

Luz, C.F.P., Barth, O.M. & Silva, C.G., 2005. Spatial distribution of palynomorphs in the surface sediments of the Lagoa do Campelo lake, North region of Rio de Janeiro State, Brazil. *Acta Botanica Brasilica*, 19(4), pp.741–752.

Martin, A.R.H., 1962. Evidence relating to the Quaternary history of the Wilderness Lakes. *Transactions of the Geological Society of South Africa*, 65, pp.19–45.

Martin, A.R.H., 1968. Pollen Analysis of Groenvlei Lake Sediments, Knysna (South Africa). *Review of Palaeobotany and Palynology*, 7, pp.107–144.

Meadows, M.E., Baxter, A.J. & Parkington, J., 1996. Late Holocene Environments at Verlorenvlei, Western Cape Province, South Africa. *Quaternary International*, 33, pp.81–95.

Midgley, J.J., Cowling, R.M., Seydack, A.H.W. & van Wyk, G.F., 2004. Forest. In R. M. Cowling, D. M. Richardson, & S. M. Pierce, eds. *Vegetation of Southern Africa*. Cambridge: Cambridge University Press, Cambridge, UK, pp. 278–296.

Moore, P.D., Webb, J.A. & Collinson, M.E., 1991. *Pollen Analysis* 2nd ed., Oxford: Blackwell Scientific Publications.

Mucina, L. & Rutherford, M.C., 2006. *The vegetation of South Africa, Lesotho and Swaziland*, Pretoria: South African National Biodiveristy Institute, Sterlitzia.

Nakagawa, T., Brugiapaglia, E., Digerfeldt, G., Reille, M., De Beaulieu, J.-L. & Yasuda, Y., 1998. Dense media separation as a more efficient pollen extraction method for use with organic sediment/deposit samples: comparison with the conventional method. *Boreas*, 27, pp.15–24.

du Plessis, N., Chase, B.M., Quick, L.J., Haberzettl, T., Kasper, T. & Meadows, M.E., 2020. Vegetation and climate change during the Medieval Climate Anomaly and the Little Ice Age on the southern Cape coast of South Africa: Pollen evidence from Bo Langvlei. *The Holocene*, 30(12), pp.1716–1727.

Quick, L.J., Chase, B.M., Wundsch, M., Kirsten, K.L., Chevalier, M., Mausbacher, R., Meadows, M.E. & Haberzettl, T., 2018. A high-resolution record of Holocene climate and vegetation dynamics from the southern Cape coast of South Africa : pollen and microcharcoal evidence from Eilandvlei. *Journal of Quaternary Science*, 33(5), pp.487–500.

Reimer, P.J., Bard, E., Bayliss, A., Beck, J.W., Blackwell, P.G., Ramsey, C.B., Buck, C.E., Cheng, H., Edwards, R.L., Friedrich, M., Grootes, P.M., Guilderson, T.P., Haflidason, H., Hajdas, I., Hatté, C., Heaton, T.J., Hoffmann, D.L., Hogg, A.G., Hughen, K.A., Kaiser, K.F., Kromer, B., Manning, S.W., Niu, M., Reimer, R.W., Richards, D.A., Scott, E.M., Southon, J.R., Staff, R.A., Turney, C.S.M. & van der Plicht, J., 2013. IntCal13 and Marine13 Radiocarbon Age Calibration Curves 0–50,000 Years cal BP. *Radiocarbon*, 55(04), pp.1869–1887.

Reimer, P.J., Brown, T.A. & Reimer, R.W., 2004. Discussion: Reporting and Calibration of Post-Bomb 14C Data. *Radiocarbon*, 46(3), pp.1299–1304.

Roy, I., Ranhotra, P.S., Shekhar, M., Bhattacharyya, A., Pal, A.K., Sharma, Y.K., Singh, S.P. & Singh, U., 2018. Over-representation of some taxa in surface pollen analysis misleads the interpretation of fossil pollen spectra in terms of extant vegetation. *Tropical Ecology*, 59(2), pp.339–350.

Scott, L., 1982. Late quaternary fossil pollen grains from the Transvaal, South Africa. *Review of Palaeobotany and Palynology*, 36(3–4), pp.241–278.

Tinner, W. & Hu, F.S., 2003. Size parameters, size-class distribution and area-number relationship of microscopic charcoal: relevance for fire reconstruction. *The Holocene*, 13(4), pp.499–505.

Welman, W.G. & Kuhn, L., 1970. *South African pollen grains and spores, Volume VI*, Amsterdam-Cape Town: Balkema.

Wündsch, M., Haberzettl, T., Cawthra, H.C., Kirsten, K.L., Quick, L.J., Zabel, M., Frenzel, P., Hahn,

A., Baade, J., Daut, G., Kasper, T., Meadows, M.E. & Mäusbacher, R., 2018. Holocene environmental change along the southern Cape coast of South Africa - Insights from the Eilandvlei sediment record spanning the last 8.9kyr. *Global and Planetary Change*, 163, pp.51–66.

Wündsch, M., Haberzettl, T., Kirsten, K.L., Kasper, T., Zabel, M., Dietze, E., Baade, J., Daut, G., Meschner, S., Meadows, M.E. & Mäusbacher, R., 2016a. Sea level and climate change at the southern Cape coast , South Africa , during the past 4.2 kyr. *Palaeogeography, Palaeoclimatology, Palaeoecology*, 446, pp.295–307.

Wündsch, M., Haberzettl, T., Meadows, M.E., Kirsten, K.L., Kasper, T., Baade, J., Daut, G., Stoner, J.S. & Mäusbacher, R., 2016b. The impact of changing reservoir effects on the 14C chronology of a Holocene sediment record from South Africa. *Quaternary Geochronology*, 36, pp.148–160.

Van Zinderen Bakker, E.M., 1953. *South African Pollen Grains and Spores, Volume I*, AA Balkema.

Van Zinderen Bakker, E.M. & Coetzee, J.A., 1959. *South African Pollen Grains and Spores, Volume III*, Cape Town: AA Balkema.

Chapter 5

Revisiting Vankervelsvlei: A ~650 year pollen and microcharcoal record from an endorheic wetland, southern Cape coast, South Africa

---

N du Plessis[1]

BM Chase[1, 2]

LJ Quick[3]

P Strobel[4]

T Haberzettl[5]

ME Meadows[1, 6, 7]

[1]*Department of Environmental and Geographical Science, University of Cape Town, Rondebosch, South Africa*

[2]*Centre National de la Recherche Scientifique, Institut des Sciences de l'Evolution-Montpellier, Université Montpellier, Montpellier, France*

[3]*African Centre for Coastal Palaeoscience, Nelson Mandela University, Port Elizabeth, South Africa*

[4]*Physical Geography, Institute of Geography, Friedrich Schiller University Jena, Germany*

[5]*Physical Geography, Institute of Geography and Geology, University of Greifswald, Germany*

[6]*School of Geographic Sciences, East China Normal University, Shanghai, China*

[7]*College of Geography and Environmental Sciences, Zhejiang Normal University, China*

Status: Accepted: *Palaeoecology of Africa Volume 35: Quaternary Vegetation Dynamics. Special Edition: Contributions to the African Pollen Database*

5.1. Introduction

Vankervelsvlei presents a unique environment for both palaeoecological and palaeoclimatological study, not only due to its location within the modern year round rainfall zone (*sensu* Chase and Meadows, 2007) but also as it is situated at the ecotone between the Afrotemperate Forest and Fynbos biomes. Furthermore, there is still debate about the exact nature of this waterbody - characterised previously as a floating bog or Schwingmoor (Irving and Meadows 1997; Quick 2013; Quick et al. 2016) and more recently reinterpreted as a fen (Strobel et al. 2019).

Although the sediments at Vankervelsvlei have been the subject of several palaeoenvironmental reconstructions, the late Holocene has not thus far been well resolved, leaving scope for further investigation. In light of this, the aim of this study was to obtain a more complete late Holocene record of palaeoenvironmental change in and around Vankervelsvlei to try and resolve this information gap.

A brief review of the previous studies from Vankervelsvlei are presented first in order to provide a basis for the current ongoing work while also highlighting the challenges and constraints involved in obtaining suitable samples and robust chronologies from this complex depositional environment. This is followed by an introduction to this unusual waterbody and a sediment description of the top section of composite core VVV16 on which this study is based. Details relating to the dating and age model for this section of VVV16 are further provided before presenting a description and interpretation of the results from the ~650 year fossil pollen and microcharcoal record[1]. This record is then analysed in comparison to the existing pollen records.

[1] This record has been submitted to Palaeoecology of Africa Volume 35: Quaternary Vegetation Dynamics, Special Edition: Contributions to the African Pollen Database in the form of a data paper and will broadly follow that format from section 5.3 to 5.6.

5.2. Previous studies from Vankervelsvlei

5.2.1. Why do we keep going back?

Peat bogs (or peatlands) are considered to be rather scarce in the southern Hemisphere in general, although they have been extensively studied from a palaeoenvironmental perspective especially in eastern North America and parts of western Europe (Moore 2002). In South Africa, such deposits are unusual, mainly due to the relatively arid climates and steep topography, although they are more frequent in northern KwaZulu-Natal along the tropical coastal plain (Thamm et al. 1996; Grundling et al. 1998; Finch and Hill 2008; Ellery et al. 2012). As such, the discovery of Vankervelsvlei presents a rare opportunity to delve into the origin and development of such a landform in this particular environmental and climatic setting. The fact that there is well-preserved organic sediments within the basin together with its ecotonal location has resulted in it being very attractive from a palaeoecological perspective.

5.2.2. The beginning: Irving and Meadows (1997), Irving (1998)

The early work from Irving (1998) and Irving and Meadows (1997) provided a seminal baseline from which to further explore the palaeoenvironmental history of this distinctive waterbody. Two cores, VVVA and VVVB (Figure 5-1), were obtained in 1992 and 1996 respectively, using a vibracorer. The radiocarbon dating results (Table 5-1) provided a nominally infinite basal age of 39 900 ± 1000 yr BP for VVVA and indicated an age reversal at the base of VVVB (Irving and Meadows 1997; Irving 1998).

VVVA produced a pollen record for the period ~39 900 to ~3170 BP with a hiatus between ~25 000 and ~7100 BP, with the pollen record from VVVB covering ~45 000 to ~4700 BP. Quick (2013) highlighted several issues with these records including poor chronological control and problems with taxonomic identification leading to uncertainty in reconstruction. Nonetheless, important inroads were made towards understanding vegetation dynamics in this ecotonal region as well as the development of Vankervelsvlei. From these records two periods of forest expansion were identified - from 43 000 to 40 000 BP and again between 4000 and 3000 BP (Irving 1998). Given the scarcity of

Last Glacial Maximum (LGM) records for southern Africa in general, the inferences made about this period were of particular interest and, while the its reconstruction as a period of cooler temperatures was to be expected, conditions appear not to have been as dry at this time as suggested for other regions of southern Africa (Irving 1998). Analysis of the chronostratigraphic results from VVVA and VVVB suggest that two major depositional phases have taken place over the last ~40 000 years (Irving and Meadows 1997; Irving 1998). The first phase is characterised by finer inwashed clay and is identifiable in both VVVA and VVVB (Irving and Meadows 1997; Irving 1998). The second more recent phase is only visible in VVVA and mainly consists of organic rich peaty sediments (Irving and Meadows 1997; Irving 1998).

Table 5-1: Radiocarbon dating results for VVVA and VVVB
[adapted from Irving and Meadows (1997) and Irving (1998)]

Core Name	Sample reference	Depth from core surface (cm)	^{14}C age (yr BP)	2 σ cal range (cal BP)*	Median cal age (cal BP)
VVVA	Pta - 6583	6 - 16	3170 ± 60	3203 - 3454 3475 - 3479	3339
VVVA	Pta - 6585	407 - 413	7130 ± 40	7799 - 7807 7835 - 8011	7920
VVVA	Pta - 6584	500 - 507	19 500 ± 20	23 260 - 23 749	23 543
VVVA	Pta - 6361	695 - 700	39 900 ± 1000	42 262 - 44 568	43 317
VVVB	Pta - 7258	19 - 23	7240 ± 60	7877 - 7889 7931 - 8173	8014
VVVB	Pta - 7130	117 - 124	19 300 ± 210	22 837 - 23 793	23 253
VVVB	Pta - 7259	378 - 381	38 400 ± 1100	41 068 - 44 041	42 401
VVVB	Pta - 7124	520 - 528	31 600 ± 1200	33 696 - 39 256	36 081

*The ^{14}C ages were calibrated with the SHCal20 dataset (Hogg et al. 2020) using the online version of CALIB 8.2 (Stuiver et al. 2020).

Irving (1998) also investigated modern pollen sequences from surface samples in and around Vankervelsvlei. Interestingly it was found that in samples from the vegetation mat, the concentration of Cyperaceae pollen was not as high as anticipated (Irving 1998; Quick 2013). It was further indicated that Ericaceae pollen concentrations were highest in the open transitional area between the forest and the wetland and confirmed that Afrotemperate forest taxa are likely to be generally underrepresented in pollen assemblages at this site (Irving 1998; Quick 2013).

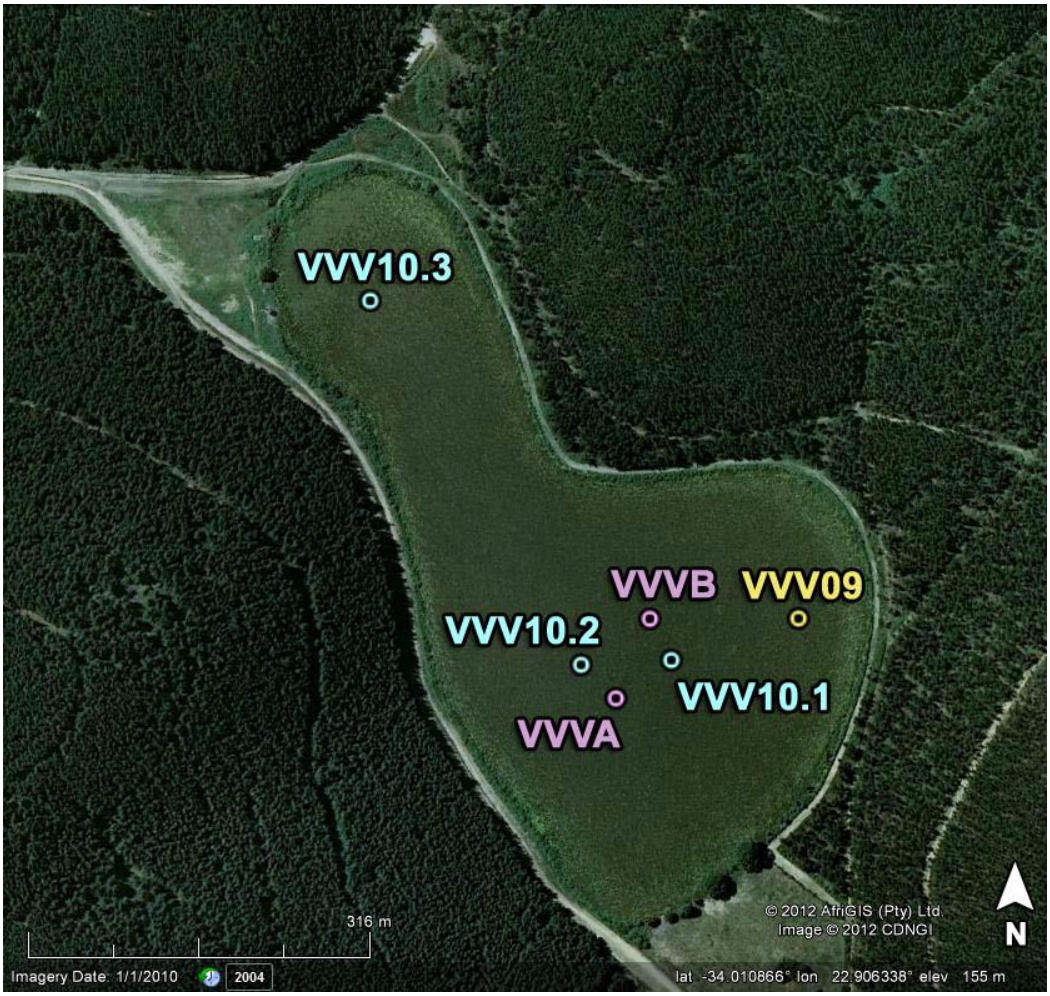

Figure 5-1: The locations of extracted cores from Vankervelsvlei, excluding this study.
VVA and VVB (Irving and Meadows 1997; Irving 1998); VVV10.1 (Quick 2013; Quick et al. 2016); VVV10.2 and VVV10.3 (not analysed). [from Quick (2013)]

5.2.3. Return, reanalysis: Quick (2013), Quick et al. (2016)

Further field investigations were conducted at Vankervelsvlei in 2009 and 2010 yielding four sediment cores – VVV09, VVV10.1, VVV10.2 and VVV10.3 (Figure 5-1) – also retrieved with a vibracorer. VVV10.1 showed the most promise for palynological investigation (Quick 2013).

The chronology for VVV10.1 was obtained through the use of both ^{14}C and optically stimulated luminescence (OSL) dating methods and delivered results that are challenging to interpret. Three of the ages were deemed to be outliers by Quick (2013) and Quick et al. (2016) with an age reversal indicated at 271 cm. Taking this into account, the age-depth model (Figure 5-2) provided an interpolated basal age for VVV10.1 of ~140 ka (Quick 2013; Quick et al. 2016).

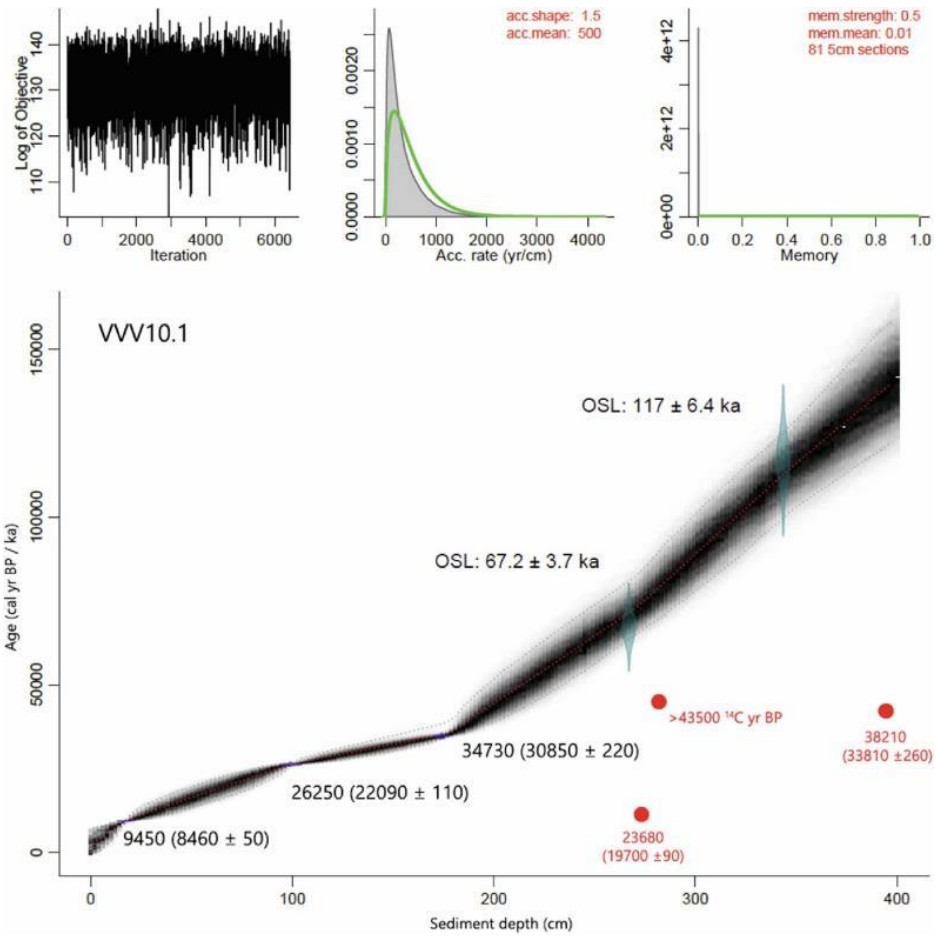

Figure 5-2: The VVV10.1 age-depth model. The ages presented in red were deemed to be outliers and as such excluded from the model (Quick 2013; Quick et al. 2016).

Pollen preservation proved to be an added concern with no pollen present between c.140 and 122 ka, and only two viable samples, at 6.9 and 5ka, available for the Holocene period. These limitations aside, VVV10.1 produced the longest pollen record yet for the southern Cape coast region (Quick 2013; Quick et al. 2016). Salient features from this record include a period of extensive forest development between c.108 and 96 ka as a result of enhanced summer rainfall counteracting increased potential evapotranspiration under warmer conditions (Quick 2013; Quick et al. 2016). In addition, it is suggested that Vankervelsvlei was a more open, shallow waterbody at this time which might reflect the initial phase of lake development (Quick 2013; Quick et al. 2016). After c.96 ka, cooler conditions are inferred by the dominance of fynbos but moisture availability appears to remain high (Quick 2013; Quick et al. 2016). Cool conditions continue between 59 and 37 ka as fynbos remain prominent in the record, with a change towards increasing summer aridity linked to lower Agulhas Current sea surface temperatures (SST) (Quick 2013; Quick et al. 2016). Water levels in Vankervelsvlei were possibly lower at this time as well (Quick 2013; Quick et al. 2016). Around c.36 ka, a notable shift in environmental conditions seemed to occur with increased temperatures and moisture availability until 27 ka (Quick 2013; Quick et al. 2016). It is proposed that the absence of pollen after 27 ka is likely related to drier conditions during the LGM in the southern Cape (Quick 2013; Quick et al. 2016). Around 2 ka sediment accumulation ceased which could indicate that Vankervelsvlei became completely closed over by this time (Quick 2013; Quick et al. 2016). It is also suggested that vegetation succession and the development of the waterbody are the main drivers behind changes observed in the pollen record as opposed to variations in moisture availability (Quick 2013; Quick et al. 2016).

5.2.4. Additional proxies: Strobel et al. (2019)

Another fieldwork campaign was undertaken in 2016, when several cores – including those in this study - were recovered by means of a piston corer. The Strobel et al. (2019) study focused on two parallel cores, VVV16-1 and VVV16-6, and considered the results of leaf wax biomarkers, organic macro-remains and both organic and inorganic geochemical analyses. As with VVV10.1, radiocarbon dating revealed a complex chronology with an age offset between the upper and lower sections of the

composite sequence. Accordingly, the two sections were modelled separately (Figure 5-3) resulting in a basal age of 37 720 cal BP and a hiatus between 28 520 and 8360 cal BP (Strobel et al. 2019).

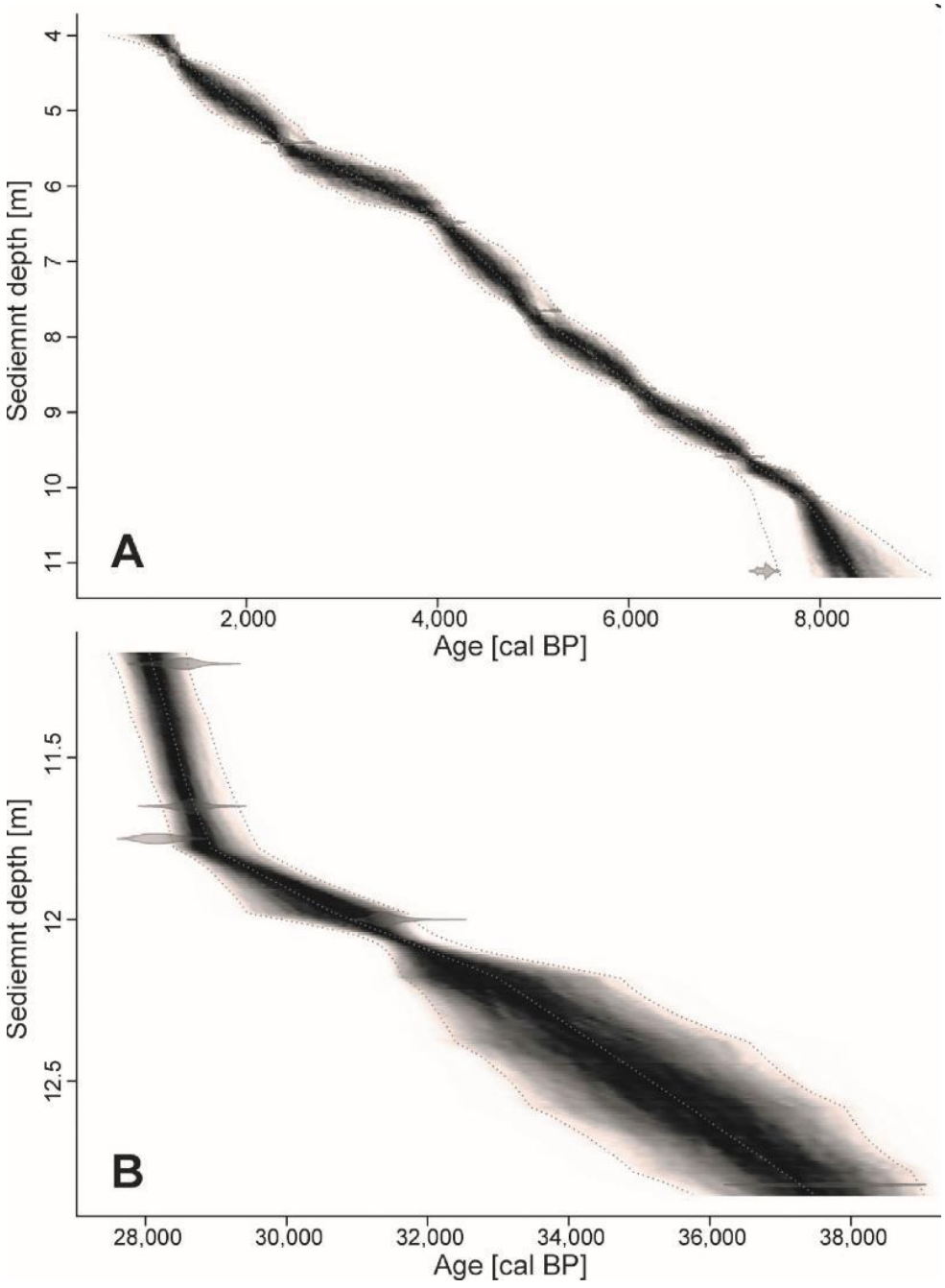

Figure 5-3: The VVV16 age-depth models. **A:** upper section, composite depth: 11.18 – 4m; **B:** lower section, composite depth: 12.85 – 11.18 m (Strobel et al. 2019).

This multi proxy record identified three major phases of environmental change over the last ~37 700 years. During the first phase, 37 700 to 28 500 cal BP, drier conditions are inferred for the region as a result of reduced summer rainfall and greater evapotranspiration driven by increased wind strength (Strobel et al. 2019). The hiatus between 28 520 and 8360 cal BP represents the second phase, reflecting the driest climatic conditions in the record likely due to increased rainfall seasonality at this time (Strobel et al. 2019). It is proposed that the hiatus is related to more arid conditions resulting in the degradation and desiccation of accumulated peat layers (Strobel et al. 2019). Peat formation and accumulation started again in Vankervelsvlei from 6800 to 1200 cal yr BP, the third phase, leading to the inference of wetter conditions in the area during this period (Strobel et al. 2019).

It is further suggested that climatic mechanisms vary between centennial/millennial and orbital time scales (Strobel et al. 2019). Wind induced evapotranspiration is suggested as the main driver on a centennial/millennial scale, while on orbital scales, climate dynamics are driven by a combination of evapotranspiration and rainfall amounts (Strobel et al. 2019). Additionally, it is proposed that wind has a much greater influence on evapotranspiration at Vankervelsvlei in relation to temperature, and that the system is primarily controlled by evaporation (Strobel et al. 2019).

5.3. Site details

Vankervelsvlei is situated along the southern Cape coast of South Africa, about 5 km inland, in the aseasonal rainfall zone (Figure 5-4). It is surrounded by a lithified aeolian dune of middle to Late Pleistocene age at an elevation of ~150 mamsl (Figure 5-5) (Bateman et al. 2011; Illenberger 1996). It is has been proposed that Vankervelsvlei formed following the stabilisation of the dune cordon within MIS 9 – MIS 7, behind the Landward barrier dune (*sensu* Illenberger 1996) (Irving and Meadows 1997). Today, Vankervelsvlei is a ~0.5 km^2 irregular shaped waterbody with no surface inflow or outlet, exclusively fed by rainfall (Irving and Meadows 1997; Parsons 2009).

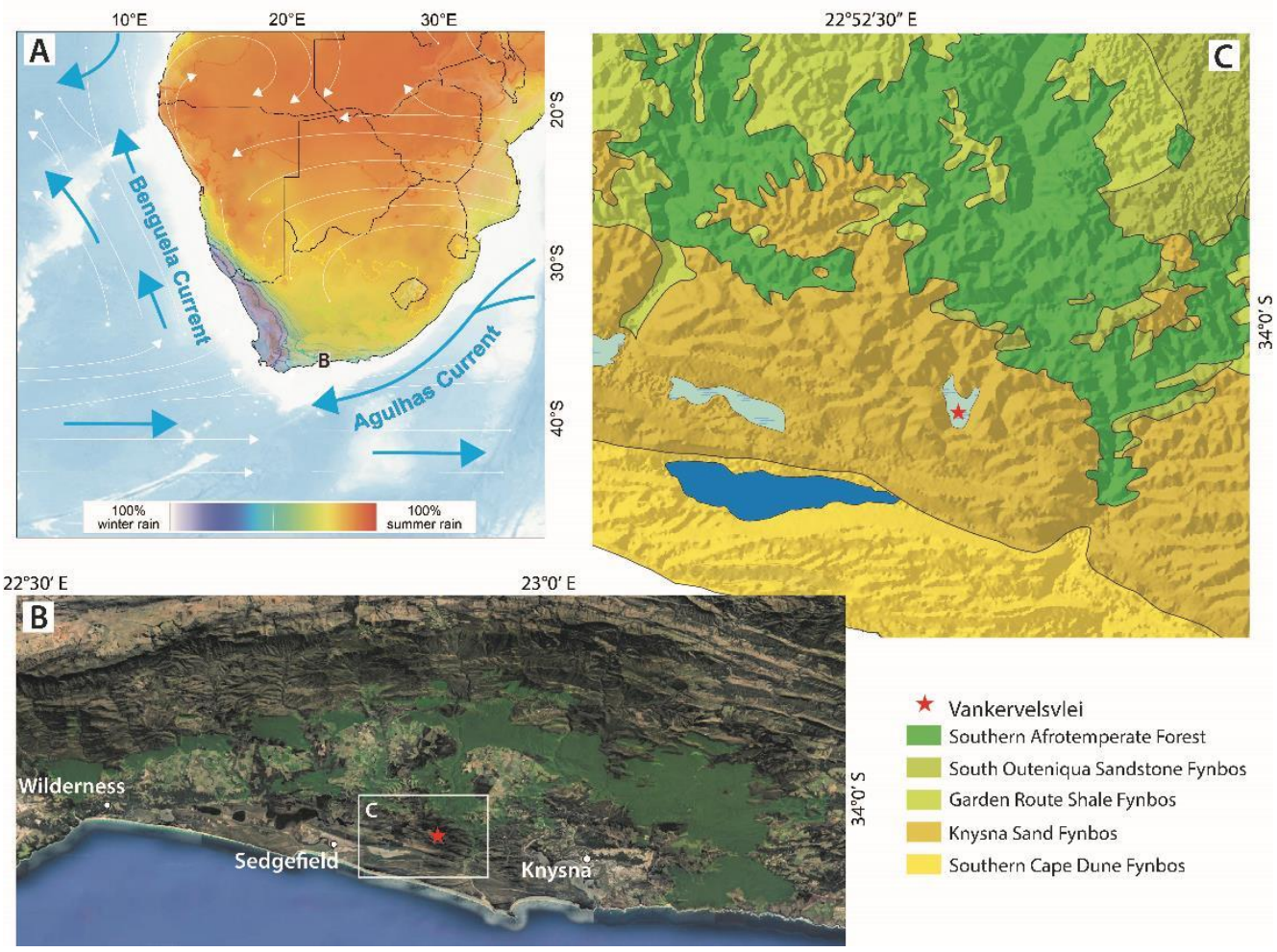

Figure 5-4: A. Map of southern Africa showing seasonality of rainfall and sharp climatic gradients dictated by the zones of summer/tropical (red) and winter/temperate (blue) rainfall dominance. Major atmospheric (white arrows) and oceanic (blue arrows) circulation systems are indicated. **B.** A section of the southern Cape coast between the towns of Wilderness and Knysna indicating the location of Vankervelsvlei and the current extent of Afrotemperate forest in the region. **C.** The location of VVV16 and the contemporary distribution of the dominant vegetation types (Mucina and Rutherford 2006).

This enclosed and endorheic wetland is covered with a floating vegetation mat primarily comprising of several Cyperaceae species as well as some Bryophytes and Pteridophytes (Irving and Meadows 1997; Quick et al. 2016). The surrounding fossil dune is covered by pine plantations (*Pinus)* of various ages, with scrub forest elements (e.g. *Cassine*, *Euclea*, *Kiggelaria*) occupying the area between the plantations and the wetland. Along the edges, vegetation predominantly consists of fynbos pioneer communities (*Erica*, Restionaceae, *Leucadendron* (Proteaceae), *Passerina*) (Quick et al. 2016).

Northward of Vankervelsvlei, Southern Afrotemperate forest is present in patches, largely represented by *Ocotea bullata*, *Olea capensis*, *Afrocarpus falcatus* and *Podocarpus latifolius* (in the pollen record we cannot differentiate between these species, as such these are all labelled *Podocarpus* for the purpose of this chapter) (Midgley et al. 2004).

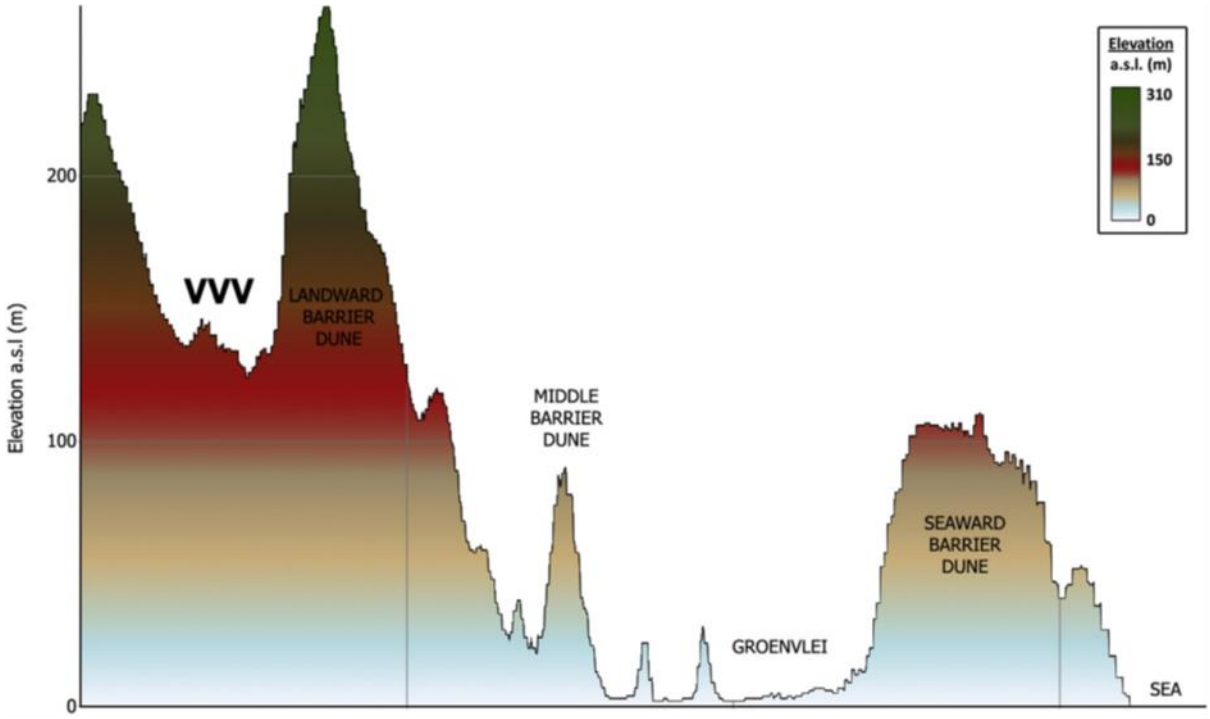

Figure 5-5: A longitudinal profile illustrating the setting of the Vankervelsvlei basin relative to important geomorphic features in the area (Quick 2013; Quick et al. 2016).

5.4. Sediment description and methods

VVV16-4 and VVV16-1-1-1/2 (34°0'46.8'' S, 22°54'14.4'' E) (Figure 5-6) were recovered using a UWITEC piston corer. Combined, the core sections are used here to create a 205 cm long record. Due to the nature of this waterbody, VVV16-4 was a push core from the surface while VVV16-1 started at a depth of 80 cm below the surface resulting in the ~25 cm gap between the two sections.

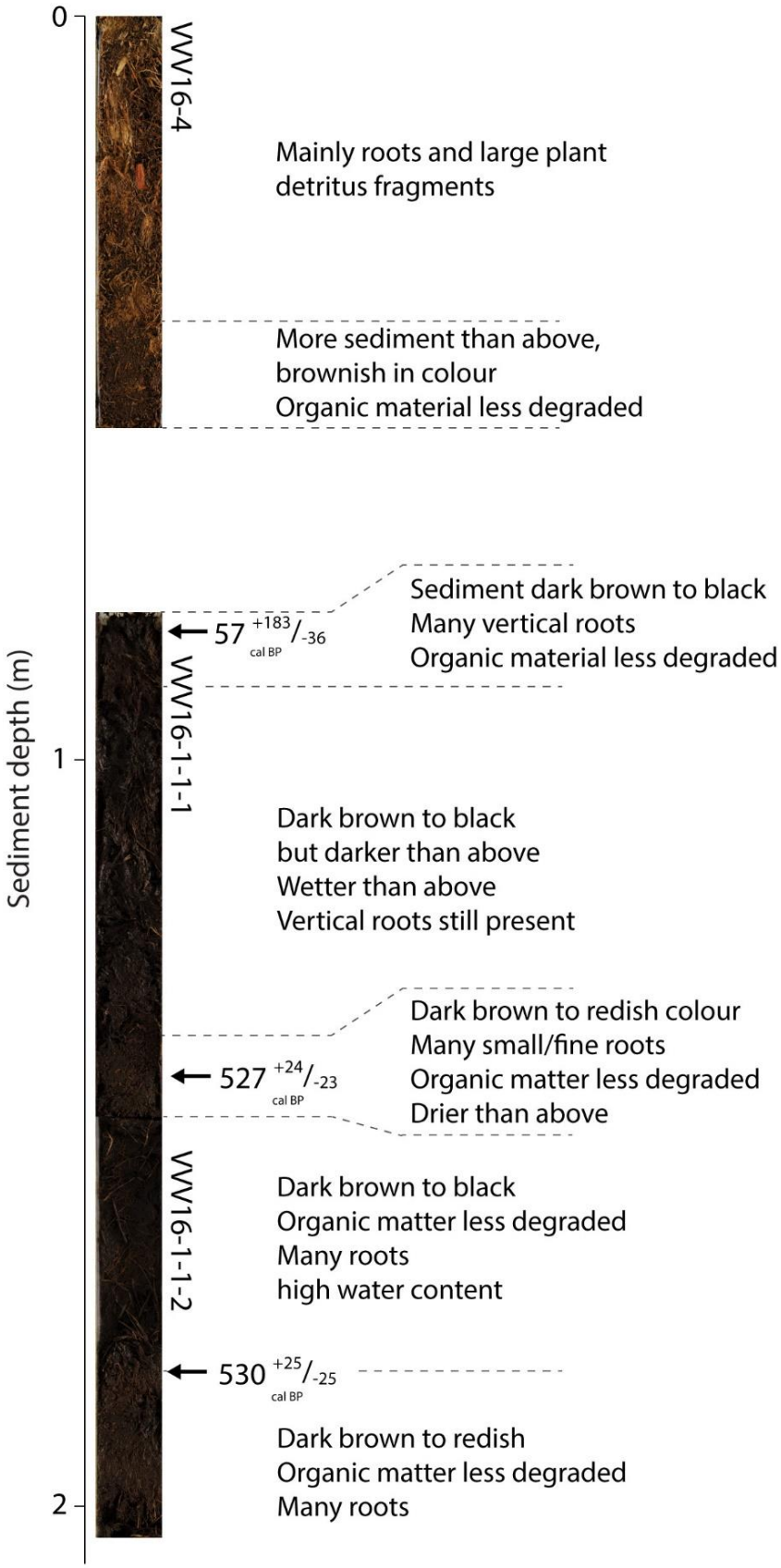

Figure 5-6: Core image and sediment descriptions for VVV16-4, VVV16-1-1-1 and VVV16-1-1-2. The arrows indicate the depths at which the ^{14}C samples were taken with the corresponding uncalibrated ages.

A total of 24 samples, with a minimum weight of 2 g, were processed using standard palynological methods as per Faegri and Iversen (1989) and Moore *et al.* (1991) with adaptations for dense media separation (Nakagawa *et al.* 1998). LacCore's polystaene microsphere pollen spike (0.5 ml per sample; 5.0 x 10^4 sph/ml ± 7%) was added to each sample to determine pollen concentrations. Pollen grains were examined and counted using a Zeiss Axiostar Plus microscope. Identification of pollen were based on comparison with reference material from the Environmental and Geographical Science department at the University of Cape Town, and published images (Van Zinderen Bakker 1953, Van Zinderen Bakker and Coetzee 1959, Welman and Kuhn 1970 and Scott 1982). Charcoal particles were counted together with pollen grains using the particle count method (Tinner and Hu 2003), and were classified according to size: 10 – 100 µm and >100 µm. Counts of 300 terrestrial pollen grains, or three slides, were performed for each sample. Three samples were excluded due to insufficient pollen concentrations; depths 50, 54 and 182 cm.

5.5. Dating

The age-depth model for this section of the VVV16 composite record is based on three AMS ^{14}C ages from organic macro-particles in VVV16-1-1-1 and VVV16-1-1-2 (Figure 5-6, Table 5-2) and compliments an age-depth model previously published by (Strobel et al. 2019) (Figure 5-3). The samples were dated at the Poznan Radiocarbon Laboratory (Poland). The resultant ages were calibrated using the SHCal13 curve (Hogg et al. 2013). The age-depth model was developed with the R software package Bacon (v2.3) (Blaauw and Christen 2011).

Table 5-2: Radiocarbon dating details for VVV16-1-1-1/2

Lab ID	Depth under surface (cm)	Core section depth (cm)	^{14}C age (BP)	1σ error	Calibration curve	2σ cal age range (cal BP)	Median cal age (cal BP)
Poz-92269	83	3	10	30	SHcal13	21 - 240	57
Poz-92270	143	63	545	30	SHcal13	504 - 551	527
Poz-102442	182	35	560	30	SHcal13	505 - 555	530

5.6. Results and interpretation

Fifty-nine different taxa were identified from this section of the VVV16 record, spanning the period ~AD 1300 to present. Due to the core composition, the assemblage was divided into two zones – the first comprising cores VVV16-1-1-1 and 16-1-1-2 and the second VVV16-4. Pollen concentrations in VVV16-1-1-1/2 vary from 2.34 x 10^3 to 1.15 x 10^4 grains.g^{-1}, and in VVV16-4 these range between 2.56 x 10^3 and 6.20 x 10^4 grains.g^{-1} (Figure 5-8).

The pollen assemblage is summarised according to the ecological affinity of the primary contemporary vegetation types in the region (Figure 5-7). The most prominent vegetation group includes aquatic and/or riparian taxa, of which Haloragaceae is most prevalent. All aquatic/riparian taxa were excluded from the total pollen sum due to the sites environmental setting and hence the likelihood of these taxa being overrepresented in the record. In terms of terrestrial vegetation, the fynbos vegetation group is the main contributor to the assemblage, largely represented by Ericaceae, Restionaceae and *Stoebe*-type. *Euphorbia* and *Pentzia*-type are the main components in the succulent/drought resistant group while the coastal thicket group is dominated by *Morella* with *Euclea* and *Olea* also present. The most prominent taxa in the Afrotemperate forest group is *Podocarpus*, and *Kiggelaria* in the top section (VVV16-4) of the assemblage. The minimal presence of other forest taxa can largely be ascribed to the low pollen output of some forest taxa as well as the different pollen dispersal methods (Jackson and Kearsley 1998; Jackson and Williams 2004; Lowe and Walker 1997). Due to its morphology, *Podocarpus* pollen is very successfully distributed over long distances through wind (Jackson and Kearsley 1998; Jackson and Williams 2004; Roy et al. 2018). As a result of this, the presence of *Podocarpus* pollen in a sequence could rather be indicative of more regional climatic conditions due to long-distance transport, which may further result in *Podocarpus* being overrepresented in the pollen record (Jackson and Kearsley 1998; Jackson and Williams 2004; Roy et al. 2018). Despite these considerations *Podocarpus* has been shown to be valuable indicators of aridity/humidity in the region (e.g. du Plessis et al. 2020; Quick et al. 2018) (with aridity/humidity being distinct from rainfall amount per se [see Chevalier & Chase 2016]).

VVV16-1-1-1/2: *AD 1300 – 1720 (650 – 230 cal yr BP)*

Coastal thicket is prominent from the start of the record remaining elevated until c. AD 1420. This group is mainly represented by *Morella* – most likely the dune, scrub and heath species *M. quercifolia and M. cordifolia* (Martin 1968). Afrotemperate forest pollen percentages are low, increasing after c. AD 1400 to near maximum values (5.2%) at c. AD 1420. Haloragaceae is similarly elevated here. Fynbos pollen percentages increase towards c. AD 1460, Restionaceae displays a similar trend. Ericaceae generally follows this pattern with *Stoebe*-type also present. The thermophilous taxon *Pentzia*-type is present at maximum percentages near the start of the sequence at c. AD 1310, followed by a decline in both this taxon and the succulent/drought resistant group to near minimum values at c.AD1460. *Euphorbia* is present in relatively substantial proportions throughout the record (with peaks at c. AD 1430, 1580 and 1690). This sustained presence of *Euphorbia* could be related to enhanced dune movement in the region as opposed to being a climatic response (Schalke 1973). These trends might indicate generally warmer and drier conditions around AD 1300 with moisture availability increasing towards c. AD 1420, and a decline in temperature moving into the Little Ice Age (LIA).

After c. AD 1420, coastal thicket percentages are lower until c. AD 1580. Afrotemperate forest taxa (mainly *Podocarpus*) are more prominent in the assemblage during this period which could reflect a stage of vegetation succession and/or climatic conditions more conducive to enhanced forest spread. Both Cyperaceae and *Podocarpus* are present at maximum percentages at c. AD 1500 which could suggest a preceding period of enhanced moisture availability and/or reduced rainfall seasonality.

Maximum charcoal concentrations at c. AD 1460 are followed by a notable increase in drier asteraceous fynbos (Asteraceae HS) until c. AD 1580. This could indicate a progressively drier environment or alternatively a local vegetation response to a large fire event, as inferred from the peak in charcoal concentrations. *Stoebe*-type values increase after c. AD 1500, remaining elevated toward the top of this section of the record, c. AD 1690, probably reflecting a colder LIA environment.

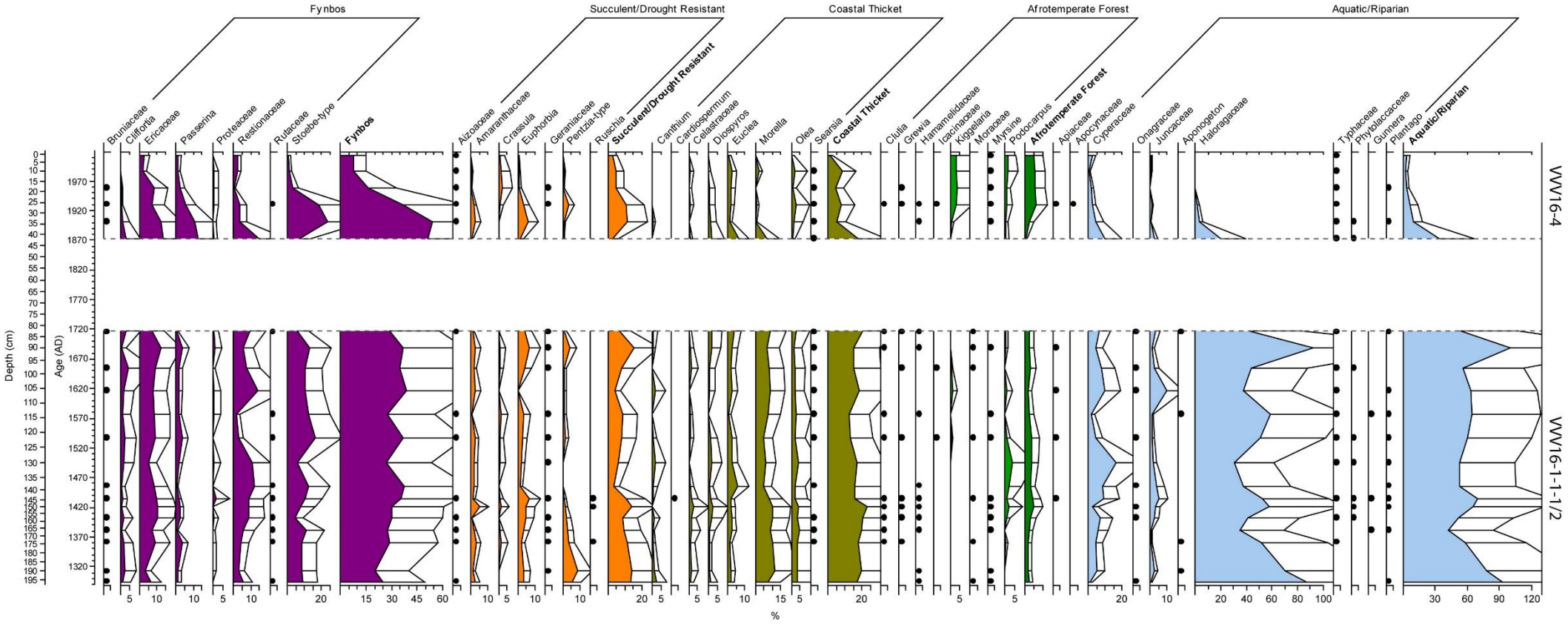

Figure 5-7.1: Relative pollen percentage diagram for VVV16-4 and VVV16-1-1-1/2 organized according to ecological affinity (fynbos - aquatic/riparian vegetation).

Pollen taxa occurring at less than 1% are shown only as presence points. Exaggeration curves are 4x for taxa present between 5 and 2% and 2x for those above 5%

Throughout this part of the record Cyperaceae and Restionaceae display similar trends, while Haloragaceae, likely *Myriophyllum spicatum* (Howard-Williams 1979; Neumann et al. 2008; Weyl and Coetzee 2014; Weyl et al. 2016), the most prominent taxon in the record, exhibits the opposite. These trends are possibly related to changing water levels in Vankervelsvlei.

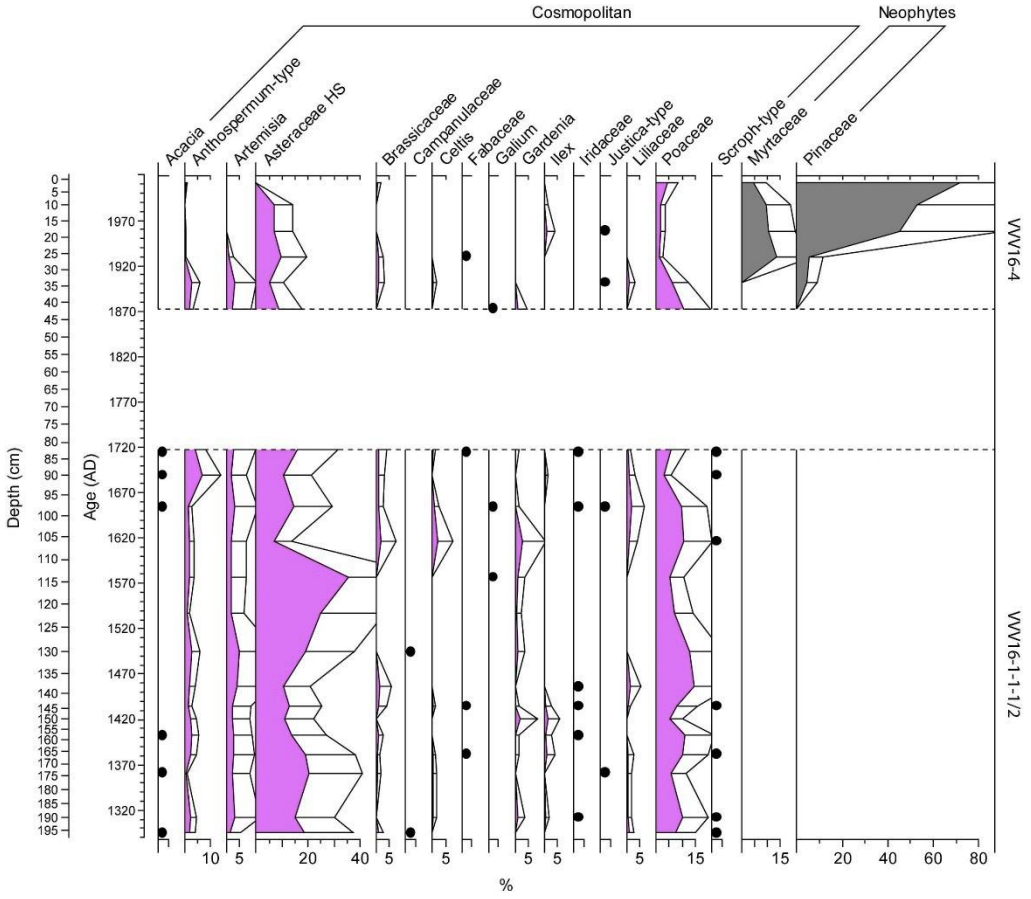

Figure 5-7.2: Relative pollen percentage diagram for VVV16-4 and VVV16-1-1-1/2 organized according to ecological affinity (cosmopolitan vegetation and neophytes). Pollen taxa occurring at less than 1% are shown only as presence points. Exaggeration values are 4x for taxa present between 5 and 2% and 2x for those above 5%.

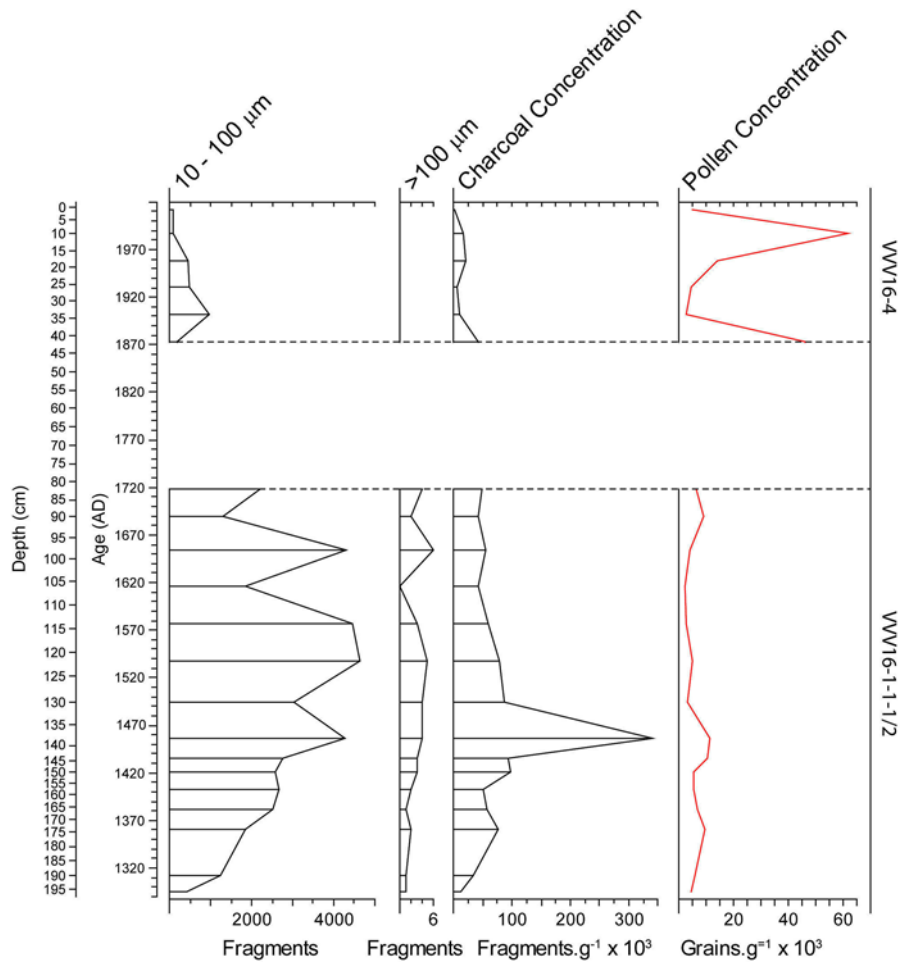

Figure 5-8: Charcoal counts and charcoal and pollen concentrations for VVV16-4 and VVV16-1-1-1/2. Charcoal and pollen concentrations were calculated in the same manner using microsphere counts.

VVV16-4: *AD 1870 – 2010/Present*

Pinus is first seen in the record from c. AD 1900, with Myrtaceae (most likely *Eucalyptus*) present from AD 1930, reflecting the influences of the forestry industry that became established in the late AD 1700's and still remains active in the region today.

Kiggelaria, largely absent from the pollen assemblage, becomes more prevalent from c. AD 1900. As *Kiggelaria* percentages increase, scrub forest and thicket elements, i.e. *Euclea* and *Morella*, decline which could reflect a change in forest species composition. As a forest pioneer (Manders and Richardson 1992; Manders and Smith 1992), the presence of *Kiggelaria* here may possibly indicate the

recovery of indigenous forests. This stage of vegetation succession may have been triggered by the establishment of the pine plantations and/or better forest management practices.

5.7. VVV16 vs VVV10.1

The main trends identified in the VVV16[2] pollen record are now considered in comparison to the record from VVV10.1 (Quick 2013; Quick et al. 2016) in order to ascertain if, and how, vegetation and environmental dynamics have changed in and around Vankervelsvlei during these different time periods. Due to the issues highlighted in section 5.2.2, the records from VVVA and VVVB (Irving 1998) are not included here.

5.7.1. Vegetation succession and forest development

From the start of the VVV16 record, c. AD 1300, until c. AD 1420, *Morella* is the most prevalent coastal thicket taxon, whereas *Euclea*, also a component of this groups, and the forest taxon *Podocarpus* are present at low percentages (Figure 5-9). This trend is similarly seen in the VVV10.1 record between c. 84 and 53 kBP (Figure 5-9). The opposite, i.e. elevated percentages of *Podocarpus* and *Euclea* pollen together with a decline in *Morella*, is noted in the VVV16 record after c. AD 1420 until around c. AD 1500, and in VVV10.1 between c. 101 and 95 kBP.

In both records, during periods when *Podocarpus* is more dominant, it is generally inferred that rainfall seasonality and drought stress were reduced. Quick et al. (2016) suggests that the occurrence of other coastal thicket elements (i.e. *Euclea, Olea*) together with *Podocarpus* indicate the presence of transitional scrub forest patches and thicket on the surrounding dunes. Additionally, *Euclea schimperi* is often found as a small tree in very dry scrub forest (Von Breitenbach 1972) together with *Podocarpus/Afrocarpus falcatus* which could explain the strong association between *Euclea* and *Podocarpus* seen in both records at these times.

[2] From here onward the composite record VVV16-4, VVV16-1-1-1/2 will be referred to as VVV16

In contrast, when *Morella* is the most prevalent taxon, the evidence suggests drier conditions, or at least increased rainfall seasonality and potentially reduced summer rainfall (Quick 2013; Quick et al. 2016). The strong positive relationship between *Morella* and succulent/drought resistant taxa in both records (in VVV16 from c. AD 1300 to around AD 1580, and in VVV10.1 from c. 80 to around 50 kBP) could further substantiate a drier environment. In addition, as suggested previously for the VVV16 record, the presence of *Morella* at these times might very likely represent the drier dune species *M. quercifolia* and *M. cordifolia* (Martin 1968). *Morella cordifolia* is also common as a shrub in very very dry scrub on littoral dunes (Von Breitenbach 1972). However, the increase in *Canthium* together with *Morella* in the VVV10.1 record after c. 85 kBP, led Quick et al. (2016) to suggest that moisture availability was in fact not restricted at this time as cooler temperatures and reduced potential evapotranspiration would result in less drought stress and more effective rainfall. Furthermore, according to Quick et al. (2016), the contemporary distribution of *Podocarpus*, *Morella* and *Canthium* are very similar, primarily found in areas with low drought stress. Consequently it was suggested that the decrease in *Podocarpus* seen here results from vegetation succession and the changing morphology of Vankervelsvlei itself, rather than as a response to changing climate dynamics. This does, however, appear contradictory to the argument of drier conditions at this time as indicated by the increased presence of pollen from succulent/drought resistant taxa.

In the VVV16 record the sharp decline in *Podocarpus* after c. AD 1500 is, however, concomitant with the increasing presence of the cryophilic taxon *Stoebe*-type, reflecting cooler temperatures. This trend is similarly seen in the Bo Langvlei pollen record (this thesis) indicating cool and dry conditions during the latter part of the LIA, particularly between c. AD 1600 and 1850. This cold and dry environment could further be responsible for the cessation of sedimentation as seen in the VVV16 core between 54 and 80 cm (Figure 5-6) (c. AD 1775 to 1860), equating to a time gap of ~85 years (~155 years between samples).

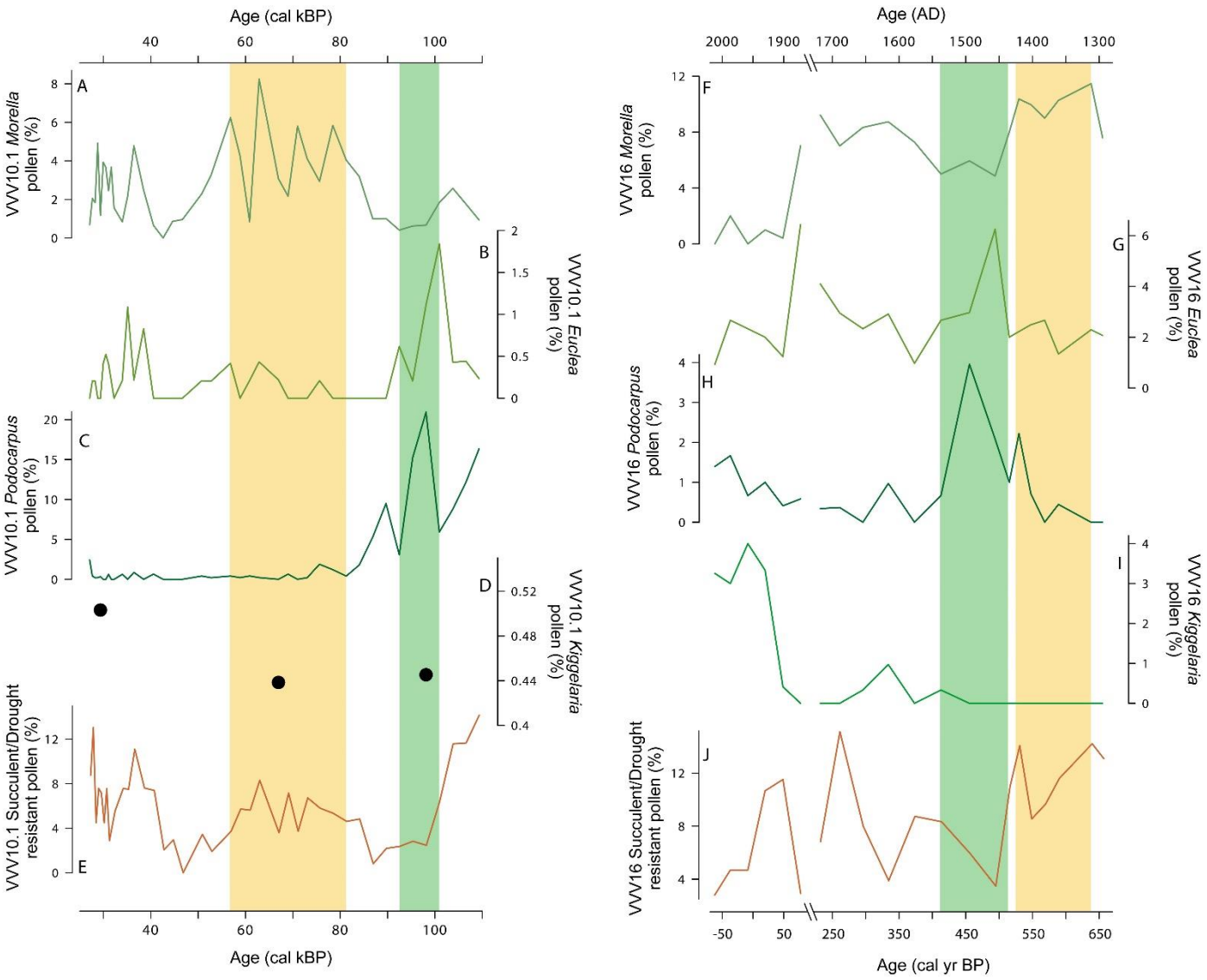

Figure 5-9: Comparison of coastal thicket and Afrotemperate forest elements between the VVV16 (right) and VVV10.1 (Quick 2013; Quick et al. 2016) (left) pollen records: **A**. VVV10.1 *Morella* pollen percentages; **B**. VVV10.1 *Euclea* pollen percentages; **C**. VVV10.1 *Podocarpus* pollen percentages; **D**. VVV10.1 *Kiggelaria* pollen percentages; **E.** VVV10.1 Succulent/drought resistant taxa pollen percentages; **F**. VVV16 *Morella* pollen percentages; **G**. VVV16 *Euclea* pollen percentages; **H**. VVV16 *Podocarpus* pollen percentages; **I**. VVV16 *Kiggelaria* pollen percentages; **J.** VVV16 Succulent/drought resistant taxa pollen percentages. Suggested drier periods when *Morella* is more dominant are indicated by orange shading and green shading indicates periods when *Podocarpus* is more dominant and drought stress is limited.

From the comparisons above it is concluded that these two records (VVV16 and VVV10.1), although representing very different time periods, do tend to display similar trends with regard to vegetation succession. It does, however, seem that the triggers initiating these successional changes are different.

5.7.2. Wetland vegetation and water levels

For the VVV10.1 record it was proposed that the increased presence of wetland taxa reflects shallow conditions in Vankervelsvlei, likely associated with increased aridity (Quick et al. 2016). Cyperaceae was excluded from this group as today it is the primary component of the floating vegetation mat covering the wetland. Accordingly, low Cyperaceae pollen percentages in the VVV10.1 record indicated a more open waterbody (Quick et al. 2016). Cyperaceae and the aquatic/riparian group does tend to display a similar trend throughout the VVV10.1 record (Figure 5-10: A, C) which may suggest a negative relationship between the water level in, and the sedge cover of, Vankervelsvlei during the time period covered by this record. A positive association is further noted between the aquatic/riparian and succulent/drought resistant groups (Figure 5-10: C, D), supporting the proposition of increased wetland taxa representing lower water levels during drier conditions.

This trend of increased wetland taxa pollen during drier periods is also exhibited in the VVV16 record (Figure 5-10). Cyperaceae does, however, not mimic the aquatic/riparian group as in VVV10.1, instead generally displaying an opposite pattern, except at the very top of the sequence (VVV16-4). Quick et al. (2016) suggested that the cyperaceous mat was fully established by c. 2000 cal yr BP, which likely explains the differences in the presence of Cyperaceae pollen as observed in the two records.

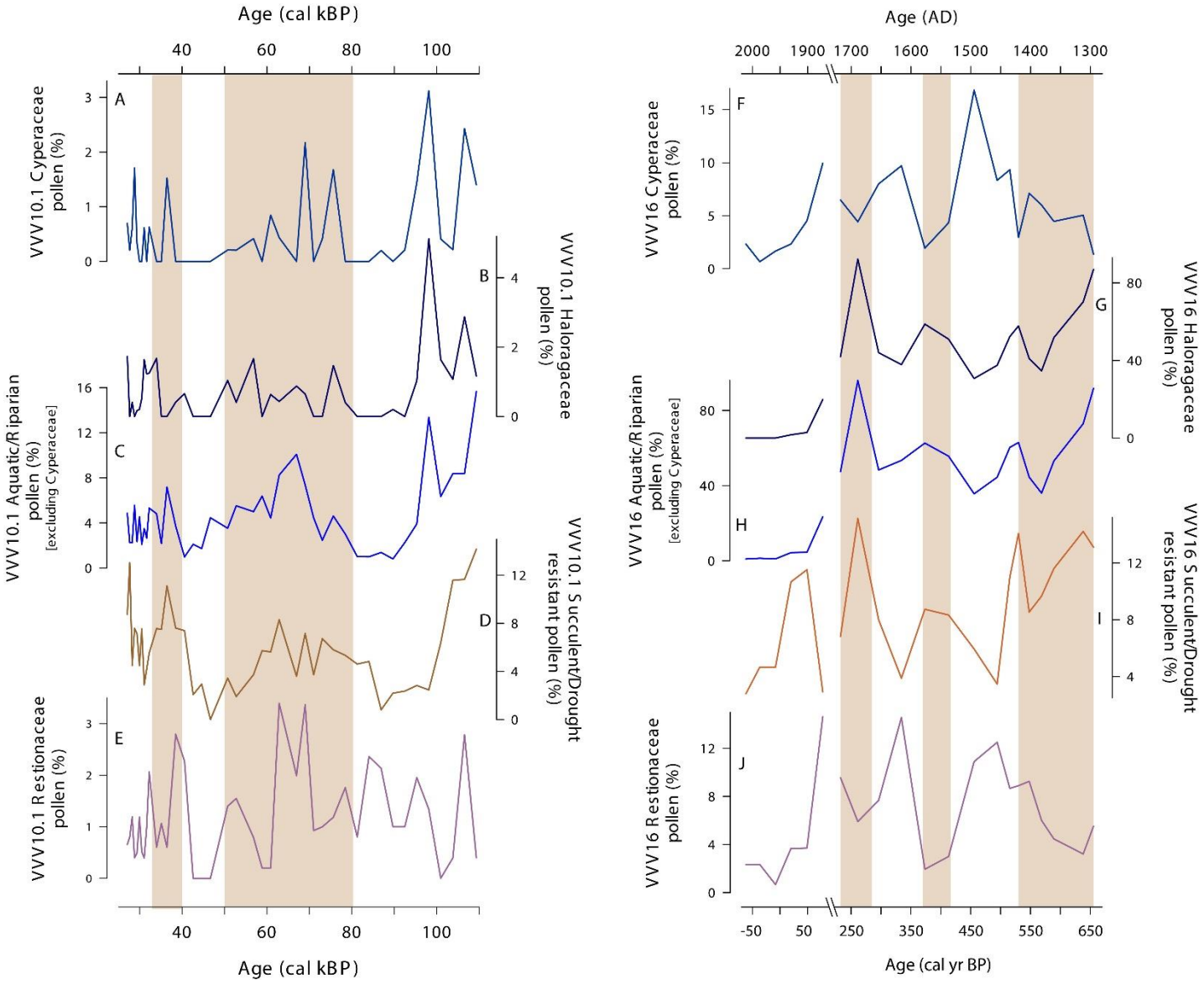

Figure 5-10: Comparison of wetland elements and succulent/drought resistant vegetation between the VVV16 (right) and VVV10.1 (left) pollen records. **A**. VVV10.1 Cyperaceae pollen percentages; **B**. VVV10.1 Haloragaceae pollen percentages; **C**. the sum of aquatic/riparian pollen percentages in the VVV10.1 record (excluding Cyperaceae); **D**. the sum of succulent/drought resistant pollen percentages in the VVV10.1 record; **E.** VVV10.1 Restionaceae pollen percentages; **F**. VVV16 Cyperaceae pollen percentages; **G**. VVV16 Haloragaceae pollen percentages; **H**. the sum of aquatic/riparian pollen percentages in the VVV16 record (excluding Cyperaceae); **I**. the sum of succulent/drought resistant pollen percentages in the VVV16 record; **J.** VVV16 Restionaceae pollen percentages. The brown shading indicates drier periods as inferred from the pollen records.

The trends observed in Cyperaceae, Restionaceae and Haolagaceae in the VVV16 record were highlighted in section 5.6, i.e. Cyperaceae and Restionaceae having a positive relationship, and Haloragaceae displaying the opposite. The increased presence of Haloragaceae have previously been associated with higher water levels in lakes (Howard-Williams 1979; Neumann et al. 2008) while elevated Restionaceae percentages have been related to a rise in the groundwater table (Martin 1968). From both the Vankervelsvlei pollen records considered here, indications are, however, that the increased presence of Haloragaceae instead equates to drier periods, consequent to lower water levels.

In the VVV10.1 record Cyperaceae and Restionaceae does not display any significant relationship as seen for VVV16 (Figure 5-10). Again, this difference is most likely related to the state of the cyperaceous vegetation mat. In both records Restionaceae and succulent/drought resistant taxa display opposite trends (Figure 5-10), suggesting that the increased presence of this taxon may be related to periods with enhanced rainfall, and indeed an elevated groundwater table. It is worth noting that in his study, Parsons (2009) proposed that Vankervelsvlei is not recharged by groundwater from the underlying Table Mountain Aquifer and is solely dependent on rainfall for freshwater input. Nevertheless, it is suggested that the positive correlation between Cyperaceae and Restionaceae, as observed in the VVV16 record, is related to rainfall amount, with increased rainfall resulting in both a higher groundwater table and higher water levels in Vankervelsvlei. Furthermore, it would appear that the cyperaceous vegetation mat becomes denser as the water levels in Vankervelsvlei rise. This dynamic is not illustrated in the VVV10.1 record, suggesting a change in the response of Cyperaceae to fluctuating water levels as the waterbody became fully closed over after c. 2000 cal yr BP (Quick et al. 2016).

As found in the previous section, VVV16 and VVV10.1 tend to display largely similar trends. The evidence further suggests that the pattern of expanding wetland vegetation during drier periods, and lower water levels in Vankervelsvlei, have largely remained in place during the last ~100 000 years. This proposition does exclude Cyperaceae, as the data indicate very different patterns in the two records with regard to this taxon, as outlined above.

5.8. Conclusion

This chapter presented a ~650 year pollen and microcharcoal record from Vankervelsvlei. Although relatively short, interesting patterns have emerged from this most recent section of the VVV16 sequence.

The data indicate warmer and drier conditions at the onset of the record c. AD 1300, followed by a decline in temperature moving into the LIA. Moisture availability appears to be rather variable, but as suggested by Quick et al. (2016), vegetation succession may play a more important role in vegetation dynamics than climate, especially in relation to forest species composition. After c. AD 1500 the record reflects the markedly colder and drier latter part of the LIA which is also present in the pollen record from nearby Bo Langvlei (this thesis). Additionally, these drier conditions were, in all likelihood, the driver behind the cessation of sedimentation seen toward the top of VVV16.

In comparing the key trends in the VVV16 pollen record with that of the previously obtained VVV10.1 record, it was established that the records do tend to exhibit similar patterns regarding vegetation succession; the triggers initiating these changes do, however, appear to be different. It was further concluded that the positive relationship between the increased presence of wetland taxa pollen during drier periods have largely remained in place over the last ~100 000 years. This expansion of wetland taxa as water levels decline are, however, not generally noted in lacustrine systems (e.g. Howard-Williams 1980; Neumann et al. 2008), indicating that commonly applied assumptions with regard to indicator taxa as applied in lakes, cannot necessarily be readily carried over to this type of waterbody.

5.9. Acknowledgements

This study was funded by the German Federal Ministry of Education and Research (BMBF). The investigations were conducted as part of a pilot study for the collaborative project 'Regional Archives for Integrated Investigations' (RAiN), embedded in the international research program SPACES (Science Partnership for the Assessment of Complex Earth System Processes).

5.10. References

Bateman, M.D., Carr, A.S., Dunajko, A.C., Holmes, P.J., Roberts, D.L., McLaren, S.J., Bryant, R.G., Marker, M.E. & Murray-Wallace, C.V., 2011. The evolution of coastal barrier systems: a case study of the Middle-Late Pleistocene Wilderness barriers, South Africa. *Quaternary Science Reviews*, 30(1–2), pp.63–81.

Blaauw, M. & Christen, J.A., 2011. Flexible paleoclimate age-depth models using an autoregressive gamma process. *Bayesian Analysis*, 6(3), pp.457–474.

Von Breitenbach, F., 1972. Indigenous forests of the southern Cape. *Veld & Flora*, 58(1), pp.18–47.

Chase, B.M. & Meadows, M.E., 2007. Late Quaternary dynamics of southern Africa's winter rainfall zone. *Earth-Science Reviews*, 84(3–4), pp.103–138.

Chevalier, M. & Chase, B.M., 2016. Determining the drivers of long-term aridity variability: A southern African case study. *Journal of Quaternary Science*, 31(2), pp.143–151.

Ellery, W.N., Grenfell, S.E., Grenfell, M.C., Humphries, M.S., Barnes, K., Dahlberg, A. & Kindness, A., 2012. Peat formation in the context of the development of the Mkuze floodplain on the coastal plain of Maputaland, South Africa. *Geomorphology*, 141–142, pp.11–20.

Faegri, K. & Iversen, J., 1989. *Textbook of Pollen Analysis*, Chichester: John Wiley & Sons Ltd.

Finch, J.M. & Hill, T.R., 2008. A late Quaternary pollen sequence from Mfabeni Peatland, South Africa: Reconstructing forest history in Maputaland. *Quaternary Research*, 70(3), pp.442–450.

Grundling, P.L., Mazus, H. & Baartman, L., 1998. *Peat resources in northern KwaZulu-Natal wetlands: Maputuland*, Pretoria.

Hogg, A.G., Hua, Q., Blackwell, P.G., Niu, M., Buck, C.E., Guilderson, T.P., Heaton, T.J., Palmer, J.G., Reimer, P.J., Reimer, R.W., Turney, C.S.M. & Zimmerman, S.R.H., 2013. SHCal13 Southern Hemisphere Calibration, 0–50 000 Years Cal BP. *Radiocarbon*, 55(4), pp.1889–1903.

Hogg, A.G., Heaton, T.J., Hua, Q., Palmer, J.G., Turney, C.S., Southon, J., Bayliss, A., Blackwell, P.G., Boswijk, G., Bronk Ramsey, C., Pearson, C., Petchey, F., Reimer, P., Reimer, R. & Wacker, L., 2020. SHCal20 Southern Hemisphere Calibration, 0–55,000 Years cal BP. *Radiocarbon*, 62(4), pp.759–778.

Howard-Williams, C., 1980. Aquatic macrophyte communities of the Wilderness lakes: community structure and associated environmental conditions. *Journal of the Limnological Society of Southern Africa*, 6, pp.85–92.

Howard-Williams, C., 1979. Distribution, biomass and role of aquatic macrophytes in Lake Sibaya. In B. R. Allanson, ed. *Lake Sibaya Vol 36*. The Hague, Netherlands: Dr W Junk Publishers, pp. 88–107.

Illenberger, W.K., 1996. The Geomorphological Evolution of the Wilderness Dune Cordons, South Africa. *Quaternary International*, 33, pp.11–20.

Irving, S.J.E., 1998. *Late Quaternary palaeoenvironemtns at Vankervelsvlei, near Knysna, South Africa*. University of Cape Town.

Irving, S.J.E. & Meadows, M.E., 1997. Radiocarbon Chronology and Organic Matter Accumulation at Vankervelsvlei, near Knysa, South Africa. *South African Geographical Journal*, 79(2), pp.101–105.

Jackson, S.T. & Kearsley, J.B., 1998. Quantitative Representation of Local Forest Composition in Forest-Floor Pollen Assemblages. *Journal of Ecology*, 86(3), pp.474–490.

Jackson, S.T. & Williams, J.W., 2004. Modern Analogs in Quaternary Paleoecology: Here Today, Gone Yesterday, Gone Tomorrow? *Annual Review of Earth and Planetary Sciences*, 32(1), pp.495–537.

Lowe, J.J. & Walker, M.J.C., 1997. *Reconstructing Quaternary Environments*, London: Longman.

Manders, P.T. & Richardson, D.M., 1992. Colonization of Cape fynbos communities by forest species. *Forest Ecology and Management*, 48, pp.277–293.

Manders, P.T. & Smith, R.E., 1992. Effects of artificially established depth to water table gradients and soil type on the growth of Cape fynbos and forest plants. *South African Journal of Botany*, 58(3), pp.195–201.

Martin, A.R.H., 1968. Pollen Analysis of Groenvlei Lake Sediments, Knysna (South Africa). *Review of Palaeobotany and Palynology*, 7, pp.107–144.

Midgley, J.J., Cowling, R.M., Seydack, A.H.W. & van Wyk, G.F., 2004. Forest. In R. M. Cowling, D. M. Richardson, & S. M. Pierce, eds. *Vegetation of Southern Africa*. Cambridge: Cambridge

University Press, Cambridge, UK, pp. 278–296.

Moore, P.D., 2002. The future of cool temperate bogs. *Environmental Conservation*, 29, pp.3–20.

Moore, P.D., Webb, J.A. & Collinson, M.E., 1991. *Pollen Analysis* 2nd ed., Oxford: Blackwell Scientific Publications.

Mucina, L. & Rutherford, M.C., 2006. *The vegetation of South Africa, Lesotho and Swaziland*, Pretoria: South African National Biodiveristy Institute, Sterlitzia.

Nakagawa, T., Brugiapaglia, E., Digerfeldt, G., Reille, M., De Beaulieu, J.-L. & Yasuda, Y., 1998. Dense media separation as a more efficient pollen extraction method for use with organic sediment/deposit samples: comparison with the conventional method. *Boreas*, 27, pp.15–24.

Neumann, F.H., Stager, J.C., Scott, L., Venter, H.J.T. & Weyhenmeyer, C., 2008. Holocene vegetation and climate records from Lake Sibaya, KwaZulu-Natal (South Africa). *Review of Palaeobotany and Palynology*, 152(3–4), pp.113–128.

Parsons, R., 2009. Is Groenvlei really fed by groundwater discharged from the Table Mountain Group (TMG) Aquifer ? *Water SA*, 35(5), pp.657–662.

du Plessis, N., Chase, B.M., Quick, L.J., Haberzettl, T., Kasper, T. & Meadows, M.E., 2020. Vegetation and climate change during the Medieval Climate Anomaly and the Little Ice Age on the southern Cape coast of South Africa: Pollen evidence from Bo Langvlei. *The Holocene*, 30(12), pp.1716–1727.

Quick, L.J., Chase, B.M., Wundsch, M., Kirsten, K.L., Chevalier, M., Mausbacher, R., Meadows, M.E. & Haberzettl, T., 2018. A high-resolution record of Holocene climate and vegetation dynamics from the southern Cape coast of South Africa : pollen and microcharcoal evidence from Eilandvlei. *Journal of Quaternary Science*, 33(5), pp.487–500.

Quick, L.J., 2013. *Late Quaternary palaeoenvironments of the southern Cape, South Africa: palynological evidence from three coastal wetlands*. University of Cape Town.

Quick, L.J., Meadows, M.E., Bateman, M.D., Kirsten, K.L., Mäusbacher, R., Haberzettl, T. & Chase, B.M., 2016. Vegetation and climate dynamics during the last glacial period in the fynbos-afrotemperate forest ecotone, southern Cape, South Africa. *Quaternary International*, 404, pp.136–149.

Roy, I., Ranhotra, P.S., Shekhar, M., Bhattacharyya, A., Pal, A.K., Sharma, Y.K., Singh, S.P. & Singh, U., 2018. Over-representation of some taxa in surface pollen analysis misleads the interpretation of fossil pollen spectra in terms of extant vegetation. *Tropical Ecology*, 59(2), pp.339–350.

Schalke, H.J., 1973. The Upper Quaternary of the Cape Flats Area (Cape Province, South Africa). *Scripta Geologica*, 15, pp.1–67.

Scott, L., 1982. Late quaternary fossil pollen grains from the Transvaal, South Africa. *Review of Palaeobotany and Palynology*, 36(3–4), pp.241–278.

Strobel, P., Kasper, T., Frenzel, P., Schittek, K., Quick, L.J., Meadows, M.E., Mäusbacher, R. & Haberzettl, T., 2019. Late Quaternary palaeoenvironmental change in the year-round rainfall zone of South Africa derived from peat sediments from Vankervelsvlei. *Quaternary Science Reviews*, 218, pp.200–214.

Stuiver, M., Reimer, P.J. & Reimer, R.W., 2020. CALIB 8.2.

Thamm, A.G., Grundling, P. & Mazus, H., 1996. Holocene and recent peat growth rates on the Zululand coastal plain. *Journal of African Earth Sciences*, 23(1), pp.119–124.

Tinner, W. & Hu, F.S., 2003. Size parameters, size-class distribution and area-number relationship of microscopic charcoal: relevance for fire reconstruction. *The Holocene*, 13(4), pp.499–505.

Welman, W.G. & Kuhn, L., 1970. *South African pollen grains and spores, Volume VI*, Amsterdam-Cape Town: Balkema.

Weyl, P.S.R., Thum, R.A., Moody, M.L., Newman, R.M. & Coetzee, J.A., 2016. Was Myriophyllum spicatum L. (Haloragaceae) recently introduced to South Africa from Eurasia? *Aquatic Botany*, 128, pp.7–12.

Weyl, P.S.R. & Coetzee, J.A., 2014. The invasion status of Myriophyllum spicatum L. In Southern Africa. *Management of Biological Invasions*, 5(1), pp.31–37.

Van Zinderen Bakker, E.M., 1953. *South African Pollen Grains and Spores, Volume I*, AA Balkema.

Van Zinderen Bakker, E.M. & Coetzee, J.A., 1959. *South African Pollen Grains and Spores, Volume III*, Cape Town: AA Balkema.

Chapter 6
Conclusion

6.1. Introduction

This study produced four sets of late Holocene records from three wetlands along the southern Cape coast by analysing pollen and charcoal data from sediment cores from Bo Langvlei, Eilandvlei and Vankervelsvlei, and geochemical and sedimentological data from Bo Langvlei.

Chapter 6 begins with a synthesis of the late Holocene palaeoenvironments of the Wilderness Embayment in which the key findings from this study are placed in context. This is followed by a review of the aim and objectives as outlined in Chapter 1, and concludes with ideas for future research directions.

6.2. Late Holocene palaeoenvironments of the Wilderness Embayment – the current state of knowledge

The late Holocene evolution of the Wilderness Embayment has been significantly influenced by sea level oscillations, climatic and geomorphic dynamics, and more recently, anthropogenic activities. This section serves as a reflection on how the additional work presented in the dissertation advances our understanding of the current state of knowledge of the late Holocene environmental evolution of the region.

Palaeoenvironmental synthesis of the late Holocene evolution of the Wilderness Embayment

Following the mid-Holocene sea level highstand c. 6400 to 4700 cal yr (Wündsch et al. 2018), the southern Cape coast was subjected to a series of sea level regressions and minor transgressions. As revealed in this study (Chapter 3), the development of the Wilderness Embayment during the late Holocene can essentially be divided into three phases. During the marine/lagoon phase the Wilderness lakes were transitioning from full marine conditions towards a coastal lagoon system as sea levels regressed and the inflow of seawater

became increasingly restricted. In Bo Langvlei this phase extended to c. 1200 cal yr BP with a variable marine influence still present throughout this period (Figure 6-1.B). In adjacent Eilandvlei this phase persisted from c. 4700 to 1400 cal yr BP (Kirsten et al. 2018; Wündsch et al. 2018) and at Groenvlei these conditions lasted until around 2700 cal yr BP (Martin 1959; 1968; Wündsch et al. 2016). This was a highly dynamic period in the development of the embayment with the onset of late Holocene dune sedimentation c. 3700 cal yr BP driven by increased westerly winds (Bateman et al. 2011).

As outlined in Chapter 3, the evidence from Bo Langvlei indicates that throughout this marine/lagoon phase the Wilderness lakes – Eilandvlei, Bo Langvlei and Rondevlei – were connected by much wider channels than seen today and that Eilandvlei still had strong connection to the ocean. These connections would however have narrowed over time as sea levels recede and the dunes became established, progressively isolating the lakes (mainly Eilandvlei) from the ocean as well as from each other (Figure 6-1.A).

The Wilderness region further experienced relatively dry conditions prior to c. 3000 cal yr BP (Quick et al. 2018; Wündsch et al. 2016; Wündsch et al. 2018), followed by a shift towards increasing moisture availability and reduced rainfall seasonality until at least c. 2600 cal yr BP as evidenced by the increasing percentages of Afrotemperate forest pollen in the EV11 Eilandvlei pollen record (Figure 6-2; Chapter 4). Similar conditions were inferred from the EV13 Eilandvlei (Quick et al. 2018; Wündsch et al. 2018) and Groenvlei (Wündsch et al. 2016) records. During this period of enhanced dune mobility, most of the records are however generally characterised by substantial variability – as demonstrated by the EV11 pollen record in Chapter 4 (Figure 6-2). In this regard, Martin (1968) cautions climatic interpretations based on the expansion and/or contraction of forest at this time as observed in pollen records, as extensive dune activity may have been responsible for such changes.

In the analysis of Bo Langvlei, presented in Chapter 3, a sea level lowstand was identified after 2600 cal yr BP (Figure 6-1.B), consistent with indications of lower sea levels at Groenvlei (Deevey et al. 1959; Martin 1968) and a lowstand recorded along the west coast of South Africa between c. 2500 and 1800 cal yr BP (Baxter 1997; Compton 2001; 2006). This regression is also evident at Eilandvlei in the expansion of salt marsh vegetation (high percentages of the halophytic taxon Amaranthaceae in the EV11

record) from c. 2600 to around 1900 cal yr BP (Figure 6-1.B). An offset in the timing of this salt marsh expansion was noted between the EV11and EV13 (Quick et al. 2018) pollen records and, as indicated in Chapter 4, this might be ascribed to the different coring locations and internal lake hydrodynamics.

From around c. 1300 to 1200 cal yr BP, the embayment underwent a short transitional phase (Figure 6-1.A). The geochemical and sedimentological evidence from Bo Langvlei (Chapter 3) indicate a rather abrupt shift from marine/lagoon to lacustrine conditions, likely triggered by a flood event around c. 1210 cal yr BP (Figure 6-1.B). This is supported by findings from Groenvlei (Wündsch et al. 2016). This event also resulted in a distinct narrowing, or possible cut off, of the connection between Bo Langvlei and Eilandvlei as outlined in Chapter 3. Following this, the lakes developed conditions broadly consistent with the contemporary scenario.

After ~1200 cal yr BP the EV13 Eilandvlei records suggest wetter, more humid conditions with reduced rainfall seasonality for the remainder of the late Holocene (Quick et al. 2018; Wündsch et al. 2018). The evidence from this study however has revealed finer scale climatic dynamics during the last ~1200 years (Figure 6-2):

Drier conditions are indicated in both the pollen and geochemical records from Bo Langvlei after c. 1200 cal yr BP until around 800 cal yr BP (Chapter 2, 3). Evidenced by a decline in Afrotemperate forest pollen and decreased minerogenic input, it is suggested that the MCA in the region was relatively arid with more enhanced rainfall seasonality related to the greater influence of temperate circulation systems at this time. From around 750 to 550 cal yr BP a period of forest expansion and increased rainfall is indicated in the Bo Langvlei records with wetter than present conditions also inferred at Groenvlei between 700 and 600 cal yr BP (Wündsch et al. 2016). Warmer and slightly drier conditions are indicated in the pollen record from Vankervelsvlei (Chapter 5) around c. 650 cal yr BP with moisture availability increasing towards c. 530 cal yr BP. As indicated in Chapter 2, the transition from the MCA to the LIA was warm and humid in the Wilderness region with reduced rainfall seasonality resulting from the increased influence of tropical moisture bearing systems. In the EV11 Eilandvlei pollen record, however, the phase of forest expansion (with onset after c. 1600 cal yr BP) extends until c. 710 cal yr BP.

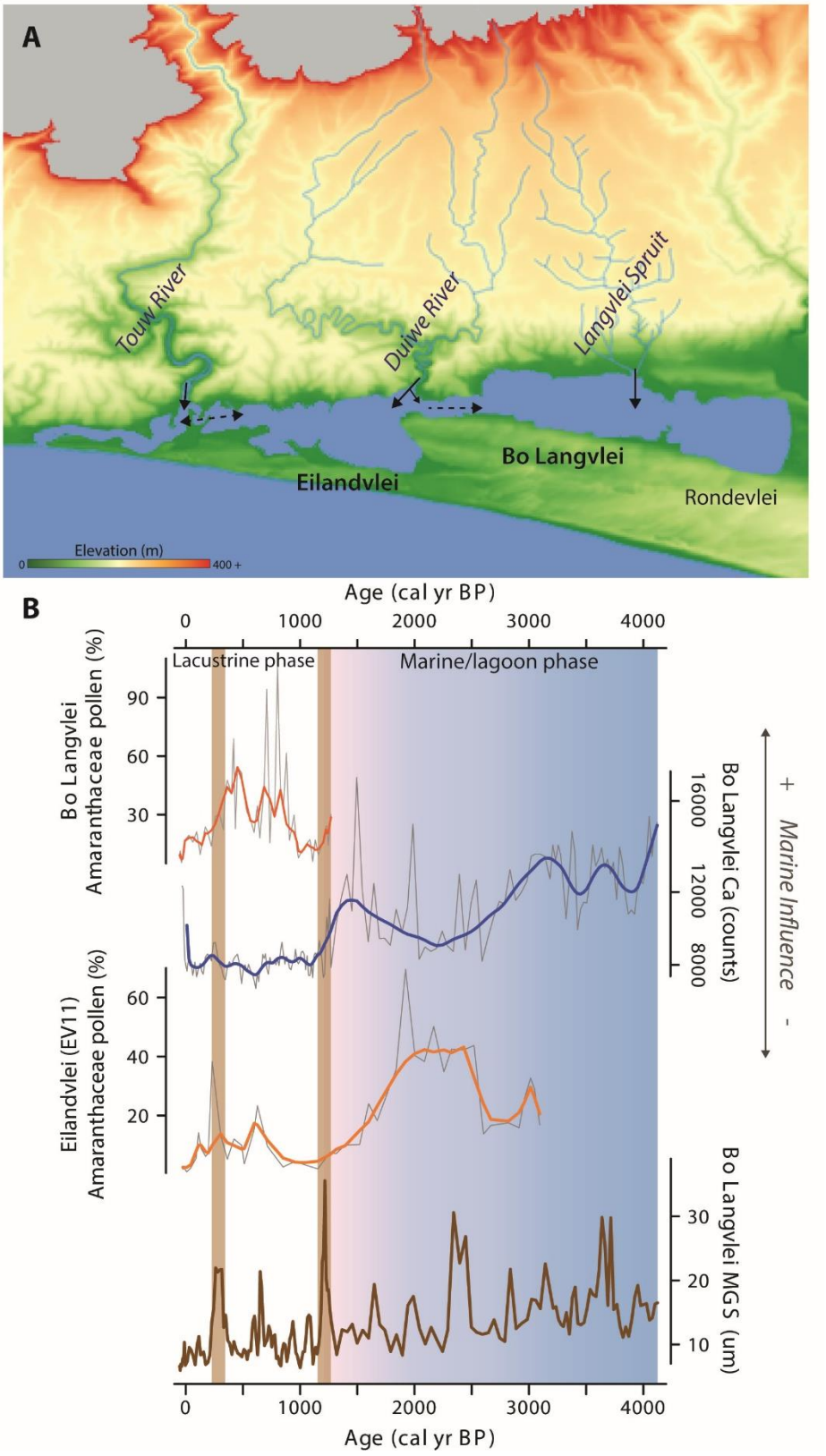

Figure 6-1: Summary of the Holocene evolution of the Wilderness Embayment as impacted by marine transgressions and regressions, and flood events: **A.** Illustration of the hydrology during the *Transitional Phase* of the Wilderness Embayment, as termed in Chapter 3; **B.** Pollen (Bo Langvlei and Eilandvlei) and geochemical (Bo Langvlei) records generated in this study demonstrating sea level change and the consequent vegetation responses. The brown shading indicates the two flood events, at ~1210 and ~310 cal yr BP respectively, as identified in the BoLa 13.2 record, and the blue shading indicates the marine, or lagoon, phase in the Embayment.

After c. 550 cal yr BP, a cooler and drier environment, concomitant with a period of forest retreat, is seen at Bo Langvlei with similar conditions indicated in the Vankervelsvlei record around this time. Generally dry conditions were also experienced then at Groenvlei (Wündsch et al. 2016). On the other hand, increased percentages of Afrotemperate forest pollen are seen in the EV11 Eilandvlei record from c. 600 to 360 cal yr BP. However, based on the Bo Langvlei records, the period c. 550 to 350 cal yr BP appears to have been especially variable, with marked shifts between warm-wet and cool-dry conditions. A resurgence in dune activity is indicated from c. 600 to 430 cal yr BP (Bateman et al. 2011). Accordingly the evidence from this study suggests cooler and drier conditions during the first part of the LIA, while geomorphic activity (i.e. dune accretion) may have affected the area on a more local scale as reflected in the variability observed in the pollen records.

Substantially drier and cooler conditions characterised the latter part of the LIA with a marked decline in Afrotemperate forest pollen in both the Bo Langvlei and EV11 Eilandvlei pollen records after c. 350 cal yr BP (AD 1600). A similar distinct decrease in minerogenic input, hence rainfall, is apparent at Bo Langvlei after a large flood event around c. 310 cal yr BP (AD 1640), with the drier conditions recorded at Groenvlei extending until c. 140 cal yr BP (AD 1810) (Wündsch et al. 2016). The break in sedimentation in composite core VVV16 from c. 175 to 110 cal yr BP (AD 1775 to 1860) may indeed be a response to these drier conditions.

As suggested in Chapter 2, the colder and drier conditions during the LIA may be ascribed to limited rainfall associated with tropical systems or relating to higher Agulhas Current sea-surface temperatures. In addition, the limited impact of increased frontal systems on rainfall during the LIA reinforces the proposed importance of summer rainfall in regulating moisture availability along the southern Cape coast, as suggested by (Quick et al. 2018).

After c. AD 1850 (c. 100 cal yr BP), the increased presence of Afrotemperate forest pollen in the Bo Langvlei and EV11 Eilandvlei records suggests warmer and more humid conditions, also recorded at Groenvlei (Wündsch et al. 2016). This period is, however, notable for increasing levels of human disturbance in the region, evidenced by the presence of *Pinus* in the Bo Langvlei record from c. AD 1850, in EV11 from AD 1910 and, in the record from Vankervelsvlei, *Pinus* is present from c. AD 1900 and

Myrtaceae (likely *Eucalyptus*) from c. AD 1930. Accordingly, some of the variability observed in the most recent records may be related to non-climatic influences.

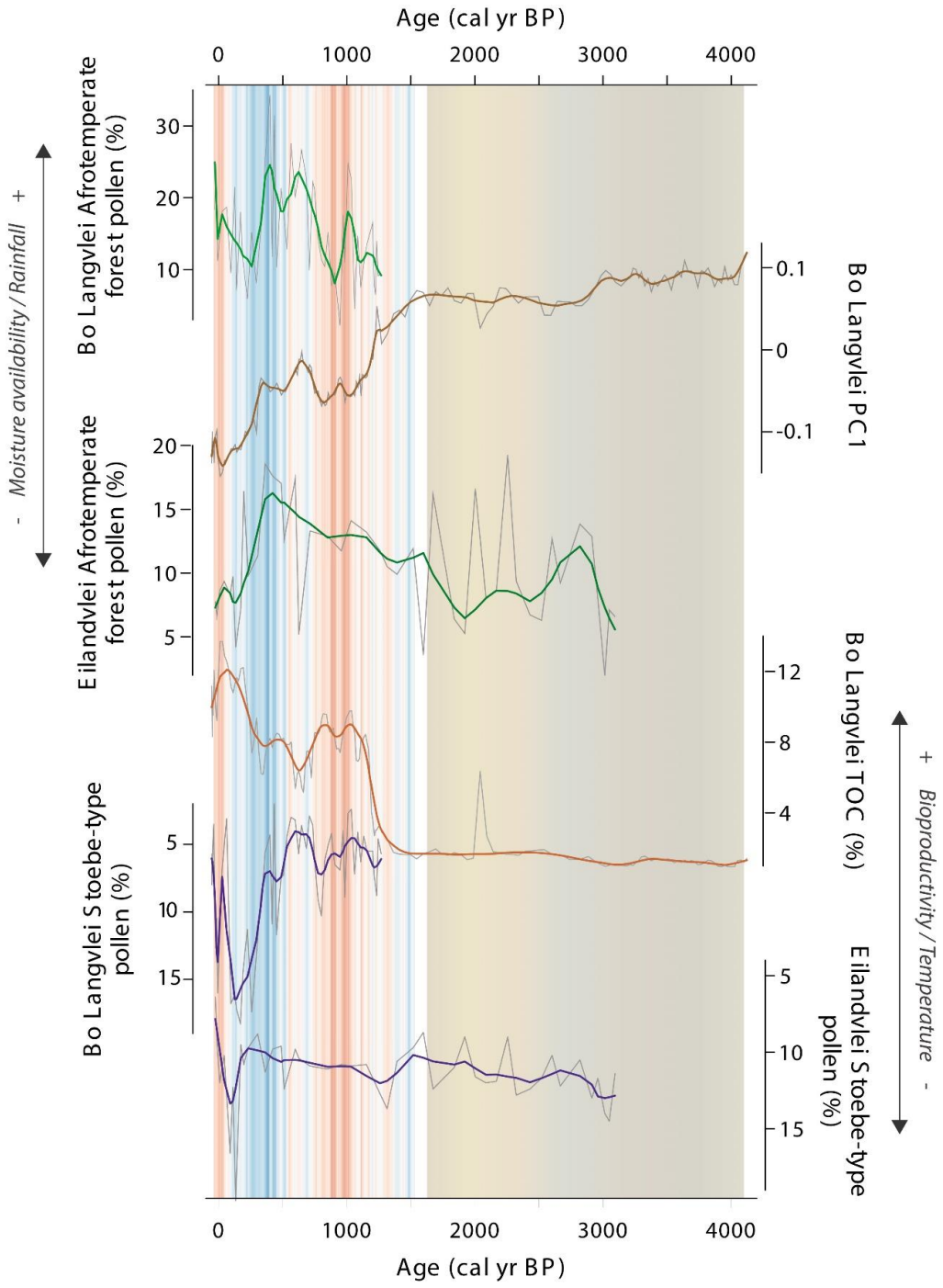

Figure 6-2: Summary of Late Holocene vegetation and climate change in the Wilderness Embayment as recorded by the pollen (Bo Langvlei and Eilandvlei) and geochemical (Bo Langvlei) records from Bo Langvlei and Eilandvlei. The red and blue shading indicates the reconstructed temperature anomaly in the Northern Hemisphere, as in Chapter

2. The blue/brown shading indicates the period during which the main drivers behind environmental and landscape change in the region were sea level fluctuations and dune accretion.

The records presented here are of better temporal resolution than those previously obtained from the Wilderness region, offering more detailed insights on finer scale environmental and climate dynamics both regionally and more locally. In addition, the records from Bo Langvlei present evidence from a new site while also contributing to the understanding of inter-basin dynamics in this area specifically. Accordingly, this study has greatly added to the existing body of work from the region by providing a more comprehensive picture of environmental and climate change along the southern Cape coast during the late Holocene.

6.3. Review of aims and objectives

This study aimed to investigate and reveal vegetation, climatic and landscape dynamics in the Wilderness Embayment during the late Holocene using a multi-proxy approach combining pollen, microscopic charcoal, geochemical and grain size analyses. This aim has been achieved in meeting the specific objectives as set out in Chapter 1.

Objective 1: Retrieve sediment cores from the specified study sites within the Wilderness Embayment

This objective was successfully achieved by retrieving sediment cores from Bo Langvlei, Eilandvlei and Vankervelsvlei and applying the multi-proxy methodologies and analysis as outlined in the relevant chapters.

Objective 2.1: Obtain high resolution chronologies through radiocarbon and ^{210}Pb dating

It has proved possible to establish high resolution chronologies for each of the sequences through the use of radiocarbon dating. For Bo Langvlei additional ^{210}Pb dating was employed for the most recent section of the sequence.

Objective 2.2: Obtain palynological records of long term vegetation change, and the associated charcoal records

Through the extraction and identification of pollen and charcoal from the Bo Langvlei (BoLa 13.2), Eilandvlei (EV11) and Vankervelsvlei (VVV16-4, VVV16-1-1-1/2) sediment cores, palynological records of vegetation and climate change have been successfully constructed for each of the study sites.

More specifically, the BoLa 13.2 pollen record covers the last ~1300 years and is analysed in Chapter 2; the pollen record from sediment core EV11 extends from c. 3000 cal yr BP to the present and is discussed in Chapter 4; the composite pollen record from VVV16-4 and VVV16-1-1-1/2 includes the last ~650 years and is presented in Chapter 5.

Objective 2.3: Obtain sediment, elemental- and organic geochemical records to investigate the landscape evolution of the area

Through the use of the methodologies set out in Chapter 3, sediment, elemental- and organic geochemical records have been generated for sediment core BoLa 13.2. These ~4200 year multi-proxy records provide for a more robust environmental reconstruction illustrating the late Holocene evolution of Bo Langvlei and the Wilderness lakes as a whole.

Objective 3: Assessment of these records in order to reconstruct late Holocene palaeoenvironmental conditions for the study sites

Credible palaeoenvironmental reconstructions for the sites in question have indeed been completed and presented in each of the relevant chapters

Objective 4: Evaluate these findings in the context of local, regional and appropriate broader palaeoenvironmental records

As with objective 3, each record has been described, analysed and discussed in relation to the wider environmental context in the relevant chapters, with section 6.2 providing a summary of the findings from this study.

6.4. Future research directions

While providing new records and contributing new insights to the expanding state of knowledge regarding the late Holocene evolution of the southern Cape coast, this study also highlighted several areas where further investigation is warranted. These include:

- long-term fire ecology in the Wilderness region and its association with the Afrotemperate Forest Biome
- the effects of internal lake hydrodynamics and external forcings on pollen accumulation and preservation in a lake basin
- the connection, if any, between water level fluctuations in Vankervelsvlei and the density of the sedge cover of the floating vegetation mat

6.5. A final word

This study successfully produced four new late Holocene records of environmental, vegetation and climate change for the southern Cape coast of South Africa. These records provide invaluable information to improve our understanding of both past and future environmental dynamics in southern Africa.

In closing,

‘Science can only help us if we use it to show how the present is a product of the past, and to remind us that we are now shaping our future. It is the privilege of the paleoecologist to reconstruct a [temporal ecological] continuum so convincing that the lesson will be heeded. . . . It may well be that [paleoecological] findings will, in the end, mean far more to the future of mankind than [we] now suspect’ (Sears 1962, p 5).

[Birks 2019]

6.6. References

Bateman, M.D., Carr, A.S., Dunajko, A.C., Holmes, P.J., Roberts, D.L., McLaren, S.J., Bryant, R.G., Marker, M.E. & Murray-Wallace, C.V., 2011. The evolution of coastal barrier systems: a case study of the Middle-Late Pleistocene Wilderness barriers, South Africa. *Quaternary Science Reviews*, 30(1–2), pp.63–81.

Baxter, A.J., 1997. *Late Quaternary palaeoenvironments of the Sandveld, Western Cape Province, South Africa*. University of Cape Town.

Birks, H.J.B., 2019. Contributions of Quaternary botany to modern ecology and biogeography. *Plant Ecology and Diversity*, 12(3–4), pp.189–385.

Compton, J.S., 2001. Holocene sea-level fluctuations inferred from the evolution of depositional environments of the southern Langebaan Lagoon salt marsh, South Africa. *The Holocene*, 11(4), pp.395–405.

Compton, J.S., 2006. The mid-Holocene sea-level highstand at Bogenfels Pan on the southwest coast of Namibia. *Quaternary Research*, 66(2), pp.303–310.

Deevey, E.S., Gralenski, L.J. & Hoffren, V., 1959. Yale natural radiocarbon measurements IV. *Radiocarbon*, 1, pp.144–159.

Kirsten, K.L., Haberzettl, T., Wündsch, M., Meschner, S., Smit, A.J., Quick, L.J. & Meadows, M.E., 2018. A multiproxy study of the ocean-atmospheric forcing and the impact of sea-level changes on the southern Cape coast, South Africa during the Holocene. *Palaeogeography, Palaeoclimatology, Palaeoecology*, 496, pp.282–291.

Martin, A.R.H., 1968. Pollen Analysis of Groenvlei Lake Sediments, Knysna (South Africa). *Review of Palaeobotany and Palynology*, 7, pp.107–144.

Martin, A.R.H., 1959. The Stratigraphy and History of Groenvlei, a South African Coastal Fen. *Australian Journal of Botany*.

Quick, L.J., Chase, B.M., Wundsch, M., Kirsten, K.L., Chevalier, M., Mausbacher, R., Meadows, M.E. & Haberzettl, T., 2018. A high-resolution record of Holocene climate and vegetation dynamics from the southern Cape coast of South Africa : pollen and microcharcoal evidence from Eilandvlei. *Journal of Quaternary Science*, 33(5), pp.487–500.

Sears, P.B., 1962. The goals of paleoecological reconstruction. In J. J. Hester & J. Schoenwetter, eds. *The reconstruction of past environments*. Fort Burwin Research Centre, Taos, NM, pp. 4–6.

Wündsch, M., Haberzettl, T., Cawthra, H.C., Kirsten, K.L., Quick, L.J., Zabel, M., Frenzel, P., Hahn, A., Baade, J., Daut, G., Kasper, T., Meadows, M.E. & Mäusbacher, R., 2018. Holocene environmental change along the southern Cape coast of South Africa - Insights from the Eilandvlei sediment record spanning the last 8.9kyr. *Global and Planetary Change*, 163, pp.51–66.

Wündsch, M., Haberzettl, T., Kirsten, K.L., Kasper, T., Zabel, M., Dietze, E., Baade, J., Daut, G., Meschner, S., Meadows, M.E. & Mäusbacher, R., 2016. Sea level and climate change at the southern Cape coast , South Africa , during the past 4.2 kyr. *Palaeogeography, Palaeoclimatology, Palaeoecology*, 446, pp.295–307.

Appendix A

BoLa13.2 Pollen and microcharcoal

Sample	13-2-2	13-2-3	13-2-4	13-2-5	13-2-6	13-2-7	13-2-8	13-2-9
Depth (cm)	2	3	4	5	6	7	8	9
Age (cal yr BP	-54.1	-51.2	-48.5	-45.8	-38.2	-30.5	-22.9	-15.3
Artemisia	3	3	0	2	0	9	11	4
Pentzia-type	3	3	0	4	0	0	1	0
Proteaceae	0	1	2	3	0	1	1	0
Ericaceae	14	8	8	5	8	18	9	10
Cliffortia	4	3	1	4	1	3	6	4
Bruniaceae	0	0	1	0	1	0	0	0
Anthospermum-type	12	0	0	1	2	7	1	1
Apiaceae	0	0	0	0	0	0	0	0
Fabaceae	0	0	1	1	0	0	2	0
Phylica	0	0	0	0	0	1	1	0
Rutaceae	0	0	0	0	0	0	0	1
Santalaceae	0	2	0	1	1	0	1	1
Scroph-type	0	0	0	2	1	0	0	0
Thymelaeaceae	0	5	2	4	3	9	11	6
Passerina	12	9	15	4	5	42	33	17
Canthium	0	0	0	0	0	0	0	0
Icacinaceae	4	0	0	0	0	1	1	0
Encephalartos	0	0	0	0	0	0	0	0
Euclea	1	5	1	1	1	4	2	3
Grewia	0	0	0	0	0	1	0	0
Ilex	1	0	1	0	0	1	1	1
Morella	0	0	0	0	0	4	2	0
Myrsine	1	0	1	1	0	0	0	0
Myrtaceae	0	0	0	0	0	0	0	0
Olea	11	3	6	5	4	4	0	6
Exotics	175	65	591	133	53	1433	1115	185
Cyperaceae	6	12	5	5	3	4	5	1
Restionaceae	14	16	5	11	8	12	8	14
Poaceae	17	22	7	9	6	28	10	15
Asteraceae HS	7	7	5	3	6	2	9	6
Stoebe-type	21	14	17	13	9	25	34	20
Geraniaceae	1	1	0	0	0	0	0	1
Montinaceae	0	0	0	0	0	0	0	0
Oxygonum	0	0	0	0	0	0	0	0
Polygonum	0	0	0	0	0	0	0	0
Celastraceae	4	1	2	1	3	2	0	2
Celtis	1	0	0	0	0	0	0	0
Diospyros	2	0	0	2	0	0	2	4
Dodonaea	0	0	0	0	0	0	0	0
Euphorbia	5	9	7	7	4	14	12	7
Clutia	0	0	0	0	0	0	0	0
Amaranthaceae	21	28	30	22	15	23	20	25
Crassula	3	0	2	2	0	1	0	2

Sample	13-2-2	13-2-3	13-2-4	13-2-5	13-2-6	13-2-7	13-2-8	13-2-9
Depth (cm)	2	3	4	5	6	7	8	9
Age (cal yr BP	-54.1	-51.2	-48.5	-45.8	-38.2	-30.5	-22.9	-15.3
Ruschia	0	0	0	0	0	0	0	1
Juncaceae	0	0	0	2	0	0	0	0
Liliaceae	0	2	1	0	1	0	1	1
Iridaceae	0	0	0	1	0	0	0	0
Amarylliaceae	0	0	1	0	0	0	0	0
Scabiosa	0	0	0	0	0	2	2	0
Aponogeton	0	0	2	0	0	0	0	6
Haloraginaceae	0	1	0	0	0	0	0	0
Typhaceae	2	2	0	2	0	0	1	0
Zygophyllaceae	0	0	0	0	0	0	0	0
Unidentifiable	2	4	1	2	1	3	4	2
Broken	4	4	3	3	0	4	3	3
Justica-type	0	0	0	1	0	0	0	0
Pinaceae	31	50	100	104	95	22	38	12
Podocarpus	86	73	69	64	115	47	66	40
Rhus	0	0	1	4	0	2	1	0
Dioscoreaceae	0	0	0	0	0	0	0	0
Aizoaceae	4	8	0	4	3	2	0	6
Euphorbiaceae undif	0	0	0	0	0	0	0	0
Aloe-type	0	0	0	0	0	0	0	0
Brassicaceae	2	1	3	0	0	2	0	0
Caryophyllaceae	0	2	0	0	0	0	0	0
Gunnera	1	0	0	0	1	0	0	0
Polygala	0	0	0	0	0	0	0	0
Cardiospermum	0	1	0	0	0	0	0	0
Lauraceae	0	0	0	0	0	0	0	0
Combretaceae	0	0	0	0	0	0	0	0
Nymphaea	0	0	0	0	0	0	0	0
Oxalis	0	0	0	0	1	0	0	0
Plumbaginaceae	0	0	0	0	0	0	0	0
Portulaceae	0	0	0	0	2	0	0	0
Plantago	0	0	0	0	0	0	0	0
10 - 100 um	0	0	0	0	0	0	0	0
>100 um	0	0	0	0	0	0	0	0
Moraceae	0	0	0	0	0	0	0	0
Potamogetonaceae	0	0	0	0	0	0	1	0
NAP	300	300	300	300	300	300	300	222
All total	475	365	891	433	353	1733	1415	410

Sample	13-2-10	13-2-12	13-2-14	13-2-16	13-2-18	13-2-19	13-2-21	13-2-22
Depth (cm)	10	12	14	16	18	19	21	22
Age (cal yr BP	-7.7	27.4	61.9	95.4	126.1	139.3	170.5	189.5
Artemisia	4	1	0	6	0	19	3	8
Pentzia-type	3	1	0	2	0	8	3	3
Proteaceae	5	2	2	6	0	1	0	8
Ericaceae	17	6	15	9	17	24	15	21
Cliffortia	4	2	4	3	4	4	3	4
Bruniaceae	0	3	2	2	0	2	0	1
Anthospermum-type	2	1	2	6	8	5	10	4
Apiaceae	1	0	0	0	0	0	0	1
Fabaceae	0	0	0	1	0	0	0	1
Phylica	0	1	1	0	0	1	3	0
Rutaceae	0	0	0	0	0	0	0	0
Santalaceae	0	0	0	0	0	2	0	0
Scroph-type	0	1	0	0	0	0	0	0
Thymelaeaceae	6	6	3	10	7	5	8	2
Passerina	6	10	20	12	17	44	6	17
Canthium	0	0	0	0	1	1	0	0
Icacinaceae	5	0	0	3	1	0	2	1
Encephalartos	0	0	1	0	0	0	0	1
Euclea	2	4	3	1	1	1	4	4
Grewia	0	0	0	0	0	0	0	2
Ilex	3	0	0	2	0	0	3	0
Morella	4	0	0	4	0	4	1	3
Myrsine	0	0	1	0	0	0	0	0
Myrtaceae	0	0	0	0	0	0	0	0
Olea	11	8	12	18	15	6	11	7
Exotics	196	222	58	202	114	860	217	641
Cyperaceae	11	4	7	14	10	7	14	3
Restionaceae	12	13	16	15	18	11	25	23
Poaceae	12	18	9	14	29	5	14	28
Asteraceae HS	6	9	11	5	10	15	3	8
Stoebe-type	38	16	7	38	41	43	41	34
Geraniaceae	2	0	2	1	0	2	0	0
Montinaceae	0	0	0	0	0	0	0	0
Oxygonum	0	0	0	0	0	0	1	0
Polygonum	0	0	1	0	0	0	0	0
Celastraceae	2	3	1	2	5	0	1	2
Celtis	0	2	2	2	0	1	2	0
Diospyros	3	3	1	4	2	2	1	0
Dodonaea	0	0	0	0	0	0	0	0
Euphorbia	16	8	4	12	7	14	11	20
Clutia	1	0	0	1	1	0	0	0
Amaranthaceae	41	48	40	49	25	36	54	51
Crassula	3	3	2	2	4	3	4	0

Sample	13-2-10	13-2-12	13-2-14	13-2-16	13-2-18	13-2-19	13-2-21	13-2-22
Depth (cm)	10	12	14	16	18	19	21	22
Age (cal yr BP	-7.7	27.4	61.9	95.4	126.1	139.3	170.5	189.5
Ruschia	0	0	0	1	0	0	0	0
Juncaceae	1	1	0	1	2	1	0	0
Liliaceae	0	0	1	1	0	2	0	1
Iridaceae	0	0	0	0	0	0	0	3
Amarylliaceae	0	0	0	0	0	0	0	0
Scabiosa	0	0	0	2	0	1	0	0
Aponogeton	0	0	0	0	0	0	0	0
Haloraginaceae	0	0	0	0	0	0	0	0
Typhaceae	5	0	2	5	3	1	4	7
Zygophyllaceae	0	0	0	0	0	0	0	0
Unidentifiable	4	3	3	4	4	3	1	3
Broken	3	2	3	4	5	2	5	3
Justica-type	0	0	0	0	0	0	0	0
Pinaceae	33	0	73	12	0	0	0	0
Podocarpus	18	108	46	16	53	18	36	24
Rhus	7	5	0	4	1	0	5	2
Dioscoreaceae	1	0	0	0	0	0	0	0
Aizoaceae	7	5	2	4	7	0	3	0
Euphorbiaceae undif	0	0	0	0	0	0	0	0
Aloe-type	0	0	0	0	0	0	0	0
Brassicaceae	0	0	0	1	0	4	1	0
Caryophyllaceae	0	0	0	0	0	0	0	0
Gunnera	0	1	0	1	0	0	1	0
Polygala	0	0	0	0	0	0	0	0
Cardiospermum	0	2	0	0	0	0	0	0
Lauraceae	0	0	0	0	0	0	0	0
Combretaceae	1	0	0	0	0	0	0	0
Nymphaea	0	0	0	0	0	0	0	0
Oxalis	0	0	0	0	0	0	0	0
Plumbaginaceae	0	0	0	0	0	0	0	0
Portulaceae	0	0	0	0	0	0	0	0
Plantago	0	0	0	0	0	0	1	0
10 - 100 um	0	0	0	0	1075	0	0	0
>100 um	0	0	0	0	0	0	0	1
Moraceae	0	0	0	0	1	0	0	0
Potamogetonaceae	0	0	1	0	1	2	0	0
NAP	300	300	300	300	300	300	300	300
All total	496	522	358	502	1489	1160	517	942

Sample	13-2-24	13-2-26	13-2-28	13-2-30	13-2-31	13-2-32	13-2-34	13-2-35
Depth (cm)	24	26	28	30	31	32	34	35
Age (cal yr BP	224.3	257.8	293.7	328.6	345.3	362.9	399.7	417.6
Artemisia	7	0	5	0	8	2	0	7
Pentzia-type	3	9	6	4	4	4	1	2
Proteaceae	2	4	0	4	2	1	0	3
Ericaceae	6	14	19	19	20	8	19	9
Cliffortia	5	7	5	8	7	4	1	1
Bruniaceae	0	1	1	1	2	0	2	3
Anthospermum-type	11	5	6	8	4	8	8	3
Apiaceae	0	0	0	0	0	0	0	0
Fabaceae	0	0	2	0	0	0	0	0
Phylica	0	0	0	0	0	1	0	0
Rutaceae	0	0	0	0	0	0	0	0
Santalaceae	0	2	0	3	0	0	0	0
Scroph-type	0	0	0	0	0	0	0	0
Thymelaeaceae	9	5	6	0	0	5	1	2
Passerina	27	7	19	6	9	3	0	4
Canthium	0	0	0	0	5	0	0	0
Icacinaceae	0	0	0	0	1	1	1	4
Encephalartos	1	0	0	0	0	0	0	0
Euclea	10	4	4	1	1	3	3	2
Grewia	1	0	0	0	0	0	0	0
Ilex	1	1	3	0	2	2	0	3
Morella	0	2	0	0	2	0	0	4
Myrsine	0	0	1	0	1	0	2	1
Myrtaceae	0	0	0	0	0	0	0	0
Olea	9	8	11	11	14	11	18	9
Exotics	315	136	203	188	569	109	24	224
Cyperaceae	9	14	6	13	8	21	19	11
Restionaceae	25	13	18	25	14	22	19	9
Poaceae	20	17	20	37	11	16	17	7
Asteraceae HS	11	10	12	10	3	3	2	8
Stoebe-type	28	37	29	20	15	10	8	18
Geraniaceae	2	0	0	0	0	1	0	4
Montinaceae	0	0	0	0	0	0	0	0
Oxygonum	0	0	0	0	0	0	0	0
Polygonum	0	0	0	0	0	0	0	0
Celastraceae	4	1	1	4	4	3	1	2
Celtis	1	1	3	2	1	0	1	0
Diospyros	2	2	2	2	1	0	0	1
Dodonaea	0	0	0	0	0	0	0	1
Euphorbia	16	13	18	14	16	10	8	28
Clutia	0	0	0	0	1	0	1	0
Amaranthaceae	35	63	68	52	86	89	81	117
Crassula	3	4	4	0	0	3	2	0

Sample	13-2-24	13-2-26	13-2-28	13-2-30	13-2-31	13-2-32	13-2-34	13-2-35
Depth (cm)	24	26	28	30	31	32	34	35
Age (cal yr BP	224.3	257.8	293.7	328.6	345.3	362.9	399.7	417.6
Ruschia	0	0	0	0	0	0	0	0
Juncaceae	0	1	1	1	2	2	0	0
Liliaceae	4	3	0	0	1	4	3	1
Iridaceae	1	0	0	0	0	0	1	0
Amarylliaceae	0	1	0	0	0	0	0	0
Scabiosa	0	1	0	0	0	0	0	2
Aponogeton	3	0	0	0	0	0	0	0
Haloraginaceae	0	0	0	0	0	0	0	0
Typhaceae	2	5	3	1	3	1	2	2
Zygophyllaceae	0	0	0	0	0	0	0	0
Unidentifiable	4	2	3	2	4	4	2	6
Broken	2	4	5	5	3	3	2	2
Justica-type	0	0	0	0	0	0	0	0
Pinaceae	0	0	0	0	0	0	0	0
Podocarpus	11	32	14	35	31	44	64	12
Rhus	5	2	1	1	6	4	0	1
Dioscoreaceae	0	0	0	0	0	0	0	0
Aizoaceae	12	3	2	8	2	4	7	5
Euphorbiaceae undif	0	0	0	0	0	0	0	0
Aloe-type	0	0	0	0	0	0	0	0
Brassicaceae	5	0	1	1	5	0	4	1
Caryophyllaceae	0	0	1	0	1	1	0	3
Gunnera	0	2	0	1	0	2	0	2
Polygala	0	0	0	0	0	0	0	0
Cardiospermum	0	0	0	0	0	0	0	0
Lauraceae	2	0	0	1	0	0	0	0
Combretaceae	0	0	0	0	0	0	0	0
Nymphaea	0	0	0	0	0	0	0	0
Oxalis	1	0	0	0	0	0	0	0
Plumbaginaceae	0	0	0	0	0	0	0	0
Portulaceae	0	0	0	0	0	0	0	0
Plantago	0	0	0	0	0	0	0	0
10 - 100 um	0	0	0	0	0	0	0	0
>100 um	0	0	0	0	0	0	0	0
Moraceae	0	0	0	0	0	0	0	0
Potamogetonaceae	0	0	0	0	0	0	0	0
NAP	300	300	300	300	300	300	300	300
All total	615	436	503	488	869	409	324	524

Sample	13-2-36	13-2-37	13-2-39	13-2-40	13-2-42	13-2-44	13-2-46	13-2-48
Depth (cm)	36	37	39	40	42	44	46	48
Age (cal yr BP	434	451.8	487.2	505.1	533.1	564.8	597.4	624.6
Artemisia	4	8	5	2	9	5	19	8
Pentzia-type	0	7	10	7	0	2	1	5
Proteaceae	3	2	5	1	1	5	5	1
Ericaceae	13	19	7	6	12	14	17	13
Cliffortia	2	1	0	4	1	2	5	4
Bruniaceae	0	2	0	0	1	2	0	1
Anthospermum-type	12	4	1	11	17	4	8	0
Apiaceae	0	1	0	0	0	0	0	1
Fabaceae	0	2	0	0	0	0	1	1
Phylica	0	0	2	3	0	0	0	1
Rutaceae	0	0	1	0	0	0	0	0
Santalaceae	0	0	0	2	2	0	0	0
Scroph-type	0	0	0	0	0	0	0	0
Thymelaeaceae	3	3	2	0	2	2	3	1
Passerina	5	7	1	7	8	3	1	3
Canthium	1	0	1	0	4	1	3	0
Icacinaceae	0	0	0	0	0	1	4	2
Encephalartos	0	0	0	0	0	0	0	0
Euclea	4	3	9	3	2	5	0	2
Grewia	0	0	0	0	0	0	2	0
Ilex	0	0	3	1	1	0	0	1
Morella	0	0	0	1	2	2	1	2
Myrsine	2	2	0	0	0	1	0	0
Myrtaceae	0	0	0	1	0	0	0	0
Olea	16	10	16	10	11	9	7	11
Exotics	602	467	56	98	390	101	607	181
Cyperaceae	8	11	19	15	11	13	11	22
Restionaceae	27	15	10	23	34	15	25	18
Poaceae	19	11	15	26	26	17	41	24
Asteraceae HS	4	4	6	7	8	4	6	5
Stoebe-type	4	21	13	14	9	6	7	11
Geraniaceae	1	1	0	2	1	0	1	0
Montinaceae	0	0	0	0	0	0	0	0
Oxygonum	0	0	0	0	0	0	0	0
Polygonum	0	0	0	0	0	0	0	0
Celastraceae	2	3	1	4	2	4	2	0
Celtis	3	0	0	2	1	4	1	0
Diospyros	2	2	3	0	2	0	1	1
Dodonaea	0	1	0	0	0	0	0	0
Euphorbia	15	20	16	9	17	28	19	22
Clutia	0	0	0	0	0	0	0	0
Amaranthaceae	53	100	94	85	69	61	50	70
Crassula	3	3	5	1	2	2	1	1

Sample	13-2-36	13-2-37	13-2-39	13-2-40	13-2-42	13-2-44	13-2-46	13-2-48
Depth (cm)	36	37	39	40	42	44	46	48
Age (cal yr BP	434	451.8	487.2	505.1	533.1	564.8	597.4	624.6
Ruschia	0	0	0	0	0	0	0	0
Juncaceae	1	4	3	0	1	3	0	2
Liliaceae	1	4	0	0	3	3	1	2
Iridaceae	0	1	0	0	0	0	0	0
Amarylliaceae	0	0	0	0	0	1	1	0
Scabiosa	1	0	0	0	0	0	2	5
Aponogeton	0	0	0	0	1	0	0	0
Haloraginaceae	0	0	0	0	0	0	0	0
Typhaceae	6	1	1	1	0	2	0	3
Zygophyllaceae	0	0	0	0	0	0	0	0
Unidentifiable	3	5	4	2	3	5	2	4
Broken	4	0	4	3	4	3	1	5
Justica-type	0	0	0	0	0	0	0	0
Pinaceae	0	0	0	0	0	0	0	0
Podocarpus	71	17	36	35	27	59	42	44
Rhus	1	2	3	0	0	2	0	3
Dioscoreaceae	0	0	0	0	0	0	0	0
Aizoaceae	5	1	4	7	3	4	3	0
Euphorbiaceae undif	0	0	0	0	0	0	0	0
Aloe-type	0	0	0	0	0	1	0	0
Brassicaceae	0	2	0	4	3	1	5	1
Caryophyllaceae	0	0	0	0	0	0	0	0
Gunnera	0	0	0	0	0	2	0	0
Polygala	0	0	0	0	0	0	0	0
Cardiospermum	0	0	0	1	0	0	0	0
Lauraceae	0	0	0	0	0	0	0	0
Combretaceae	0	0	0	0	0	0	0	0
Nymphaea	0	0	0	0	0	0	0	0
Oxalis	1	0	0	0	0	0	0	0
Plumbaginaceae	0	0	0	0	0	0	0	0
Portulaceae	0	0	0	0	0	0	1	0
Plantago	0	0	0	0	0	1	0	0
10 - 100 um	0	0	0	0	0	0	0	0
>100 um	0	0	0	0	0	0	0	0
Moraceae	0	0	0	0	0	0	0	0
Potamogetonaceae	0	0	0	0	0	1	0	0
NAP	300	300	300	300	300	300	300	300
All total	902	767	356	398	690	401	907	481

Sample	13-2-50	13-2-53	13-2-55	13-2-57	13-2-58	13-2-60	13-2-62	13-2-64
Depth (cm)	50	53	55	57	58	60	62	64
Age (cal yr BP	647.1	684.9	708.1	735.2	748.6	775.5	802.1	828
Artemisia	5	0	12	6	13	14	12	2
Pentzia-type	4	6	1	2	4	3	4	1
Proteaceae	2	0	3	4	3	3	1	4
Ericaceae	12	9	19	16	18	13	11	4
Cliffortia	2	2	3	7	4	3	3	4
Bruniaceae	0	0	0	0	4	2	1	1
Anthospermum-type	29	12	9	14	2	3	0	7
Apiaceae	0	0	0	0	0	0	0	0
Fabaceae	0	0	1	0	0	2	0	0
Phylica	0	0	0	0	0	1	0	0
Rutaceae	0	1	0	0	2	0	0	0
Santalaceae	2	0	0	0	1	0	0	0
Scroph-type	0	0	0	0	0	0	0	0
Thymelaeaceae	0	2	1	2	6	0	3	1
Passerina	9	7	7	7	5	14	14	10
Canthium	1	0	2	0	0	2	0	2
Icacinaceae	2	2	0	1	0	0	4	0
Encephalartos	0	0	0	0	0	0	0	0
Euclea	2	0	1	3	0	3	1	6
Grewia	2	0	0	0	0	2	0	0
Ilex	0	0	1	0	0	1	3	0
Morella	2	0	0	0	0	2	0	0
Myrsine	0	2	1	0	0	2	3	3
Myrtaceae	0	0	0	0	0	0	0	0
Olea	10	19	3	11	6	16	4	16
Exotics	442	269	817	641	47	200	724	171
Cyperaceae	10	10	4	14	20	12	7	9
Restionaceae	16	24	20	32	15	13	15	20
Poaceae	29	16	12	28	16	23	10	34
Asteraceae HS	5	5	4	5	3	5	2	7
Stoebe-type	8	10	4	8	12	19	14	12
Geraniaceae	0	3	2	1	0	2	1	2
Montinaceae	0	0	0	0	0	0	0	0
Oxygonum	0	0	0	0	0	0	0	0
Polygonum	0	0	0	0	0	0	0	0
Celastraceae	1	9	1	4	0	3	0	4
Celtis	0	2	0	0	1	0	3	1
Diospyros	1	3	0	1	0	2	0	0
Dodonaea	0	0	0	0	0	0	1	0
Euphorbia	28	6	21	15	29	18	11	10
Clutia	0	0	0	0	0	0	0	0
Amaranthaceae	44	88	143	38	71	63	148	86
Crassula	2	6	0	1	1	2	1	4

Sample	13-2-50	13-2-53	13-2-55	13-2-57	13-2-58	13-2-60	13-2-62	13-2-64
Depth (cm)	50	53	55	57	58	60	62	64
Age (cal yr BP	647.1	684.9	708.1	735.2	748.6	775.5	802.1	828
Ruschia	0	0	0	0	0	0	0	0
Juncaceae	2	1	0	1	1	2	3	0
Liliaceae	1	0	1	1	0	1	1	3
Iridaceae	0	0	0	1	0	0	0	0
Amarylliaceae	0	0	0	0	0	0	0	0
Scabiosa	0	1	0	0	1	0	0	0
Aponogeton	0	0	0	2	0	0	0	1
Haloraginaceae	0	0	0	0	0	0	0	0
Typhaceae	1	2	1	4	5	6	2	3
Zygophyllaceae	0	0	0	0	0	0	0	0
Unidentifiable	1	1	4	4	4	3	5	3
Broken	2	5	3	3	3	5	1	5
Justica-type	0	0	0	0	1	0	0	0
Pinaceae	0	0	0	0	0	0	0	0
Podocarpus	61	41	13	53	43	26	6	18
Rhus	2	1	2	1	1	4	1	3
Dioscoreaceae	0	0	0	0	0	0	0	0
Aizoaceae	1	3	1	2	3	2	3	9
Euphorbiaceae undif	0	0	0	0	0	1	0	1
Aloe-type	0	0	0	0	0	0	0	0
Brassicaceae	1	0	0	4	2	0	1	4
Caryophyllaceae	0	0	0	0	0	1	0	0
Gunnera	0	0	0	2	0	0	0	0
Polygala	0	0	0	0	0	0	0	0
Cardiospermum	0	0	0	0	0	0	0	0
Lauraceae	0	0	0	0	0	0	0	0
Combretaceae	0	0	0	0	0	0	0	0
Nymphaea	0	1	0	0	0	0	0	0
Oxalis	0	0	0	2	0	0	0	0
Plumbaginaceae	0	0	0	0	0	1	0	0
Portulaceae	0	0	0	0	0	0	0	0
Plantago	0	0	0	0	0	0	0	0
10 - 100 um	0	5556	0	0	0	0	0	0
>100 um	0	0	0	0	0	0	1	0
Moraceae	0	0	0	0	0	0	0	0
Potamogetonaceae	0	0	0	0	0	0	0	0
NAP	300	300	300	300	300	300	300	300
All total	742	6133	1117	941	347	500	1025	472

Sample	13-2-66	13-2-68	13-2-70	13-2-73	13-2-75	13-2-76	13-2-78	13-2-80
Depth (cm)	66	68	70	73	75	76	78	80
Age (cal yr BP	853.1	880.1	906	946.6	972.1	984.6	1009.3	1035.2
Artemisia	3	12	12	20	1	11	3	2
Pentzia-type	3	5	5	4	4	5	0	2
Proteaceae	3	7	1	3	0	3	2	3
Ericaceae	23	17	30	39	22	20	18	16
Cliffortia	1	3	6	3	1	4	4	2
Bruniaceae	1	2	0	0	2	0	3	1
Anthospermum-type	5	11	18	11	22	4	6	6
Apiaceae	0	0	0	0	0	0	0	0
Fabaceae	0	0	1	2	0	0	2	3
Phylica	0	0	0	0	1	0	3	1
Rutaceae	0	0	0	0	0	0	0	0
Santalaceae	0	0	1	0	0	1	0	2
Scroph-type	0	0	0	0	0	0	0	0
Thymelaeaceae	2	2	8	3	4	4	4	0
Passerina	10	13	3	15	10	8	7	8
Canthium	0	0	0	0	0	2	0	1
Icacinaceae	1	4	1	4	2	0	2	0
Encephalartos	0	0	0	0	0	0	0	0
Euclea	5	1	3	3	3	6	7	2
Grewia	0	1	0	0	0	0	2	0
Ilex	0	2	2	0	0	2	3	0
Morella	1	2	1	3	0	0	4	0
Myrsine	0	0	1	0	1	1	0	1
Myrtaceae	0	0	0	0	0	0	0	1
Olea	13	7	11	8	16	14	14	17
Exotics	81	468	329	751	143	198	84	592
Cyperaceae	15	8	11	2	16	14	8	14
Restionaceae	21	11	23	14	18	25	14	22
Poaceae	33	9	32	20	32	29	40	27
Asteraceae HS	5	7	5	3	9	9	7	6
Stoebe-type	10	7	15	15	9	22	6	5
Geraniaceae	2	0	6	5	2	1	1	3
Montinaceae	0	0	0	0	0	0	0	0
Oxygonum	0	0	0	0	0	0	0	0
Polygonum	0	0	0	0	0	0	0	0
Celastraceae	1	1	3	0	11	2	2	6
Celtis	0	2	4	0	0	1	0	3
Diospyros	0	0	0	0	0	0	3	3
Dodonaea	0	0	0	0	0	0	0	0
Euphorbia	15	23	12	32	16	32	14	21
Clutia	0	0	0	0	0	0	0	0
Amaranthaceae	71	110	41	68	30	20	28	29
Crassula	0	2	2	2	1	1	5	1

Sample	13-2-66	13-2-68	13-2-70	13-2-73	13-2-75	13-2-76	13-2-78	13-2-80
Depth (cm)	66	68	70	73	75	76	78	80
Age (cal yr BP	853.1	880.1	906	946.6	972.1	984.6	1009.3	1035.2
Ruschia	0	0	0	0	0	0	0	0
Juncaceae	3	0	2	0	1	3	0	3
Liliaceae	4	3	0	2	0	2	2	4
Iridaceae	1	0	0	1	0	0	0	2
Amarylliaceae	0	0	0	0	0	0	0	1
Scabiosa	0	3	1	2	0	1	0	0
Aponogeton	2	0	0	0	1	0	0	1
Haloraginaceae	0	0	0	0	0	0	0	0
Typhaceae	1	3	4	2	8	8	10	11
Zygophyllaceae	0	0	0	0	0	0	0	0
Unidentifiable	2	3	3	4	3	2	3	4
Broken	2	2	2	5	6	6	5	3
Justica-type	0	0	0	0	0	0	1	0
Pinaceae	0	0	0	0	0	0	0	0
Podocarpus	31	7	19	1	40	24	56	54
Rhus	5	1	1	3	2	5	1	0
Dioscoreaceae	0	0	0	0	0	0	0	0
Aizoaceae	4	5	7	0	5	1	3	4
Euphorbiaceae undif	0	0	0	0	0	2	0	2
Aloe-type	0	0	0	0	0	0	0	0
Brassicaceae	0	1	0	1	1	3	0	2
Caryophyllaceae	0	0	0	0	0	0	0	0
Gunnera	0	1	0	0	0	0	3	0
Polygala	1	0	0	0	0	0	0	0
Cardiospermum	0	0	0	0	0	0	0	0
Lauraceae	0	0	0	0	0	1	0	0
Combretaceae	0	0	0	0	0	0	0	0
Nymphaea	0	0	0	0	0	0	0	0
Oxalis	0	1	3	0	0	1	0	1
Plumbaginaceae	0	0	0	0	0	0	0	0
Portulaceae	0	0	0	0	0	0	0	0
Plantago	0	0	0	0	0	0	0	0
10 - 100 um	0	0	0	0	0	0	0	0
>100 um	0	0	0	3	0	0	2	0
Moraceae	0	0	0	0	0	0	0	0
Potamogetonaceae	0	1	0	0	0	0	4	0
NAP	300	300	300	300	300	300	300	300
All total	381	768	629	1054	443	498	386	892

Sample	13-2-82	13-2-84	13-2-86	13-2-88	13-2-90	13-2-94	13-2-95	13-2-96
Depth (cm)	82	84	86	88	90	94	95	96
Age (cal yr BP	1060.8	1085.8	1109.2	1132.2	1157.2	1201.9	1213.2	1223.7
Artemisia	16	6	7	7	20	8	16	21
Pentzia-type	6	9	2	0	3	2	4	2
Proteaceae	10	2	6	4	1	0	3	6
Ericaceae	43	18	20	22	25	25	18	27
Cliffortia	3	2	8	6	5	5	1	0
Bruniaceae	1	1	0	2	1	1	0	1
Anthospermum-type	5	6	18	0	3	2	2	6
Apiaceae	0	0	0	1	0	1	1	0
Fabaceae	0	1	2	2	5	4	0	0
Phylica	0	0	0	2	1	1	0	2
Rutaceae	0	1	0	2	0	0	0	0
Santalaceae	0	0	1	0	0	0	1	0
Scroph-type	0	0	3	0	0	0	0	0
Thymelaeaceae	1	2	3	1	0	2	0	0
Passerina	17	14	6	10	2	7	7	13
Canthium	1	0	2	0	0	0	2	0
Icacinaceae	4	0	2	1	0	1	2	1
Encephalartos	0	0	0	0	0	0	0	1
Euclea	3	3	5	11	5	7	7	2
Grewia	2	0	3	0	1	0	0	0
Ilex	2	3	0	3	0	1	2	3
Morella	0	0	0	0	1	0	3	3
Myrsine	0	1	2	0	0	0	0	0
Myrtaceae	0	0	0	0	0	0	0	0
Olea	12	15	15	20	8	10	11	7
Exotics	2515	171	622	216	243	449	835	718
Cyperaceae	10	12	9	21	10	25	23	10
Restionaceae	21	13	22	18	24	19	35	22
Poaceae	15	27	29	15	32	15	16	23
Asteraceae HS	7	7	5	8	9	5	6	3
Stoebe-type	17	9	16	9	13	12	16	18
Geraniaceae	4	2	4	0	1	2	2	1
Montinaceae	0	0	0	2	0	0	0	0
Oxygonum	0	0	0	0	0	0	0	0
Polygonum	0	0	0	1	1	0	0	1
Celastraceae	2	3	5	6	2	0	2	0
Celtis	0	2	2	3	0	1	0	0
Diospyros	4	1	2	2	3	0	2	1
Dodonaea	0	0	0	0	1	0	0	0
Euphorbia	32	34	24	15	24	32	35	35
Clutia	0	2	0	0	0	0	0	0
Amaranthaceae	38	41	16	38	24	37	42	55
Crassula	2	4	1	4	3	5	0	1

Sample	13-2-82	13-2-84	13-2-86	13-2-88	13-2-90	13-2-94	13-2-95	13-2-96
Depth (cm)	82	84	86	88	90	94	95	96
Age (cal yr BP	1060.8	1085.8	1109.2	1132.2	1157.2	1201.9	1213.2	1223.7
Ruschia	0	2	0	0	0	0	0	0
Juncaceae	1	0	0	3	2	1	0	0
Liliaceae	0	1	4	1	2	3	3	2
Iridaceae	1	0	3	1	0	1	1	1
Amarylliaceae	0	0	0	0	0	0	0	0
Scabiosa	0	3	0	0	0	0	2	2
Aponogeton	0	0	3	1	0	0	1	0
Haloraginaceae	0	0	0	0	0	0	0	0
Typhaceae	5	9	8	16	12	6	8	2
Zygophyllaceae	0	0	0	0	1	0	0	0
Unidentifiable	4	4	7	2	7	8	2	2
Broken	2	5	6	5	8	9	2	4
Justica-type	0	0	0	0	0	0	0	0
Pinaceae	0	0	0	0	0	0	0	0
Podocarpus	3	29	13	19	33	36	14	11
Rhus	1	1	1	4	0	0	2	2
Dioscoreaceae	0	0	0	0	1	0	0	0
Aizoaceae	2	2	7	3	4	2	3	5
Euphorbiaceae undif	0	1	2	2	0	0	0	0
Aloe-type	0	0	0	0	0	0	0	0
Brassicaceae	3	1	4	2	2	1	2	3
Caryophyllaceae	0	0	0	0	0	0	0	0
Gunnera	0	0	0	1	0	2	0	0
Polygala	0	0	0	0	0	0	0	0
Cardiospermum	0	0	0	0	0	0	0	0
Lauraceae	0	0	0	0	0	0	0	0
Combretaceae	0	0	0	0	0	0	0	0
Nymphaea	0	0	0	0	0	0	0	0
Oxalis	0	1	2	3	0	1	0	0
Plumbaginaceae	0	0	0	0	0	0	0	0
Portulaceae	0	0	0	0	0	0	0	0
Plantago	0	0	0	0	0	0	0	0
10 - 100 um	0	0	0	0	0	0	0	0
>100 um	0	0	0	0	0	0	0	0
Moraceae	0	0	0	1	0	0	0	0
Potamogetonaceae	0	0	0	0	0	0	1	0
NAP	300	300	300	300	300	300	300	299
All total	2815	471	922	516	543	749	1135	1017

Sample	13-2-97	13-2-98	13-2-100
Depth (cm)	97	98	100
Age (cal yr BP	1233.9	1244.7	1269
Artemisia	4	17	14
Pentzia-type	3	0	4
Proteaceae	3	5	2
Ericaceae	13	16	11
Cliffortia	4	8	4
Bruniaceae	0	0	2
Anthospermum-type	11	13	8
Apiaceae	0	0	0
Fabaceae	0	0	0
Phylica	0	0	0
Rutaceae	0	0	0
Santalaceae	1	0	0
Scroph-type	0	0	0
Thymelaeaceae	4	2	6
Passerina	7	8	11
Canthium	0	1	2
Icacinaceae	0	0	3
Encephalartos	0	0	0
Euclea	1	6	5
Grewia	0	3	0
Ilex	2	2	1
Morella	1	2	2
Myrsine	0	0	1
Myrtaceae	0	2	1
Olea	16	14	11
Exotics	250	508	453
Cyperaceae	7	15	10
Restionaceae	23	20	18
Poaceae	24	22	27
Asteraceae HS	2	5	3
Stoebe-type	20	10	12
Geraniaceae	1	1	2
Montinaceae	0	0	0
Oxygonum	0	0	0
Polygonum	0	0	1
Celastraceae	7	2	2
Celtis	4	0	1
Diospyros	3	3	0
Dodonaea	0	0	0
Euphorbia	15	24	23
Clutia	0	0	1
Amaranthaceae	57	33	67
Crassula	5	2	3

Sample	13-2-97	13-2-98	13-2-100
Depth (cm)	97	98	100
Age (cal yr BP	1233.9	1244.7	1269
Ruschia	0	0	0
Juncaceae	0	0	0
Liliaceae	2	5	2
Iridaceae	1	2	1
Amarylliaceae	0	0	0
Scabiosa	0	1	0
Aponogeton	0	1	0
Haloraginaceae	0	0	0
Typhaceae	1	1	1
Zygophyllaceae	0	0	0
Unidentifiable	5	4	3
Broken	5	5	5
Justica-type	0	0	0
Pinaceae	0	0	0
Podocarpus	31	16	15
Rhus	3	2	2
Dioscoreaceae	0	0	0
Aizoaceae	10	2	6
Euphorbiaceae undif	0	0	0
Aloe-type	0	0	0
Brassicaceae	3	1	4
Caryophyllaceae	1	0	0
Gunnera	0	0	0
Polygala	0	0	1
Cardiospermum	0	0	0
Lauraceae	0	0	0
Combretaceae	0	0	0
Nymphaea	0	0	0
Oxalis	0	3	2
Plumbaginaceae	0	0	0
Portulaceae	0	0	0
Plantago	0	0	0
10 - 100 um	0	0	0
>100 um	0	0	0
Moraceae	0	0	0
Potamogetonaceae	0	1	0
NAP	300	280	300
All total	559	788	753

Appendix B

BoLa13.2 XRF Data

Depth (cm)	Age (cal BP)	Al	Si	S	Cl	K	Ca	Ti
1	-56.8	616	10235	5197	33578	4373	31426	5800
2	-54.1	493	7387	4935	34260	3367	16720	5591
3	-51.2	794	11277	7243	33580	4950	39046	7574
4	-48.5	685	10741	7315	34652	4522	63244	7091
5	-45.8	354	7338	5265	35244	3659	34727	5881
6	-38.2	466	8109	5736	35011	3927	35708	6078
7	-30.5	670	10404	7023	33315	5143	13531	7042
8	-22.9	841	11555	7735	32825	5434	10496	7264
9	-15.3	646	10715	7243	32982	5192	8874	7032
10	-7.7	465	8451	6186	33030	4906	9125	6281
11	10.1	643	9370	6899	32990	4415	7834	5782
12	27.4	587	9211	7572	32822	4540	8226	5778
13	44.7	656	10355	7407	32582	4733	7952	6048
14	61.9	669	9893	7431	32963	4686	7837	6170
15	79.1	686	10256	7797	32756	5011	8037	6403
16	95.4	488	8130	6066	33348	4245	7552	5911
17	111.4	568	9406	6885	32588	4797	7771	6247
18	126.1	769	11403	8162	32214	5314	7984	6523
19	139.3	597	9066	6902	32263	4896	7750	6371
20	152.4	397	7268	5658	32350	4433	7714	5627
21	170.5	569	9475	7075	32412	5015	8051	5962
22	189.5	883	12815	9001	31206	6369	8517	7224
23	207.2	983	13727	8612	31313	6425	8265	7374
24	224.3	1034	13114	8187	31517	5949	8295	6965
25	240.9	814	11970	7789	31580	5587	8541	6370
26	257.8	688	11832	7950	31805	5252	8844	6326
27	275.8	918	13121	8542	31123	5090	8894	6310
28	293.7	842	12552	8209	31885	4938	8236	5769
29	311.8	1099	16781	8790	30169	6838	7940	7232
30	328.6	1312	17285	8483	30183	7610	7653	7835
31	345.3	1100	14947	10032	30590	6830	7279	7472
32	362.9	1465	19052	10523	30864	8409	7723	8423
33	381.6	1553	18809	10121	32259	8357	8288	8415
34	399.7	1553	19296	9498	33448	8167	7946	8196
35	417.6	1658	19613	10703	32913	8450	8273	8286
36	434.0	1564	18612	9791	32476	8352	8272	8429
37	451.8	1810	21302	9868	33855	8946	8257	8868
38	470.0	1584	20354	9938	33374	8619	8219	8367
39	487.2	1283	15876	8315	31806	7527	7428	7668
40	505.1	1411	17648	9197	31429	7916	7659	7767
41	518.8	1281	16708	8731	33217	8112	8009	7733
42	533.1	1142	15102	7605	34296	7611	7544	7805
43	548.5	1451	18698	8984	36518	8790	8015	
44	564.8	1481	18356	9092	36898	8661	8005	8791
45	582.1	1343	18634	7894	34668	8614	7711	8104

Depth (cm)	Age (cal BP)	Al	Si	S	Cl	K	Ca	Ti
46	597.4	1413	18587	8576	33235	8067	7371	8044
47	611.8	1274	15705	8434	33417	7924	7002	7884
48	624.6	1942	21982	10065	32339	9584	7502	8914
49	636.0	2003	23672	10342	30626	9417	7355	9130
50	647.1	1857	23684	8515	32332	9710	7765	9073
51	660.1	1711	22078	11722	30761	9459	7799	8669
52	673.2	1787	21987	10417	31610	9712	8420	9455
53	684.9	1884	21758	9277	33380	10059	8364	9859
54	697.0	1506	19879	9014	36140	9509	8438	9584
55	708.1	1695	20621	9422	31631	9348	7986	9257
56	721.9	1450	18372	9614	31935	8765	7832	8785
57	735.2	1518	18816	10141	28963	8847	8261	8788
58	748.6	1523	18562	10153	30524	8631	8280	8424
59	762.0	1326	18294	9021	28858	8380	8079	8170
60	775.5	1288	17908	10007	28829	8269	8038	8127
61	788.3	1339	17364	10155	30038	7961	7871	7658
62	802.1	1261	17171	9781	31709	7545	8069	7470
63	815.1	1404	19483	10568	30655	7971	8077	7911
64	828.0	1434	19338	10606	32339	7994	8567	7864
65	840.0	1492	19678	11525	34667	8142	8856	7949
66	853.1	1622	20483	10713	36193	8213	8403	8580
67	866.7	1387	18235	10816	35270	7893	8397	8043
68	880.1	1737	20667	11716	32570	8417	8431	8329
69	893.2	1556	20117	10825	31846	8286	8235	8417
70	906.0	1470	20650	10058	32460	8316	8024	7910
71	919.2	1451	19273	11459	29581	7907	7768	7677
72	933.2	1673	21120	9895	29181	8390	7909	8275
73	946.6	1819	22427	10710	30593	9432	8301	8618
74	959.4	1762	21713	10759	31013	9304	8442	8542
75	972.1	1492	19614	10983	32128	8968	8278	8572
76	984.6	1314	16626	10257	32977	7735	8034	7824
77	997.0	1575	19220	10402	33097	7973	8141	8335
78	1009.3	1628	19905	10127	36071	8792	8414	8362
79	1022.4	1393	18452	9432	34375	8603	8566	8225
80	1035.2	1510	20174	9627	33480	8526	8505	8616
81	1047.8	1327	18328	8848	34792	8328	8169	8537
82	1060.8	1049	16316	9865	35750	7967	8108	7990
83	1073.0	988	15895	7819	32570	7431	7767	7578
84	1085.8	773	12247	7557	34088	6872	7442	6936
85	1098.2	1036	14841	8201	31387	8328	7996	7978
86	1109.2	1113	15029	6745	29809	7593	7630	7418
87	1120.5	1364	18656	7736	31388	9231	8516	8526
88	1132.2	1398	18918	7955	30479	9244	8684	9217
89	1144.6	1564	20496	8087	30047	9461	8491	8571
90	1157.2	1614	21518	8577	29806	9812	8669	8818
91	1167.9	1666	22966	8274	29304	9948	8840	8709
92	1179.1	1161	18279	7594	30183	8528	8430	7765
93	1190.3	1367	22059	8056	29480	8947	8301	7739
94	1201.9	831	18046	7213	30167	7893	11278	6603

Depth (cm)	Age (cal BP)	Al	Si	S	Cl	K	Ca	Ti
95	1213.2	1313	22441	8494	28698	10598	7988	7658
96	1223.7	1567	22581	8582	29672	12698	10338	9175
97	1233.9	2120	26188	8951	30367	14191	9594	9387
98	1244.7	1746	19908	7322	32387	12385	9520	9439
99	1257.0	686	11147	5138	33003	10370	10106	8711
100	1269.0	625	11081	4917	33047	9444	8587	8179
101	1316.0	806	13599	5347	31417	10201	9955	8464
102	1363.5	1543	22662	6282	28428	12050	11400	8842
103	1408.9	1745	24842	6237	27659	12291	12178	9080
104	1452.3	1801	25828	6050	27785	12605	10698	9192
105	1494.7	1780	24284	5721	28780	12712	14205	9345
106	1543.5	1648	23495	5525	28314	13760	10341	10189
107	1595.1	1607	20777	5089	30007	12947	12244	10376
108	1644.2	1693	21295	4981	29630	12831	10841	9753
109	1691.9	2045	25534	5527	28936	13399	9158	10275
110	1737.0	1685	22704	5216	29436	13284	9225	10014
111	1787.5	1765	24266	5206	28826	13288	9867	9968
112	1838.6	1552	20807	5129	29389	12016	12248	9357
113	1890.3	1361	19782	5220	29770	12175	8885	9851
114	1938.5	1874	24581	5603	29115	12750	10316	10142
115	1985.9	1826	24932	5057	28212	12534	12050	9440
116	2039.5	1307	17543	4036	28567	9224	8152	7445
117	2090.9	1705	22154	4873	27112	11921	8534	9345
118	2141.7	1753	23428	5365	27613	12556	8756	9896
119	2191.0	2188	27680	5755	27647	14032	11429	10658
120	2241.3	2192	27998	5622	27952	13822	9500	10308
121	2286.7	1842	24325	4858	28855	12623	8687	9857
122	2338.1	1636	22782	4732	28587	12294	10313	9497
123	2391.3	1862	25657	4935	27463	12980	10659	9749
124	2442.9	1940	24662	5126	28699	13622	9276	10273
125	2492.5	1942	25369	4892	28072	13807	9631	9901
126	2539.2	1402	18890	4472	30178	11111	10772	8840
127	2589.4	1277	16784	4056	29928	10685	8343	8878
128	2641.6	2115	25334	5303	26828	13694	9626	9870
129	2691.4	1872	23877	5036	27422	12733	10833	9932
130	2741.0	1739	24279	5357	28033	12472	10759	9166
131	2785.0	1706	23546	4640	27662	11675	11169	8839
132	2833.7	2081	26945	5052	27233	12578	12584	9498
133	2883.7	2267	27727	5049	26551	13712	11220	9974
134	2934.4	2398	31485	4974	27051	14680	13577	10522
135	2982.4	2372	31715	4436	28274	14161	12766	9987
136	3019.0	2546	34231	4579	28169	14516	12361	10288
137	3055.9	2427	32896	4362	26936	14159	13108	9938
138	3096.0	2405	32178	4402	26345	13587	13847	9690
139	3139.5	2458	32787	4527	26442	13487	12329	10035
140	3183.5	2322	32311	4302	26535	13205	12475	9576
141	3208.4	2644	36040	4579	25806	14574	13935	10233
142	3232.9	2884	36670	4448	25648	15271	12677	10827
143	3255.7	2540	33985	5087	26826	14974	13769	10490

Depth (cm)	Age (cal BP)	Al	Si	S	Cl	K	Ca	Ti
144	3277.7	2421	33329	5492	27276	15077	12141	10449
145	3297.6	2669	34331	5406	26975	15726	11100	10969
146	3324.2	2247	28875	5294	27667	14731	10181	10453
147	3349.9	2388	29821	5407	27828	14638	11135	10757
148	3375.6	2168	28551	4967	27690	13837	12918	10201
149	3400.5	2012	27671	4605	28218	14207	11565	10577
150	3424.7	2123	28275	4610	28334	14626	10416	10709
151	3450.6	2385	30741	5128	27048	15287	12440	11118
152	3478.0	2235	29985	4813	27493	14851	10982	10638
153	3504.9	2481	34509	4928	26767	14616	10763	10506
154	3531.7	1765	25121	4237	28222	13365	11118	9959
155	3557.0	2874	37913	5367	26166	15679	13741	10473
156	3583.1	2331	30427	4529	27694	14442	14087	10445
157	3609.5	2284	28699	4600	27983	14339	13197	10007
158	3635.1	3114	38880	5584	26256	16665	13729	11399
159	3661.6	2434	32269	5107	27519	15450	12015	11159
160	3686.4	2780	35100	5300	27126	15392	12586	10854
161	3711.8	2459	32025	4831	26886	14255	11881	10413
162	3737.8	2127	29285	4510	27035	14286	12021	10034
163	3765.6	2462	32067	4375	26906	15420	11166	10934
164	3792.3	2552	34069	5028	27204	15241	15294	10467
165	3818.6	2898	36284	5315	26424	16167	12350	10975
166	3843.1	2238	29092	4909	27457	14518	11629	10472
167	3868.9	1903	25836	4755	27831	14258	10442	10109
168	3895.7	1943	24330	4349	27820	13952	9978	10413
169	3922.4	2478	32213	5071	26633	15726	10562	10920
170	3948.3	2661	34161	4770	25809	15602	11668	10776
171	3973.2	2136	30364	4156	27107	13746	11600	10030
172	3997.8	2317	32282	4405	27076	14377	11811	10202
173	4023.9	2026	26987	4220	27918	13648	12709	9610
174	4050.7	2048	26088	4823	28939	13619	14286	10228
175	4075.8	2619	33924	5505	27874	16689	14380	11246
176	4098.5	2934	36945	5297	27111	17804	13636	12146
177	4120.5	3518	43344	5441	25735	18115	14480	11902

Depth (cm)	Age (cal BP)	Mn	Fe	Rh	Ni	Cu	Zn	Br
1	-56.8	1167	52807	32233	192	1396	1242	2501
2	-54.1	1292	52950	35857	174	1398	1301	2409
3	-51.2	1148	63294	32773	162	1431	1262	2354
4	-48.5	1058	57117	31620	176	1390	1242	2404
5	-45.8	739	49822	33191	150	1396	1222	2654
6	-38.2	985	50365	33688	182	1441	1200	2681
7	-30.5	1115	61760	34766	175	1415	1281	2499
8	-22.9	1091	61031	33639	175	1432	1314	2480
9	-15.3	1105	61927	34338	180	1443	1266	2348
10	-7.7	1057	56247	35919	185	1399	1247	2688
11	10.1	1170	54004	34738	162	1392	1250	2784
12	27.4	1164	54978	33083	165	1463	1308	2667
13	44.7	1081	57720	33621	171	1411	1293	2580
14	61.9	894	59155	33199	190	1435	1290	2491
15	79.1	1123	61923	33272	192	1432	1229	2583
16	95.4	901	55278	34420	155	1412	1223	2327
17	111.4	1001	54992	34869	170	1355	1272	2487
18	126.1	1219	61840	34746	198	1419	1293	2502
19	139.3	1042	58342	34755	174	1365	1260	2355
20	152.4	1086	54200	34742	207	1425	1267	2130
21	170.5	1037	55262	33853	180	1457	1270	2260
22	189.5	829	65559	33862	210	1443	1262	2352
23	207.2	1187	63922	34126	201	1407	1293	2269
24	224.3	863	59028	34238	186	1425	1276	2370
25	240.9	762	55622	34107	176	1415	1271	2288
26	257.8	704	48828	33530	157	1443	1317	1883
27	275.8	898	47644	33304	207	1428	1235	1699
28	293.7	918	50893	33382	194	1408	1276	1707
29	311.8	1051	61487	33614	211	1457	1285	1356
30	328.6	1022	69629	34045	200	1420	1262	1250
31	345.3	739	93453	33352	198	1457	1259	1262
32	362.9	910	82464	32628	224	1443	1275	1520
33	381.6	1062	79855	33611	180	1362	1352	1611
34	399.7	811	74753	32690	205	1436	1330	1679
35	417.6	779	83961	32251	175	1365	1312	1765
36	434.0	1230	78876	33160	229	1372	1325	1738
37	451.8	1039	74245	32293	188	1398	1303	1704
38	470.0	921	75093	32632	216	1449	1350	1646
39	487.2	823	71384	35705	154	1431	1311	1588
40	505.1	759	77823	35160	182	1410	1282	1494
41	518.8	1156	73994	33121	177	1405	1230	1507
42	533.1	1077	69715	35319	176	1357	1287	1546
43	548.5	1139	76750	34034	217	1394	1346	1618
44	564.8	818	77376	32548	199	1414	1302	1684
45	582.1	944	65921	33616	202	1416	1313	1367

Depth (cm)	Age (cal BP)	Mn	Fe	Rh	Ni	Cu	Zn	Br
46	597.4	1050	72030	32825	179	1436	1265	1147
47	611.8	1120	79805	34605	194	1418	1243	1196
48	624.6	1206	80456	33204	191	1438	1265	1299
49	636.0	1350	81703	31808	205	1405	1263	1308
50	647.1	1112	69789	33020	202	1426	1355	1372
51	660.1	948	98863	33039	178	1390	1328	1403
52	673.2	1450	87211	31517	172	1404	1327	1589
53	684.9	1102	78788	31720	204	1368	1296	1554
54	697.0	1140	77508	32427	185	1479	1307	1587
55	708.1	972	79114	31674	174	1394	1270	1464
56	721.9	952	84722	31183	179	1400	1288	1362
57	735.2	1174	84832	31142	200	1460	1317	1687
58	748.6	1268	78355	29789	170	1353	1318	1678
59	762.0	1214	70274	29832	199	1361	1343	1667
60	775.5	1275	76186	31596	177	1399	1303	1476
61	788.3	1329	72057	30634	176	1439	1313	1420
62	802.1	1098	66483	32445	197	1413	1321	1477
63	815.1	1140	68939	30520	150	1432	1299	1575
64	828.0	1112	70328	29753	181	1454	1365	1539
65	840.0	1174	76219	30048	195	1398	1297	1612
66	853.1	1059	70245	30246	188	1441	1248	1616
67	866.7	1202	78305	31647	191	1447	1283	1519
68	880.1	1513	83157	32320	207	1405	1262	1585
69	893.2	1362	74218	32498	174	1381	1241	1629
70	906.0	1006	71005	31891	187	1445	1295	1458
71	919.2	882	80957	31590	199	1456	1325	1176
72	933.2	1142	68948	30322	179	1493	1283	1263
73	946.6	669	73134	31903	165	1406	1257	1263
74	959.4	856	77817	31626	203	1524	1348	1378
75	972.1	1044	79698	30162	191	1452	1309	1432
76	984.6	1151	75906	30994	172	1456	1327	1534
77	997.0	1031	74025	31357	227	1450	1346	1566
78	1009.3	1106	71292	31847	187	1413	1294	1616
79	1022.4	1113	69335	33019	194	1466	1251	1654
80	1035.2	918	68296	31088	193	1390	1308	1700
81	1047.8	955	67333	31189	190	1369	1293	1623
82	1060.8	827	75819	32424	173	1459	1327	1491
83	1073.0	870	60709	32844	187	1365	1255	1332
84	1085.8	920	71588	33968	193	1426	1295	1305
85	1098.2	825	77961	34436	210	1417	1326	1276
86	1109.2	972	66065	32318	171	1428	1275	1217
87	1120.5	873	71069	32912	185	1398	1297	1487
88	1132.2	877	72941	33416	167	1370	1266	1504
89	1144.6	930	72336	34673	191	1410	1322	1499
90	1157.2	978	72968	32598	208	1464	1268	1499
91	1167.9	866	69261	33772	156	1470	1280	1315
92	1179.1	738	65127	34828	181	1342	1308	1255
93	1190.3	655	55985	34383	178	1393	1224	955
94	1201.9	784	57246	34208	151	1413	1192	784

Depth (cm)	Age (cal BP)	Mn	Fe	Rh	Ni	Cu	Zn	Br
95	1213.2	1163	67735	33923	151	1379	1275	623
96	1223.7	917	76686	30833	172	1407	1301	778
97	1233.9	1283	78473	30891	163	1413	1298	828
98	1244.7	1050	75197	32963	176	1431	1302	792
99	1257.0	1074	72448	34533	204	1378	1295	763
100	1269.0	903	69063	34172	175	1450	1300	774
101	1316.0	949	65981	32392	181	1439	1240	686
102	1363.5	1151	66081	33262	198	1429	1271	609
103	1408.9	1086	66862	33619	186	1440	1263	558
104	1452.3	1170	68287	33509	193	1424	1256	547
105	1494.7	1112	71101	33366	197	1471	1291	525
106	1543.5	1319	79877	32822	129	1431	1272	532
107	1595.1	1453	86021	33364	192	1423	1345	596
108	1644.2	1512	86603	33159	196	1410	1290	631
109	1691.9	1380	84961	31285	194	1484	1309	678
110	1737.0	1464	81502	32446	194	1400	1283	688
111	1787.5	1362	80342	33015	207	1411	1277	681
112	1838.6	1025	79206	32662	186	1407	1290	650
113	1890.3	1023	83599	31411	190	1431	1268	633
114	1938.5	915	78990	31637	174	1382	1272	519
115	1985.9	1076	74815	30657	188	1450	1252	506
116	2039.5	895	63347	29584	185	1425	1274	546
117	2090.9	1233	77836	30969	175	1434	1311	658
118	2141.7	1440	83219	29655	182	1407	1298	751
119	2191.0	1203	86682	30063	191	1405	1284	691
120	2241.3	1167	82396	31151	184	1416	1324	761
121	2286.7	1189	77202	30860	181	1432	1298	659
122	2338.1	943	75749	30907	182	1406	1285	649
123	2391.3	1193	75409	30798	193	1399	1290	625
124	2442.9	1195	80898	31320	193	1438	1306	671
125	2492.5	1209	81088	31407	157	1384	1267	696
126	2539.2	1063	78611	31612	201	1395	1234	714
127	2589.4	1177	79964	30480	191	1423	1327	726
128	2641.6	1197	80604	29798	164	1394	1262	700
129	2691.4	1159	75888	29288	190	1423	1270	597
130	2741.0	969	73471	29758	190	1452	1295	610
131	2785.0	897	68640	31090	175	1479	1238	581
132	2833.7	977	68576	28918	183	1340	1201	595
133	2883.7	944	74630	30019	162	1384	1281	571
134	2934.4	1251	75327	30136	186	1413	1218	581
135	2982.4	1129	68628	30616	192	1360	1262	422
136	3019.0	1037	67911	30080	182	1419	1317	440
137	3055.9	1077	66862	29929	186	1429	1225	435
138	3096.0	866	64770	29574	191	1392	1295	449
139	3139.5	826	65033	30026	185	1400	1223	421
140	3183.5	881	62933	30242	182	1411	1248	443
141	3208.4	993	68027	29581	199	1400	1279	473
142	3232.9	1034	71476	30699	207	1373	1300	510
143	3255.7	911	74947	31207	187	1394	1288	532

Depth (cm)	Age (cal BP)	Mn	Fe	Rh	Ni	Cu	Zn	Br
144	3277.7	997	78541	31700	176	1406	1318	571
145	3297.6	1161	81497	32007	201	1438	1250	612
146	3324.2	1106	82987	32096	211	1388	1258	630
147	3349.9	1269	83739	31503	200	1397	1322	640
148	3375.6	1141	78297	31679	210	1417	1247	579
149	3400.5	1191	78716	32148	195	1414	1320	558
150	3424.7	1109	83007	31741	182	1428	1304	640
151	3450.6	1116	85034	32298	191	1415	1328	609
152	3478.0	945	80969	31837	181	1431	1248	609
153	3504.9	1007	77278	30847	196	1385	1275	602
154	3531.7	1068	77449	32246	173	1405	1348	574
155	3557.0	1338	73777	31712	184	1473	1261	516
156	3583.1	1161	75976	31739	193	1442	1290	487
157	3609.5	816	76493	31710	197	1416	1251	505
158	3635.1	1132	81955	30817	167	1418	1323	547
159	3661.6	1138	80986	31925	182	1400	1232	588
160	3686.4	1069	78940	30341	156	1416	1271	556
161	3711.8	1146	74704	30136	198	1391	1302	511
162	3737.8	925	73419	30474	162	1410	1264	506
163	3765.6	1028	76586	30474	185	1421	1234	481
164	3792.3	862	75618	30471	162	1410	1274	452
165	3818.6	1233	80295	30424	180	1407	1266	511
166	3843.1	1078	76930	30796	223	1466	1262	498
167	3868.9	993	76408	31115	210	1403	1291	573
168	3895.7	859	78144	30514	167	1407	1287	514
169	3922.4	984	76997	29462	194	1462	1366	501
170	3948.3	829	74316	29166	201	1415	1248	512
171	3973.2	809	66440	30130	188	1410	1241	408
172	3997.8	741	67719	29768	159	1340	1296	398
173	4023.9	778	72307	30885	202	1429	1243	478
174	4050.7	910	76109	30031	168	1423	1230	467
175	4075.8	1092	85159	30325	185	1458	1307	538
176	4098.5	975	82995	31784	179	1430	1337	539
177	4120.5	1183	79750	31401	219	1460	1328	490

Depth (cm)	Age (cal BP)	Rb	Sr	Zr	Nb	Mo	Pb
1	-56.8	1043	2432	2555	505	1016	224
2	-54.1	996	2076	1947	467	1027	264
3	-51.2	1102	3463	2962	631	1056	264
4	-48.5	989	4026	1919	450	1208	250
5	-45.8	933	4191	2018	390	1141	226
6	-38.2	1024	2886	2155	392	1172	215
7	-30.5	1176	1432	3607	605	1184	236
8	-22.9	1234	1240	2991	443	1098	233
9	-15.3	1155	1137	3786	560	1170	254
10	-7.7	998	1231	2034	428	1038	214
11	10.1	906	1037	1825	500	1143	210
12	27.4	983	1038	1874	566	1096	212
13	44.7	1021	1080	2224	529	1053	208
14	61.9	1064	1165	2132	489	1007	234
15	79.1	1040	1064	2396	499	1018	218
16	95.4	1015	1145	2658	515	962	194
17	111.4	1051	1104	2440	513	1212	213
18	126.1	1177	1211	2760	552	1167	227
19	139.3	1010	1116	2602	490	1162	202
20	152.4	1070	1122	2295	630	882	169
21	170.5	1026	1165	2276	574	1133	209
22	189.5	1245	1237	2569	557	1165	215
23	207.2	1187	1279	2951	760	1188	201
24	224.3	1066	1222	4618	445	1105	199
25	240.9	1107	1210	5062	539	1297	207
26	257.8	948	1154	6438	669	1281	206
27	275.8	993	1263	5801	443	1118	206
28	293.7	965	1214	5859	469	1045	188
29	311.8	1084	1136	6783	518	960	197
30	328.6	1334	1181	6104	544	872	249
31	345.3	1266	1221	5769	472	960	255
32	362.9	1386	1219	2874	480	992	258
33	381.6	1508	1175	3503	590	999	236
34	399.7	1428	1253	3642	624	1106	247
35	417.6	1359	1120	2909	503	961	227
36	434.0	1557	1249	3063	583	896	237
37	451.8	1645	1325	3200	543	1043	260
38	470.0	1497	1176	3017	563	1055	221
39	487.2	1445	1232	3234	664	1055	237
40	505.1	1335	1262	4064	539	987	230
41	518.8	1433	1207	2711	643	1243	215
42	533.1	1518	1272	3320	484	975	235
43	548.5	1521	1285	3129	484	1115	248
44	564.8	1621	1307	3568	494	1046	222
45	582.1	1460	1255	6025	473	987	213

Depth (cm)	Age (cal BP)	Rb	Sr	Zr	Nb	Mo	Pb
46	597.4	1391	1179	5417	556	845	257
47	611.8	1432	1177	3565	534	786	226
48	624.6	1594	1241	3760	617	1139	226
49	636.0	1492	1389	4559	504	1151	235
50	647.1	1480	1366	6391	652	1046	235
51	660.1	1363	1284	4916	564	1095	293
52	673.2	1641	1294	3349	384	968	262
53	684.9	1636	1301	3554	471	1230	226
54	697.0	1660	1282	3389	498	1033	257
55	708.1	1674	1435	4691	450	967	256
56	721.9	1520	1362	4051	553	959	247
57	735.2	1481	1297	3136	661	1011	281
58	748.6	1530	1174	2720	610	935	275
59	762.0	1469	1189	3075	473	919	219
60	775.5	1398	1205	2854	500	1066	242
61	788.3	1289	1119	2427	536	1015	221
62	802.1	1284	1079	2513	426	846	188
63	815.1	1440	1137	2363	580	968	231
64	828.0	1324	1138	2028	548	1097	214
65	840.0	1364	1197	2458	540	889	205
66	853.1	1425	1181	2617	626	1064	186
67	866.7	1420	1223	2615	579	948	244
68	880.1	1433	1191	2262	456	895	238
69	893.2	1410	1257	2827	557	987	237
70	906.0	1326	1073	3749	573	942	217
71	919.2	1270	1025	3169	492	966	246
72	933.2	1392	1225	3472	566	1065	244
73	946.6	1493	1198	3481	567	867	223
74	959.4	1456	1248	3257	615	970	224
75	972.1	1507	1200	2691	604	1228	218
76	984.6	1418	1121	2331	639	1039	230
77	997.0	1463	1270	2477	507	909	226
78	1009.3	1476	1208	2446	501	1009	200
79	1022.4	1534	1288	2869	650	1176	245
80	1035.2	1401	1304	3294	607	1203	228
81	1047.8	1528	1295	3640	641	1151	235
82	1060.8	1298	1241	3535	480	828	209
83	1073.0	1431	1334	5634	367	970	219
84	1085.8	1406	1256	4476	502	927	231
85	1098.2	1487	1210	3783	600	1005	229
86	1109.2	1318	1156	2125	672	947	222
87	1120.5	1613	1339	3048	522	967	214
88	1132.2	1657	1435	3535	696	1113	246
89	1144.6	1541	1299	3070	549	1124	270
90	1157.2	1450	1320	3320	681	1007	248
91	1167.9	1523	1403	3816	608	1068	221
92	1179.1	1384	1290	5959	529	1096	257
93	1190.3	1158	1352	11342	572	1210	228
94	1201.9	1160	1442	12027	579	901	261

Depth (cm)	Age (cal BP)	Rb	Sr	Zr	Nb	Mo	Pb
95	1213.2	1241	1457	13316	476	1006	240
96	1223.7	1622	2049	7782	446	886	263
97	1233.9	1863	1777	8227	382	837	240
98	1244.7	1784	1629	7929	443	1031	239
99	1257.0	1651	2142	9984	534	840	233
100	1269.0	1645	1886	7974	592	930	233
101	1316.0	1412	2615	7930	567	903	229
102	1363.5	1378	2711	9200	570	886	251
103	1408.9	1395	2282	8540	526	967	229
104	1452.3	1364	2078	8323	493	807	223
105	1494.7	1422	3755	9048	457	821	222
106	1543.5	1557	1812	9949	559	879	237
107	1595.1	1567	4639	6927	483	845	267
108	1644.2	1605	4897	5311	404	859	259
109	1691.9	1739	1729	8573	403	1040	251
110	1737.0	1689	1733	7907	576	842	271
111	1787.5	1598	2638	9091	432	722	266
112	1838.6	1577	2480	9369	559	851	249
113	1890.3	1619	1906	8600	472	936	278
114	1938.5	1514	2563	9336	620	825	272
115	1985.9	1497	2904	8765	359	828	242
116	2039.5	1419	1604	7835	423	949	237
117	2090.9	1609	1733	6231	514	967	261
118	2141.7	1799	1687	6273	544	902	270
119	2191.0	1877	1732	7577	652	854	271
120	2241.3	1762	1701	7266	458	995	267
121	2286.7	1754	1729	7932	564	832	264
122	2338.1	1652	2034	7873	401	987	261
123	2391.3	1587	1724	7526	555	913	243
124	2442.9	1702	1756	7072	425	849	235
125	2492.5	1755	1675	7168	480	995	281
126	2539.2	1594	2905	6062	448	876	309
127	2589.4	1674	3061	4363	523	796	247
128	2641.6	1623	2193	6587	553	785	246
129	2691.4	1428	2934	5849	498	750	239
130	2741.0	1617	1849	8412	457	936	258
131	2785.0	1506	2058	8364	563	928	209
132	2833.7	1351	2274	7888	499	839	248
133	2883.7	1442	2486	7284	509	882	254
134	2934.4	1618	1970	7566	569	1036	250
135	2982.4	1490	3189	8793	533	945	246
136	3019.0	1509	2239	9800	480	811	233
137	3055.9	1606	2266	8580	524	905	240
138	3096.0	1455	2716	7997	449	854	232
139	3139.5	1373	2918	8187	422	828	224
140	3183.5	1463	2632	8305	423	833	233
141	3208.4	1515	2779	8785	586	838	244
142	3232.9	1614	1981	9825	482	870	262
143	3255.7	1623	2133	9079	475	842	256

Depth (cm)	Age (cal BP)	Rb	Sr	Zr	Nb	Mo	Pb
144	3277.7	1612	2043	8156	465	917	254
145	3297.6	1681	2107	8784	432	1005	278
146	3324.2	1608	1792	7572	455	763	258
147	3349.9	1705	1985	7592	440	827	248
148	3375.6	1528	3192	6403	481	772	253
149	3400.5	1761	2554	7903	534	792	276
150	3424.7	1748	1689	7801	481	927	283
151	3450.6	1786	1837	7232	532	925	293
152	3478.0	1755	1868	7454	584	826	290
153	3504.9	1695	1829	7553	736	876	259
154	3531.7	1709	1741	8549	463	923	277
155	3557.0	1521	2181	9108	522	730	247
156	3583.1	1572	3171	6651	426	851	278
157	3609.5	1440	3979	7943	443	799	261
158	3635.1	1814	2099	7989	484	1001	247
159	3661.6	1825	1895	7979	538	877	259
160	3686.4	1708	2002	8513	453	920	241
161	3711.8	1535	3418	6993	497	882	250
162	3737.8	1561	2237	7842	521	777	245
163	3765.6	1699	2187	8634	483	781	256
164	3792.3	1522	3574	8306	479	939	235
165	3818.6	1638	2890	8078	455	982	276
166	3843.1	1661	2434	7461	441	842	250
167	3868.9	1702	1999	8472	489	790	250
168	3895.7	1762	1817	8090	568	974	257
169	3922.4	1725	1727	8702	507	814	283
170	3948.3	1664	1830	8414	610	1071	253
171	3973.2	1544	1954	11197	533	984	249
172	3997.8	1565	2177	10863	526	814	269
173	4023.9	1716	2825	8768	419	871	246
174	4050.7	1564	3820	8780	592	831	238
175	4075.8	1944	2326	8505	472	1061	309
176	4098.5	1871	2052	9524	600	966	290
177	4120.5	1788	2010	9150	511	778	276

Appendix C

BoLa13.2 CNS data

depth (cm)	Age (cal BP)	TN	TOC	depth (cm)	Age (cal BP)	TN	TOC
1	-56.8	1.238	11.172	46	597.4	0.469	5.375
2	-54.1	1.108	10.51	47	611.8	0.53	6.229
3	-51.2	0.871	8.319	48	624.6	0.551	6.35
4	-48.5	1.095	10.09	49	636	0.51	6
5	-45.8	0.953	9.528	50	647.1	0.459	5.425
6	-38.2	1.223	12.077	51	660.1	0.447	5.153
7	-30.5	1.073	10.817	52	673.2	0.555	6.596
8	-22.9	0.923	9.603	53	684.9	0.627	7.47
9	-15.3	0.93	9.221	54	697	0.632	7.505
10	-7.7	1.129	11.283	55	708.1	0.591	7.087
11	10.1	1.358	13.712	56	721.9	0.503	5.98
12	27.4	1.326	13.7	57	735.2	0.634	7.66
13	44.7	1.263	12.87	58	748.6	0.699	8.546
14	61.9	1.223	12.547	59	762	0.672	8.516
15	79.1	1.159	12.037	60	775.5	0.681	8.477
16	95.4	1.054	11.123	61	788.3	0.716	8.666
17	111.4	1.029	10.799	62	802.1	0.76	9.313
18	126.1	1.099	11.314	63	815.1	0.778	9.614
19	139.3	1.157	11.647	64	828	0.796	9.57
20	152.4	1.089	11.446	65	840	0.819	9.568
21	170.5	1.142	12.159	66	853.1	0.765	8.848
22	189.5	1.204	12.231	67	866.7	0.727	8.567
23	207.2	1.038	11.098	68	880.1	0.768	8.647
24	224.3	0.931	10.015	69	893.2	0.756	8.795
25	240.9	0.868	8.967	70	906	0.707	8.169
26	257.8	0.689	7.388	71	919.2	0.652	7.618
27	275.8	0.776	8.102	72	933.2	0.637	7.656
28	293.7	0.906	9.367	73	946.6	0.608	7.408
29	311.8	0.68	7.454	74	959.4	0.669	8.122
30	328.6	0.554	6.236	75	972.1	0.698	8.467
31	345.3	0.555	6.168	76	984.6	0.74	8.958
32	362.9	0.635	7.257	77	997	0.764	9.407
33	381.6	0.722	7.979	78	1009.3	0.78	9.583
34	399.7	0.726	8.214	79	1022.4	0.791	9.771
35	417.6	0.694	7.681	80	1035.2	0.783	9.773
36	434	0.728	8.262	81	1047.8	0.729	8.954
37	451.8	0.755	8.51	82	1060.8	0.686	8.477
38	470	0.738	8.442	83	1073	0.554	6.967
39	487.2	0.714	8.155	84	1085.8	0.557	6.921
40	505.1	0.732	8.218	85	1098.2	0.57	7.077
41	518.8	0.687	7.745	86	1109.2	0.662	8.259
42	533.1	0.675	7.876	87	1120.5	0.644	8.026
43	548.5	0.667	7.851	88	1132.2	0.671	8.295
44	564.8	0.676	8.01	89	1144.6	0.682	8.447
45	582.1	0.545	6.369	90	1157.2	0.645	7.956

depth (cm)	Age (cal BP)	TN	TOC	depth (cm)	Age (cal BP)	TN	TOC
91	1167.9	0.622	7.605	140	3183.5	0.099	0.988
92	1179.1	0.503	6.22	141	3208.4	0.103	1.066
93	1190.3	0.337	4.035	142	3232.9	0.102	1.025
94	1201.9	0.3	3.568	143	3255.7	0.118	1.186
95	1213.2	0.239	2.706	144	3277.7	0.13	1.297
96	1223.7	0.267	3.014	145	3297.6	0.141	1.499
97	1233.9	0.265	3.047	146	3324.2	0.145	1.544
98	1244.7	0.279	3.208	147	3349.9	0.132	1.435
99	1257	0.297	3.298	148	3375.6	0.123	1.281
100	1269	0.255	2.932	149	3400.5	0.126	1.386
101	1316	0.222	2.477	150	3424.7	0.142	1.422
102	1363.5	0.165	1.748	151	3450.6	0.134	1.375
103	1408.9	0.154	1.664	152	3478	0.126	1.327
104	1452.3	0.157	1.637	153	3504.9	0.141	1.401
105	1494.7	0.173	1.629	154	3531.7	0.128	1.3
106	1543.5	0.146	1.392	155	3557	0.13	1.173
107	1595.1	0.155	1.676	156	3583.1	0.089	1.303
108	1644.2	0.17	1.797	157	3609.5	0.075	1.197
109	1691.9	0.181	1.952	158	3635.1	0.097	1.325
110	1737	0.153	1.687	159	3661.6	0.094	1.219
111	1787.5	0.139	1.596	160	3686.4	0.092	1.298
112	1838.6	0.155	1.747	161	3711.8	0.098	1.244
113	1890.3	0.156	1.621	162	3737.8	0.084	1.057
114	1938.5	0.132	1.343	163	3765.6	0.081	1.09
115	1985.9	0.136	1.432	164	3792.3	0.096	1.191
116	2039.5	0.278	6.348	165	3818.6	0.104	1.323
117	2090.9	0.187	2.683	166	3843.1	0.103	1.286
118	2141.7	0.153	1.787	167	3868.9	0.094	1.165
119	2191	0.155	1.755	168	3895.7	0.079	0.976
120	2241.3	0.146	1.655	169	3922.4	0.076	0.942
121	2286.7	0.146	1.651	170	3948.3	0.125	1.031
122	2338.1	0.13	1.594	171	3973.2	0.109	0.947
123	2391.3	0.153	1.821	172	3997.8	0.12	0.935
124	2442.9	0.152	1.851	173	4023.9	0.092	0.955
125	2492.5	0.162	1.894	174	4050.7	0.14	1.308
126	2539.2	0.162	1.914	175	4075.8	0.123	1.324
127	2589.4	0.177	1.693	176	4098.5	0.105	1.209
128	2641.6	0.158	1.594	177	4120.5	0.117	1.415
129	2691.4	0.169	1.536				
130	2741	0.14	1.347				
131	2785	0.141	1.356				
132	2833.7	0.137	1.4				
133	2883.7	0.154	1.523				
134	2934.4	0.127	1.262				
135	2982.4	0.113	1.077				
136	3019	0.099	0.967				
137	3055.9	0.104	1.062				
138	3096	0.114	1.09				
139	3139.5	0.101	1.03				

Appendix D

BoLa13.2 grain size data

depth (cm)	Age (cal yr BP)	Coarse Sand 500 - 2000 µm	Medium Sand 250 - 500 µm	Fine Sand 125-250 µm	V Fine Sand 63-125 µm	V Coarse Silt 31-63 µm
1	-56.8	0	0.096648225	7.918670357	5.647331724	7.394549238
2	-54.1	0	0.000159613	1.901881941	7.343211394	8.269745504
3	-51.2	0	0.008761337	2.78609924	5.93005022	9.309794956
4	-48.5	0	0.072835675	6.393823705	7.896322974	8.472608201
5	-45.8	0	0.010447396	3.956236846	9.126576664	9.647087471
6	-38.2	0	0.000293482	2.812544062	9.194850665	11.83803968
7	-30.5	0	0.02528091	4.570832896	11.46142045	12.31339167
8	-22.9	0	0.00029486	3.40344957	10.16041225	13.51290411
9	-15.3	0	2.258927262	13.04187101	8.042299325	9.785790393
10	-7.7	0	0.034025572	4.330994214	7.485017844	10.90469441
11	10.1	0	0	3.172781273	10.28819128	10.64725528
12	27.4	0	0.031422934	6.912259213	11.85321069	12.01234193
13	44.7	0	0.006607298	6.83212346	9.684564355	13.39693892
14	61.9	0	0.018285147	5.440982875	8.323369054	13.04212873
15	79.1	0	0	1.572774969	7.63364729	12.80881746
16	95.4	0	0.272328889	8.474526427	9.24114202	13.38385164
17	111.4	0	0.56712701	10.52564474	8.594670449	14.03786225
18	126.1	0	0.003956675	4.544510405	8.960882899	13.47628189
19	139.3	0	0.019514986	4.935136861	7.818629136	14.07695251
20	152.4	0	0.051044516	5.309938045	8.048647883	14.27414387
21	170.5	0	0.008853704	2.711756033	7.117273691	11.34917178
22	189.5	0	0.017009348	3.164903436	7.64772732	11.33149167
23	207.2	0	0.078229871	5.77595228	8.96140445	11.72809584
24	224.3	0	1.726574976	11.18794162	11.74663047	14.82613165
25	240.9	0	2.940811992	11.47699552	12.05950309	16.98841601
26	257.8	0	4.777926251	15.34363291	14.59968147	17.35747193
27	275.8	0	4.948850012	13.56356733	14.07091841	18.60325208
28	293.7	0.488517646	5.858119784	11.59631137	14.87204484	19.2015888
29	311.8	1.419207936	7.5908105	10.01982111	11.83281814	17.27060517
30	328.6	0	0.073664968	5.031804774	11.95352752	18.98466051
31	345.3	0	0.52430165	7.189939725	11.01517256	20.66188083
32	362.9	0	0.132337584	7.746539276	8.379035494	13.47757149
33	381.6	0	0.22334007	8.144341269	7.887591823	11.18792375
34	399.7	0	0.024206384	3.205459525	7.197536115	13.20115232
35	417.6	0	0.104371866	7.243893502	6.784524805	13.6960797
36	434.0	0	0.028430761	7.90903323	7.796436738	11.49662731
37	451.8	0	0.223028361	5.59203882	7.242869465	11.56317054
38	470.0	0	0.00313357	5.279192701	6.772996589	12.2416852
39	487.2	0	0.002398459	3.802019028	5.781994037	12.98860452
40	505.1	0	0.035174316	3.988834528	6.732593472	14.89394282
41	518.8	0	0.103885469	6.607034676	5.807781986	11.49648925
42	533.1	0	0.006794635	2.055585292	5.456167308	11.63939489
43	548.5	0	0.007142052	5.0188705	5.851290989	12.21090935
44	564.8	0	0.116827238	6.063166505	6.334202462	11.32121928

depth (cm)	Age (cal yr BP)	Coarse Sand 500 - 2000 µm	Medium Sand 250 - 500 µm	Fine Sand 125-250 µm	V Fine Sand 63-125 µm	V Coarse Silt 31-63 µm
45	582.1	0	1.113960347	8.796161432	9.741718921	16.28239256
46	597.4	0	0.482211154	6.594235966	11.41419996	20.36148058
47	611.8	0	0.145374693	7.722192776	8.022836592	15.07995028
48	624.6	0	0.023453855	5.149496724	5.772274804	11.7819763
49	636.0	0	0.454614544	7.637208493	6.565405665	13.75936793
50	647.1	2.852009037	7.835526884	10.07244061	8.806376739	14.83799329
51	660.1	0.172146529	4.053376609	10.88329637	11.9322449	17.69989518
52	673.2	0	4.174750133	10.71224212	7.315804141	10.41190545
53	684.9	0	0.662855686	8.206374065	6.541164114	10.01082069
54	697.0	0	0.814247755	9.267230743	6.883901679	10.46722612
55	708.1	0	0.364532012	7.187262361	6.603657046	13.35403139
56	721.9	0	0.856187305	7.579240529	7.711125565	16.1639949
57	735.2	0	0.342747689	7.751803836	7.931525439	14.37930451
58	748.6	0	0.020326956	8.205490626	6.911590972	10.26831816
59	762.0	0	0.517677698	10.50873102	7.858957229	10.48051725
60	775.5	0.18534233	1.533109972	9.773823732	7.340751152	10.6546425
61	788.3	0	0.229913883	7.207903245	5.292659877	8.653509767
62	802.1	0	0.186664398	8.500602611	6.051580969	8.586786566
63	815.1	0	0.020503385	6.314238015	5.185476247	7.888217338
64	828.0	0	0.010162363	3.325263676	5.734699617	8.304922287
65	840.0	0	0.081574116	9.228134592	6.885667302	8.414050033
66	853.1	0	0.324415545	8.518489533	8.122719414	10.13419425
67	866.7	0	0.701936685	9.687250309	6.569626121	9.416958959
68	880.1	0	0.019280738	4.78271025	5.305768435	8.957855168
69	893.2	0	0.264390139	8.088106433	6.054746498	9.242708888
70	906.0	0	0.392045644	9.126868456	8.579073896	12.17071209
71	919.2	0	0.204505923	7.105495067	9.471655988	14.55503517
72	933.2	0	1.01168078	10.13965221	8.651833069	13.5658128
73	946.6	0	0.083693498	6.590118579	8.379410781	13.95097913
74	959.4	0	0.115424744	4.930002475	7.420455233	11.35031527
75	972.1	0	0.174570842	7.032687418	6.06797963	9.4717931
76	984.6	0	0.027857761	5.788467509	5.786805979	8.203591381
77	997.0	0	0.024313615	3.829676176	5.318528443	7.449643448
78	1009.3	0	0.153431582	6.105839228	6.769698397	8.520129451
79	1022.4	0	0.013621997	7.718695147	6.855735988	10.1289325
80	1035.2	0	0.038012265	6.874722612	6.770275826	11.061811
81	1047.8	0	0.687263278	7.526149778	6.027247463	12.03612924
82	1060.8	0	3.465019889	9.719174559	9.861492759	13.57160655
83	1073.0	0	0.905727243	8.30193996	10.64379265	17.84440128
84	1085.8	0	0.578698117	7.760443163	9.804757363	17.98548389
85	1098.2	0	0.392626887	8.557282845	7.015119372	9.412959311
86	1109.2	0	0.001856674	2.862849573	5.011061346	8.248784651
87	1120.5	0	0.141055506	6.258106207	6.609204971	9.325328503
88	1132.2	0	0.139053223	6.60802284	7.026035899	10.04724546
89	1144.6	0	0.014178557	5.5361267	6.188148629	9.18784416
90	1157.2	0	0.027137639	5.497391451	6.815367761	11.02995738
91	1167.9	0	0.074416188	7.479691955	8.863528883	11.72813623
92	1179.1	0	0.600201281	9.981266248	12.9945784	13.56410151

depth (cm)	Age (cal yr BP)	Coarse Sand 500 - 2000 µm	Medium Sand 250 - 500 µm	Fine Sand 125-250 µm	V Fine Sand 63-125 µm	V Coarse Silt 31-63 µm
93	1190.3	0	1.210799867	11.57796738	22.45685507	17.54068491
94	1201.9	0	0.857795465	8.54415469	24.22561168	22.70983208
95	1213.2	1.436035447	4.521938563	11.19432354	22.65781489	25.31478773
96	1223.7	0.166552385	1.465392174	8.672085974	14.58246561	21.40404939
97	1233.9	0	0.93228196	7.583232631	13.94408226	20.75873446
98	1244.7	0	1.479062056	7.557914845	14.11195879	20.42787276
99	1257.0	0	0.022187314	6.420463382	13.21105112	19.04035593
100	1269.0	0	1.266279635	8.048659305	9.528012582	16.25215164
101	1316.0	0	0.023571031	6.805521962	6.40885422	9.97915207
102	1363.5	0	0.288790269	4.079017209	11.50085795	19.38313774
103	1408.9	0	0	0.672894507	13.24707743	21.67772735
104	1452.3	0	0	2.294025791	16.26151251	20.09366946
105	1494.7	0	0	0.57804374	6.402960638	23.31945504
106	1543.5	0	0.024633187	3.84555584	9.816238765	20.58660291
107	1595.1	0	0	0.347624653	8.512977307	22.37536101
108	1644.2	0	4.154686126	10.27577998	10.33804863	18.38715756
109	1691.9	0	0.119360418	6.925332916	9.51501158	19.10065288
110	1737.0	0	0.136610831	5.92027515	10.26439861	17.9533316
111	1787.5	0	0	0.220870435	6.428325826	19.58128353
112	1838.6	0	0	1.863025429	12.94569787	18.65213466
113	1890.3	0	0	0.481361282	3.989623557	18.8647065
114	1938.5	0	0.12011734	10.02606842	13.08070525	19.28133704
115	1985.9	0	0.81197211	9.565478633	14.09429724	21.22982241
116	2039.5	0	0.008792139	2.092245731	11.21950877	22.94378008
117	2090.9	0	0.003231007	1.82968389	5.894814305	17.88979488
118	2141.7	0	0.041184661	4.107807645	7.425032428	18.30732409
119	2191.0	0	0.007080536	4.902131952	7.134590672	17.24908238
120	2241.3	0	0.012932006	1.413652819	4.528335211	18.40603018
121	2286.7	0.000282704	2.137759297	10.04984893	6.316288658	14.05654831
122	2338.1	2.882347965	14.31627349	15.74117969	8.61092681	11.92005441
123	2391.3	0.412949336	6.87630196	14.85101366	10.47989025	15.87189274
124	2442.9	2.099851444	11.21949256	12.52546525	10.0419258	15.74580547
125	2492.5	0	0.279942913	4.971439276	9.740480244	18.85210764
126	2539.2	0	0.130151373	7.38482218	7.90808747	16.99817246
127	2589.4	0	0.118919173	7.070980787	8.02665428	17.08178708
128	2641.6	0	0.113434997	7.803601058	7.006734723	17.89486838
129	2691.4	0	0.499582129	8.698796339	10.01416989	19.28744965
130	2741.0	0	0.00172118	1.496090915	9.471140033	22.01656494
131	2785.0	0	0.024159663	1.767348166	7.828975487	21.07779329
132	2833.7	0.337315336	5.866055983	13.55274896	11.11443727	17.67817208
133	2883.7	0	0.002880217	2.947907113	10.93815385	21.10443817
134	2934.4	0	0.403071277	8.324786966	9.39962596	18.66388015
135	2982.4	0	0.595627947	8.016752895	9.819123081	19.60688629
136	3019.0	0	0.586897828	8.219227791	12.84634854	23.15745717
137	3055.9	0	0.225103573	7.210086467	12.84159184	24.26464851
138	3096.0	0	0.066085391	3.948993929	14.08537149	25.14625452
139	3139.5	0	2.414351547	11.97673124	15.35175354	22.20830845
140	3183.5	0	0.267020587	4.550875268	16.49665405	26.17848665

depth (cm)	Age (cal yr BP)	Coarse Sand 500 - 2000 µm	Medium Sand 250 - 500 µm	Fine Sand 125-250 µm	V Fine Sand 63-125 µm	V Coarse Silt 31-63 µm
141	3208.4	0	0.073670755	3.627092463	12.26181519	26.86146656
142	3232.9	0	0.164607696	6.026351409	12.02804281	24.38660043
143	3255.7	0	0.023980045	6.57813031	11.01387368	21.07800088
144	3277.7	0	0.003692794	2.216530821	11.55352061	22.39476346
145	3297.6	0	0.159727587	6.654910662	9.458578319	19.31339424
146	3324.2	0	0.085332864	6.684634778	10.92687819	22.88253954
147	3349.9	0	0	0.679847102	9.927640044	22.13415067
148	3375.6	0	0.945284343	8.993181232	12.52236941	22.26151238
149	3400.5	0.209319271	4.951789454	8.598588494	11.10703441	20.45416031
150	3424.7	0	0.01526979	2.917422652	12.19996882	21.99133046
151	3450.6	0	0.014009055	3.389205673	11.80235529	21.63525761
152	3478.0	0	0.008866144	5.075038654	9.715190635	22.30596414
153	3504.9	0	0.084607483	6.758247606	12.37329154	22.67753567
154	3531.7	0	2.225217094	9.600436505	12.72103429	21.74410397
155	3557.0	0	0.772535113	9.437688206	12.51304942	22.18780506
156	3583.1	0	0.401868157	5.724825424	13.16232274	26.38107391
157	3609.5	0	2.030296677	8.567754478	16.86298782	24.1388507
158	3635.1	2.331986581	9.524030472	11.26483214	12.78809638	20.37492748
159	3661.6	0.769429657	6.853014389	11.95078413	14.33881808	19.74202607
160	3686.4	0	0.289142195	6.834991611	12.80931835	23.33715298
161	3711.8	2.062832968	10.18874442	11.20230567	13.5100539	19.25997317
162	3737.8	0	0.028127641	3.909890033	12.68655733	22.00582766
163	3765.6	0	0.000633616	2.241953984	17.40722495	24.82330807
164	3792.3	0	0.002729953	1.201434278	12.9512192	23.57134302
165	3818.6	0	0	0.145099525	10.04481588	22.67399071
166	3843.1	0	0	1.486397627	13.09347282	22.16893699
167	3868.9	0	0	0.41896524	11.40647874	21.69748228
168	3895.7	0	0	2.028335634	14.44442939	23.17839898
169	3922.4	0	0.06801873	7.67882785	13.68383426	24.03312833
170	3948.3	0	0.40179964	7.873005124	15.35754948	24.7842631
171	3973.2	0	0	1.05195688	16.58541006	26.29811266
172	3997.8	0	0	1.21001011	17.1398201	25.94237349
173	4023.9	0	0.007145272	3.618752138	14.41356347	24.30765816
174	4050.7	0	0.000766903	3.166444253	11.1408613	20.80524875
175	4075.8	0	0.03797023	6.402402191	10.73750929	21.37291901
176	4098.5	0	0.535883272	8.539587161	11.80396802	21.71884346
177	4120.5	0	0.445375391	7.133503366	14.77851503	20.68893679

depth (cm)	Age (cal yr BP)	Coarse Silt 16-31 µm	Medium Silt 8-16 µm	Fine Silt 4-8 µm	V Fine Silt 2-4 µm	Clay 0-2 µm
1	-56.8	7.392102877	9.362733245	14.70069812	21.2732273	26.214039
2	-54.1	8.648693516	11.97900185	16.30094065	20.6398453	24.91652
3	-51.2	9.896384581	11.80857508	13.9528425	18.0539482	28.253544
4	-48.5	8.005903376	9.54403198	13.30042753	19.2249803	27.089066
5	-45.8	8.206504967	10.48007717	14.60441788	18.7787723	25.189879
6	-38.2	8.868570411	8.798273516	12.05030137	17.5208319	28.916295
7	-30.5	8.594594986	8.607115758	11.29889812	15.7946454	27.33382
8	-22.9	9.802876963	10.61518048	11.79006886	15.2447659	25.470047
9	-15.3	7.24435173	8.37679439	11.11596668	16.169832	23.964167
10	-7.7	9.289006016	10.6231961	12.71974801	16.3363823	28.276936
11	10.1	7.977645279	8.252343374	15.55160805	22.8357956	21.27438
12	27.4	9.086529326	9.174613486	12.5047765	17.8863336	20.538512
13	44.7	10.52778511	10.40553395	10.88470366	14.4408181	23.820925
14	61.9	11.20685208	10.65569963	11.07961039	14.8392761	25.393796
15	79.1	11.20164761	10.7175905	12.61485579	17.700407	25.750259
16	95.4	10.45723292	9.989124478	10.77054179	15.1685155	22.242736
17	111.4	11.700118	11.24768457	10.29897187	11.3051369	21.722784
18	126.1	11.59812755	10.58970429	11.12522877	15.9523133	23.748994
19	139.3	12.38824415	10.71695574	11.31281462	15.2746991	23.457053
20	152.4	12.64478323	11.3914194	11.05170815	13.7558464	23.472469
21	170.5	10.88665278	11.42292757	13.34723657	17.9317495	25.224378
22	189.5	10.99486387	11.86672242	13.18337319	16.8261011	24.967808
23	207.2	10.0330578	11.03778589	12.8267695	16.58282	22.975884
24	224.3	9.709601029	9.72015413	9.97183699	12.1958664	18.915263
25	240.9	10.0480142	7.709543029	9.102085728	12.9323251	16.742305
26	257.8	9.161176797	6.504555505	8.018919602	11.1010782	13.135557
27	275.8	9.865499727	7.53973649	7.659144084	10.2049124	13.544119
28	293.7	9.833581774	6.829397055	7.267892789	10.1851695	13.867376
29	311.8	11.54946668	10.06876383	8.280427837	8.70085259	13.267226
30	328.6	14.07802085	12.3577268	9.494109236	11.3544678	16.672018
31	345.3	14.70615585	12.68223868	8.488375336	8.82825678	15.903679
32	362.9	13.04723737	15.0976063	10.55846367	11.7057602	19.855449
33	381.6	12.35050042	16.68262916	11.6562657	11.5608007	20.306607
34	399.7	13.11277431	16.91929239	11.76005271	12.3063177	22.273209
35	417.6	14.06408768	16.9907207	11.30233058	10.4388428	19.375148
36	434.0	11.64108085	14.71952943	11.63545115	12.6540169	22.119394
37	451.8	12.22624442	15.89261166	12.69058797	11.6176655	22.951783
38	470.0	12.05523945	15.11393756	12.20448862	13.6097724	22.719554
39	487.2	13.3208811	15.41363368	12.29292407	13.9279641	22.469581
40	505.1	14.46471437	15.31435193	11.570512	12.5786203	20.421256
41	518.8	13.84608099	16.50063068	11.96651466	11.7588473	21.912735
42	533.1	14.8294417	18.08528867	12.50547507	12.8241485	22.597704
43	548.5	15.10996766	17.7870215	11.79218291	11.6575579	20.565057
44	564.8	13.22818163	17.46844008	12.49952007	11.6509361	21.317507

depth (cm)	Age (cal yr BP)	Coarse Silt 16-31 µm	Medium Silt 8-16 µm	Fine Silt 4-8 µm	V Fine Silt 2-4 µm	Clay 0-2 µm
45	582.1	13.1041228	14.53625643	10.10683388	8.99074634	17.327807
46	597.4	14.55073472	13.84966093	8.847131808	8.0768022	15.823543
47	611.8	13.67238034	14.67182401	11.02925594	10.2257834	19.430402
48	624.6	13.66470029	15.872465	12.4626296	12.9927393	22.280264
49	636.0	16.10021729	15.8203314	10.95896363	9.91684944	18.787042
50	647.1	13.70448348	12.67709881	8.029955689	6.92640515	14.25771
51	660.1	13.54791815	11.87093605	8.052789902	7.32159206	14.465804
52	673.2	13.10108724	15.15110806	10.6391076	9.98759375	18.506402
53	684.9	13.30778927	16.78016083	12.33211827	11.8294174	20.3293
54	697.0	13.02398559	16.15930178	11.99341228	10.922196	20.468498
55	708.1	15.23958123	16.7236049	11.43077531	10.1179953	18.97856
56	721.9	16.64694517	15.88158685	10.03063299	8.46362739	16.666659
57	735.2	16.25120068	16.57310422	10.54326512	9.04548255	17.181566
58	748.6	13.65141303	16.58776779	12.33814136	10.9894388	21.027512
59	762.0	13.46241002	16.01920715	11.33949515	10.3274479	19.485557
60	775.5	13.53913649	15.76684461	11.55607021	10.5234343	19.126845
61	788.3	11.70008152	15.84936347	13.47531843	13.1759369	24.415313
62	802.1	10.78636877	14.90549799	13.23038314	13.1652046	24.586911
63	815.1	10.52998244	15.36561095	14.16370244	14.6547229	25.877546
64	828.0	11.73835128	16.51630487	14.54349036	14.0209909	25.805815
65	840.0	11.43978105	16.60640236	12.77062904	12.4838849	22.089877
66	853.1	12.14123498	17.27003728	11.98319763	11.1849395	20.320772
67	866.7	12.03716369	16.94967784	11.68533333	11.6757639	21.276289
68	880.1	12.05851306	17.99135048	13.57222042	13.0040109	24.308291
69	893.2	11.34952876	16.70524729	13.16406466	12.1992948	22.931913
70	906.0	12.05611876	15.00502536	11.36254993	11.027365	20.280241
71	919.2	14.42986685	15.83598576	10.37363629	9.44967618	18.574143
72	933.2	15.58798728	16.04108916	9.364694972	8.98310854	16.654141
73	946.6	15.42458506	16.41897261	10.41910139	9.9624741	18.770665
74	959.4	13.22758598	16.63551865	12.84069147	11.2891858	22.19082
75	972.1	11.9186952	15.97922708	13.37586748	12.3058045	23.673375
76	984.6	10.65513423	15.57886795	14.00908433	14.5899838	25.360207
77	997.0	10.22428197	17.14462983	15.26970517	14.2854338	26.453788
78	1009.3	10.48316401	16.19167991	13.88975695	13.5849149	24.301386
79	1022.4	11.71629474	15.99328487	12.88122737	12.3547522	22.337455
80	1035.2	12.45237135	15.92619256	12.40954965	12.2624822	22.204583
81	1047.8	15.80103392	18.54818356	12.40014062	10.3102955	16.663557
82	1060.8	12.52617075	13.40634545	9.821515203	10.4735313	17.155144
83	1073.0	14.85688045	13.70479496	8.983760066	9.36709626	15.391607
84	1085.8	15.64864426	14.91899643	9.582636886	9.05476869	14.665571
85	1098.2	12.04811234	18.47363042	15.15019943	12.739914	16.210155
86	1109.2	12.46634854	19.48282835	13.92120707	15.077999	22.927065
87	1120.5	12.90240694	19.33847152	12.81355062	12.6309151	19.980961
88	1132.2	13.29813339	18.62220059	12.48686835	13.0849472	18.687493
89	1144.6	13.10587044	19.20813593	12.53930326	13.6586076	20.561785
90	1157.2	14.70321274	20.20868143	11.91326114	11.9072957	17.897695
91	1167.9	14.42969138	19.27880873	10.63777408	10.555488	16.952465
92	1179.1	13.32492646	16.42631291	9.584958185	8.55708011	14.966575

depth (cm)	Age (cal yr BP)	Coarse Silt 16-31 µm	Medium Silt 8-16 µm	Fine Silt 4-8 µm	V Fine Silt 2-4 µm	Clay 0-2 µm
93	1190.3	10.84187949	10.88785806	6.776509071	7.1213172	11.586129
94	1201.9	11.88360571	9.392251842	5.992997454	6.02397075	10.36978
95	1213.2	11.85757215	7.214500628	4.302231053	4.08949527	7.4113007
96	1223.7	16.19598372	12.65551947	7.953640528	5.92102894	10.983282
97	1233.9	16.76211319	13.47200314	8.472978356	6.58932024	11.485254
98	1244.7	15.99481493	13.40421825	8.738274517	6.79556193	11.490322
99	1257.0	16.1869663	12.20890212	10.19628635	10.9582013	11.755586
100	1269.0	13.01600455	10.01699448	13.88618552	16.6082189	11.377493
101	1316.0	12.1597332	11.95301245	13.99298054	18.8314169	19.845758
102	1363.5	12.54515774	8.74182704	13.60642619	17.6207465	12.234039
103	1408.9	13.77367661	9.607725756	11.36196188	15.7541129	13.904824
104	1452.3	12.3354957	8.746382896	11.47761745	15.6833667	13.107929
105	1494.7	15.72329708	11.9111585	11.28200877	13.9628872	16.820107
106	1543.5	14.52449432	11.84262705	11.68589511	13.4719808	14.201972
107	1595.1	16.24041582	13.61021166	11.14106916	11.8460912	15.926249
108	1644.2	14.5919807	13.03241671	9.879199317	8.62426625	10.716465
109	1691.9	14.34711256	11.41774206	11.01005988	13.2468833	14.317844
110	1737.0	12.93591738	10.43279147	12.95839828	15.706206	13.692071
111	1787.5	14.2121331	11.1359028	13.75696822	17.8369698	16.827546
112	1838.6	13.47689386	10.53893465	12.58667952	15.6167109	14.319914
113	1890.3	14.23476879	10.9197568	15.71823111	20.0787026	15.712849
114	1938.5	12.84495832	9.116392299	10.08803865	13.0927992	12.349584
115	1985.9	12.67676556	8.659305928	8.980762428	11.3479185	12.633677
116	2039.5	14.69200442	10.19714438	10.88358277	13.9843714	13.97857
117	2090.9	16.90931089	14.59548796	13.90701514	14.5714988	14.399163
118	2141.7	18.22996099	17.1043846	12.72755771	9.83086184	12.225886
119	2191.0	15.46463536	13.44526146	11.65420737	13.2905	16.85251
120	2241.3	16.25505151	13.60831921	12.78259042	14.7788668	18.214222
121	2286.7	12.98698636	11.92539377	11.73311769	13.9807497	16.813025
122	2338.1	9.792671497	7.068001323	8.367507106	11.1581788	10.142859
123	2391.3	12.08904019	9.155275326	8.521089109	10.1332097	11.609338
124	2442.9	11.49992673	8.267063216	8.013770754	9.84072016	10.745979
125	2492.5	15.82072637	12.63350769	10.89344147	12.2706231	14.537731
126	2539.2	14.73830621	12.76057204	11.14502026	12.3607988	16.574069
127	2589.4	13.77539448	12.66504833	11.60694726	12.926153	16.728116
128	2641.6	13.96584042	12.15901554	11.52276615	13.3188273	16.214911
129	2691.4	12.80289734	10.28882689	10.44595617	13.0332222	14.929099
130	2741.0	14.31248322	12.18628949	10.99839059	12.5325523	16.984767
131	2785.0	14.13913098	11.66433676	12.59912681	15.347097	15.552032
132	2833.7	11.76466174	9.055348626	8.64088938	10.0597769	11.930594
133	2883.7	15.30885282	12.27653232	10.67771357	11.7625127	14.981009
134	2934.4	13.79335503	10.64267288	10.36368412	13.0494375	15.359486
135	2982.4	14.08857537	10.45685931	10.01223474	12.5554957	14.848445
136	3019.0	13.95324577	9.808946033	8.405461994	9.93062652	13.091788
137	3055.9	14.78835399	10.1649842	8.273118068	9.51328204	12.718831
138	3096.0	14.29107939	9.449968251	9.225840744	11.3176576	12.468749
139	3139.5	12.8810559	7.900067303	7.627859421	9.38274656	10.257126
140	3183.5	14.46118269	9.394670025	8.054605488	9.28997464	11.306531

depth (cm)	Age (cal yr BP)	Coarse Silt 16-31 µm	Medium Silt 8-16 µm	Fine Silt 4-8 µm	V Fine Silt 2-4 µm	Clay 0-2 µm
141	3208.4	15.67853777	9.82535203	8.852449606	10.5478742	12.271741
142	3232.9	15.45270442	10.37371032	8.537357331	9.9230447	13.107581
143	3255.7	14.33696477	10.42869653	9.752704548	12.1837724	14.603877
144	3277.7	16.46400257	12.5513084	9.766381494	10.3673732	14.682427
145	3297.6	14.44269392	11.0787106	10.70295949	13.045165	15.14386
146	3324.2	15.210807	10.68262601	9.029825405	10.6816681	13.815688
147	3349.9	16.35616451	12.93509576	11.13967045	11.6661217	15.16131
148	3375.6	14.15712794	10.30684054	8.126118382	9.17323918	13.514327
149	3400.5	14.00559495	9.736372647	8.395762006	9.90412306	12.637255
150	3424.7	15.58842806	10.71519802	10.19124087	12.2607443	14.120397
151	3450.6	15.31757805	10.51482357	10.26137824	12.7531507	14.312242
152	3478.0	16.04676161	11.31640308	9.615725647	11.0718791	14.844171
153	3504.9	14.98470485	10.961738	8.783099797	9.7351791	13.641596
154	3531.7	13.58033801	9.901187283	8.138948576	9.30281399	12.78592
155	3557.0	14.35734903	10.38273799	8.441375123	9.40176214	12.505698
156	3583.1	15.59281041	10.34827911	7.689901278	8.16286411	12.536055
157	3609.5	13.36108339	8.887825423	7.168393776	8.17739226	10.805415
158	3635.1	12.01723891	7.805078757	6.438958319	7.58814441	9.8667066
159	3661.6	11.58924949	7.721209798	7.397373128	9.17875108	10.459344
160	3686.4	14.46044356	9.874523549	8.766740774	10.3600845	13.267602
161	3711.8	11.7608118	7.799164987	6.425077868	7.52017683	10.270858
162	3737.8	17.22807948	13.5708145	10.07251808	9.21667669	11.281509
163	3765.6	14.98117763	10.24643032	8.335853623	9.17074332	12.792674
164	3792.3	14.62147409	9.988390204	10.50585766	13.0258835	14.131668
165	3818.6	15.81480873	11.55217485	10.61614073	12.8506745	16.302295
166	3843.1	14.83212569	10.69341018	10.6567171	12.6726008	14.396339
167	3868.9	14.84392004	10.11873036	11.62379895	14.8012097	15.089415
168	3895.7	15.13082371	10.44147962	9.413223231	11.2557326	14.107522
169	3922.4	15.15835675	9.687052554	7.948600714	9.23863401	12.503547
170	3948.3	14.68742724	9.020026864	7.514995806	8.79407917	11.566854
171	3973.2	15.6098281	9.771439007	8.785006311	10.1707124	11.727535
172	3997.8	15.89124587	10.25426351	7.970314176	8.9358339	12.656139
173	4023.9	16.84299387	11.28208025	8.792597558	9.16220245	11.573007
174	4050.7	17.06480138	14.86958937	10.84530107	9.63139531	12.475592
175	4075.8	15.61775353	11.60245039	9.148437472	10.1247355	14.955822
176	4098.5	14.85739996	10.47104034	8.551278795	9.76598152	13.756017
177	4120.5	14.37041386	10.47166343	8.948432503	10.1959989	12.967161

depth (cm)	Age (cal yr BP)	MMG (µm) Mean	MMG (µm) Sorting	MMG (µm) Skewness	MMG (µm) Kurtosis
1	-56.8	6.584223393	5.163917484	0.580365779	2.286093125
2	-54.1	6.053808779	4.330198904	0.448167936	2.276514122
3	-51.2	5.95418798	4.5917064	0.396532999	2.171750024
4	-48.5	6.843176062	5.251316571	0.457799814	2.077970477
5	-45.8	6.936606769	4.920504875	0.370247285	2.034575919
6	-38.2	6.587926788	5.084061899	0.319575028	1.876469837
7	-30.5	7.78453539	5.507806636	0.217660304	1.756973606
8	-22.9	7.872225584	5.124409825	0.151482267	1.805807796
9	-15.3	10.32544184	6.610828944	0.255528965	1.749427205
10	-7.7	6.728979128	5.100169463	0.328496584	1.984162553
11	10.1	7.352290728	4.694886715	0.407864358	1.992668094
12	27.4	9.545788893	5.322075603	0.168662039	1.775379114
13	44.7	9.08922093	5.426895872	0.103268122	1.79204447
14	61.9	8.148221309	5.260352056	0.154864126	1.838909623
15	79.1	6.836621862	4.619598915	0.226996142	1.900686699
16	95.4	9.85452368	5.565067667	0.119588997	1.809590026
17	111.4	11.24728253	5.813687078	-0.003711241	1.845550555
18	126.1	8.364590797	5.065916826	0.135679608	1.827172535
19	139.3	8.478617641	5.046589455	0.115278174	1.863081936
20	152.4	8.830546657	5.143742783	0.0685481	1.863716377
21	170.5	6.858132725	4.64504093	0.286221441	2.013294035
22	189.5	7.164743932	4.758939469	0.250483202	1.990380282
23	207.2	8.363328692	5.133707007	0.21952267	1.907056699
24	224.3	13.53591151	5.998704337	-0.073569489	1.781683111
25	240.9	15.62730438	6.013809168	-0.139572365	1.781052526
26	257.8	21.95267297	6.055994833	-0.360587723	1.883272586
27	275.8	21.29275207	5.938756978	-0.363835811	1.948943916
28	293.7	21.63661294	6.075967519	-0.352087519	1.984602992
29	311.8	21.70173768	6.171843558	-0.227993194	2.08271323
30	328.6	12.65813115	4.855101292	-0.257351933	1.94404725
31	345.3	14.57173831	5.001965622	-0.342514322	2.108446977
32	362.9	10.64803974	5.126152394	-0.018524457	1.96872385
33	381.6	10.11953069	5.138845737	0.050951785	2.021365438
34	399.7	8.444510084	4.644298521	0.012862025	2.012172888
35	417.6	10.43943692	4.916623912	-0.049671665	2.08389603
36	434.0	9.378281832	5.219980821	0.093947659	1.948870576
37	451.8	8.638096756	5.023302413	0.085206579	2.037998608
38	470.0	8.389855811	4.855548437	0.113378774	1.999928268
39	487.2	8.074915177	4.60292137	0.078864036	2.01857961
40	505.1	9.219428362	4.642167114	-0.038244538	2.007157677
41	518.8	8.968164243	4.929042343	0.07455969	2.083098767
42	533.1	7.653816285	4.317716531	0.012132463	2.088797142
43	548.5	9.051148785	4.610616365	-0.003998437	2.113891099
44	564.8	8.983145829	4.842995347	0.06987518	2.111804393

depth (cm)	Age (cal yr BP)	MMG (µm) Mean	MMG (µm) Sorting	MMG (µm) Skewness	MMG (µm) Kurtosis
45	582.1	13.38849663	5.321386709	-0.171828333	2.047518657
46	597.4	14.41125716	4.918472318	-0.370072998	2.152886401
47	611.8	11.08841751	5.125163977	-0.092245448	2.002394367
48	624.6	8.374870568	4.734431233	0.097526821	2.078011196
49	636.0	11.08660158	4.990436999	-0.069488812	2.119707237
50	647.1	21.38527513	6.480801114	-0.143355953	2.143560348
51	660.1	18.84075523	5.642307976	-0.325145886	2.151343437
52	673.2	13.13677317	5.921855785	0.037995279	2.000216328
53	684.9	9.819277021	5.121816793	0.117350173	2.11519687
54	697.0	10.36839658	5.343279079	0.077636357	2.057928693
55	708.1	10.66027075	4.927059601	-0.051903184	2.128599444
56	721.9	12.88382346	4.959703989	-0.192826257	2.202736048
57	735.2	12.12359078	4.91260523	-0.15520398	2.157299115
58	748.6	9.623004854	5.08817521	0.053533232	2.059407878
59	762.0	11.29501674	5.408997771	0.014255062	2.018257381
60	775.5	11.49904798	5.485384383	0.054517819	2.075123465
61	788.3	7.823806186	5.072508603	0.25314244	2.156842523
62	802.1	8.141585377	5.326699865	0.255429168	2.07799575
63	815.1	6.989679194	4.902444592	0.330369154	2.207227198
64	828.0	6.651346243	4.558767982	0.238922303	2.194838134
65	840.0	9.085974888	5.239628563	0.173288612	2.049886581
66	853.1	10.13982581	5.197607367	0.06372879	2.041492732
67	866.7	9.919089538	5.385018566	0.13916051	2.058086119
68	880.1	7.338478732	4.660310137	0.193088279	2.191490145
69	893.2	8.625256255	5.179581981	0.189190283	2.104138848
70	906.0	10.8351768	5.402292584	0.014313481	1.965143284
71	919.2	11.63391286	5.045497046	-0.153568766	2.042862095
72	933.2	13.58836441	5.230390371	-0.142813427	2.108631165
73	946.6	11.03283202	4.897920659	-0.123841187	2.072349166
74	959.4	8.70982139	4.870912658	0.046822873	2.06597791
75	972.1	8.234114907	5.095234862	0.185923583	2.103472846
76	984.6	7.130959016	4.866069966	0.307236249	2.186625132
77	997.0	6.37268844	4.564787326	0.314124433	2.30468701
78	1009.3	7.694702469	4.993469867	0.255083931	2.137331332
79	1022.4	8.858995592	5.106410367	0.134586764	2.038167189
80	1035.2	8.886641836	5.024677279	0.10233021	2.038238123
81	1047.8	11.12441075	4.73158495	-0.010566055	2.264565721
82	1060.8	14.17490261	5.73381704	-0.066342594	1.967439557
83	1073.0	14.57450249	5.053055348	-0.257129164	2.102773889
84	1085.8	14.2995706	4.837035546	-0.262752461	2.183717162
85	1098.2	10.45514979	4.776299866	0.155893223	2.219585894
86	1109.2	6.943918595	4.206780475	0.196079061	2.279844922
87	1120.5	9.002705262	4.703217874	0.127160747	2.198409783
88	1132.2	9.565532926	4.694948632	0.10587799	2.165064749
89	1144.6	8.495452378	4.574355635	0.14660979	2.197375686
90	1157.2	9.767434483	4.473194346	0.004551622	2.21261399
91	1167.9	11.417658	4.772024061	-0.068683236	2.13674126

depth (cm)	Age (cal yr BP)	MMG (µm) Mean	MMG (µm) Sorting	MMG (µm) Skewness	MMG (µm) Kurtosis
92	1179.1	15.00584225	5.152131636	-0.231002497	2.092037686
93	1190.3	22.90034671	5.127156122	-0.612513042	2.309911649
94	1201.9	24.49412161	4.677964863	-0.806669566	2.687741499
95	1213.2	35.56959797	4.573205555	-0.850032626	3.36520855
96	1223.7	20.33073419	4.698494025	-0.535032288	2.573103878
97	1233.9	18.44170785	4.59822118	-0.506184823	2.482920633
98	1244.7	18.57547308	4.683502544	-0.469561194	2.440694121
99	1257.0	15.41282538	4.48095845	-0.341474776	2.106672381
100	1269.0	13.52142216	4.781673325	0.072452215	1.930397446
101	1316.0	8.420492861	4.735780341	0.308276565	2.069547618
102	1363.5	12.30094729	4.485033014	-0.024837376	1.820000595
103	1408.9	11.97367363	4.331071008	-0.22893931	1.764597037
104	1452.3	13.15386675	4.552983873	-0.216117046	1.748836104
105	1494.7	10.20754941	4.19176078	-0.279007555	1.856083168
106	1543.5	12.23139171	4.438123135	-0.209615569	1.958186968
107	1595.1	10.98754282	4.173386197	-0.36616591	1.974924819
108	1644.2	19.37115953	5.052746315	-0.247552591	2.22922312
109	1691.9	13.08448733	4.733294125	-0.152383504	1.972669036
110	1737.0	12.22198663	4.651696799	-0.040738429	1.901492335
111	1787.5	8.894924237	4.054252991	-0.066126452	1.78519702
112	1838.6	11.50902645	4.414998066	-0.146214378	1.817688559
113	1890.3	8.330420712	3.828444857	0.042834291	1.835179936
114	1938.5	16.10481739	4.942730638	-0.248903444	1.900864737
115	1985.9	17.50539304	5.063996439	-0.340027225	2.007516997
116	2039.5	12.48174632	4.371273889	-0.287862271	1.889551458
117	2090.9	10.08844529	3.968423189	-0.140175194	2.055013569
118	2141.7	12.67339607	4.066517128	-0.285327246	2.348819312
119	2191.0	10.73630333	4.546863434	-0.099438569	2.003319329
120	2241.3	8.9157473	4.141872191	-0.109759118	1.966214073
121	2286.7	12.23447379	5.390190773	0.087012353	1.982228593
122	2338.1	30.59379518	6.963767847	-0.260752804	1.808903242
123	2391.3	22.71725319	5.927024027	-0.260098622	1.971710532
124	2442.9	26.85331155	6.377950608	-0.246059324	1.986016132
125	2492.5	12.70917735	4.578162252	-0.20015348	2.038850711
126	2539.2	11.90899694	4.863099776	-0.10273325	1.996051098
127	2589.4	11.58993087	4.859831569	-0.075242359	1.972661119
128	2641.6	11.81946032	4.845049815	-0.068667584	1.974646972
129	2691.4	13.84247525	5.064896033	-0.149391047	1.916743915
130	2741.0	11.01064143	4.458172662	-0.269948261	1.89886348
131	2785.0	10.47011105	4.278787217	-0.141922544	1.890954071
132	2833.7	21.72725994	5.798739965	-0.274066952	2.005897588
133	2883.7	12.47714073	4.474275849	-0.311190891	1.994668149
134	2934.4	13.31190622	5.007767279	-0.139383506	1.932063989
135	2982.4	13.91308901	4.986901432	-0.176996813	1.964179144
136	3019.0	17.04413717	4.893295952	-0.412015011	2.126008514
137	3055.9	16.91185467	4.686352936	-0.477967835	2.193383113
138	3096.0	15.58912482	4.500228752	-0.457491487	2.066763674

depth (cm)	Age (cal yr BP)	MMG (µm) Mean	MMG (µm) Sorting	MMG (µm) Skewness	MMG (µm) Kurtosis
139	3139.5	22.58321583	5.017648992	-0.491613651	2.227799762
140	3183.5	18.11039561	4.455654298	-0.601873155	2.298616443
141	3208.4	15.64279694	4.363563107	-0.517140893	2.172793743
142	3232.9	15.90390841	4.613583507	-0.459175304	2.168466759
143	3255.7	13.871106	4.784118415	-0.275570102	1.958256073
144	3277.7	13.10738251	4.403193817	-0.417862624	2.08766112
145	3297.6	12.80417882	4.791278928	-0.165199471	1.9599
146	3324.2	14.97111784	4.6946605	-0.375436641	2.077087495
147	3349.9	11.62481404	4.229587744	-0.373802587	2.006258955
148	3375.6	17.33002988	5.009441146	-0.407351616	2.150671146
149	3400.5	18.95406341	5.386117249	-0.261226483	2.138985061
150	3424.7	13.24234882	4.475049685	-0.340358428	1.978523333
151	3450.6	13.06161183	4.519551526	-0.304130987	1.951168985
152	3478.0	13.41631516	4.596804734	-0.340524071	2.050879773
153	3504.9	15.65929834	4.72293192	-0.425477993	2.129452884
154	3531.7	18.5899068	5.13397409	-0.382784563	2.151303588
155	3557.0	17.78601391	4.901974793	-0.409060028	2.173339474
156	3583.1	17.47885046	4.574095615	-0.576380083	2.363790476
157	3609.5	21.60692068	4.813964431	-0.57428444	2.3834889
158	3635.1	29.83802852	5.86908423	-0.395286417	2.309158565
159	3661.6	25.39234059	5.615891391	-0.392185397	2.172464576
160	3686.4	16.10265538	4.768134274	-0.411213074	2.101293082
161	3711.8	29.77829892	5.974786457	-0.406477788	2.279190905
162	3737.8	15.44895911	4.210871951	-0.470754341	2.310134219
163	3765.6	16.26309788	4.451275516	-0.60551053	2.217831393
164	3792.3	12.84396948	4.390410562	-0.365010951	1.9099986
165	3818.6	11.11744367	4.300136924	-0.339099485	1.882237742
166	3843.1	12.73596306	4.431505606	-0.342468648	1.922628235
167	3868.9	11.26896434	4.305100554	-0.25691607	1.815315632
168	3895.7	13.94866344	4.489075294	-0.441510201	2.005693123
169	3922.4	17.49889896	4.685514939	-0.519017774	2.225166632
170	3948.3	19.2233483	4.679369624	-0.568271607	2.317739161
171	3973.2	16.05347246	4.247819306	-0.612506948	2.203078303
172	3997.8	16.21736701	4.339826756	-0.658506548	2.2768897
173	4023.9	16.38117158	4.283036468	-0.570357258	2.305543509
174	4050.7	13.79847857	4.193290266	-0.414024117	2.24603235
175	4075.8	14.1682897	4.753751666	-0.354096043	2.080148074
176	4098.5	16.29898978	4.936995061	-0.371886735	2.120728665
177	4120.5	16.50651365	4.837173968	-0.38907089	2.105767972

Appendix E

EV11 Pollen and microcharcoal

Sample name	EV11-1	EV11-3	EV11-5	EV11-7	EV11-9	EV11-9.1	EV11-10
Depth (cm)	12	16.5	22	26	30.5	32.5	34.5
Age (cal yr BP)	-26	-14	8	43	90	111	133
Artemisia	16	4	3	3	6	5	13
Pentzia-type	4	3	6	2	4	4	8
Proteaceae	4	2	1	2	0	1	4
Ericaceae	8	22	14	19	14	8	13
Cliffortia	3	7	5	8	0	0	11
Bruniaceae	8	6	0	1	0	0	2
Anthospermum-type	7	17	23	22	3	2	11
Apiaceae	0	0	0	0	0	0	0
Fabaceae	1	0	0	0	0	0	0
Rhamnaceae	0	0	0	0	0	0	0
Rutaceae	2	6	0	2	0	0	4
Santalaceae	0	0	0	1	0	0	0
Scroph-type	0	0	0	0	0	0	0
Passerina	7	7	8	11	8	2	13
Cunoniaceae	1	3	0	0	1	0	0
Canthium	3	1	0	1	0	0	0
Gnidia	0	0	0	0	0	1	0
Euclea	8	7	1	2	5	0	6
Grewia	0	0	0	0	0	0	0
Ilex	1	1	1	5	0	0	0
Myrica	3	1	0	0	0	0	0
Myrsine	2	0	0	0	0	1	0
Myrtaceae	3	6	0	1	0	0	0
Olea	7	11	8	16	4	7	10
Cyperaceae	84	57	47	63	23	14	74
Restionaceae	13	9	17	28	13	6	44
Poaceae	38	51	49	70	44	27	66
Asteraceae HS	15	14	8	8	10	7	11
Stoebe-type	1	13	26	17	19	7	52
Geraniaceae	0	0	0	0	2	0	6
Onagraceae	0	0	0	0	0	0	0
Icacinaceae	0	0	0	1	0	1	0
Polygonium	1	1	1	0	1	0	0
Acacia	5	7	6	1	0	0	0
Celastraceae	3	5	3	6	1	0	7
Celtis	1	0	0	0	0	0	0
Diospyros	4	5	4	6	0	0	3
Euphorbia	4	15	10	7	11	4	18
Clutia	3	4	0	2	0	0	0
ChenAm-type	7	9	4	9	10	16	34
Crassula	1	4	1	2	3	0	6
Gunneraceae	0	0	0	1	0	0	0
Juncaceae	8	9	4	9	0	0	10

Sample name	EV11-1	EV11-3	EV11-5	EV11-7	EV11-9	EV11-9.1	EV11-10
Depth (cm)	12	16.5	22	26	30.5	32.5	34.5
Age (cal yr BP)	-26	-14	8	43	90	111	133
Liliaceae	5	4	2	5	2	0	9
Iridaceae	2	2	0	2	0	3	5
Urticaceae	0	3	2	0	0	0	0
Verbenaceae	0	0	0	0	0	0	0
Haloraginaceae	0	0	0	0	0	0	0
Typha	3	2	3	1	0	3	0
Zygophyllaceae	0	0	0	0	0	0	0
Lauraceae	1	0	1	1	0	0	0
Loranthaceae	2	0	0	0	0	0	0
Plantago	1	4	4	4	0	0	0
Acanthaceae	0	0	0	0	0	0	0
Pinaceae	123	76	168	71	0	0	0
Podocarpus	26	24	36	32	14	8	16
Rhus	6	5	6	10	2	4	4
Aizoaceae	10	4	5	2	2	1	1
Euphorbiaceae undif	0	0	0	0	3	3	4
Brassicaceae	5	9	1	2	2	2	8
Campanulaceae	0	0	0	0	0	0	0
Caryophyllaceae	0	0	0	0	0	0	0
Moraceae	0	0	0	0	0	1	0
Polygala	0	0	0	2	0	0	0
Oxalis	0	0	2	2	0	0	3
Unidentifiable	19	28	8	18	2	3	9
Broken	16	26	10	19	3	3	11
Unknown	5	6	2	3	2	2	4
10 - 50 µm	795	892	720	1498	3669	1278	2917
50 - 100 µm	1	4	6	5	0	0	2

Sample name	EV11-11	EV11-11.1	EV11-12.1	EV11-13.1	EV11-14.1
Depth (cm)	38	40	42.5	48	52
Age (cal yr BP)	173	196	231	305	363
Artemisia	6	5	6	1	1
Pentzia-type	6	7	8	4	0
Proteaceae	2	3	1	0	0
Ericaceae	16	16	8	7	7
Cliffortia	11	4	3	2	1
Bruniaceae	2	6	2	3	0
Anthospermum-type	16	20	15	8	8
Apiaceae	0	2	0	0	0
Fabaceae	0	0	0	0	0
Rhamnaceae	0	0	0	0	0
Rutaceae	2	6	5	1	0
Santalaceae	0	1	3	0	0
Scroph-type	0	0	0	0	0
Passerina	10	18	15	3	1
Cunoniaceae	0	1	1	0	0
Canthium	0	0	0	0	0
Gnidia	0	2	2	0	0
Euclea	13	5	11	1	1
Grewia	0	0	0	0	0
Ilex	0	7	2	1	1
Myrica	0	0	0	0	0
Myrsine	0	0	0	0	0
Myrtaceae	0	0	0	0	0
Olea	15	18	8	9	3
Cyperaceae	109	55	73	16	12
Restionaceae	66	32	39	17	7
Poaceae	93	76	61	33	22
Asteraceae HS	13	11	7	3	2
Stoebe-type	12	19	11	4	5
Geraniaceae	3	0	1	0	0
Onagraceae	0	0	0	0	0
Icacinaceae	1	0	0	0	0
Polygonium	0	0	0	0	0
Acacia	0	2	0	1	0
Celastraceae	2	5	1	4	1
Celtis	0	0	0	0	0
Diospyros	0	5	4	1	1
Euphorbia	3	2	15	1	1
Clutia	0	0	0	0	0
ChenAm-type	22	29	117	20	5
Crassula	6	4	3	0	0
Gunneraceae	0	0	0	0	0
Juncaceae	11	10	4	2	0

Sample name	EV11-11	EV11-11.1	EV11-12.1	EV11-13.1	EV11-14.1
Depth (cm)	38	40	42.5	48	52
Age (cal yr BP)	173	196	231	305	363
Liliaceae	6	7	6	3	3
Iridaceae	2	3	1	3	0
Urticaceae	0	3	0	0	0
Verbenaceae	0	0	0	0	0
Haloraginaceae	0	1	0	0	0
Typha	0	1	0	0	1
Zygophyllaceae	0	0	0	0	0
Lauraceae	0	2	1	0	0
Loranthaceae	0	0	0	0	0
Plantago	0	3	0	0	0
Acanthaceae	0	0	0	0	0
Pinaceae	0	0	0	0	0
Podocarpus	25	56	26	16	17
Rhus	5	11	9	4	5
Aizoaceae	4	6	4	3	0
Euphorbiaceae undif	3	1	2	0	0
Brassicaceae	3	5	4	1	0
Campanulaceae	0	0	0	0	0
Caryophyllaceae	0	0	0	0	0
Moraceae	0	0	0	0	0
Polygala	0	1	0	0	0
Oxalis	1	2	4	0	0
Unidentifiable	4	12	4	1	1
Broken	7	13	10	6	1
Unknown	0	2	3	9	8
10 - 50 µm	1632	1966	4931	1366	1086
50 - 100 µm	0	4	2	5	3

Sample name	EV11-16	EV11-18	EV11-19	EV11-21	EV11-22
Depth (cm)	56	60.5	62	68	70
Age (cal yr BP)	421	488	511	598	626
Artemisia	2	12	2	13	5
Pentzia-type	10	18	0	7	5
Proteaceae	3	2	0	1	0
Ericaceae	23	23	8	16	3
Cliffortia	4	2	0	1	2
Bruniaceae	1	2	0	1	0
Anthospermum-type	15	16	5	6	3
Apiaceae	0	0	0	0	0
Fabaceae	0	0	0	0	0
Rhamnaceae	0	0	0	0	0
Rutaceae	1	0	0	3	4
Santalaceae	0	0	0	0	0
Scroph-type	0	0	0	0	0
Passerina	11	10	6	12	2
Cunoniaceae	0	0	0	0	0
Canthium	0	2	0	0	0
Gnidia	0	1	0	3	0
Euclea	3	6	0	9	4
Grewia	0	0	0	0	0
Ilex	2	4	1	7	0
Myrica	0	2	0	2	0
Myrsine	2	0	0	0	0
Myrtaceae	0	0	0	0	0
Olea	15	17	5	21	11
Cyperaceae	53	45	12	46	37
Restionaceae	34	49	14	38	13
Poaceae	96	84	28	85	24
Asteraceae HS	10	8	1	11	7
Stoebe-type	14	14	7	14	5
Geraniaceae	0	1	0	2	2
Onagraceae	0	0	0	0	0
Icacinaceae	2	0	0	0	0
Polygonium	0	0	0	0	0
Acacia	0	0	0	0	0
Celastraceae	6	6	1	5	0
Celtis	0	0	0	0	0
Diospyros	1	2	0	3	0
Euphorbia	11	12	0	11	5
Clutia	0	0	0	1	0
ChenAm-type	45	40	4	58	27
Crassula	5	8	0	3	1
Gunneraceae	0	0	0	0	0
Juncaceae	8	4	1	6	0

Sample name	EV11-16	EV11-18	EV11-19	EV11-21	EV11-22
Depth (cm)	56	60.5	62	68	70
Age (cal yr BP)	421	488	511	598	626
Liliaceae	7	4	5	5	3
Iridaceae	4	1	1	3	1
Urticaceae	1	0	0	0	0
Verbenaceae	0	0	0	0	0
Haloraginaceae	1	0	0	0	0
Typha	4	3	1	8	0
Zygophyllaceae	0	0	0	0	0
Lauraceae	0	0	0	0	0
Loranthaceae	0	0	0	0	0
Plantago	0	1	0	0	0
Acanthaceae	0	0	0	0	0
Pinaceae	0	0	0	0	0
Podocarpus	60	65	13	59	6
Rhus	3	5	6	8	0
Aizoaceae	4	1	0	2	1
Euphorbiaceae undif	4	4	0	7	0
Brassicaceae	5	1	0	4	4
Campanulaceae	0	0	0	0	0
Caryophyllaceae	0	2	0	0	0
Moraceae	0	0	0	0	0
Polygala	2	0	1	2	0
Oxalis	2	2	0	0	0
Unidentifiable	4	8	0	9	0
Broken	8	11	3	6	3
Unknown	0	2	4	2	2
10 - 50 µm	2281	1167	2629	2041	1740
50 - 100 µm	7	10	7	4	7

Sample name	EV11-25	EV11-26	EV11-27	EV11-29	EV11-30	EV11-32
Depth (cm)	76	80	82	85.5	88	92
Age (cal yr BP)	713	788	850	957	1033	1153
Artemisia	6	2	9	14	15	0
Pentzia-type	3	1	5	22	9	0
Proteaceae	0	1	3	2	2	1
Ericaceae	12	2	15	30	30	8
Cliffortia	2	0	2	7	9	1
Bruniaceae	2	1	2	8	1	0
Anthospermum-type	8	3	16	25	8	5
Apiaceae	0	1	1	0	0	0
Fabaceae	0	0	0	0	0	0
Rhamnaceae	0	1	0	1	0	0
Rutaceae	2	1	3	3	2	0
Santalaceae	0	0	0	1	0	0
Scroph-type	0	0	0	0	0	0
Passerina	4	2	15	19	9	2
Cunoniaceae	0	0	0	1	1	0
Canthium	0	0	1	4	0	0
Gnidia	0	1	2	2	0	0
Euclea	1	0	5	10	11	2
Grewia	0	0	0	0	0	0
Ilex	1	0	0	2	2	0
Myrica	0	0	0	0	3	0
Myrsine	0	0	0	0	0	0
Myrtaceae	1	0	0	0	1	1
Olea	9	2	16	35	15	8
Cyperaceae	16	10	36	42	51	4
Restionaceae	15	8	22	24	38	9
Poaceae	45	23	70	39	83	24
Asteraceae HS	5	2	16	25	20	2
Stoebe-type	9	4	16	20	20	5
Geraniaceae	1	0	1	0	2	2
Onagraceae	0	0	0	0	0	0
Icacinaceae	0	0	0	7	1	0
Polygonium	0	0	0	0	0	0
Acacia	0	0	1	0	0	0
Celastraceae	2	1	6	14	6	1
Celtis	0	0	0	0	0	0
Diospyros	0	1	3	2	5	0
Euphorbia	3	0	5	10	12	0
Clutia	0	0	0	0	0	0
ChenAm-type	18	3	8	19	14	2
Crassula	2	0	2	11	1	0
Gunneraceae	0	0	0	0	1	0
Juncaceae	2	1	5	3	5	2

Sample name	EV11-25	EV11-26	EV11-27	EV11-29	EV11-30	EV11-32
Depth (cm)	76	80	82	85.5	88	92
Age (cal yr BP)	713	788	850	957	1033	1153
Liliaceae	1	0	4	5	5	3
Iridaceae	0	0	1	2	2	1
Urticaceae	1	0	0	0	0	0
Verbenaceae	0	0	0	0	0	0
Haloraginaceae	0	0	0	1	0	0
Typha	0	2	3	9	11	5
Zygophyllaceae	0	0	1	0	0	0
Lauraceae	0	0	0	0	0	0
Loranthaceae	0	0	0	0	0	0
Plantago	1	0	1	0	0	0
Acanthaceae	0	0	0	0	0	0
Pinaceae	0	0	0	0	0	0
Podocarpus	24	6	41	40	55	14
Rhus	8	1	6	19	4	2
Aizoaceae	1	1	3	0	3	2
Euphorbiaceae undif	0	0	0	0	9	0
Brassicaceae	3	0	5	8	6	4
Campanulaceae	0	0	0	1	0	0
Caryophyllaceae	0	0	1	0	0	0
Moraceae	0	0	0	0	0	0
Polygala	0	0	0	0	2	0
Oxalis	1	0	0	0	2	0
Unidentifiable	4	1	10	4	7	2
Broken	4	0	4	8	11	2
Unknown	7	0	5	1	6	5
10 - 50 µm	2723	1670	2420	1582	2615	4217
50 - 100 µm	2	0	3	3	3	3

Sample name	EV11-34	EV11-35	EV11-36	EV11-37	EV11-38	EV11-39	EV11-40
Depth (cm)	95.5	97.5	100	104	106	108	112
Age (cal yr BP)	1259	1315	1392	1519	1598	1673	1839
Artemisia	9	13	16	12	5	7	6
Pentzia-type	6	8	2	0	0	5	6
Proteaceae	2	3	5	1	1	4	3
Ericaceae	14	23	28	38	4	20	16
Cliffortia	7	6	13	6	5	1	7
Bruniaceae	3	2	1	2	1	1	3
Anthospermum-type	10	32	3	6	18	14	13
Apiaceae	0	0	0	0	0	0	0
Fabaceae	0	0	0	0	0	0	0
Rhamnaceae	0	0	0	0	0	0	0
Rutaceae	0	1	7	3	3	2	4
Santalaceae	0	0	0	0	1	0	0
Scroph-type	0	0	2	0	0	0	1
Passerina	8	11	8	17	6	7	16
Cunoniaceae	0	0	0	1	0	0	0
Canthium	0	0	0	2	0	0	1
Gnidia	0	0	1	1	0	0	1
Euclea	5	8	6	10	9	12	8
Grewia	1	0	0	0	0	0	2
Ilex	1	0	1	3	3	5	3
Myrica	0	0	0	0	1	0	0
Myrsine	1	0	2	0	0	3	3
Myrtaceae	0	0	0	1	0	0	0
Olea	17	17	18	25	15	11	8
Cyperaceae	52	49	48	60	44	35	49
Restionaceae	25	36	53	43	23	30	51
Poaceae	36	78	88	93	21	85	41
Asteraceae HS	9	18	7	9	8	7	4
Stoebe-type	18	31	18	14	5	24	16
Geraniaceae	9	1	2	1	4	3	3
Onagraceae	0	0	0	0	0	0	0
Icacinaceae	1	0	3	0	0	3	0
Polygonium	1	1	0	0	0	0	0
Acacia	0	0	0	0	0	2	0
Celastraceae	3	3	4	3	2	5	3
Celtis	0	0	0	0	0	0	3
Diospyros	2	3	7	1	2	3	2
Euphorbia	11	10	15	18	8	13	8
Clutia	0	1	0	0	0	1	0
ChenAm-type	20	29	40	40	47	70	117
Crassula	1	5	1	5	3	5	2
Gunneraceae	0	0	0	0	0	0	0
Juncaceae	1	6	0	2	1	6	0

Sample name	EV11-34	EV11-35	EV11-36	EV11-37	EV11-38	EV11-39	EV11-40
Depth (cm)	95.5	97.5	100	104	106	108	112
Age (cal yr BP)	1259	1315	1392	1519	1598	1673	1839
Liliaceae	4	5	8	1	8	4	13
Iridaceae	0	3	4	0	2	4	8
Urticaceae	0	1	0	0	0	0	1
Verbenaceae	0	0	0	1	0	0	0
Haloraginaceae	0	0	0	1	0	0	0
Typha	0	0	8	4	0	6	6
Zygophyllaceae	0	0	0	0	0	0	0
Lauraceae	0	0	0	0	0	0	0
Loranthaceae	0	0	0	0	0	0	0
Plantago	0	0	0	0	0	0	0
Acanthaceae	0	0	0	0	0	0	0
Pinaceae	0	0	0	0	0	0	0
Podocarpus	28	43	34	41	4	44	13
Rhus	14	6	13	8	12	6	14
Aizoaceae	4	4	2	3	0	0	0
Euphorbiaceae undif	4	2	6	9	1	5	3
Brassicaceae	5	5	4	2	6	4	7
Campanulaceae	0	0	0	0	0	0	0
Caryophyllaceae	0	0	0	0	0	5	1
Moraceae	0	0	0	2	0	7	0
Polygala	0	1	1	1	0	0	2
Oxalis	1	2	1	0	0	0	0
Unidentifiable	7	9	6	6	6	11	17
Broken	4	7	8	2	4	10	7
Unknown	1	10	6	2	5	10	8
10 - 50 µm	3801	12077	5462	1416	5981	9796	3904
50 - 100 µm	2	13	13	13	12	9	12

Sample name	EV11-40.1	EV11-41	EV11-42	EV11-43	EV11-44	EV11-45	EV11-46
Depth (cm)	114	116	118	120	122	123.5	126
Age (cal yr BP)	1921	2003	2086	2167	2256	2323	2430
Artemisia	6	7	9	6	6	8	3
Pentzia-type	1	10	4	3	3	3	1
Proteaceae	0	1	2	1	3	3	0
Ericaceae	7	15	13	12	17	11	8
Cliffortia	2	2	3	4	5	2	1
Bruniaceae	2	0	2	0	4	2	3
Anthospermum-type	6	7	8	9	6	3	8
Apiaceae	1	0	0	0	0	0	0
Fabaceae	0	0	0	0	0	0	0
Rhamnaceae	0	0	0	0	0	1	0
Rutaceae	1	1	3	2	1	11	3
Santalaceae	2	0	0	1	0	1	2
Scroph-type	0	0	1	0	0	0	0
Passerina	8	5	15	11	7	7	11
Cunoniaceae	0	0	0	0	1	0	0
Canthium	0	0	1	0	0	0	0
Gnidia	2	1	3	4	0	3	2
Euclea	5	7	10	9	5	8	8
Grewia	0	0	0	0	0	2	0
Ilex	1	0	2	0	4	2	1
Myrica	1	0	1	0	0	0	1
Myrsine	0	0	0	0	0	0	1
Myrtaceae	0	0	0	0	0	1	0
Olea	5	17	19	14	19	15	10
Cyperaceae	66	36	50	59	24	69	52
Restionaceae	31	21	35	43	32	31	40
Poaceae	29	69	60	46	32	49	37
Asteraceae HS	1	3	11	7	2	7	3
Stoebe-type	5	18	19	17	7	20	16
Geraniaceae	6	5	0	2	0	8	4
Onagraceae	0	0	0	0	0	0	0
Icacinaceae	1	1	0	1	1	3	1
Polygonium	0	0	0	0	0	0	0
Acacia	0	0	0	0	0	0	0
Celastraceae	2	7	3	0	4	1	3
Celtis	0	0	0	0	1	0	0
Diospyros	2	1	2	0	2	2	2
Euphorbia	5	13	14	10	9	10	8
Clutia	0	0	0	0	0	0	0
ChenAm-type	119	131	123	146	85	127	107
Crassula	2	2	8	0	4	2	3
Gunneraceae	0	0	0	0	0	0	0
Juncaceae	0	3	2	1	2	5	3

Sample name	EV11-40.1	EV11-41	EV11-42	EV11-43	EV11-44	EV11-45	EV11-46
Depth (cm)	114	116	118	120	122	123.5	126
Age (cal yr BP)	1921	2003	2086	2167	2256	2323	2430
Liliaceae	7	7	5	10	2	6	8
Iridaceae	5	1	4	5	2	4	7
Urticaceae	0	0	0	0	0	0	0
Verbenaceae	0	0	0	0	0	0	0
Haloraginaceae	0	0	0	0	0	0	0
Typha	1	5	4	3	0	0	1
Zygophyllaceae	0	0	0	0	0	0	0
Lauraceae	0	1	2	0	0	0	0
Loranthaceae	0	0	0	0	0	0	0
Plantago	0	1	1	0	1	0	0
Acanthaceae	0	0	0	0	0	0	0
Pinaceae	0	0	0	0	0	0	0
Podocarpus	7	45	22	24	36	16	14
Rhus	5	10	10	8	5	10	2
Aizoaceae	0	2	3	7	2	2	6
Euphorbiaceae undif	0	6	8	3	4	5	2
Brassicaceae	3	5	5	9	0	9	9
Campanulaceae	0	0	0	0	0	0	0
Caryophyllaceae	0	3	0	0	0	0	0
Moraceae	0	7	0	0	5	5	0
Polygala	1	1	1	0	0	0	1
Oxalis	0	0	0	1	0	0	2
Unidentifiable	2	6	5	9	5	10	7
Broken	4	7	3	7	5	11	8
Unknown	4	10	4	6	2	5	7
10 - 50 µm	4185	8827	2409	3625	7994	2530	4223
50 - 100 µm	14	10	0	6	11	5	13

Sample name	EV11-47	EV11-48	EV11-49	EV11-50	EV11-51	EV11-52	EV11-53
Depth (cm)	128	130	131.5	136	138	140	142
Age (cal yr BP)	2520	2602	2667	2820	2868	2913	2960
Artemisia	7	11	8	21	4	1	3
Pentzia-type	0	5	8	3	1	0	6
Proteaceae	2	6	5	3	1	0	2
Ericaceae	12	32	22	28	8	5	13
Cliffortia	4	3	5	11	0	0	7
Bruniaceae	5	7	7	0	1	1	5
Anthospermum-type	12	20	6	6	1	1	11
Apiaceae	1	0	0	0	0	0	0
Fabaceae	0	0	0	0	0	0	0
Rhamnaceae	0	0	0	0	0	0	0
Rutaceae	2	2	4	5	0	1	3
Santalaceae	0	0	0	2	0	0	0
Scroph-type	0	0	0	1	0	0	1
Passerina	14	9	18	13	1	1	14
Cunoniaceae	0	0	0	0	0	0	1
Canthium	0	0	0	2	0	0	0
Gnidia	0	1	0	2	0	0	1
Euclea	11	17	7	10	2	4	12
Grewia	6	0	1	4	0	0	5
Ilex	2	6	4	8	0	0	2
Myrica	1	0	1	1	0	1	0
Myrsine	3	0	2	0	0	1	0
Myrtaceae	2	0	0	0	0	0	0
Olea	15	23	18	8	4	6	13
Cyperaceae	59	48	56	39	5	7	65
Restionaceae	40	28	37	41	8	10	45
Poaceae	30	65	77	69	8	16	43
Asteraceae HS	8	10	7	7	1	3	15
Stoebe-type	17	16	23	17	5	7	19
Geraniaceae	3	6	1	2	0	0	3
Onagraceae	0	2	0	0	0	0	0
Icacinaceae	0	4	4	4	1	0	0
Polygonium	1	0	0	0	0	0	0
Acacia	0	0	0	0	0	0	0
Celastraceae	0	4	3	3	0	2	1
Celtis	1	0	0	0	0	0	2
Diospyros	1	1	6	3	0	2	7
Euphorbia	16	17	14	17	4	4	16
Clutia	0	0	0	0	0	0	0
ChenAm-type	132	53	63	67	19	16	88
Crassula	5	4	8	5	1	2	3
Gunneraceae	0	0	0	2	0	1	1
Juncaceae	3	0	2	2	0	0	3

Sample name	EV11-47	EV11-48	EV11-49	EV11-50	EV11-51	EV11-52	EV11-53
Depth (cm)	128	130	131.5	136	138	140	142
Age (cal yr BP)	2520	2602	2667	2820	2868	2913	2960
Liliaceae	8	5	5	2	1	2	8
Iridaceae	3	4	3	0	0	1	5
Urticaceae	0	0	0	1	0	0	0
Verbenaceae	0	0	0	0	0	0	0
Haloraginaceae	0	0	0	0	0	0	0
Typha	3	7	0	7	0	1	1
Zygophyllaceae	0	0	0	0	0	0	0
Lauraceae	0	2	0	0	0	0	0
Loranthaceae	0	0	0	0	0	0	0
Plantago	0	0	0	0	0	0	0
Acanthaceae	0	0	0	0	0	0	1
Pinaceae	0	0	0	0	0	0	0
Podocarpus	8	37	24	34	9	8	19
Rhus	17	14	16	19	4	5	10
Aizoaceae	7	3	4	3	0	2	7
Euphorbiaceae undif	5	5	6	1	0	2	1
Brassicaceae	5	6	6	7	1	0	7
Campanulaceae	0	0	0	0	0	0	0
Caryophyllaceae	0	0	0	0	0	1	0
Moraceae	0	0	0	3	0	4	0
Polygala	2	2	0	0	0	0	0
Oxalis	0	0	0	0	0	1	1
Unidentifiable	8	9	8	7	1	2	15
Broken	10	4	7	6	1	2	10
Unknown	9	2	4	4	1	3	5
10 - 50 µm	3838	9438	2777	3738	4451	6143	5273
50 - 100 µm	12	26	0	3	11	2	21

Sample name	EV11-54	EV11-55	EV11-56
Depth (cm)	144.5	146	148
Age (cal yr BP)	3014	3049	3094
Artemisia	2	0	11
Pentzia-type	1	5	2
Proteaceae	0	4	3
Ericaceae	2	6	23
Cliffortia	2	0	4
Bruniaceae	0	1	6
Anthospermum-type	4	4	11
Apiaceae	0	1	0
Fabaceae	0	0	0
Rhamnaceae	0	0	0
Rutaceae	0	1	4
Santalaceae	0	0	0
Scroph-type	0	0	0
Passerina	4	9	9
Cunoniaceae	0	0	0
Canthium	0	0	0
Gnidia	0	0	1
Euclea	3	10	15
Grewia	0	0	0
Ilex	0	1	3
Myrica	0	1	2
Myrsine	0	2	0
Myrtaceae	0	0	0
Olea	7	18	14
Cyperaceae	18	40	46
Restionaceae	16	23	36
Poaceae	12	29	83
Asteraceae HS	2	4	11
Stoebe-type	8	19	20
Geraniaceae	2	3	2
Onagraceae	0	0	0
Icacinaceae	0	0	3
Polygonium	1	0	0
Acacia	0	0	0
Celastraceae	0	0	1
Celtis	2	1	0
Diospyros	2	6	2
Euphorbia	5	13	17
Clutia	1	0	2
ChenAm-type	33	65	64
Crassula	1	4	6
Gunneraceae	0	0	1
Juncaceae	0	3	3

Sample name	EV11-54	EV11-55	EV11-56
Depth (cm)	144.5	146	148
Age (cal yr BP)	3014	3049	3094
Liliaceae	4	7	5
Iridaceae	0	4	3
Urticaceae	0	0	0
Verbenaceae	0	0	0
Haloraginaceae	0	0	0
Typha	1	0	6
Zygophyllaceae	0	0	0
Lauraceae	0	0	0
Loranthaceae	0	0	0
Plantago	0	0	0
Acanthaceae	0	0	0
Pinaceae	0	0	0
Podocarpus	2	13	19
Rhus	2	6	21
Aizoaceae	0	10	0
Euphorbiaceae undif	1	1	9
Brassicaceae	4	5	6
Campanulaceae	0	0	0
Caryophyllaceae	0	0	1
Moraceae	0	0	0
Polygala	0	0	1
Oxalis	0	0	0
Unidentifiable	4	6	10
Broken	2	5	8
Unknown	5	4	6
10 - 50 µm	5006	4942	6462
50 - 100 µm	10	18	13

Appendix F

VVV16 Pollen and microcharcoal

Sample name	VVV16-4-2	VVV16-4-10	VVV16-4-18	VVV16-4-26	VVV16-4-34	VVV16-4-42	VVV16-1-1-1-2
Depth (cm)	1	10	18	26	34	42	82
Age (cal yr BP)	-62.09	-36.88	-8.4	19.65	48.65	77.33	232.03
Artemisia	0	0	0	2	7	4	8
Pentzia-type	0	2	1	10	2	1	3
Proteaceae	0	2	2	2	1	1	2
Ericaceae	6	6	25	22	30	23	21
Cliffortia	0	0	1	1	3	5	9
Bruniaceae	0	0	1	2	4	0	4
Anthospermum-type	1	0	1	1	7	3	12
Fabaceae	0	0	0	1	0	0	1
Phylica	1	0	1	2	0	0	2
Rutaceae	0	0	0	1	0	0	1
Scroph-type	0	0	0	0	0	0	1
Passerina	3	4	8	17	27	22	2
Galium	0	0	0	0	0	1	0
Canthium	0	0	0	0	1	0	2
Icacinaceae	0	0	0	2	0	0	0
Euclea	2	8	7	6	3	11	12
Grewia	0	0	1	1	0	0	1
Ilex	0	1	3	0	0	0	0
Morella	0	6	0	3	1	12	27
Myrsine	1	3	2	1	1	0	0
Olea	1	7	2	8	4	1	8
Restionaceae	5	7	2	11	9	25	28
Poaceae	9	5	5	4	15	18	17
Asteraceae HS	0	21	21	29	13	15	46
Stoebe-type	2	4	10	55	57	12	18
Geraniaceae	0	0	1	1	0	0	1
Gardenia	0	0	0	0	0	2	1
Polygonum	0	0	0	0	0	0	1
Acacia	0	0	0	0	0	0	2
Celastraceae	0	2	1	2	0	1	1
Celtis	0	0	0	0	1	0	1
Diospyros	0	1	3	3	3	4	6
Dodonaea	0	1	0	3	0	1	6
Euphorbia	1	2	3	10	15	3	12
Clutia	0	0	0	1	0	0	2
Amaranthaceae	0	2	1	5	7	1	3
Crassula	2	5	6	2	0	0	0
Ruschia	0	0	0	0	0	0	0
Liliaceae	0	0	0	0	2	0	1
Iridaceae	0	0	0	0	0	0	3
Hamamelidaceae	0	0	0	1	3	0	1
Unidentifiable	0	2	2	3	2	0	5
Broken	2	4	5	5	2	3	3

Sample name	VVV16-4-2	VVV16-4-10	VVV16-4-18	VVV16-4-26	VVV16-4-34	VVV16-4-42	VVV16-1-1-1-2
Depth (cm)	1	10	18	26	34	42	82
Age (cal yr BP)	-62.09	-36.88	-8.4	19.65	48.65	77.33	232.03
Pittosporaceae	0	0	0	0	0	0	1
Justica-type	0	0	1	0	2	0	0
Pinaceae	154	159	136	17	11	0	0
Podocarpus	3	5	2	3	1	1	1
Rhus	0	1	1	2	1	1	3
Aizoaceae	3	3	2	4	4	0	1
Brassicaceae	1	0	0	2	2	0	3
Campanulaceae	0	0	0	0	0	0	0
Caryophyllaceae	0	0	0	1	0	0	0
Polygala	0	0	0	1	0	0	0
Cardiospermum	0	0	0	0	0	0	0
Rosaceae	0	0	0	0	0	0	4
Myrtaceae	10	28	31	41	0	0	0
Kiggelaria	7	9	12	10	1	0	0
Solanum	1	0	0	2	1	0	4
Sideroxylon	0	0	0	0	0	0	0
Moraceae	0	0	0	0	0	0	2
Gentian	0	0	0	0	0	0	0
Spheres	254	50	159	416	687	38	424
10-100 µm	71	81	437	467	949	158	2205
>100 µm	0	0	0	0	0	0	4

Sample name	16-1-1-1-10	16-1-1-1-18	16-1-1-1-26	16-1-1-1-34	16-1-1-1-42	16-1-1-1-50	16-1-1-1-58
Depth (cm)	90	98	106	114	122	130	138
Age (cal yr BP)	261.05	295.81	333.89	373.15	412.79	455.5	494.01
Artemisia	5	9	2	4	5	5	6
Pentzia-type	11	3	1	2	5	0	0
Proteaceae	3	1	1	2	0	1	0
Ericaceae	33	27	8	18	27	5	12
Cliffortia	2	14	2	3	7	2	1
Bruniaceae	0	3	1	0	2	0	2
Anthospermum-type	19	4	2	4	3	3	3
Fabaceae	0	0	0	0	0	0	0
Phylica	2	0	1	2	0	0	1
Rutaceae	0	0	0	1	5	0	2
Scroph-type	2	0	1	0	0	0	0
Passerina	10	6	2	3	11	2	1
Galium	0	1	0	1	0	0	0
Canthium	1	0	2	0	2	2	1
Icacinaceae	0	4	0	0	1	0	0
Euclea	8	7	3	2	8	3	9
Grewia	0	2	0	0	3	0	0
Ilex	1	0	0	0	0	0	0
Morella	19	25	9	15	15	6	7
Myrsine	1	0	0	1	1	0	0
Olea	4	6	2	6	6	4	3
Restionaceae	16	23	15	4	9	11	18
Poaceae	8	29	11	11	21	13	21
Asteraceae HS	29	44	7	73	74	19	15
Stoebe-type	35	31	11	26	49	6	18
Geraniaceae	1	2	0	2	1	1	0
Gardenia	0	1	3	2	2	1	0
Polygonum	0	1	0	0	0	0	0
Acacia	3	2	0	0	0	0	0
Celastraceae	2	4	0	1	2	0	1
Celtis	0	2	2	0	0	0	0
Diospyros	5	3	1	0	4	2	1
Dodonaea	2	2	0	1	0	0	0
Euphorbia	18	12	0	8	8	2	2
Clutia	1	0	0	2	3	0	0
Amaranthaceae	8	5	3	1	7	2	3
Crassula	3	2	0	3	2	1	0
Ruschia	0	0	0	0	0	0	0
Liliaceae	2	5	1	0	0	0	2
Iridaceae	0	2	0	0	0	0	1
Hamamelidaceae	3	0	0	2	0	0	1
Unidentifiable	2	4	2	0	3	1	0
Broken	4	4	3	3	5	3	2

Sample name	16-1-1-1-10	16-1-1-1-18	16-1-1-1-26	16-1-1-1-34	16-1-1-1-42	16-1-1-1-50	16-1-1-1-58
Depth (cm)	90	98	106	114	122	130	138
Age (cal yr BP)	261.05	295.81	333.89	373.15	412.79	455.5	494.01
Pittosporaceae	0	0	0	0	0	0	1
Justica-type	0	1	0	0	0	0	0
Pinaceae	0	0	0	0	0	0	0
Podocarpus	1	0	1	0	2	4	3
Rhus	2	1	2	1	2	0	1
Aizoaceae	0	0	0	2	2	0	0
Brassicaceae	2	2	2	0	0	0	2
Campanulaceae	0	0	0	0	0	1	0
Caryophyllaceae	0	0	0	0	0	0	0
Polygala	0	0	0	0	0	0	0
Cardiospermum	0	0	0	0	0	0	0
Rosaceae	0	0	0	0	1	1	0
Myrtaceae	0	0	0	0	0	0	0
Kiggelaria	0	1	1	0	1	0	0
Solanum	2	2	1	0	0	0	0
Sideroxylon	0	0	0	0	0	0	0
Moraceae	1	3	0	0	1	0	0
Gentian	0	0	0	0	0	0	0
Spheres	278	515	399	734	468	296	126
10-100 µm	1304	4320	1830	4467	4655	3018	4270
>100 µm	2	6	0	3	5	4	4

Sample name	16-1-1-1-64	16-1-1-2-2	16-1-1-2-10	16-1-1-2-18	16-1-1-2-26	16-1-1-2-42	16-1-1-2-48
Depth (cm)	144	150	158	166	174	190	196
Age (cal yr BP)	515.24	529.7	547.63	568.32	588.93	637.92	655.17
Artemisia	7	3	7	8	5	7	2
Pentzia-type	3	2	7	9	8	19	8
Proteaceae	6	0	2	1	1	1	0
Ericaceae	30	14	29	21	20	7	9
Cliffortia	3	1	5	2	4	5	2
Bruniaceae	4	0	2	1	1	2	1
Anthospermum-type	4	3	8	7	1	5	3
Fabaceae	1	0	0	1	0	0	0
Phylica	2	1	4	3	5	1	3
Rutaceae	1	0	1	4	1	0	1
Scroph-type	1	0	0	1	0	1	1
Passerina	5	3	6	2	8	3	2
Galium	0	0	0	0	0	0	0
Canthium	1	0	3	1	1	2	3
Icacinaceae	0	0	0	0	0	0	0
Euclea	6	3	7	8	3	5	3
Grewia	1	1	2	0	1	0	0
Ilex	2	2	2	3	0	1	0
Morella	24	14	28	27	23	25	11
Myrsine	1	1	1	2	0	2	1
Olea	7	6	9	14	8	7	5
Restionaceae	26	12	26	18	10	7	8
Poaceae	24	7	31	30	13	22	11
Asteraceae HS	38	15	38	57	46	33	27
Stoebe-type	31	11	13	33	19	19	13
Geraniaceae	1	0	2	1	1	1	0
Gardenia	1	3	1	1	0	2	0
Polygonum	0	0	0	0	0	1	0
Acacia	0	0	2	0	3	0	1
Celastraceae	4	4	3	5	2	3	1
Celtis	1	0	0	1	1	1	0
Diospyros	4	4	6	3	1	1	2
Dodonaea	4	0	2	1	3	2	0
Euphorbia	20	7	13	10	5	8	5
Clutia	2	1	2	4	1	0	0
Amaranthaceae	4	7	1	5	7	3	4
Crassula	2	2	0	2	3	0	0
Ruschia	1	1	0	0	1	0	0
Liliaceae	1	0	0	2	1	1	1
Iridaceae	2	0	1	0	0	2	0
Hamamelidaceae	3	1	2	1	0	2	1
Unidentifiable	1	0	0	1	3	2	2
Broken	4	3	6	4	5	4	3

Sample name	16-1-1-1-64	16-1-1-2-2	16-1-1-2-10	16-1-1-2-18	16-1-1-2-26	16-1-1-2-42	16-1-1-2-48
Depth (cm)	144	150	158	166	174	190	196
Age (cal yr BP)	515.24	529.7	547.63	568.32	588.93	637.92	655.17
Pittosporaceae	1	0	0	0	0	2	1
Justica-type	0	0	0	0	1	0	0
Pinaceae	0	0	0	0	0	0	0
Podocarpus	3	3	2	0	1	0	0
Rhus	0	0	2	1	1	0	0
Aizoaceae	2	0	1	2	1	0	2
Brassicaceae	3	0	2	1	1	0	1
Campanulaceae	0	0	0	0	0	0	1
Caryophyllaceae	0	0	0	0	0	0	0
Polygala	0	0	0	0	0	0	0
Cardiospermum	1	0	0	0	0	0	0
Rosaceae	0	0	0	1	1	0	0
Myrtaceae	0	0	0	0	0	0	0
Kiggelaria	0	0	0	0	0	0	0
Solanum	3	0	2	0	2	8	3
Sideroxylon	1	0	0	1	0	1	1
Moraceae	3	0	0	0	1	0	1
Gentian	0	0	0	0	0	0	1
Spheres	328	206	534	472	263	283	202
10-100 µm	2751	2586	2669	2528	1855	1223	409
>100 µm	3	3	2	1	2	1	1